The Role of Protein Kinase N in Gastric Cancer

Lizbeth Minerva Jiménez Flores

The Role of Protein Kinase N in Gastric Cancer

by

Lizbeth Minerva Jiménez Flores

A thesis submitted in fulfillment of the requirements for the title of PhD by the University of Barcelona

PhD program in Biomedicine

The thesis was carried out at

Group of Biomedical Research in Digestive Tract Tumors

Centre for Molecular Biology and Biochemistry Investigation in Nanomedice (CIBBIM-Nanomedicine)

Vall d'Hebron Research Institute

Director:

Diego Arango del Corro

Co-Director:

José Higinio Dopeso González

PhD candidate:

Lizbeth Minerva Jiménez Flores

Esta tesis doctoral ha sido apoyada por el gobierno de los Estados Unidos Mexicanos, a través del programa nacional de Becas en el extranjero (convocatoria de 2014 segundo periodo)

Registro y Solicitud de Beca No. 269733/383724

Número de Becario 389474

A mis padres y a mi hermana

Abstract

Gastric cancer (GC) is one of the most common types of cancer in the Western World and accounts for over 700,000 deaths every year worldwide. The prognosis is dismal, with an average 5-year survival rate of less than 20%, mainly because of late diagnosis, due to the early stages are clinically silent. The cause of GC is multifactorial, as infectious agents, enviromental or/and genetic factors. Based on Lauren's histologic classification, there are 2 types of GC: intestinal (IGC) and diffuse (DGC). Diffuse carcinoma cells lacks cohesion and invade tissues independently or in small clusters, is more common in young patients and behaves more aggressively than the intestinal type. Recent findings published in Nature and Nature Genetics identified frequent hotspots (14-24%) mutations in the small GTPase RHOA in the diffuse type of gastric tumors. To investigate the mechanism that underlies downstream of RHOA we analyzed the capacity of the mutations more commonly found in gastric tumors to bind to different effectors. We observed that the mutations found in gastric tumors specifically affect the capacity of RHOA to bind to PKN effector family. Therefore, in this thesis we study and characterized the role of PKN1 in GC. We demonstrated that the downregulation of PKN1 with shRNA or the deletion mediated by CRISPR/Cas9 results in the increase of proliferation in the diffuse gastric cell lines "*in vitro*" and "*in vivo*". Moreover, the opposite effect is observed when we overexpress the constitutively active form of PKN1 in diffuse gastric cell lines with moderate or low levels of PKN1. In addition, we use a novel mouse model with conditional expression in the gastric mucosa of the RHOA-Y42C mutation (the most frequent mutation found in DGC) to investigate the role of RHOA in gastric tumorogenesis initiated by either N-methyl-N-nitrosourea (MNU) or *Apc* mutations. The mice with expression of the RHOA-Y42C have a significant increase in the number of tumors indicating that RhoA-Y42C is important for progression of the gastric tumors. Finally, we performed a preclinical testing of a new therapeutic approach, such as dietary supplements of arachidonic acid, a well-established activator of PKN1. The work carried out in this thesis will shed light on the newly identified deregulation of RHOA-PKN signaling in gastric cancer and provide a solid rationale for therapeutic targeting of this pathway.

Resumen

El cáncer gástrico (CG) es uno de los tipos de cáncer más comunes en el mundo occidental y representa más de 700,000 muertes cada año en todo el mundo. El pronóstico es bajo, con una tasa de supervivencia promedio de 5 años de menos del 20%, principalmente debido a un diagnóstico tardío, debido a que las etapas tempranas son clínicamente silenciosas. La causa del CG es multifactorial, como agentes infecciosos, factores ambientales y/o genéticos. Según la clasificación histológica de Lauren, hay 2 tipos de CG: intestinal (CGI) y difuso (CGD). Las células de carcinoma de tipo difuso carecen de cohesión e invaden los tejidos de forma independiente o en pequeños grupos, es más común en pacientes jóvenes y se comporta de forma más agresiva que el tipo intestinal. Hallazgos recientes publicados en Nature and Nature Genetics identificaron mutaciones frecuentes en sitios específicos o hotspots (14-24%) en la proteína GTPasa RHOA en los tumores gástricos de tipo difuso. Para investigar el mecanismo que subyace en la vía de señalización de RHOA, analizamos la capacidad de las mutaciones más recurrentes encontradas en tumores gástricos para unirse a sus diferentes efectores. Observamos que las mutaciones encontradas en los tumores gástricos afectan específicamente la capacidad de RHOA para unirse los efectores de la familia de proteínas kinasas PKN. Por lo tanto, en esta tesis estudiamos y caracterizamos el papel de PKN1 en el CG. Demostramos que la depleción de PKN1 mediante shRNA o la deleción mediada por CRISPR/Cas9 da como resultado el aumento de la proliferación en las líneas celulares gástricas difusas "*in vitro*" e "*in vivo*". Además, el efecto opuesto se observa cuando sobreexpresamos la forma constitutivamente activa de PKN1 en líneas celulares gástricas difusas con niveles de expresión moderados o bajos de PKN1. Así mismo, utilizamos un nuevo modelo murino con expresión condicional en la membrana mucosa gástrica de la mutación RHOA-Y42C (la mutación más frecuente encontrada en CGD) para investigar el papel de RHOA en la tumorogénesis gástrica iniciada por N-metil-N-nitrosourea (MNU) o por mutaciones de *Apc*. Los ratones con expresión de RHOA-Y42C presentaron un aumento significativo en el número de tumores, lo cual indica que RHOA-Y42C tiene un papel importante en la progresión de los tumores gástricos. Finalmente, realizamos una prueba preclínica de un nuevo enfoque terapéutico, como los suplementos dietéticos de ácido araquidónico, un activador bien establecido de PKN1. El trabajo llevado a cabo en esta tesis destacará la importancia de la desregulación recientemente identificada de la señalización RHOA-PKN en el cáncer gástrico y proporcionará una base sólida para la orientación terapéutica de esta vía.

INDEX

Figure index

Table index

INTRODUCTION

CHAPTER I. INTRODUCTION

1. The human gastrointestinal system

1.1 Overview

The human gastrointestinal system comprises a number of organs and glands responsible for the processing and digestion of food, allowing the absorption of nutrients. The digestive system consists of a large tube stretching from the mouth to the anus, comprising the esophagus, stomach, small and large intestines, along with several glands, such as the salivary glands, liver, gall bladder, and pancreas whose secretions are important for the digestive process (**Figure 1**) (1).

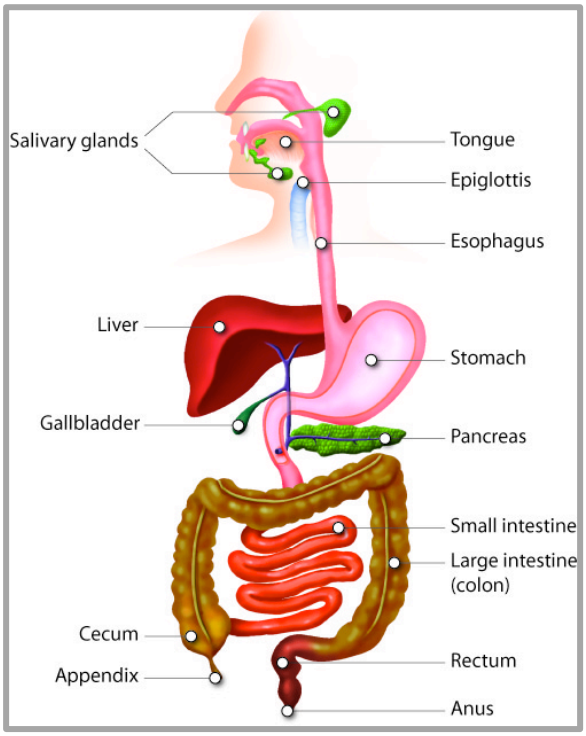

Figure 1. **The human digestive system.**
The digestive system consists of the gastrointestinal tract plus the accessory organs of digestion (the tongue, salivary glands, pancreas, liver, and gallbladder). Source: https://www.maureekai.com

1.2 Anatomy of the stomach

The stomach is a muscular, J-shaped organ in the upper part of the abdomen. It is part of the digestive system, which extends from the mouth to the anus (**Figure 1**). The size of the stomach varies from person to person, having a capacity of 1000–1500 mL in the regular adult. It is situated between the end of the oesophagus and the duodenum, the beginning of the small intestine. It lies in the epigastric, umbilical, and left hypochondrial regions of the abdomen, and occupies a recess bounded by the upper abdominal viscera, the anterior abdominal wall and the diaphragm (1).

2. Function and Structure

An important function of the stomach is to serve as a temporary holding chamber for the ingested food, which passes from the esophagus to the stomach where it is held for 2 hours approximately. Other important function is the mixing and chemical breakdown of the food with hydrochloric acid, mucus and pepsin (which digest proteins), **lipase** (which digest fats), and then release the resulting chyme, at a controlled rate into the duodenum by contraction and relaxation of the three layers of **smooth muscle** in the muscularis layer. The stomach plays many important roles in chemical digestion, including the continued digestion of carbohydrates and the initial digestion of proteins and triglycerides. Little if any nutrient absorption occurs in the stomach (1).

The stomach is divided into five main regions: the cardia, fundus, body, antrum and pylorus (**Figure 2**). The **cardia** is the first part of the stomach below the esophagus. It contains the cardiac sphincter, which is a thin ring of muscle that helps to prevent stomach contents from going back up into the esophagus. Located inferior to the diaphragm, above and to the left of the cardia, is the dome-shaped **fundus**. Below the fundus is the **body,** the largest and main part of the stomach. This is where food is mixed and starts to be digested. The **antrum** is the lower part of the stomach where it holds the predigested food until it is ready to be released into the small intestine. It is sometimes called the pyloric antrum. The **pylorus** is the part of the stomach that connects to the small intestine. This region includes the pyloric sphincter, which is a thick ring of muscle that acts as a valve to control the emptying of stomach contents (chyme) into the duodenum (first part of the small intestine). The pyloric sphincter also prevents the contents of the duodenum from going back into the stomach (1).

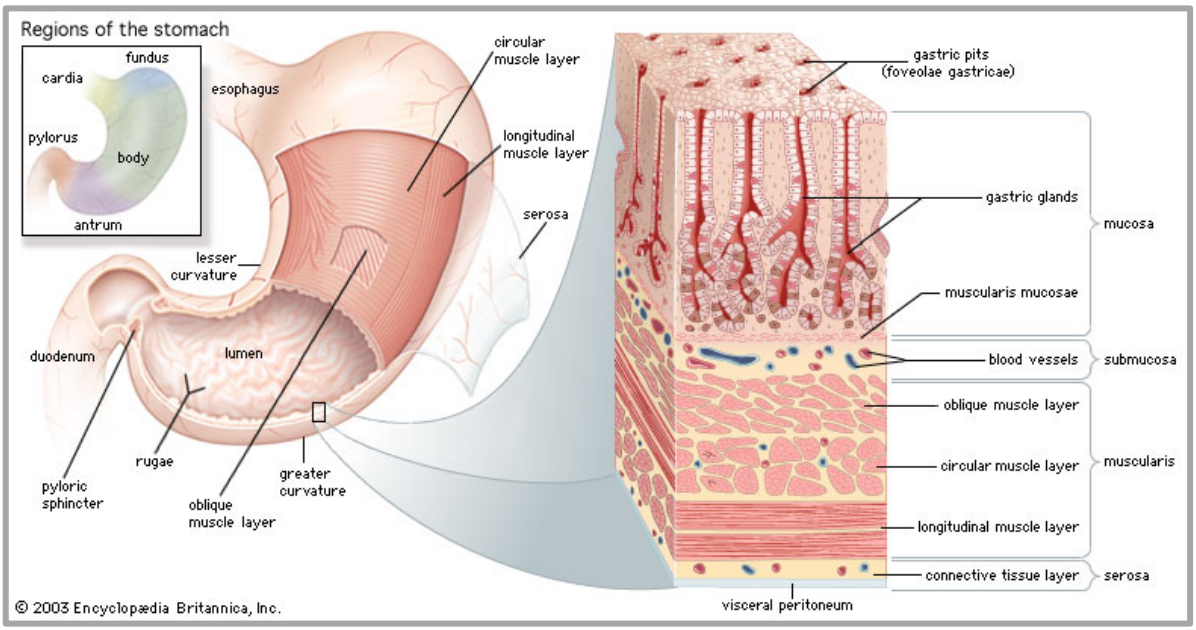

Figure 2. **Anatomy of Stomach.**

The stomach has five major regions: the cardia, fundus, body, antrum and pylorus. The inner oblique smooth muscle layer gives the muscularis the ability to vigorously churn and mix food. In the epithelium, gastric pits lead to gastric glands, which secrete gastric juice. The gastric glands (shown enlarged on the right) contain different types of cells that secrete a variety of chemical substances and enzymes, including hydrochloride acid, which activates the protein-digesting enzyme pepsin. Source: Encyclopedia Britannica, Inc.

3. Histology of human gastric ephitelia

The wall of the stomach is made of the same four layers as most of the rest of the alimentary canal, but with adaptations to the mucosa and muscularis for the unique functions of this organ (**Figure 2**).

- The **mucosa** (mucous membrane) is the inner lining of the stomach, consisting mainly of epithelial cells, cardiac, fundic and pyloric glands are found in this layer depending on the stomach area. When the stomach is empty the mucosa has a ridged appearance. These ridges (rugae) flatten out as the stomach fills with food.
- The **submucosa** covers the mucosa. It is made up of connective tissue that contains larger blood and lymph vessels, nerve cells and fibres.
- The **muscularis propria** (or muscularis externa) is the next layer that covers the submucosa. It is the main muscle of the stomach and is made up of 3 layers of muscle: longitudinal, circular and oblique, which gives the muscularis the ability to vigorously churn and mix food.

- The **serosa** is the fibrous membrane that covers the outside of the stomach.

The stomach mucosa's epithelial lining (oxyntic epithelium) consists only of surface mucus cells, which secrete a protective coat of alkaline mucus. A vast number of **gastric pits** dot the surface of the epithelium and mark the entry to each **gastric gland**, which secretes a complex digestive fluid known as as gastric juice (**Figure 3**). The cellular composition of these gastric units varies depending on the anatomical region of the stomach (2).

- The **cardiac glands** are found in the cardia of the stomach and they primarily secrete mucus. There are two kinds - either simple tubular with short ducts or compound racemose resembling the duodenal Brunner's glands, wich are found in that portion of the duodenum and produce a mucus-rich alkaline secretion in order to protect and lubricate the duodenal walls.
- The **fundic glands** (or oxyntic glands) are found in the fundus and body of the stomach, the site of most chemical digestion. They are simple almost straight tubes, they secrete hydrochloric acid (HCl) and intrinsic factor, a glycoprotein produced by the parietal cells of the stomach necessary for the absorption of vitamin B12 in the small intestine.
- The **pyloric glands** are located in the antrum of the pylorus. They secrete mucus and a number of hormones, including the majority of the stimulatory hormone, gastrin a peptide hormone that stimulates secretion of gastric acid (HCl) by the parietal cells and aids in gastric motility, produced by their G cells (enteroendocrine cells).

These glands are made up of a variety of secretory cells (**Figure 3**) (3):

- **Parietal cells** or acid secreting cells are located primarily in the middle region of the gastric glands, these cells produce a) hydrochloric acid (HCl), responsible for the high acidity (pH 1.5 to 3.5) of the stomach contents and is needed to activate the protein-digesting enzyme, pepsin and b) intrinsic factor a glycoprotein necessary for the absorption of vitamin B12 in the small intestine.
- **Chief cells** are located primarily in the basal regions of gastric glands, which contain zymogen granules and they secrete pepsinogen**,** the inactive proenzyme form of pepsin.
- **Mucous neck cells** are located in the upper part of gastric glands, which secrete thin acidic mucus and bicarbonate that protects it from the corrosive nature of gastric acid.
- **Enteroendocrine cells** (Chief cells, D cells, G cells) found in the lower base of gastric glands, secrete various peptide hormones into the interstitial fluid of the lamina propria

(e.g. Gastrin, Somatostatin, Histamine, and Leptin) that have effects on the endocrine system. For example, Somatostatin inhibits insulin and glucagon secretion, Histamine stimulates parietal cells to produce carbonic acid that finally dissociates into hydrogen and bicarbonate ions to equilibrate pH of the stomach and Leptin that helps to regulate energy balance by inhibiting hunger.

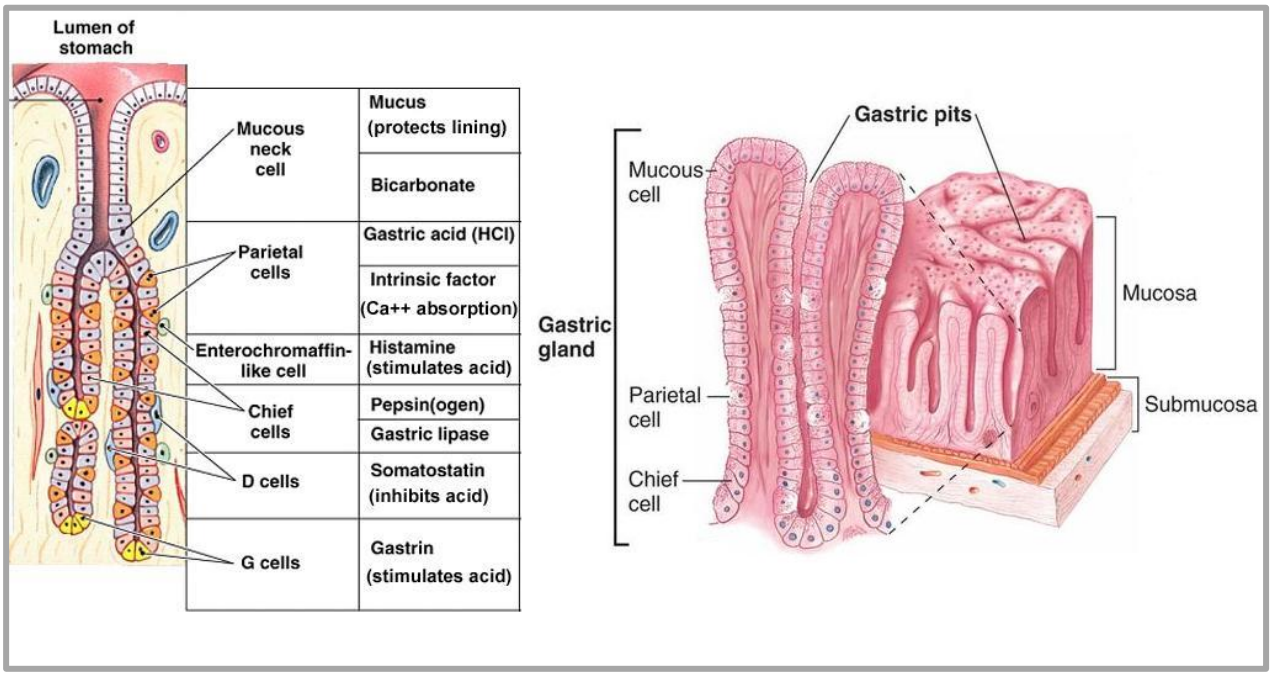

Figure 3. **Human gastric units.**

Diagrammatic representation of the gastric gland. Different types of cells are present in each gland including endocrinal (G cell, D cell) and neuroendocrinal (enterochromaffin like cell- ECL cell). Neck cells present in the glands secrete mucus. Parietal and chief cells secrete acid. D cells when stimulated secrete somatostatin, which decreases acid secretion. G cells when stimulated secrete gastrin, which increases secretion of acid through ECL cells. Source: Karam, 2010 (4).

4. Adult gastric Homeostasis

4.1 Cell renewal

The gastric epithelium is continuously undergoing cell renewal throughout the lifetime. This renewal occurs due to the proliferation and differentiation of the multipotent stem cells that are present in the isthmus region of the adult gastric glands. Leblond, *et al.* (5) defined renewing cell

populations by two major criteria: 1) frequent mitosis which are restricted to a definite subpopulation of cells; and 2) cell loss which is required to balance cell production and to keep the steady state of the population. Moreover, are described 5 successive stages in the life history of renewing cells (5). They are first present as stem cells, which divide and produce new stem cells as well as uncommitted and/or committed progenitor cells, which represent the second stage in the renewing cell process. The uncommitted progenitor cells present dual lineage features and then become committed progenitor cells with specific features of one lineage. These progenitor cells are usually capable of undergoing mitosis and thus amplifying the population before entering the next stage. Transit cells represent the third stage during which cellular differentiation gradually occurs by synthesizing new gene products. This may be shown morphologically by gradual changes in cell structure, immunocytochemically by expression of new proteins, and biochemically by changes in enzymatic activities, protein composition and mRNA expression. The fourth stage is that of the mature cells which have completed their differentiation and become fully functional. Finally, in the fifth stage of terminal cells there is a gradual deterioration and eventually death and elimination (5, 6).

4.2 The gastric stem cell

Multicellular organisms develop from a single pluripotent embryonic stem cell. This cell has the capacity to differentiate into all type of cells of the organism while maintaining and expanding a pool of the primitive cell types of the three germ layers. In adult mammals, tissue homeostasis and repair of injured organs depends on small reservoirs of tissue-specific stem cells. Adult stem cells are defined by their ability for self renewing cell divisions (7). These divisions are defined by two characteristics: First, the cell divisions give rise to two daughter cells, of which one or both have the exact same proliferative capacity as the parent cell. Second, at least one of the daughter cells has the exact same differentiating potential as the parent cell giving rise to cells that can differentiate into one or more specialized cells of the organ (8). To maintain and repair the tissues during the lifespan of the animal, adult stem cells use three different types of cell division: 1) asymmetric divisions, generating one stem cell and one progenitor cell, 2) self-renewing symmetric division, generating two daughter stem cells to expand the stem cell population, or 3) non self-renewing symmetric division, resulting in the generation of two cell progenitors. The hierarchical organization of adult tissue consisting of stem cells, progenitors and terminally differentiated cells is suggested to have developed to help the organism recover from injury and to slow aging, while on the other hand protecting the cells from accumulating

damage that would ultimately lead to cancer. Adult stem cells have evolved as a mechanism to lower this risk by restricting their expansion, whereas their immediate offspring, the progenitor cells, strongly expand in number but their limited lifespan protects them from accumulating mutations (9). Rapidly self-renewing tissues that harbour actively cycling stem cell populations to maintain tissue homeostasis, such as small intestine and stomach, offer the opportunity to deeply study adult stem cells as well as their relationship with cancer initiation and progression. Extensive studies showed the sequential generation of these gastric epithelial cells (GEC) from gastric stem cells (GSC), as well as the most important molecular markers that delineate the cell lineages (**Figure 4**). Moreover, some studies highlighted the heterogeneity of stem cells in different regions of the stomach and even in different zones of an identical gland.

The stem cells give rise to precursors that move bidirectionally (toward the lumen and toward the base) in the gland, giving rise to three main lineages with 11 cell types, that is:

1. *Pit* (also known as surface-associated/foveolar) *cell lineage:* Pre-pit cell precursors, pre-pit cells, pit cells. Foveolar cells are mucus-producing cells that cover the inside of the stomach, protecting it from the corrosive nature of gastric acid.
2. *Zymogenic Chief Cells* (ZC) *lineage:* Pre-neck cell precursors, pre-neck cells, neck cells, pre-ZCs, and ZCs. These cells work in conjunction with the parietal cells, which releases gastric acid, converting the pepsinogen into pepsin, a digestive enzyme that helps to digest the proteins in food.
3. *Parietal Cells* (PC) *lineage:* Pre-PC precursors, pre-PCs, and PCs. Also known as oxyntic or delomorphous cells, these are the epithelial cells that secrete hydrochloric acid (HCl) and intrinsic factor that advances the digestive process.

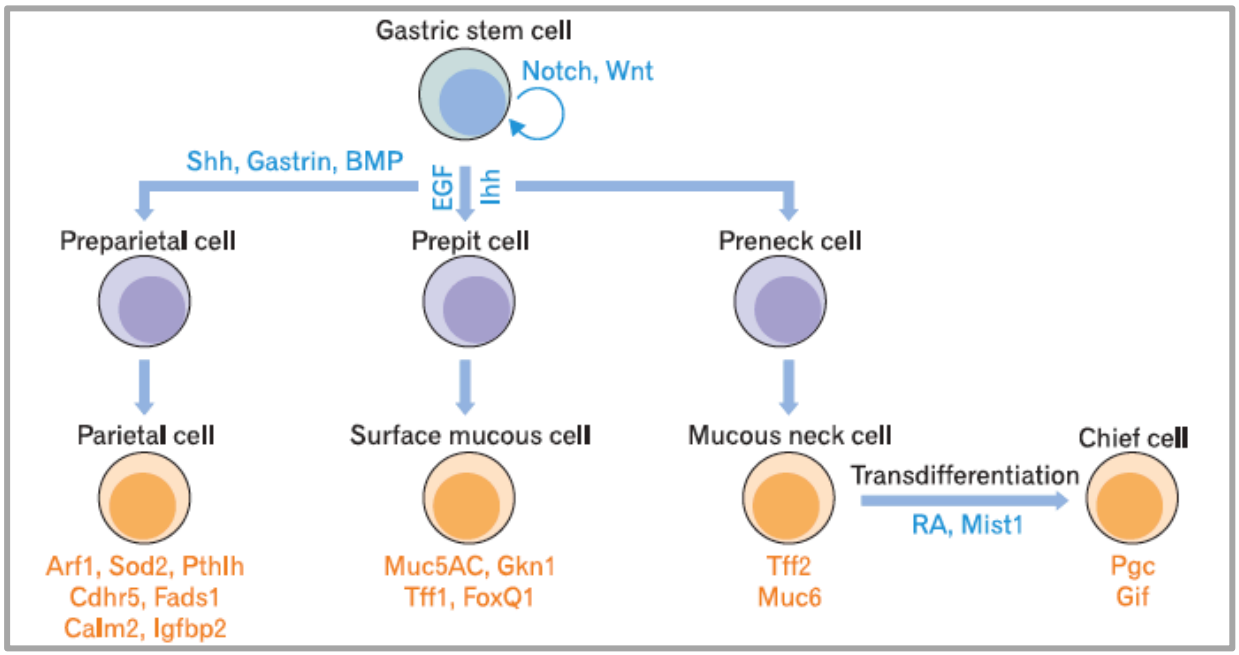

Figure 4. Self-renewal and differentiation of gastric stem cells.

Gastric stem cells have the capacity to self-renew and to differentiate into various types of daughter cells: surface mucous cells, mucus neck cells, chief cells, and parietal cells. Critical signaling pathways for each differentiation route are indicated in blue. Characteristic genes for each type of cells are indicated in orange. Arf1, ADP-ribosylation factor 1; BMP, bone morphogenetic protein; Calm2, calmodulin 2; Cdhr5, cadherin-related family member5; EGF, epidermal growth factor; Fads1, fatty acid desaturase 1; FoxQ1, forkhead box Q1; Gif, gastric intrinsic factor; Gkn1, gastrokine-1; Ihh, Indian hedgehog; Igfbp2, insulin-like growth factor binding protein 2; Mist1, basic helix-loop-helix transcription factor; Muc5AC, mucin 5AC; Muc6, mucin 6; Notch, Notch signaling pathway; Pgc, pepsinogen C; Pthlh, parathyroid hormone-like hormone; RA, retinoic acid; Shh, sonic hedgehog; Sod2, superoxide dismutase 2; Tff1, trefoil factor family 1; Tff2, trefoil factor family 2; Wnt, Wnt signaling pathway. Source: Myoung-Eun and Sae-Ock, 2013 (10).

In addition to these lineages, endocrine cells are also scattered throughout the gastric unit. The location of the stem cells within the isthmus region of the gastric corpus has been well established by ultrastructure and turnover analysis, but its molecular identity has not been well characterized (**Figure 5**) (11).

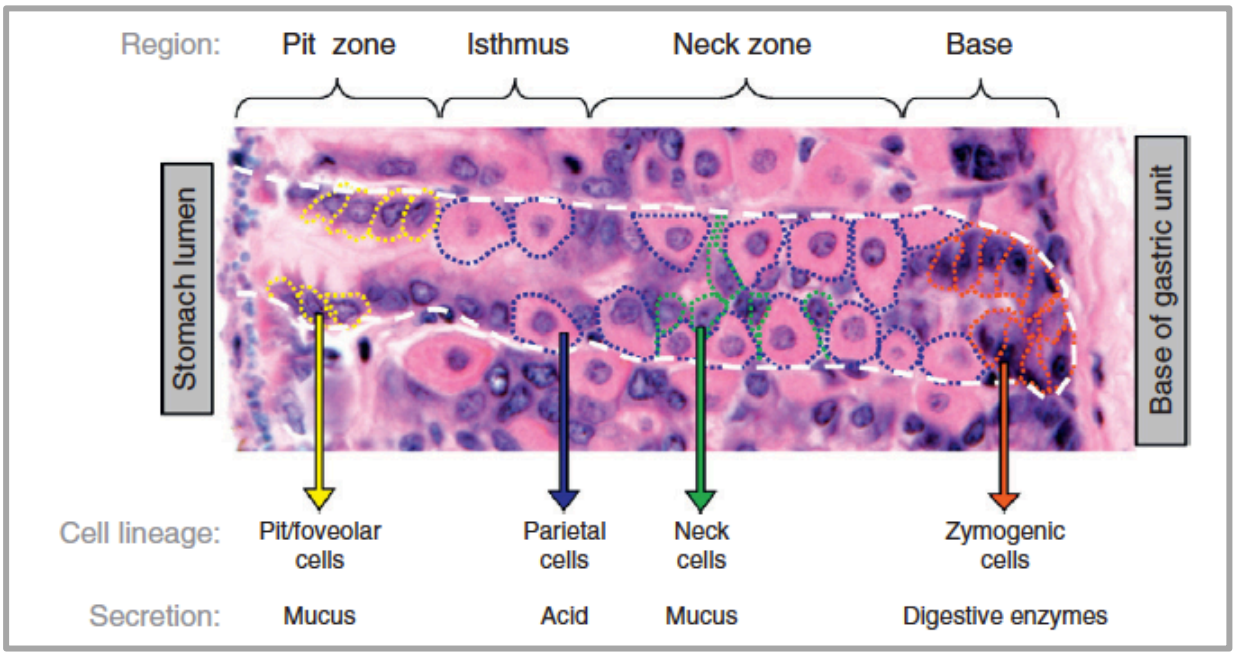

Figure 5. Normal architecture and organization of different cell types in the gastric units of the adult mouse.
The corpus (body) of the adult stomach consists of repeating invaginations called gastric units, which can be divided into four regions characterized by the presence of specific cell types in each region. Depicted is an hematoxylin and eosin stained slide of the adult mouse stomach showing a single gastric unit outlined in white, with each region labeled: 1, Pit zone, which lines the stomach lumen, consists of mucus-secreting pit foveolar cells, and narrows deeper in the unit into the isthmus region; 2, the isthmus, characterized by the presence of the multipotent gastric stem cell; 3, neck zone, where mucus-secreting neck cells and most of the acid-secreting parietal cells reside; and 4, base region, where enzyme producing zymogen cells are present. Source: Khurana and Mills (12).

The first specific identification of stem cells in situ by the Villin$^{\beta\text{-gal}/+}$ marker demonstrated that this rare subpopulation is primarily located at or below the isthmus of pyloric glands (13). Moreover, based on lineage tracing (a method that delineates all progeny produced by a marked single cell or a group of cells), cells in the isthmus region that express trefoil factor family 2 (TFF2) mRNA have also been proposed as progenitor cells (14). Multiple specific markers have also been used to distinguish stem cells from mature epithelial cells in different sites within the stomach. Lgr5 is a well-established stem cell marker in the small intestine and colon that has shown to be expressed strictly in the bottom of the adult human pyloric glands. Via stimulation of gastric units *in vitro* and lineage tracing *in vivo*, Lgr5^{+} cells have been shown to possess self-renewal capacity; therefore, Lgr5 can be considered an exclusive marker for GSCs (15). Above the bottom of the pyloric and fundic glands, Sox2^{+} stem cells without a marked overlap in Lgr5 expression were identified by using double-labelling methods and marker tracing (16). Recently,

some studies have found that a specific subpopulation of chief cells had the potential to function as reserve stem cells. A single $Troy^+$ mature chief cell located at the base of the gastric corpus glands could generate an entire gland, based on lineage tracing, and could form long-lived organoids in a three-dimensional culture system (17). Likewise, Mist1-expressing cells in the isthmus region but not in the lower third of the gastric corpus units have also been observed to have self-renewal capacity and to differentiate into multiple lineages of mature cells, such as mucus cells and chief cells. In addition, the use of transgenic mouse models also showed that $Mist1^+$ isthmus cells could expand and evolve independently of $Lgr5^+$ cells and are the origin of mature epithelial cells in the corpus units (18).

Self-renewal and differentiation of gastric stem cells are tightly regulated by the activation of specific genes (**Figure 4**). In turn, these molecular markers allowed the meticulous study of the lineage of gastric cells. For example, surface mucus cells are suggested to be generated from prepit cells derived from gastric stem cells (12, 19, 20) and the generation of surface mucus cells takes around 3 days (19-22). Mucus neck cells are generated from gastric stem cell-derived preneck cells. Interestingly, chief cells whose half-life is 194 days have been suggested to be derived by transdifferentiation of mucus neck cells, which generation takes 14 days (19, 20). The generation and differentiation of chief cells are regulated by the basic helix-loop-helix transcription factor Mist1 and retinoic acid (RA) (23-25). Parietal cells generated from gastric stem cell-derived preparietal cells (12), they are regulated by sonic hedgehog (Shh), gastrin, and bone morphogenetic protein (BMP) (26-28). Therefore, all these data imply the heterogeneity of stem cells in different regions of the stomach and even in different zones of an identical unit or gland.

The study of adult mouse gastric epithelial turnover using tritiated thymidine labelling showed that, with the exception of the parietal and chief cells, the label-retaining cells in the gland of the gastric units migrate towards the surface of the epithelium (3, 29). At birth, gastric units in both the corpus and pylorus are polyclonal. In contrats, X-chromosome inactivation and chemical mutagenesis studies have shown that 90-95% of the gastric units in the pyloric and corpus become monoclonal during adulthood. This indicates that the gastric units are derived from a single multipotent stem cell (30-33).

4.3 Cell death in the gastric epithelium

At the luminal surface of the stomach, pit and parietal cells lose their functional activities and undergo autophagic (necrosis-like) or apoptotic cell death. While necrotic cells are directly extruded into the gastric lumen (a kind of holocrine secretion), apoptotic cells are phagocytosed by healthier neighbors, which eventually undergo extrusion (20, 34, 35). In the bottom of the gastric glands, both zymogenic and parietal cells undergo degeneration and are directly extruded into the gland lumen or are phagocytosed by healthier neighbors. Connective tissue macrophages may invade the gastric gland and participate in the elimination of dead cells (34). In the pyloric glands, cell degeneration and loss occurs in both the neck and base regions. Acording to 'casacade pattern' of renewal in the glands of mouse antral units, in each gland it is estimated that about 18 cells are daily lost from the neck, 10 at the neck-base border and 1 from the base. Dead cell elimination occurs by extrusion into the gland lumen or by phagocytosis to mantain homeostasis (36). Deregulation of a normal apoptosis and cell elimination gives raise to abnormal proliferation thus initiating tumorigenesis.

5. Cancer

Cancer is a multistep process that arises over the course of several years, resulting from the accumulation and selection of succesive genetic and epigenetic changes that lead to the gain of function of oncogenes and to the loss of function of tumor suppressor genes that gives the cells the ability to proliferate independently of inhibiting signals and spread to distant organs.

The genetic changes that contribute to cancer tend to affect three main types of genes: oncogenes, tumor suppressor genes, and DNA repair genes. These changes are called "drivers" of cancer (37).

- Oncogenes are involved in normal cell growth and division. However, when these genes are altered in certain ways or are more active than normal, they may become cancer-causing genes, allowing cells to grow and survive when they should not.
- Tumor suppressor genes are also involved in controlling cell growth and division. Cells with certain alterations in tumor suppressor genes may divide in an uncontrolled manner.
- DNA repair genes are involved in fixing damaged DNA. Cells with mutations in these genes tend to develop additional mutations in other genes. Together, these mutations may cause the cells to become cancerous.

6. Gastric Cancer

6.1 Incidence

Gastric cancer (GC) accounts for a considerable amount of morbidity and mortality worldwide (38). According to GLOBOCAN (2012), 951,000 new cases of gastric cancer were estimated to have occurred in 2012 (6.8% of the total types of cancer), making it the fifth most common cancer malignancy in the world, after lung, breast, colon and prostate cancer. More than 70% of cases (677,000 cases) occur in developing countries (456,000 in men, and 221,000 in women) and half the world total occurs in Eastern Asia (mainly in China). Gastric cancer is the third leading cause of cancer death in both sexes worldwide (723,000 deaths, 8.8% of the total) (38). Stomach cancer rates are generally about twice as high in men as in women and vary widely across countries. In general, incidence rates are highest in Eastern Asia (particularly in Korea, Mongolia, Japan, and China) (**Figure 6**), Central and Eastern Europe, and South America and lowest in Northern America and most parts of Africa (39).

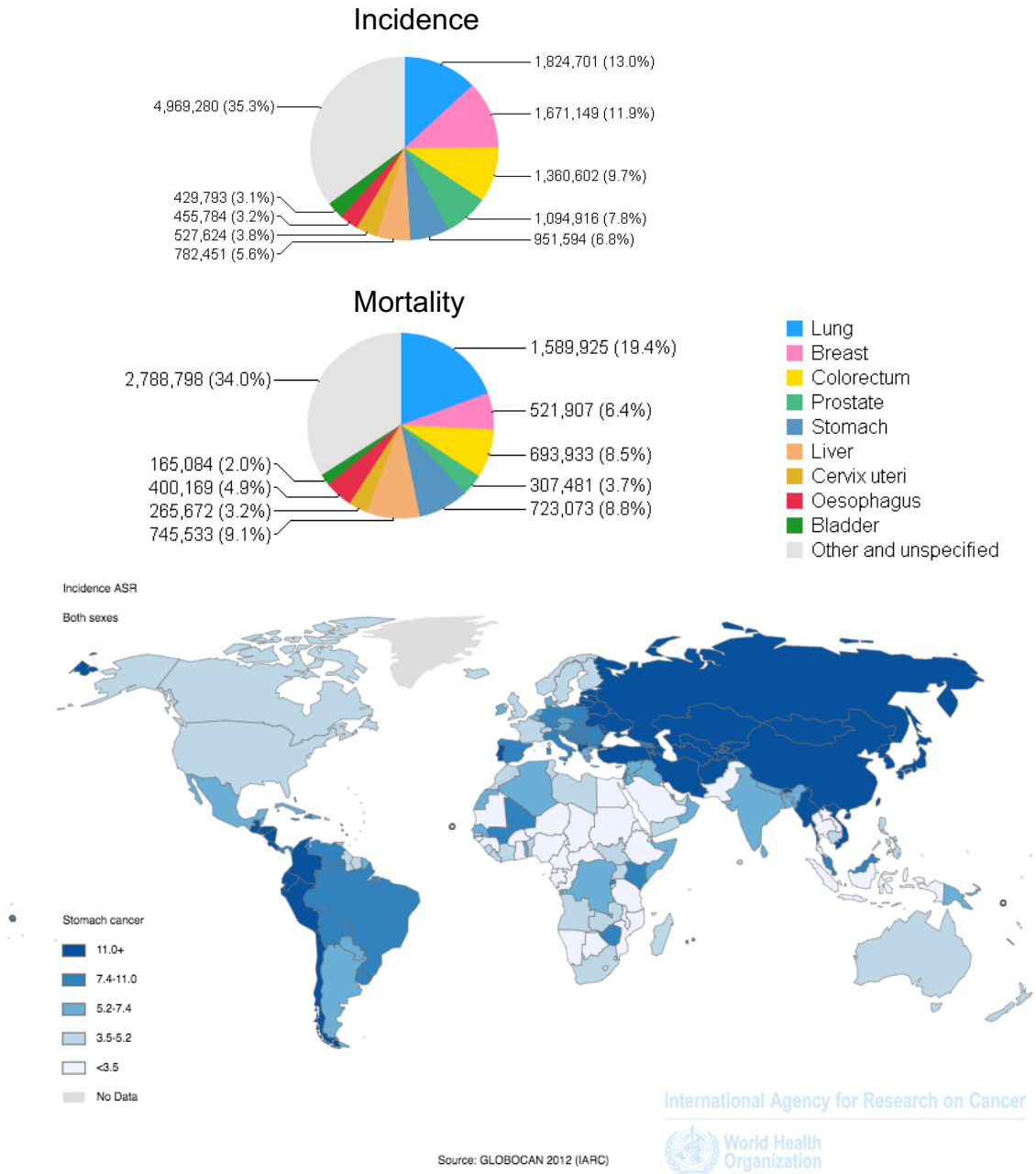

Figure 6. **The incidence and mortality of Gastric Cancer worldwide in 2012.**
Source: GLOBOCAN 2012 (IARC)

6.2 Overview

Stomach cancer is hard to detect at early stages because of the vague signs and symptoms that the patient is experiencing. Stomach cancer is most frequently diagnosed among people aged 65-74 and the age factor affects even more the cure of the patient (40). The growth of the cancer

cells usually lies in the lining of the stomach or the mucosa and can spread to nearby tissues and organs and can have different symptoms and treatments. The diagnosis of stomach cancer can be difficult at early stages, but treatment may vary according to type and stages of cancer. Apparent tumor heterogeneity exists not only between sexes but also regarding the spatial-temporal distribution of the tumor. The tumor-node-metastasis (TNM) staging system initially devised by Pierre Denoix between 1943 and 1952 bases its classification on the presence of metastasis to classify the progression of cancer. This system provides 3 key pieces of information: “T” describes how far the main (primary) tumor has grown into the wall of the stomach and whether it has grown into nearby areas; “N” describes the extent of spread to regional lymph nodes; “M” indicates whether the cancer has spread (metastasized) to other organs of the body. The numbers appearing after this letter (from 0 to 4) serve to indicate increasing severity (**Table 1**). Accurate preoperative staging of gastric cancer is important for treatment planning and prognosis prediction. Due to the development of less invasive treatment options, gastric cancer should be preoperatively staged with accuracy.

Despite considerable advances in GC treatment and decreasing trends in incidence and mortality rates, many patients still die due to cancer progression, recurrence and metastasis (41). Due to a lack of effective screening methods, more than 50% of patients are in advanced stages at initial diagnosis, at which time most of these patients do not have the opportunity for radical surgery and are reluctant to undergo treatment with adjuvant therapy (41). The response rate (RR) of patients with advanced GC (AGC) to first line chemotherapy is only 50%, and the median overall survival (OS) is less than 12 months (42, 43). Furthermore, the OS of patients after second-line therapy is only around 6 months (44).

Table 1. **TNM classification system, survival and treatment for gastric cancer staging**

TNM 2002 and AJCC Stage grouping for Gastric Cancer				5-year survival	Common treatment
Stages	**T**	**N**	**M**		
Stage 0	Tis	N0	M0		
Stage I A	T1	N0	M0	>85%	Surgery plus adjuvant chemotherapy
	T1	N1	M0		
Stage I B	T2a/b	N0	M0		
	T1	N2	M0		
Stage II	T2a/b	N1	M0	>60%	Surgery plus adjuvant chemotherapy
	T3	N0	M0		
	T2a/b	N2	M0		
Stage III A	T3	N1	M0	≤54%	Surgery plus adjuvant chemotherapy
	T4	N0	M0	~60% relapse	
Stage III B	T3	N2	M0		
	T4	N1-3	M0		
Stage IV	T1-3	N3	M0	<35%	
	Any T	Any N	M1		

AJCC= American Joint Committee on Cancer
TNM= tumor-node-metastasis staging

Once the TNM categories of a GC patient have been determined, generally after surgery, this information is combined in a process called stage grouping. The stage is expressed in Roman numerals from stage I (the least advanced) to stage IV (the most advanced). Stage I and II tumors are curable by surgical excision. The 5-year survival rates by stage for stomach cancer treated with surgery come from the National Cancer Data Base (NCDB) and were published in 2017 in the 8th edition of the AJCC Staging Manual (**Table 1**) (45). Careful tumor staging is essential to ensure that patients are appropriately selected for treatment interventions (**Figure 7**).

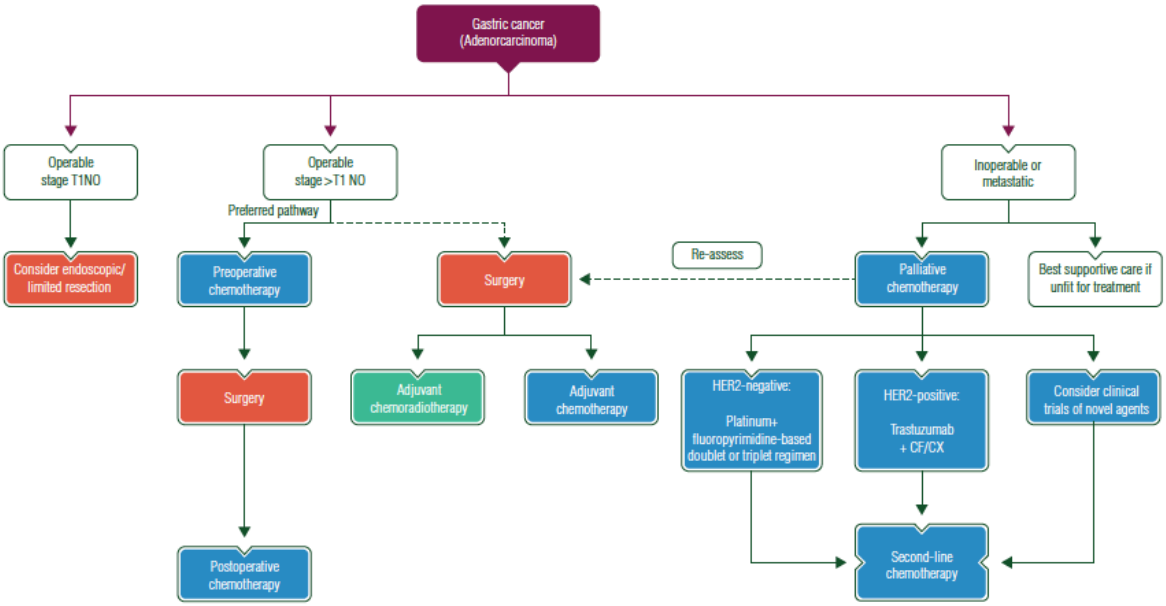

Figure 7. **Gastric Cancer treatment algorithm.**

Once a pacient is diagnosed with gastric cancer, treatment options will be definied by the stanging (TNM) and a multidisciplinary treatment planning before any treatment strategy is mandatory. HER2, human epidermal growth factor receptor 2; CF, cisplatin and 5-fluorouracil; CX, cisplatin and capecitabine. Source: Smyth, EC. *et al.* (46)

6.3 Current treatment landscape for Gastric Cancer

Despite major advances in the understanding of the biology of GC, the median survival rate of patients with advanced GC is still less than 12 months, and the development of personalized treatment strategies is the principal challenge (47). First, appropiated tumor staging is essential to ensure that patients are correctly selected for treatment interventions (**Table 1**). Once a pacient is diagnosed with GC, treatment options will be definied by the stanging and a multidisciplinary treatment planning before any treatment strategy is mandatory (**Figure 7**) (46). For example, surgical strategies as follows, endoscopic resection is appropriate for selected early tumors. Radical gastrectomy plus peritoneal washings for malignant cells are recommended in all stage IB–III gastric cancers that are considered potentially resectable, to exclude radiologically occult metastatic disease and perioperative therapy is also indicated for these patients (46). Endoscopic resection may be carried out for very early gastric cancers (T1a) if they are clearly alocated to the mucosa, well-differentiated, ≤2 cm and non-ulcerated. Perioperative (pre- and postoperative) chemotherapy with a platinum and fluoropyrimidine combination is recommended for patients with ≥stage IB resectable cancer. Capecitabine-

containing regimens can also be suggested in the perioperative setting (46). Adjuvant treatment is recommended for patients with ≥stage IB gastric cancer who have undergone surgery without administration of preoperative chemotherapy, postoperative chemoradiotherapy or adjuvant chemotherapy with the use of 5-fluorouracil (5-FU)/leucovorin plus conventionally fractionated radiotherapy (46).

Chemotherapy is the standard first-line treatment for patients with advanced GC and a good performance status (**Figure 7**). Radiotherapy plus infusional 5-fluorouracil (5-FU) remains to be the backbone of most combination adjuvant chemotherapy regimens in GC, as well as in neoadjuvant therapy to minimize tumor size before resecction. Doublet or triplet platinum/fluoropyrimidine combinations are recommended for fit patients with advanced gastric cancer (46). Second-line chemotherapy with a taxane (docetaxel, paclitaxel), or irinotecan, or ramucirumab as a single agent or in combination with paclitaxel is recommended for patients who are of performance status (PS) 0–1. In patients with symptomatic locally advanced or recurrent disease, hypofractionated radiotherapy is an effective and well-tolerated treatment modality that may palliate bleeding, obstructive symptoms or pain (46).

Available data from randomized clinical trials clearly demonstrate a statistically significant advantage of palliative chemotherapy, compared with best supportive care (BSC), in terms of palliation of symptoms and improvement of survival for patients with advanced GC (47). In general, resection of the primary tumor is not recommended in the palliative setting; but, some of the patients with initially unresectable locally advanced disease may be consider operable following a good response to systemic therapy (46). Before any systemic treatment for GC is initiated, the status of the human epidermal growth factor receptor 2 (HER2) is determined (**Figure 7**). **First-line treatment for HER2-positive GC:** Approximately 20% of GC is characterized by overexpression or/and amplification of the HER2 gene. Trastuzumab is recommended in conjunction with platinum and fluoropyrimidine-based chemotherapy for patients with HER2-positive advanced gastric cancer (46). Combining chemotherapy with trastuzumab results in a significant improvement of the survival in HER2-positive GC. In the international phase III “ToGA” trial, 594 previously untreated patients with advanced HER2-positive GC were randomized to chemotherapy (cisplatin, capecitabine, 5-FU) with or without trastuzumab, a humanized monoclonal antibody that binds to HER2-positive cells to inhibit their proliferation. Compared with chemotherapy alone, the combination of chemotherapy plus trastuzumab resulted in a statistically significant and clinically relevant improvement in response rate (RR) and overall survival (OS) (48). Up to now, this is the only prospective randomized phase III trial exploring trastuzumab in combination with chemotherapy in GC, although phase II

data with XELOX (combined chemotherapy of capecitabine and oxaliplatin) and in combination with an oral fluoropyrimidine S-1 (consists of tegafur, a prodrug of 5-FU combined with two 5-FU biochemical modulators, decreasing serious gastrointestinal toxicities) and cisplatin have shown interesting clinical activities (49, 50). There remains controversy regarding the utility of triplet regimens; however, a meta-analysis has demonstrated significant benefit from the addition of an anthracycline to a platinum and fluoropyrimidine doublet (51). Several other studies have examined the efficacy of docetaxel, fluoropyrimidine and oxaliplatin-containing regimens. The FLOT regimen (fluorouracil, leucovorin, oxaliplatin and docetaxel) resulted in a median progression-free survival (PFS) of 5.1 months and a median OS of 11 months in a small non-randomised study (52). As an alternative to platinum-based therapy, irinotecan plus leucovorin and infusional 5-FU (FOLFIRI) has been studied in both phase II trials and one phase III randomised trial in the first-line setting, and may be considered for selected patients (53, 54).

Second-line treatment for HER2-positive GC: Second-line chemotherapy with a taxane (docetaxel, paclitaxel), or irinotecan, or ramucirumab as single agent or in combination with paclitaxel is recommended for patients who are of performance status (PS) 0–1. In patients of adequate PS, second-line treatment is associated with proven improvements in OS and quality of life compared with best supportive care, with treatment options including irinotecan, docetaxel or paclitaxel, if not used before (55-58). Alternatively, in patients with disease progression >3 months following first-line chemotherapy, it may be appropriate to consider a rechallenge with the same drug combination as an additional treatment option (59).

Lapatinib is a small molecule tyrosine kinase inhibitors (TKI) that binds reversibly to epithelial growth factor receptor 1 (EGFR-1) and EGFR-2 (HER2) and blocks the activation of downstream second messengers. The phase III clinical trial, “TyTAN”, evaluated the efficacy of lapatinib in combination with paclitaxel in the second-line setting in Asian patients with HER2-positive advanced GC. A total of 261 HER2-positive patients were randomized to lapatinib plus chemotherapy *vs* chemotherapy alone (60). According to the results of this trial, the overall RR was significantly higher in patients treated with lapatinib, but the limited efficacy of lapatinib was confirmed in the first-line setting for GC in the phase III “LOGIC” trial, which investigated the activity of lapatinib in combination with capecitabine/oxaliplatin and demonstrated a non-significant prolongation of OS (61). Treatment options may be used sequentially in second and third line, but there is no clear evidence for a benefit beyond second line treatment.

Infusional 5-FU remains the backbone of most combination chemotherapy regimens in advanced GC. However, in recent years, two oral fluoropyrimidines (capecitabine and S-1) were shown to be at least equal in efficacy to 5-FU. Capecitabine was shown to be non-inferior in two

phase III trials. Treatment options for patients with **HER2-negative GC in first-line treatment** are tested in 316 patients in a randomized phase III trial comparing cisplatin plus capecitabine in a 21-day cycle to cisplatin plus 5-FU. The trial met its primary endpoint and demonstrated the non-inferiority of cisplatin plus capecitabine, compared with cisplatin plus 5-FU. Although patients receiving capecitabine had a better RR than those receiving 5-FU (41% vs 29%), progressive FS, RRs, and toxicity profiles were similar (43).

Although significant progress has been made in recent years by routinely treating patients with second- and further lines of chemotherapy, as well as integrating HER2-targeting drugs and drug combination in the routine care of patients with advanced GC, many phase III trials have had negative results, and others had to be closed prematurely due to unexpected toxicity, therefore treatment options needs further investigation (47).

Gastric cancers have been demonstrated to be highly molecularly diverse and may be driven by a number of different genetic and epigenetic abnormalities. Recently, four subtypes of gastric cancer have been described, these are the Epstein Barr Virus (EBV), microsatellite instability (MSI) high, genomically stable (GS) and chromosomal instability (CIN) subtypes (62), that will be disscused in further sections with more detail. Each subtype is enriched for selected molecular abnormalities, with some overlap. These findings have a significant impact on the therapeutic development strategies because it might guide the optimal course of treatment for different molecular tumor subtypes (**Table 2**).

Table 2. **Gastric Cancer Subtypes, molecular alterations and therapy**

GC Subtype	Molecular targets and alterations	Suggested therapeutics
EBV	PI3CA/AKT/mTOR	BYL719/ BKM120/ MK2206/ Everolimus
	PD-L1/2 overexpression	Immunotherapy
	ARID1A mutation	NA
MSI	DNA-mismatch repair deficiency	Immunotherapy/ PARP inh Not adjuvant chemotherapy
	HER3	MoAbs ERBB3
GS	CDH1 mutation	Prophylactic gastrectomy
	RHOA mutation	NA
	CLDN18-ARHGAP fusion	NA
CIN	TP53 mutation	NA
	SMAD4 mutation	NA
	APC mutation	NA
	EGFR overexpression	Cetuximab/ Panitumumab
	HER2 overexpression	Trastuzumab/ Pertuzumab/ TDM1
	EGFR/HER2 overexpression	Lapatinib
	MET overexpression	Crizotinib/ Rilotumumab/ Onartuzumab
	VEGF/VEGFR2 overexpression	Bevacizumab/ Ramucirumab
	VEGFR2/TIE2 overexpression	Regorafenib
	FGFR2 overexpression	ADZ 4547

NA: not available

6.4 Risk factors for Gastric Cancer

The etiology of GC is multifactorial and includes both dietary and nondietary factors. The major diet-related risk factors implicated in stomach cancer development include high content of nitrates and high salt intake (63). Other risk factors for gastric cancer include male gender (incidence is twice as high), *H. pylori* infection, age, tobacco, atrophic gastritis, partial gastrectomy and Ménétrier's disease (64). Most people diagnosed with stomach cancer are between their late 60s and 80s, during lifetime the cumulative effect of lesions by nitrates, salt, tobacco and others can increase the risk of cancer development and progession. Recent data also suggests that iron deficiency may be a GC risk factor, as iron depletion can accelerate the progression of carcinogenesis by augmenting *H. pylori* virulence (65). *Epstein-Barr virus* (EBV) infection is recognized as an etiological agent in 5%–10% of GCs (66). *H. pylori* is the most significant environmental risk factor for GC and is recognized as a class I carcinogen by the World Health Organization. Although more than 50% of the world population is infected with *H. pylori*, only 1%–2% of infected people will develop GC in their lifetime (67). Studies have reported that smokers have higher hazard ratios (HR) of GC in the cardia (HR, 2.86–4.10) compared to distal portions of the stomach (HR, 1.52–1.94) (68). Carcinogens in tobacco smoke, notably nitrosamines and other nitroso compounds, may exert mutagenic effects, thereby increasing GC risk (69). Smoking also increases the risk for precancerous lesions such as intestinal metaplasia and displasia (70).

The development of gastric cancer is a complex, multistep process involving multiple genetic and epigenetic alterations of oncogenes, tumor suppressor genes, DNA repair genes, cell cycle regulators, and signaling molecules (**Figure 8**) (63, 71). Adenocarcinoma is the major histological type of GC, with 90-95% of all gastric malignancies. Clinically, symptoms of gastric cancer tend to emerge late in the development of the disease and in elderly patients, stomach cancer is most frequently diagnosed among people aged 65-74 [26.3% of new cases, (72)] and thus treatment options are often limited (39). For instance, surgery and chemotherapy have low impact in advanced disease and there are very few molecular markers for targeted therapy. The 5-year survival for GC is around 30% and intense research is currently ongoing to improve our understanding the pathogenesis of the disease at the molecular level. This should in turn allow the identification of novel biomarkers to improve diagnosis and treatment of GC. Potential therapeutic targets will also be identified as a result of better understanding of the GC pathogenesis (71).

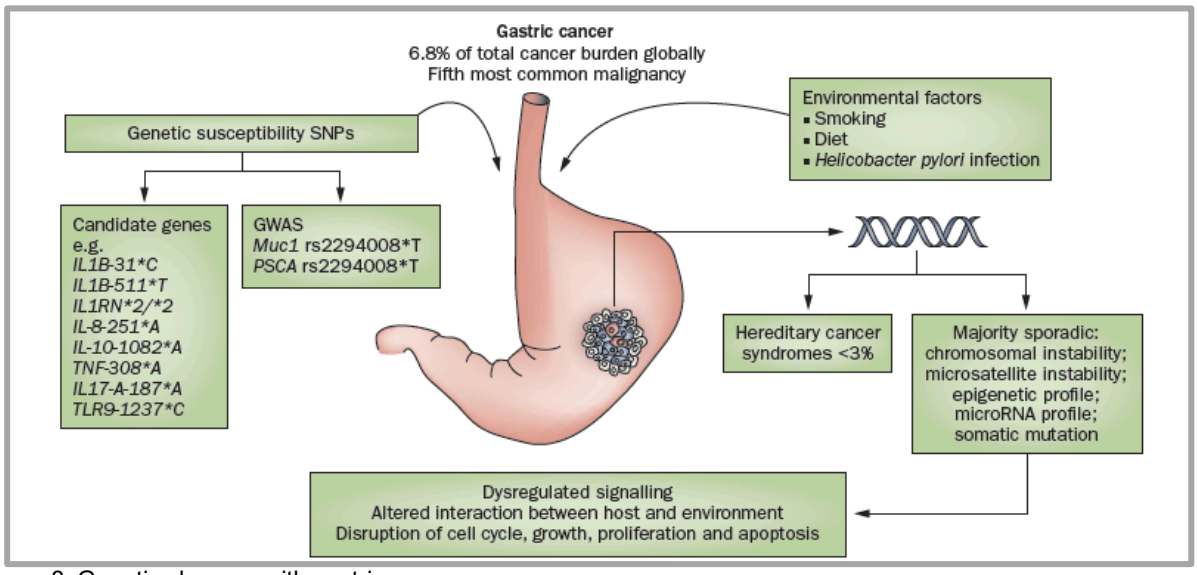

Figure 8. Genetic changes with gastric cancer.

Gastric cancer is the fifth most common malignancy worldwide. The pathogenesis of gastric cancer involves both environmental factors and genetic susceptibility. An inherited component contributes to <3% of gastric cancers. The vast majority of genetic changes associated with gastric cancer are acquired. Gastric cancer is a multifactorial and heterogeneous desease and represents a wide spectrum of several key genetic influences, includding chromosomal instability, microsatellite instability, changes in epigenetic profile including microRNA profile, somatic gene mutations or functional SNPs. Abbreviations: GWAS, genome-wide association study; SNP, single nucleotide polymorphism. Source: McLean MH et al. 2014. (71)

7. Pathology of Gastric Cancer

Gastric cancer is morphologically, biologically, and genetically heterogeneous. Most GCs are adenocarcinomas, with lymphoma, sarcomas, and carcinoids comprising <5%. Traditionally, gastric cancer is divided into two main subtypes on the basis of Lauren's classification, namely intestinal and diffuse (73). These subtypes have different molecular profiles, and their development pathways are distinct. For example, the well-differentiated intestinal type (IGC), which contains cohesive neoplastic cells, forms gland-like tubular structures that frequently ulcerate and generally arises from a premalignant gastric change. Sequential histopathological changes take place in the gastric mucosa including atrophic gastritis with loss of parietal cell mass, intestinal metaplasia (IM), and dysplasia that eventually lead to carcinoma (**Figure 9**) (74). In contrast, diffuse gastric cancer (DGC) does not seem to arise from this step-wise neoplastic progression, arising instead from normal gastric mucosa with no definitive premalignant stage. Diffuse gastric cancer is associated with pathological characteristics such as loss of cell cohesion often due the loss of E-Cadherin, or signet ring cells, and is often

associated with a negative *H. pylori* status (75, 76). DGC is more common in young patients, in whom there is a female preponderance (77), and behaves more aggressively than the intestinal type (78-81). DGC represents a subtype with poor prognosis, as a result, it has gained substantial public attention worldwide. Besides the Lauren classification, other histopathological classifications for GC have been proposed. For example, the World Health Organization classification groups GC into 4 main types based on the predominant histological pattern: tubular, papillary, mucinous and signet ring cell (82).

7.1 Gastric Premalignancy and Inflammation

Intestinal metaplasia (IM) is characterized by transformation of the gastric mucosa into an intestinal-like phenotype, replete with goblet cells and intestinal mucins. IM, associated with overexpression of the homeobox transcription factor CDX2 (83), is currently classified into three subtypes: intestinal type, gastric type, and mixed gastric-intestinal type. The latter, also known as incomplete IM, is considered to confer the highest risk for GC development. Injury to the gastric mucosa has also been observed to cause metaplastic changes with spasmolytic peptide expression. This phenomena, termed spasmolytic peptide expressing metaplasia (SPEM) or trefoil factor family 2 (TFF2) expressing metaplasia, is induced after *H. pylori* infection and chronic gastritis (84). SPEM has also been implicated as a precursor event in GC progression (85).

In most patients, the certain diagnosis of GC is often preceded by even years of chronic gastric mucosal inflammation (**Figure 9**). Chronic inflammation activates the NF-κB transcription factor, a key mediator of tumor promotion (86). Chronic inflammation also causes increased oxidative stress, due to reactive oxygen species (ROS) and nitrosamines generated by leukocytes and macrophages, which can damage proliferating cells. Moreover, the production of chemokines and cytokines may induce not only leukocyte migration but also promotes carcinogenesis.

Gastric cancer has been clearly associated with chronic inflammation (87). The expression of Cyclooxygenase-2 (COX-2), a rate-limiting enzyme for prostaglandin biosynthesis, is induced during inflammation and triggers the induction of proinflammatory prostaglandin PGE (88). The COX-2/PGE pathway plays a key role in gastric tumorigenesis (89). Transgenic mice expressing COX-2 and mPGES-1 in gastric epithelial cells develop hyperplastic lesions in the stomach (90).

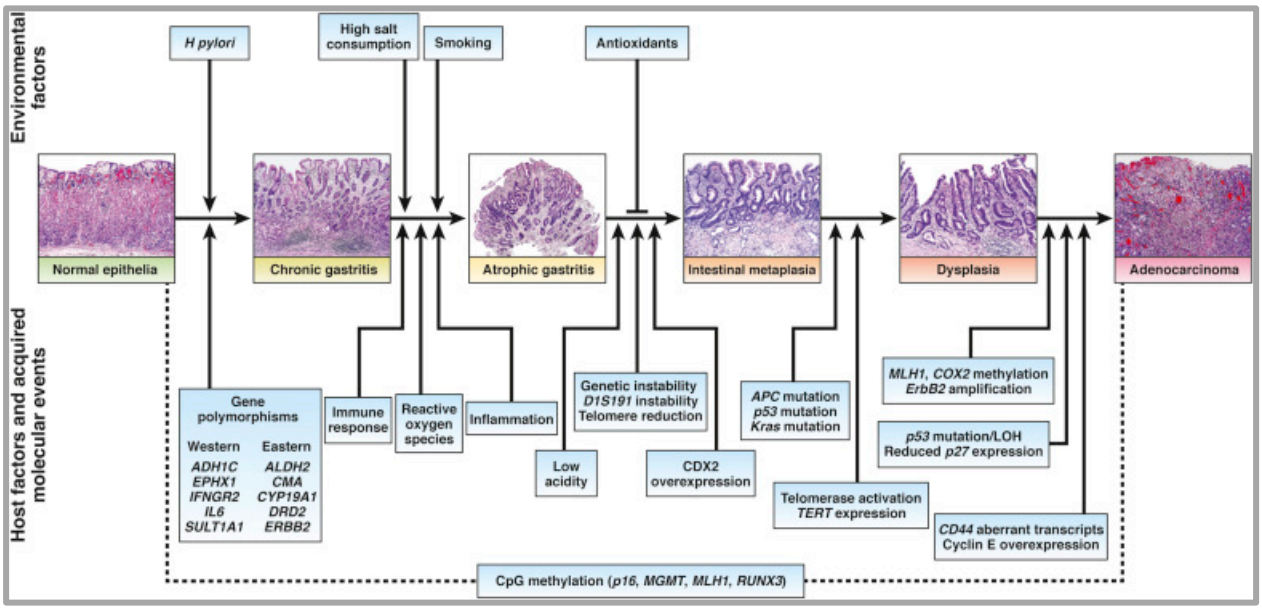

Figure 9. Cause and pathogenesis of intestinal type gastric cancer.

Sequencial stages of intestinal type GC development is shown, important host and environmental factors as well as acquired molecular events are shown. Source: Tan and Yeoh, 2015. (91)

8. Models of cancer initiation and progression

In order for a cell to become cancerous it needs to acquire a series of cellular alterations: self-sufficiency in growth signals, insensitivity to growth-inhibitory signals, evasion of programmed cell death, limitless replicative potential, sustained angiogenesis, and tissue invasion and metastasis (37). Observations of human cancers and animal models argue that tumor development proceeds via a process where each successive genetic change confers one or another type of growth advantage to the cells of the tumor. This genetic evolution of the cancer cell will cause the tumor to progress through different stages. Two fundamental questions about tumor development process has emerged: 1) which cell acquires the genetic alterations and becomes the first tumor cell? and 2) which cells are responsible for propagating the tumor after its initiation? Two models have been suggested to explain the tumor progression, the stochastic model where all cells have an equal probability to propagate the tumor and the Cancer Stem Cell (CSC) model or hierarchical model where a unique population of CSC has the potential to propagate the tumor (9).

Both the stochastic and hierarchical models are reasonable hypothesis that have been proposed to describe tumor heterogeneity, but alone, each model is insufficient to explain the diversity within tumors. In light of growing controversy, Kreso and Dick (92) proposed that the two models could be integrated into a more comprehensive explanation. By combining genetic analysis with

functional assays of tumor initiating cells (T-ICs), it was found that T-ICs also contain genetic subclones, which influence their properties (93, 94); that is, T-ICs can also evolve. Hence, it is reasonable to imagine that an early-stage tumor containing rare CSCs and other cells becomes more heterogeneous and invasive as advantageous mutations accumulate and that as the CSCs develop into several subclones, they achieve a higher capacity for self-renewal and thus form a greater proportion of the total cells (**Figure 10**). Collectively, to elucidate a unified model that is dynamically regulated by other determinants such as epigenetics (95, 96), gene expression stochasticity (97-99), the CSC niche (100), and the tumor microenvironment (TME) (101) may provide an overall explanation for complexity of the biological characteristics of the tumor, in addition may contribute for the development of new therapy strategies for GC.

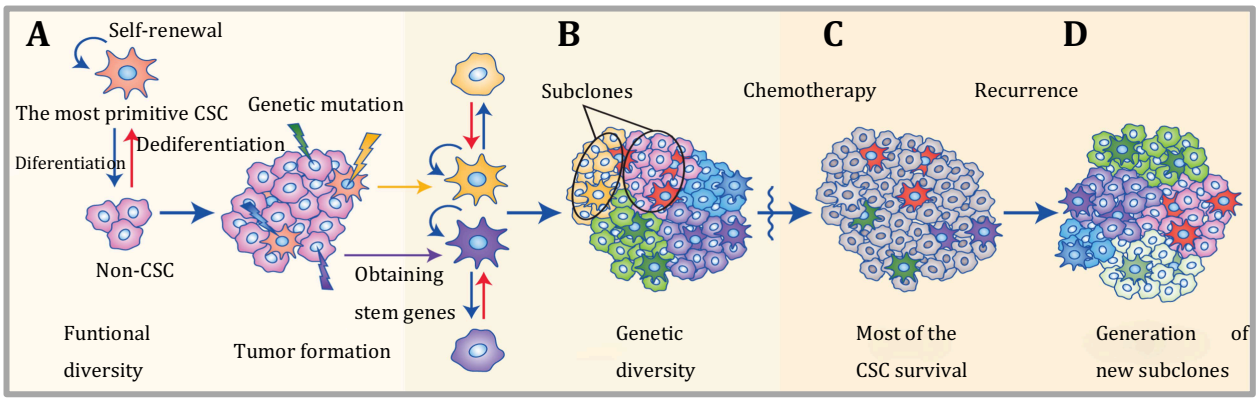

Figure 10. **The unified model of cancer.**

A) The most primitive CSCs are continuously undergoing on division, self-renewing, differentiation into non-CSCs and eventually form a tumor with functional diversity, during the course of which the cancer cells randomly develop genetic mutations that can create non-CSCs with stemness. B) The tumor becomes more heterogeneous and invasive as advantageous mutations in the CSCs accumulate; moreover, several subclones develop, and the tumor cells confer a higher capacity for self-renewal and begin to establish a greater proportion of the total cells. C) Most of the CSCs are drug-resistant and survive after chemotherapy or radiotherapy. D) The resistant CSCs cause tumor relapse, and more subclones are generated. Source: Adapted from Song, Y. *et al.* 2017 (41).

8.1 Origin of Gastric Cancer Stem Cell

The unified model of carcinogenesis depicts the tumor cells as a combination of several subpopulations of CSCs and highly homogeneous non-CSCs, these subclones could be produced by the mutation of a single CSC. Derived from this, two questions needs to be

considered: What is the precursor of CSCs? and how does a normal cell obtain the ability to infinitely self-renew? New data suggests that GSCs have heterogeneous phenotypes because they originate from multiple cell types, like gastric stem cells (GSCs), glandular cells and bone marrow-derived cells (**Figure 11A**). The unified model of carcinogenesis gives a rationale explanation for how primitive GCSCs continually optimize themselves to adapt to the ever-changing tumor microenvironment (**Figure 11B**). Regarding the mechanism of regulation of the unified model, the CSC niche is the key place for maintenance of CSC properties and plasticity, because the microenvironment is optimal to regulate stem cell fate (**Figure 11C**) (102).

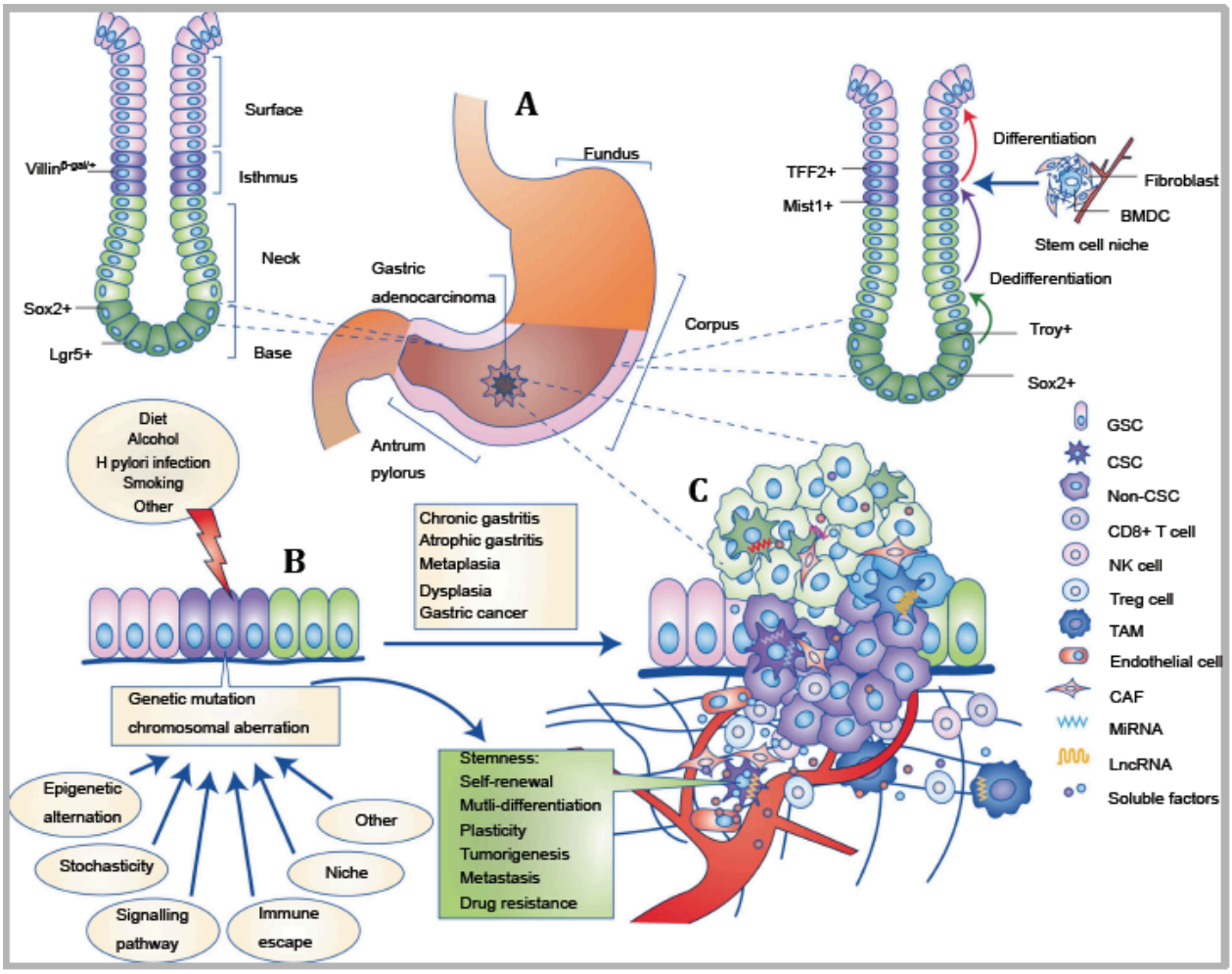

Figure 11. The combination of the hierarchical and stochastic models of GC.

A) GC stem cells originate from gastric stem cells, dedifferentiated epithelial cells or bone marrow-derived cells. B) The accumulation of cancer-associated mutations and chromosomal aberrations in the initiating cells, induced by multiple factors, such as diet, alcohol, *H. pylori* infection and smoking, promotes the pathological process of gastric adenocarcinoma, in which the gastric epithelium develops through sequential stages of chronic gastritis, atrophic

gastritis, metaplasia, dysplasia and cancer. C) The formation, invasion and metastasis of GC develops according to the unified model, dynamically regulated by other determinants such as epigenetic alternation, gene expression stochasticity, immune escape, niche, signalling pathways and networks of soluble factors. CAF: cancer-associated fibroblast. Source: Song, Y. *et al.* 2017 (41).

The mechanism of carcinogenesis is different and it depends on GSCs phenotypes, this unified model holds that a mutated GSC expands to the whole gland and forms a clonal patch by unit fission, which has been demonstrated by the detection of mitochondrial DNA mutations in normal and intestinal metaplastic mucosa adjacent to the tumor tissue of GC patients (30). With the identification of GSC-specific markers like *Villin*$^{\beta\text{-}gal/+}$, several driver mutations in the malignant progression of GSCs were verified by functional analysis in transgenic mouse models. The promoter specificity of *Villin* in adult tissues has led to the use of *Cre* recombinase-expressing transgenic mouse models (103). For example, the inactivation of the tumor suppressor gene *Krüppel-like factor 4* (*Klf4*) in *Villin*$^{+}$ gastric stem-like cells accelerated the malignant transformation of gastric mucosa in the carcinogen-induced *Villin-Cre*$^{+}$;*Klf4*$^{fl/fl}$ mice (104), and in fact, we have used the same genetic modified model strategy to generate our won murine model to carry out the experiments that will be discussed in later sections. Lineage traicing studies have identified a rare subpopulation of murine gastric progenitors cells with robust *Villin* expression predominantly in the antrum (13). These rare *Villin*-expressing gastric progenitor cells (GPCs) are quiescent in the unstimulated stomach; however, they undergo both symmetric and asymmetric division and replace multiple pyloric glands during proinflammatory insults (13). *Villin* is an actin-bundling protein found in the apical brush border of absorptive tissue (105). *Villin* is also one of the first structural genes to be transcriptionally activated in the embryonic intestinal endoderm (103). The *Villin* gene is initially expressed in the intestinal hindgut endoderm 9 days post coitum during gut tube closure. Then, *Villin* expression rapidly extends throughout the small and large intestines and distal stomach, at 16 days post coitum, intestinal cells have their highest levels of *Villin* expression, whereas neighboring stomach cells have low levels of *Villin* expression (106).

Another transgenic mouse model includes the deletion of the *adenomatous polyposis coli* (*Apc*) gene, on the carcinogenesis of *Lgr5*$^{+}$ stem cells was evaluated in the *Lgr5*-CreERT2;*Apc*$^{fl/fl}$ mouse model and the results showed that β-catenin^{hi} adenomas only in the pylorus were rapidly formed by the expansion of *Lgr5*$^{+}$ transformed stem cells after the loss of *Apc* (15). Mutations in distinct pathway components in isthmus *Mist1*$^{+}$ stem cells of the corpus gland were responsible for the differentiation within intestinal and diffuse GC. Such effects have been observed for

mutations in the *Kras* gene, facilitating the metaplastic/dysplastic transformation and expansion of *Mist1*$^{+}$ isthmus cells; aberrant *Notch* activation, resulting in the development of IGC; and mutations in *E-cadherin* and *transformation-related protein 53* (*TRP53*), inducing the formation and invasion of DGC containing numerous lineage-traced signet-ring cells in the context of chronic inflammation (18). Collectively, it is presumed that GCSCs are likely derived from aberrant GSCs and that they express its genetic and functional properties depending on the primary site where they are.

8.2 Deregulation of Signaling Pathways in Gastric Cancer Stem cells

8.2.1 Hedgehog signaling

The evolutionarily conserved Hedgehog (Hh) pathway (**Figure 12A**) is essential for normal embryonic development and plays critical roles in adult tissue maintenance, renewal and regeneration. Secreted Hh proteins act in a concentration- and time-dependent manner to initiate a series of cellular responses that range from survival and proliferation to cell fate specification and differentiation. Proper levels of Hh signaling require the regulated production, processing, secretion and trafficking of Hh-ligands, in mammals are Sonic (Shh), Indian (Ihh) and Desert (Dhh).

In the adult stomach, strictly regulated cell adherens junctions are crucial in determining epithelial cell differentiation. Parietal cells in the stomach body express the Shh protein and mRNA (107, 108). Patched 1 (Ptch1), a receptor for hedgehog signaling, is expressed in gastric epithelial cells and mesenchymal cells (108, 109). According to this expression pattern, hedgehog signaling regulated the expression of its target genes FoxA2, Isl-1, and H^{+}/K^{+} - ATPase in parietal cells and BMP4 in mesenchymal cells (108). These findings suggest that hedgehog signaling in the stomach works in both autocrine and paracrine fashions (**Figure 15**). Ihh is expressed in the surface mucus cells and may contribute to the differentiation and maintenance of this lineage (21, 110). Shh expression correlated with fundic gland differentiation of the stomach (107). In mice lacking Shh in parietal cells, the phenotypes such as decreased mucus neck cells and chief cells were reversed by treatment with the somatostatin analog, suggesting the effects of hedgehog signaling are indirect (111). Finally, the inhibition of hedgehog signaling in Immortalized Mouse Gastric Epithelial cell line-5 (IMGE-5) caused loss of E-cadherin expression accompanied by the disruption of F-actin cortical expression and stability of tight junction protein zonula occludens-1 (ZO-1) (112).

After long-term inflammation, gastric epithelial cells are transformed into neoplastic cells. During the progression of gastritis, a frequent loss of Shh expression was observed and this disappearance is consistent with that observed in parietal cells (113). The loss of Shh may promote the transformational process of gastric epitelial cells because its main role in gastric stem cells is to induce gastric differentiation. Another study showed that hedgehog signaling is essential for the maintenance of cancer stem cell-like cells in gastric cancer (114). They found that the overexpression of hedgehog signaling in tumorsphere cells and interruption of hedgehog signaling by cyclopamine or 5E1 antibody reduced the self-renewing capacity. On the other hand, the activation of hedgehog signaling promoted the proliferation and survival of gastric cancer cells and was positively correlated with poorly differentiated and aggressive gastric cancer (109, 115, 116). Moreover, hedgehog signaling enhanced the metastasis of gastric cancer cells through the activation of TGF-β signaling (117). The roles of hedgehog signaling in cancer stem cells have been described in many cancers, including multiple myeloma, glioblastoma, colorectal, and pancreatic cancer (118).

8.2.2 Wnt signaling

The conserved Wnt/β-Catenin pathway (**Figure 12B**) regulates stem cell pluripotency and cell fate decisions during development. This developmental cascade integrates signals from other pathways, including retinoic acid, FGF, TGF-β, and BMP, within different cell types and tissues (**Figure 12**). In the adult stomach, the expressions of Wnt ligands and their receptors are poorly characterized, although the expression of Wnt signaling in gastric stem cells has been suggested by the transcriptomic analysis by using laser capture microdissected gastric stem cells (119). The specific activation of Wnt signalling pathway within the mouse adult gastric epithelium via deletion of either glycogen synthase kinase 3 (*GSK3*) or *Apc* or via expression of a constitutively active β-catenin protein have showed gastric epithelial cell dedifferentiation and adenoma formation (120). In Familial Adenomatous Polyposis (FAP) patietns, characterized by germline mutations in *Apc*, hyperplastic polyps were observed in the antrum of patients (121, 122).

Like in colorectal cancer, breast cancer, and myeloid leukemia, the Wnt signaling pathway has also been suggested to regulate self-renewal of gastric cancer stem like cells (123). Blocking of Wnt signaling by the Dickkopf homolog 1 (DKK1) protein caused a reduction in the self-renewing capacity of MKN45 tumorsphere cells. Moreover, nuclear localization of β-catenin, indicating activation of Wnt signaling, was found in approximately 30% of gastric cancers (124, 125).

Mutation or loss of heterozygosity in the *Apc* gene were found in 18% or 21% of gastric cancers, respectively (126).

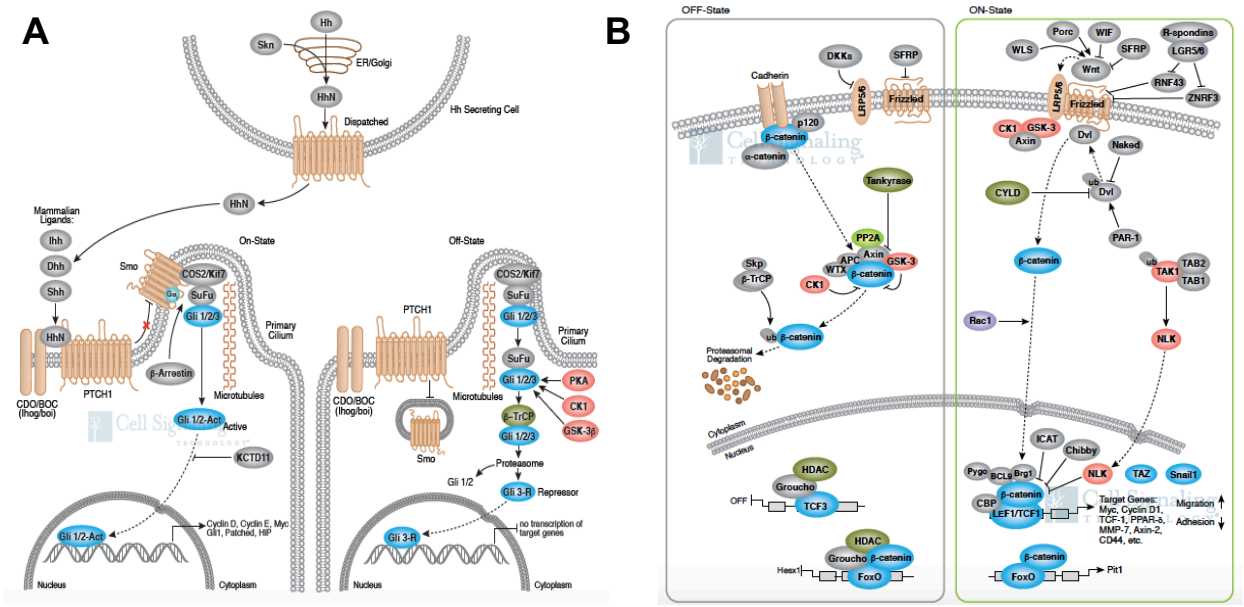

Figure 12. **Hedgehog ans Wnt signaling.**

A) The evolutionarily conserved Hedgehog (Hh) pathway is essential for normal embryonic development and plays critical roles in adult tissue maintenance, renewal and regeneration. Secreted Hh proteins act in a concentration- and time-dependent manner to initiate a series of cellular responses that range from survival and proliferation to cell fate specification and differentiation. B) The conserved Wnt/β-Catenin pathway regulates stem cell pluripotency and cell fate decisions during development. This developmental cascade integrates signals from other pathways, including retinoic acid, FGF, TGF-β, and BMP, within different cell types and tissues. Source: https://www.cellsignal.com

8.2.3 Notch signaling

Notch signaling is an evolutionarily conserved pathway in multicellular organisms that regulates cell-fate determination during development and maintains adult tissue homeostasis (**Figure 13A**). The Notch pathway mediates juxtacrine cellular signaling where in both the signal sending and receiving cells are affected through ligand-receptor crosstalk by which an array of cell fate decisions in epithelial, neuronal, cardiac, immune, and endocrine development are regulated.

Notch signaling is active in the mouse stomach epithelium during development and becomes restricted mainly to the isthmus in adult glands, similar to its known localization in the proliferative compartment of intestinal villi (127). Activation of Notch signaling in lineage-committed gastric epithelial cells is sufficient to induce dedifferentiation into stem and/or

multipotential progenitors that populate the mucosa with all major cell types. Prolonged Notch activation within dedifferentiated parietal cells eventually enhances cell proliferation and induces adenomas that show focal Wnt signaling (127). These data suggest that Notch signaling is critical for the maintenance of gastric stem cells. Another role of Notch signaling is the inhibition of enteroendocrine cell differentiation, possibly via neurogenin-3 regulation. In mice lacking of hairy and enhancer of split-1 (*Hes1*), a target gene of Notch signaling, the number of enteroendocrine cells was increased (128). Approximately 75% of primary gastric cancers expressed the Notch ligand Jag1, and its expression correlates with cancer aggressiveness and patient survival rate. Interestingly, Notch signaling promoted colony formation, migration, and invasion of gastric cancer cells partially through COX-2 (129).

8.2.4 EGF signaling

Epidermal growth factor (EGF) signaling is mediated by a typical receptor tyrosine kinase pathway (**Figure 13B**). The EGF receptors signal through Akt, MAPK, and additional pathways to regulate cell proliferation, migration, differentiation, apoptosis, and cell motility. Seven vertebrate EGF ligands are synthesized as type 1 transmembrane protein, and soluble ligands are released after proteolytic cleavage by membrane protease (130). Four kinds of EGF receptors (ErbB1, ErbB2, ErbB3, and ErbB4) have been previously described (130). EGF-ErbB family members and some of their ligands are often overexpressed, amplified, or mutated in many forms of cancer, making them important therapeutic targets. Parietal cells secrete several kinds of EGFs, including HB-EGF, amphiregulin, and transforming growth factor-alpha (TGF-α) (131). Surface epithelial cells and enteroendocrine cells also secrete TGF-α (132). Studies using TGF-α-transgenic mice, where foveolar hyperplasia occurs at the expense of parietal and chief cells, have suggested roles of EGF signaling in gastric progenitor cell differentiation (22) (**Figure 15**). Although the roles were not examined in gastric cancer stem cells, abnormal activation of EGF signaling has been reported, where amplification of ErbB2 was observed in up to 27% of gastric cancers (133). Other study showed that EGF receptor overexpression is associated with poor prognosis in gastric cancer (134, 135).

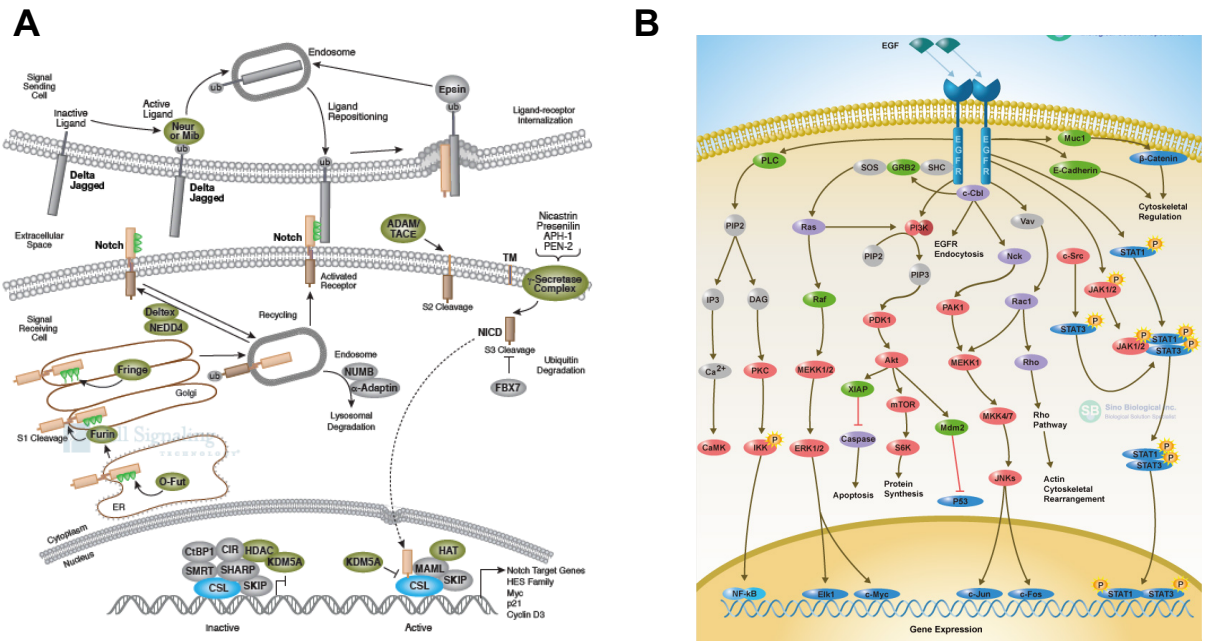

Figure 13. **Notch and EGF signaling.**

A) Notch signaling is an evolutionarily conserved pathway in multicellular organisms that regulates cell-fate determination during development and maintains adult tissue homeostasis. B) The epidermal growth factor receptor (EGFR; ErbB-1; HER1 in humans) is a transmembrane protein that is a receptor for members of the epidermal growth factor family (EGF family) of extracellular protein ligands. Deficient signaling of the EGFR and other receptor tyrosine kinases in humans is associated with diseases such as Alzheimer's, while over-expression is associated with the development of a wide variety of tumors. Source: www.cellsignal.com and www.sinobiological.com

8.2.5 TGF-β and BMP signaling

In the early stages of cancer, TGF-β signaling (**Figure 14A**) acts as a tumor suppressor by inhibiting cellular proliferation or by promoting cellular differentiation and apoptosis. However, in the later stages, TGF-β signaling enhances cancer cells invasion and metastasis (136, 137). Runx3, a target gene of TGF-β signaling, can suppress the progression of gastric cancer by inducing claudin-1 (138).

Bone Morphogenetic Proteins (BMPs) are a large subclass (more than 20 members) of the Transforming Growth Factor-beta (TGF-β) super family that is active in many tissues under normal physiologic conditions, and are regulated through reversible interactions with extracellular antagonists, including noggin, chordin, follistatin and gremlin. These interactions determine the bioavailability of different BMPs for binding to their cognate receptors and activation of downstream responses. Receptors and ligands of BMP signaling are expressed in both epithelial and mesenchymal cells of the stomach (107, 108). It has been shown that

depletion of BMPR1A from the endoderm during the early developmental period, results in reduced number of parietal cells, whereas the number of enteroendocrine cells is increased, suggesting BMP signaling regulates proliferation and commitment of enteroendocrine precursor cells (139). Other study showed that Noggin overexpression in parietal cells, decreased the number of parietal cells and increased the number of Tff2-expressing cells (27). These data suggest that BMP signaling is required for parietal cell differentiation (**Figure 15**). BMP signaling in the stomach is upregulated during inflammation and downregulated during cancer progression (124, 140). In gastric cancer tissues, the expression of BMP2 was epigenetically down-regulated (141). Moreover, BMP2 and BMP4 play tumor suppressive roles in human diffuse type gastric carcinoma (142).

8.2.6 Nuclear factor κ-light-chain-enhancer of activated B cells (NF-κB) signaling

NF-κB refers to a family of bipartite transcription factors whose members include NF-κB1, NF-κB2, c-Rel, RelA, and RelB (**Figure 14B**). The most common form in mammalian cells is the RelA/NFκ-B1 dimer. This transcription factor is normally bound by its inhibitor IκB and thereby restricted to the cytoplasm. However, upon activation by cellular stress, such as pro-inflammatory cytokines and bacterial components, IκB is phosphorylated by an IκB kinase complex and subject to proteasomal degradation, resulting in activation of NF-κB (143). In gastric cancer, NF-κB potentiates inflammation in response to *H. pylori* infection. Some studies have shown that *H. pylori* induces expression of the pro-inflammatory cytokine interleukin (IL)-8 through activation of NF-κB (124). Moreover, NF-κB amplifies the inflammatory signals of other cytokines, such as tumor necrosis factor α (TNF-α) and interferon gamma (IFN-γ) (144). Importantly, NF-κB is constitutively activated in gastric cancer (145). There is an extensive evidence related to the abnormal NF-κB activation that results in the deregulation of proliferation (145), evasion of apoptosis (145-147), genomic instability (148), increased rate of glycolysis (149) and drug resistance (150) in gastric cancer cells. NF-κB activity in self-renewal of cancer stem cells have been reported in breast cancer (151), prostate cancer (152), and glioblastoma (153).

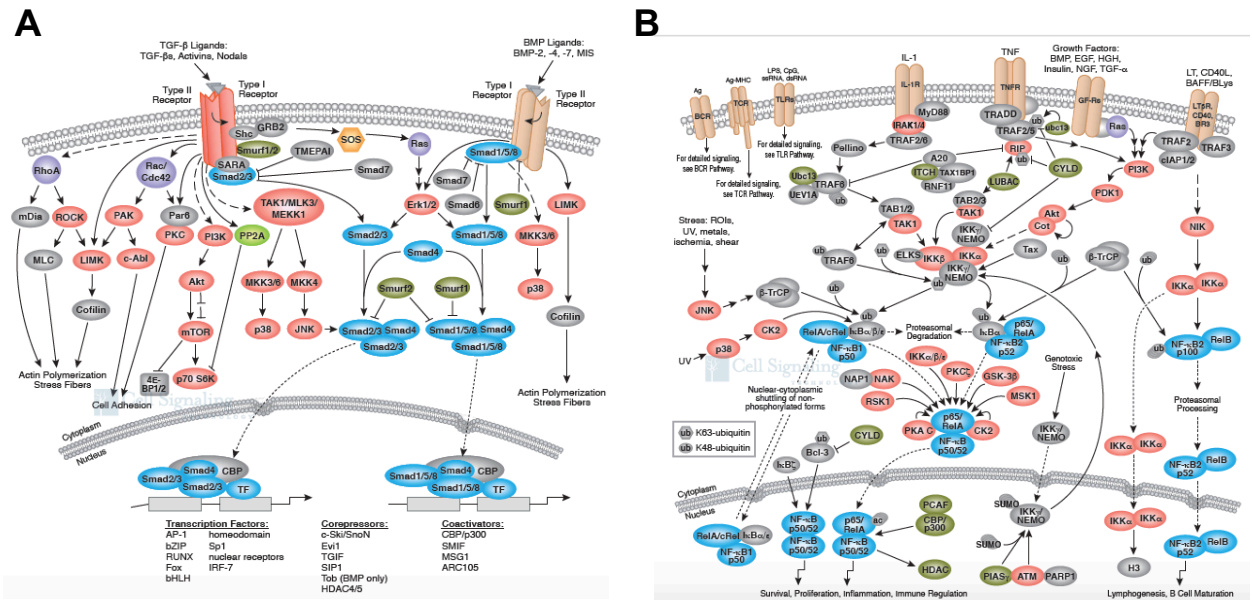

Figure 14. **TGF-β/BMP and NF-κB signaling.**

A) Transforming growth factor-β (TGF-β) superfamily signaling plays a critical role in the regulation of cell growth, differentiation, and development in a wide range of biological systems. In general, signaling is initiated with ligand-induced oligomerization of serine/threonine receptor kinases and phosphorylation of the cytoplasmic signaling molecules Smad2 and Smad3 for the TGF-β/activin pathway, or Smad1/5/9 for the bone morphogenetic protein (BMP) pathway. B) Nuclear factor-κB (NF-κB)/Rel proteins include NF-κB2 p52/p100, NF-κB1 p50/p105, c-Rel, RelA/p65, and RelB. These proteins function as dimeric transcription factors that regulate the expression of genes influencing a broad range of biological processes including innate and adaptive immunity, inflammation, stress responses, B-cell development, and lymphoid organogenesis. Source: www.cellsignal.com

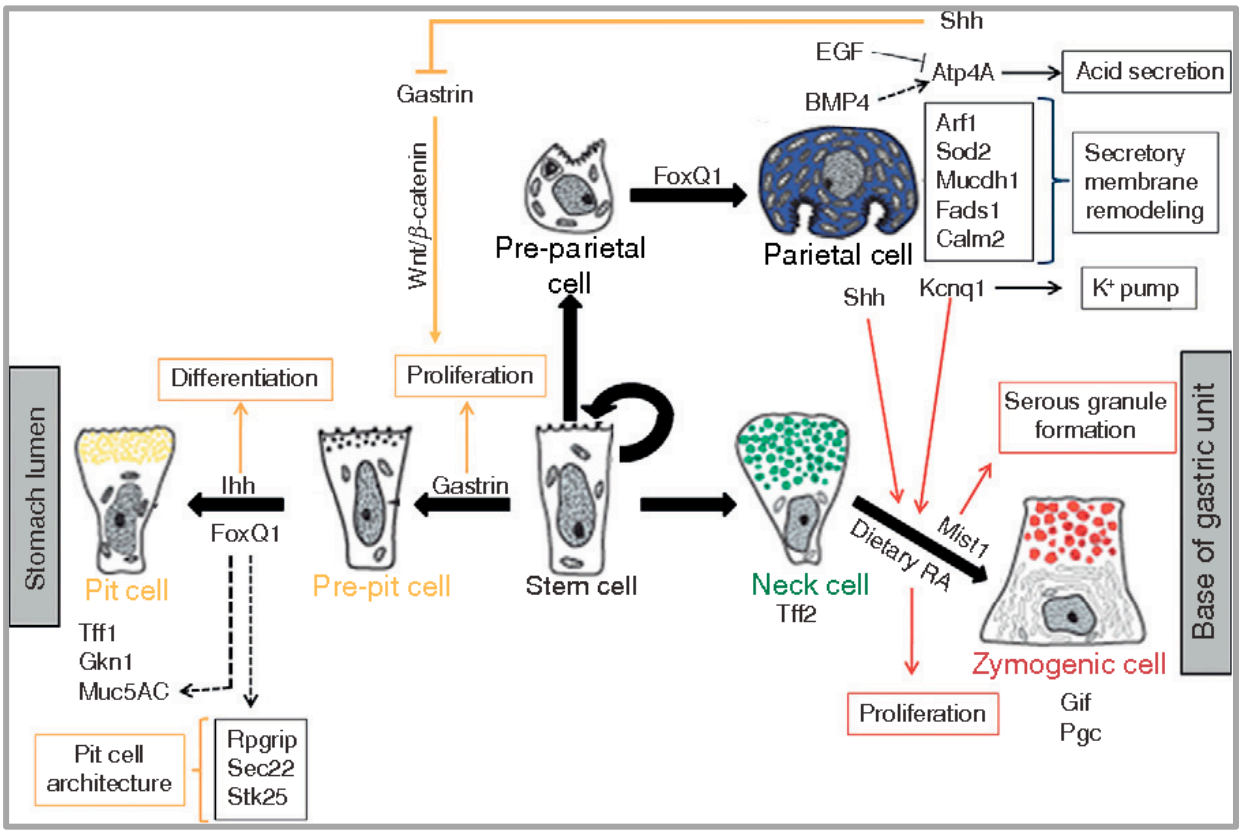

Figure 15. Interplay between developmental signaling pathways coordinating differentiation and maintenance of different cell lineages within the gastric unit.

The gastric epithelium is constantly renewing, which requires replenishment of the various differentiated cell types (each having a different life span) from multipotent stem cells. The schematic shows signaling intermediates involved in the maintenance of cell lineage homeostasis and physiology in the adult gastric gland. Sorce: Khurana and Mills, 2010 (12).

8.3 Heritable genetic factors

The development of gastric cancer is a complex, multistep process. An average of 4.18 genomic alterations has been suggested to be necessary for the development of gastric cancer (154). Hereditary GC syndromes are rare and demonstrates familial aggregation in <10% of cases, an inherited genetic predisposition is found in a small proportion of cases (<1%–3%). The most common herederitary syndromes predisposing to gastric cancer are hereditary diffuse gastric cancer (HDGC), gastric adenocarcinoma and proximal polyposis of the stomach (GAPPS), familial intestinal gastric cancer (FIGC) (155) and Peutz Jegher's sindrome (156, 157).

The hereditary diffuse gastric cancer (HDGC) is an autosomal dominant condition associated most frequently with a heterozygous germline mutation in *CDH1*, the gene that encodes cadherin 1 (also known as E-cadherin). Besides *CDH1*, other recently identified candidate HDGC genes include *CTNNA1*, *BRCA2* and *STK11* (158). Interestingly, a transgenic mouse model with Cre-loxP-controlled specific knock down of *CDH1* in gastric epitelial cells did not progress to gastric cancer, even though the mice had a reduction or absence of cadherin 1 protein and they had morphological changes in premalignant cells (159). This finding suggests that additional molecular mechanisms might be involved in the pathogenesis of this syndrome that are not currently fully understood. GAPPS, first reported in 2012, is characterized by autosomal dominant transmission of fundic gland polyposis (including dysplastic lesions or adenocarcinoma or both) restricted to the proximal stomach with no evidence of colorectal/duodenal polyposis or other hereditary gastrointestinal cancer syndromes (160), its genetic cause is as yet unknown. GC has also been associated with other hereditary cancer syndromes (155), for example Lynch syndrome (also known as hereditary nonpolyposis colorectal cancer syndrome) that is caused by mutations in one of the mismatch repair genes *MLH1, MSH2, MSH6, PMS1, PMS2, or EPCAM* (161), the familial adenomatous polyposis syndrome which is caused by *Apc* germline mutations and is characterized by the development of colonic and rectal adenomas and early development of colorectal cancer (162, 163), the Li-Fraumeni syndrome encompasses several tumor types that develop generally before 45 years of age because of inherited *TP53* mutations (164, 165) including early-onset gastric cancer, and the Juvenile polyposis syndrome an hereditary cancer syndrome characterised by numerous juvenile polyps developing in the colon or stomach, or both, and is caused by *SMAD4* or *BMPR1A* mutations (at similar frequencies) (166, 167).

8.4 Acquired genetic factors

Acquired genetic abnormalities can be the result of chromosomal insufficiency, microsatellite instability, changes in the epigenetic landscape or microRNA (miRNA) profile that profoundly affects downstream gene expression, somatic gene mutations or single nucleotide polymorphisms (SNPs) within key candidate genes. All of these mechanisms can lead to deregulated key signalling pathways (previously descibred in 8.2 section), altered interactions between the host and environment (such as in the response to intraluminal pathogens or dietary components), disruption of the cell cycle, growth proliferation or characteristics of cell death that promote the development of cancer (37). Gastric carcinoma is characterized by genomic

instability that could be either microsatellite instability (MSI) or chromosomal instability (CIN) (168) (**Figure 16**).

8.5 Molecular Subtypes of Gastric Cancer

Advances in technology, such as next-generation sequencing, have enabled the emergence of new molecular profiling in the context of gastric cancer and other solid tumors. Examples include exome-wide (DNA sequencing) and transcriptome-wide (RNA sequencing) analysis (169). The launch of large-scale consortia aimed to present openly available data from rigorous genomic profiling of a large number of internationally sourced cancer cases of different cancer types, constituted an important milestone in the field. Examples include the Cancer Genome Atlas in the USA (170), the Cancer Genome Project in the UK (171), and the International Cancer Genome Consortium (172). Gastric cancer is studied within these frameworks and data from these expansive molecular profiling efforts can be used by independent groups worldwide. The power of these global collective strategies has been highlighted in a publication presented by the Cancer Genome Atlas Research Network (173). They performed extensive molecular profiling of nearly 300 gastric cancer tissue samples using six discrete platforms with the aim of identifying novel molecular characterization of gastric cancer. They identified four defined subtypes: **1)** tumors positive for Epstein–Barr virus (EBV); **2)** tumors showing chromosomal instability (CIN); **3)** tumors with a genome stable (GS); and **4)** tumors with microsatellite instability (MSI; **Figure 16**).

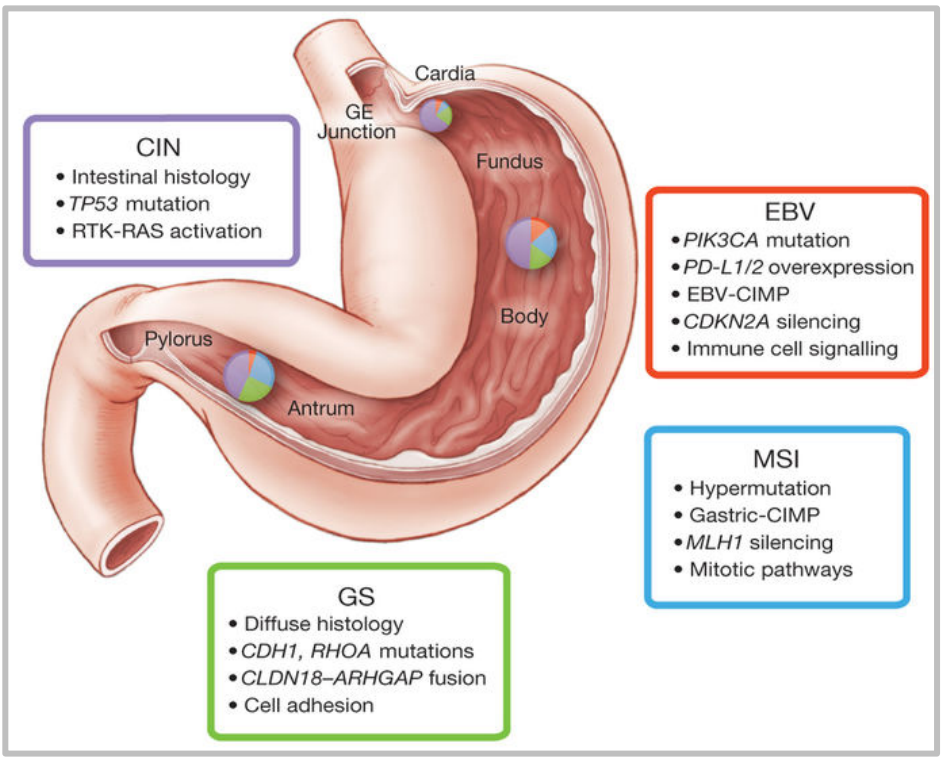

Figure 16. Key features of gastric cancer subtypes.

The schematic lists some of the salient features associated with each of the four molecular subtypes of gastric cancer. Distribution of molecular subtypes in tumors obtained from distinct regions of the stomach is represented by inset charts. EBV, Epstein Barr virus; MSI, microsatellite instability; GS, genome stable; CIN, chromosomal instability. Source: Cancer Genome Atlas Research Network (173).

8.5.1 CIN

Chromosomal instability has long been recognised as a hallmark of malignancy. The instability can occur as a change in DNA content with loss or gain of whole chromosomes leading to altered DNA copy number (aneuploidy). Alternatively, the instability might only involve part of a chromosome, which could lead to loss or gain of function of important gene families such as oncogenes, tumor suppressor genes or genes involved in DNA repair or cell cycle checkpoints, and can be a consequence of translocation, amplification, deletion or allelic loss (loss of heterozygosity, LOH) (168, 174). Chromosomal aberrations are numerous in gastric cancer (168). These changes have been linked to different histological types, for example intestinal type gastric cancer is associated with copy number gains at 8q, 17q and 20q, whereas diffuse type gastric cancer is associated with copy number gains at 12q and 13q (71).

8.5.2 MSI

Microsatellite instability is a genetic hypermutability phenomenon where microsatellite regions (regions of repetitive nucleotide sequences) in tumor genomes accumulate mutations due to defective DNA mismatch repair (MMR) enzymes, caused by mutations in one of several different DNA mismatch repair genes (i.e., *MLH1* or *MSH2*) (175). Next-generation sequencing (NGS) studies have shown that MSI occurs in about 15%-30% of GCs, and more frequently correlates with intestinal type, location in the distal part of the stomach, female gender and older age at diagnosis (62, 176, 177). The most common epigenetic change in this setting is hypermethylation of the promoter region of *MSH1*, which impairs DNA mismatch repair and resulting in multiple mutations within simple nucleotide repeats (microsatellites). These mutations impair downstream gene expression, therefore a number of cell functions such as cell cycle, cell signalling and tumor suppression can be deregulated. Gastric tumors can be categorized into those with high or low levels of microsatellite instability or those that are stable, depending on the frequency of mutations within microsatellite markers. The overall consensus from several populations is that gastric cancers with high levels of microsatellite instability are more likely to exhibit an antral location, intestinal subtype and a better survival than microsatellite stable tumors or tumors with low microsatellite instability (178, 179).

8.5.3 Epstein Barr virus

The EBV subtype highlights the viral etiology of gastric cancer; the TCGA characterization of this subtype suggests potential therapeutic targets for this group of tumors. EBV was discovered 50 years ago from Burkitt's lymphoma. EBV is carried in the blood circulation without symptoms by 90% of the adult population. However, for reasons yet-to-be identified, EBV may affect epithelial cells and become carcinogenic. It is estimated that EBV is associated with 2% of all human tumors including nasopharyngeal carcinoma, another major cancer type that is unique for Chinese population especially in the southern areas of China. In recent years, it has been increasingly recognized that the majority of gastric cancers are associated with infectious agents, including *H. pylori* and EBV. EBV is found within malignant epithelial cells in 9% of gastric cancers. The TCGA network reported that the EBV-positive gastric tumors cluster together and exhibit a higher prevalence of DNA hypermethylation (i.e., CpG island methylator phenotype –CIMP) than any other cancers (e.g., colorectal cancer, endometrial cancer, and glioblastoma) reported by TCGA before (180-182). Of therapeutic importance, there is a strong predilection for phosphatidylinositol 3-kinase, catalytic subunit alpha (PIK3CA) mutation in EBV-positive gastric cancers, with non-silent PIK3CA mutations found in 80% of this subgroup ($P < 0.001$). In contrast, tumors in other subtypes displayed fewer PIK3CA mutations (range from 3%

to 42%). PIK3CA mutations in EBV-negative gastric cancers are mostly localized in the kinase domain (exon 20) but were more dispersed in EBV-positive gastric cancers. TCGA analysis also showed that immunosuppressant proteins currently being evaluated as targets to increase antitumor immune response, such as programmed death ligand 1/2 (PD-L1/2), were elevated in EBV-positive tumors, suggesting that PD-L1/2 antagonists represent new therapeutic options for the EBV subtype of gastric cancer (183).

8.5.4 GS

Genomically stable (GS) gastric cancers are enriched for the diffuse histological variant. This subtype is characterized by mutations in the *Ras homolog* gene family, member A (RHOA) gene or fusions involving RHO-family GTPase-activating proteins (GAP). The RHO family of GTPases regulates actomyosin dynamics and other cell functions, including adhesion, proliferation, and survival. Furthermore, the RHOA signaling pathway is strongly associated with the ability of tumor cells to invade and successfully establish metastases. TCGA network identified RHOA mutation in 16 cases of gastric cancer, and these were significantly enriched in the GS subtype. RHOA, when in the active guanosine triphosphate (GTP)-bound form, acts through a variety of effectors, including Rho-associated coiled-coil-containing protein kinase 1 (ROCK1), DIAPH2, and protein kinase N (PKN), to control actin-myosin-dependent cell contractility and cellular motility and to activate signal transducer and activator of transcription 3 (STAT3) to promote tumorigenesis. Structural mapping of RHOA mutations showed that the mutations were clustered in two adjacent amino-terminal regions that are predicted to be at the interface of RHOA with ROCK1 and other effectors. The mutations found in this study may act to regulate downstream signaling of RHOA, a hypothesis validated by two recently published studies in Nature Genetics (184, 185). The importance of RHOA pathway in gastric cancer was further underscored by the discovery of recurrent structural genomic alterations. Whole genome sequencing of 107 tumors revealed numerous structural rearrangements, including 74 changes predicted to produce in-frame gene fusions. The Nature paper reports two cases with an interchromosomal translocation between CLDN18 and RHO-GTPase activating protein 26 (ARHGAP26; also known as GTPase regulator associated with focal adhesion kinase –GRAF), a GAP that facilitates conversion of RHO-GTPases to the GDP state to enhance cellular motility. CLDN18 is a protein involved in cell-cell tight junction adhesion. RNA sequencing data from tumors identified CLDN18-ARHGAP26 fusion in nine additional tumors, and two of these tumors showed CLDN18-ARHGAP26 fusion. Identification of the key mutations and gene fusions in this

subtype is an important information for future drug development targeting this group of cancers (183).

Recently, the Asian Cancer Research Group (ACRG) establish an important classification of GC using gene expression data from 300 primary GC tumor specimens, to describe four molecular subtypes linked to distinct patterns of molecular alterations, disease progression and prognosis (186). The subtype classification uses MSI and CIN stratification (from TCGA analysis) and supplements it by incorporating two key molecular mechanisms related to *TP53* activity and epithelial-to-mesenchymal transition (EMT) to further stratify GC patients. The mesenchymal-like type (MSS/EMT) includes diffuse type tumors with the worst prognosis, the tendency to occur at an earlier age and the highest recurrence frequency (63%) of the four subtypes. Microsatellite-unstable tumors (MSI) are hyper-mutated intestinal type tumors occurring in the antrum; these have the best overall prognosis and the lowest frequency of recurrence (22%) of the four subtypes. The tumor protein 53, *TP53*-active (MSS/*TP53*$^{+}$) and *TP53*-inactive (MSS/*TP53*$^{-}$) types include patients with intermediate prognosis and recurrence rates (with respect to the other two subtypes), with the *TP53*-active group showing better prognosis. They also describe key molecular alterations in each of the four GC subtypes using targeted sequencing and genome-wide copy number microarrays (**Table 3**). Collectively, this classification and the molecular screening could have important clinical implications in GC.

Table 3. Genomic alterations found in each subtype.

Gene aberrations	MSS/TP53⁻	MSS/TP53⁺	MSI	MSS/EMT	*P* value
Gene amplifications					
CCND1	4/86 (4.7%)	2/66 (3.0%)	2/61 (3.3%)	3/41 (7.3%)	0.7190
CCNE1	15/86 (17.5%)	10/66 (15.2%)	3/61 (4.9%)	5/41 (12.2%)	0.2077
EGFR	6/86 (7.0%)	2/66 (3.0%)	1/61 (1.6%)	0/41 (0.0%)	0.2685
HER2	15/86 (17.4%)	2/66 (3.0%)	0/61 (0.0%)	0/41 (0.0%)	0.0001
FGFR2	1/86 (1.2%)	2/66 (3.0%)	0/61 (0.0%)	2/41 (4.9%)	0.2594
KRAS	4/86 (4.7%)	5/66 (7.6%)	1/61 (1.6%)	1/41 (2.4%)	0.5112
MDM2	0/86 (0.0%)	5/66 (7.6%)	1/61 (1.6%)	2/41 (4.9%)	0.0316
MET	3/86 (3.5%)	2/66 (3.0%)	1/61 (1.6%)	0/41 (0.0%)	0.8028
PIK3CA	1/86 (1.1%)	0/66 (0.0%)	0/61 (0.0%)	0/41 (0.0%)	0.5805
MYC	8/86 (9.0%)	2/66 (0.0%)	0/61 (0.0%)	1/41 (2.4%)	0.0365
Somatic mutations					
ALK	2/85 (2.4%)	0/59 (0.0%)	7/43 (16.3%)	0/36 (0.0%)	0.0001
APC	7/85 (8.2%)	9/59 (15.3%)	7/43 (16.3%)	1/36 (2.8%)	0.1748
ARID1A	5/85 (5.9%)	11/59 (18.6%)	19/43 (44.2%)	5/36 (13.9%)	2.8×10^{-5}
BRAF	3/85 (3.5%)	1/59 (1.7%)	5/43 (11.6%)	1/36 (2.8%)	0.0969
CDH1	3/85 (3.5%)	1/59 (1.7%)	3/43 (7.0%)	1/36 (2.8%)	0.5657
CTNNB1	2/85 (2.4%)	3/59 (5.1%)	1/43 (2.3%)	0/36 (0.0%)	0.5158
EGFR	1/85 (1.2%)	1/59 (1.7%)	2/43 (4.7%)	0/36 (0.0%)	0.4257
ERBB2	4/85 (4.7%)	0/59 (0.0%)	7/43 (16.3%)	1/36 (2.8%)	0.0042
ERBB3	5/85 (5.9%)	3/59 (5.1%)	6/43 (14.0%)	0/36 (0.0%)	0.0916
FBWX7	2/85 (2.4%)	1/59 (1.7%)	7/43 (16.3%)	1/36 (2.8%)	0.0030
KRAS	3/85 (3.5%)	5/59 (8.5%)	10/43 (23.3%)	0/36 (0.0%)	0.0006
MTOR	3/85 (3.5%)	1/59 (1.7%)	6/43 (14.0%)	0/36 (0.0%)	0.0097
PIK3CA	4/85 (4.7%)	10/59 (16.9%)	14/43 (32.6%)	3/36 (8.3%)	0.0007
PTEN	3/85 (3.5%)	2/59 (3.4%)	6/43 (14.0%)	2/36 (5.6%)	0.1002
RHOA	3/85 (3.5%)	4/59 (6.8%)	0/43 (0.0%)	1/36 (2.8%)	0.3497
SMAD4	2/85 (2.4%)	5/59 (8.5%)	2/43 (4.7%)	1/36 (2.8%)	0.3629
TP53	51/85 (60.0%)	14/59 (23.7%)	11/43 (25.6%)	12/36 (33.3%)	0.0016

Source: Cristescu, *et al.* 2015. (186)

9. Molecular Genetics Landscape and gene mutations of Gastric Cancer

Studies from several groups over the past decade have produced a near-comprehensive catalogue of GC associated 'driver' alterations, including gene mutations, somatic copy number alterations (sCNAs), structural variants, epigenetic changes, and transcriptional changes involving mRNAs and noncoding RNAs (ncRNAs) (**Figure 17**).

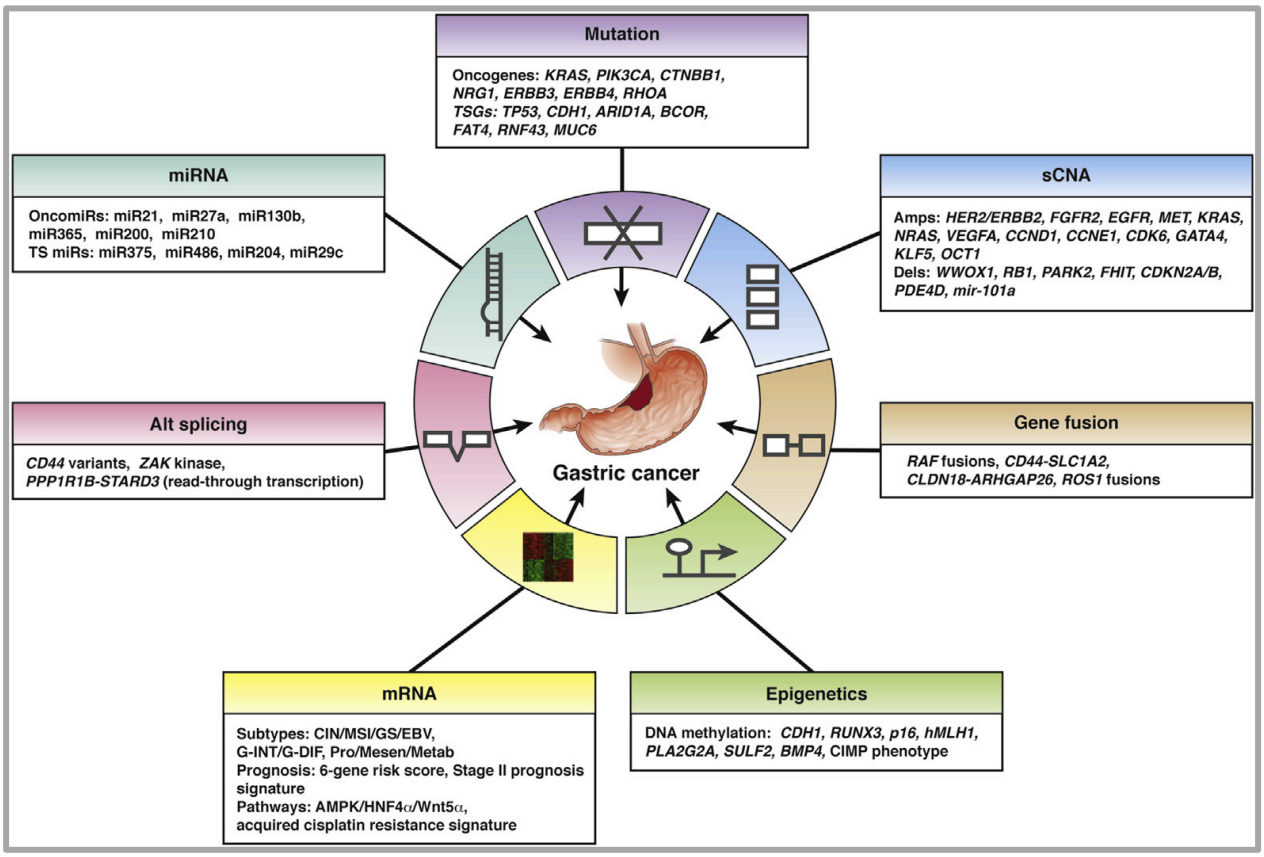

Figure 17. **Genomic features of Gastric Cancer.**
Based on the classic Hallmarks of Cancer report by Hanahan and Weinberg. Source: *Tan and Yeoh*, 2015 (91).

Mutated genes in GC can be broadly classified into three categories: **a)** high-frequency drivers displaying a high-rate of recurrence (>5%–10%) across multiple GCs; **b)** low-frequency drivers that are recurrently mutated in the 1%–10% range, but which still probably contribute to disease pathogenesis; and **c)** bystander/passenger mutations that arise as a consequence of underlying mutational processes such as CpG deamination (187), but which do not functionally contribute to tumorigenesis. Among high-frequency drivers, *TP53* is the most frequently mutated gene in GC, exhibiting aberrations in ~50% of cases (188). Reflecting TP53's cellular function as a guardian of genomic integrity, *TP53* mutated GCs often exhibit high levels of sCNAs (173, 189) involving both broad chromosomal regions and focal gene regions. GCs have also been shown to exhibit mutations in other canonical oncogenes (*KRAS, CTNNB1, PIK3CA*) and tumor suppressor genes (*SMAD4, Apc*) (190). Reflecting the importance of RTK/RAS/MAPK signaling in GC, frequent mutations in the *ERBB3, RTK* and the ligand/*RTK NRG1/ERBB4* genes have recently been reported (191, 192). Some of these mutations appear to be enriched in specific GC

subtypes, for example, EBV-positive GCs frequently exhibit *PIK3CA* mutations (173) while diffuse type GCs have been observed to exhibit frequent somatic mutations in *CDH1* (185).
Recent next-generation sequencing (NGS) studies of GC have also highlighted two new GC genes, *ARID1A* and *RHOA*. *ARID1A*, mutated in 10%–15% of GCs (193, 194) encodes a component of the SWI/SNF chromatin remodeler complex. *RHOA* was recently shown by multiple studies to exhibit recurrent mutations in diffuse type/genome-stable GCs expanding our understanding of DGC mutations by describing novel recurrent mutations of *RHOA*, encoding the small GTPase RHOA, in 14.3%–25.3% of DGC patients (184, 185), in turn giving the opportunity to elucidate the molecular mechanisms of DGC initiation and progression. *Wang et al.* (185) performed whole-genome sequencing, DNA copy number, gene expression, and DNA methylation analysis of 100 tumor and nontumor paired samples, spanning both IGC and DGC. Their analysis revealed frequent mutations in *TP53* in both subtypes, *ARID1A* in EBV-related or MSI-related cancers, and *CDH1* in DGC. *RHOA* mutation was identified recurrently within DGC and following sequencing in a larger DGC cohort, was found mutated in 14 of 98 DGC patients (14.3%). *Kakiuchi et al.* (184) initially performed whole-exome sequencing within 30 DGCs and focused sequencing in another 57 cases, finding *RHOA* mutations in 22 of 87 (25.3%) cases. Unlike *ARID1A* where mutations are dispersed throughout the gene, the *RHOA* mutations are localized to different N-terminal hot-spot regions (Tyr42, Arg5, Gly17 and Leu57), and are predicted to modulate downstream RHOA signaling. Functional analysis of these *RHOA* mutations suggest that they may impart resistance to anoikis, a form of programmed cell death occurring after cellular detachment from a solid substrate (185). Based on these genetic data is not possible to conclude whether *RHOA* signaling prevents or promotes the oncogenic process, thus further investigation is necessary to address this question.

10. RHO-GTPases

10.1 Overview

RHO-GTPases are members of the Ras superfamily of monomeric 20-30 kDa GTP-binding proteins (195). The mammalian RHO-like GTPases comprise at least 10 distinct proteins: RHOA, B, C, D and E, RAC1 and 2, RACE, CDC42s, and TC10. A comparison of the amino acid sequences of the RHO proteins from various species has revealed that they are conserved in primary structure and are 50-55% homologous to each other (196, 197).

These proteins function as molecular switches that control a wide variety of signal transduction pathways in all eukaryotic cells (197). In the GTP-bound form they are able to interact with effector or target molecules to initiate a downstream response, while an intrisic GTPase activity returns the proteins to the GDP-bound state, to complete the cycle and terminate signal transduction (195). The most important functions of RHO-GTPases are related to their capacity to regulate the actin cytoskeleton and microtubule reorganization.

10.2 Regulation of RHO-GTPase activity

As mentioned above, the activity of all small RHO-GTPases is assured by the controlled cycling between their inactive GDP-bound state and their active state, where bound GDP is replaced by GTP (195). Structurally they share a set of conserved G box GDP/GTP-binding motif elements beginning at the N-terminus: G1-GXXXXGKS/T; G2-T; G3DXXGQ/H/T; G4-T/NKXD; and G5-C/SAK/L/T. Together, these elements make up a ~20 kDa G domain (Ras residues 5-166) that has a conserved structure and biochemistry shared by all Ras superfamily proteins (**Figure 18**) (198). The two nucleotide-bound states have pronounced differences in two surface loops known as the switch I (Ras residues 30-38) and switch II (59-67) regions, with the GTP-bound conformation possessing high affinity for effector targets (**Figure 18**) (195). It is mainly through the conformational changes in these two switches that regulatory proteins and effectors 'sense' the nucleotide status of the small GTPases. A second important biochemical feature of the majority of Ras superfamiliy proteins is their post-translational modification by lipids. The majority of Ras and RHO family proteins ends with a C-terminal CAAX (C=Cys, A=aliphatic, X=any amino acid) tetrapeptide sequence. These motif, when coupled together with residues immediately upstream (e.g. cysteine residues modified by the fatty acid palmitate), comprise the membrane-targeting sequences that dictate interactions with distinct membrane compartments and subcellular locations (**Figure 18**) (198-200).

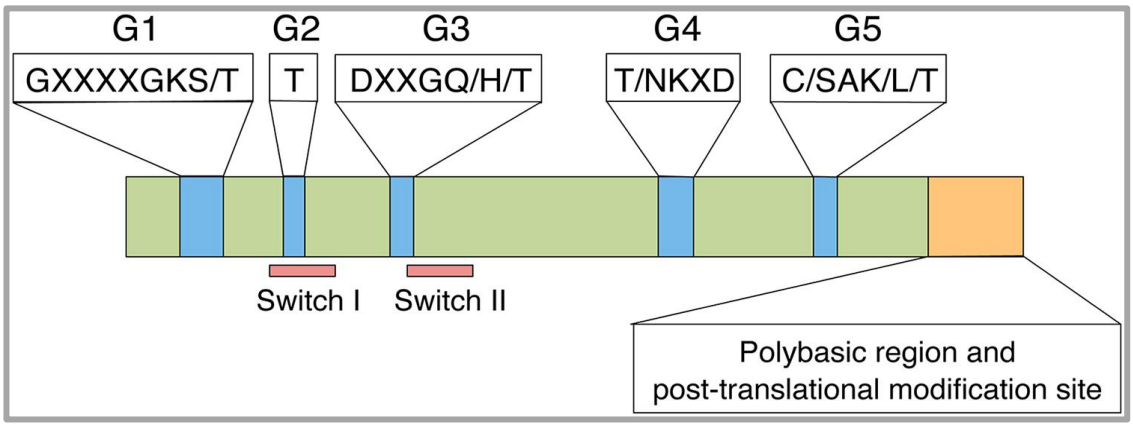

Figure 18. **Functional domains of the Rac/RHO family.**

The Rac/RHO family shares a set of five conserved G boxes (Blue), a polybasic region and a post-translational modification site (Orange). All members of this family have in common a consensus sequence for GDP/GTP union (Switch I and II); a terminal CAAX motif that facilitates membrane anchorage; and an effector domain that together with an insert loop that participate in the interaction with effectors. Source: Kawano Y *et al.* 2014 (201).

In order to ensure proper signaling responses to extracelular stimuli, cells control the activity of RHO proteins through a number of regulatory steps. These include: the control of nucleotide binding and hydrolysis by guanine-nucleotides exchange factors (**GEFs**) (202) and GTPases activating proteins (**GAPs**) (203); the regulation of their subcellular localization by guanine dissociation inhibitors (**GDIs**) specific of RHO family members (204); the modulation of their protein expression levels, and other regulatory events (200). RHOA signalling have not been deeply characterized, rencently, we have demonstrated a complex pattern of inactivation of *RHOA* gene in colorectal cancer cells through genetic, transcriptional and post-transcriptional mechanisms (205).

GDP/GTP cycle is controlled by RHO GEFs and GAPs regulatory proteins. GEFs promote the exchange of GDP for GTP molecules, thereby producing the activation of these proteins during signal transduction. All RHO GEFs contain a Dbl-homology (DH) domain which encodes the catalytic activity necessary for nucleotide exchange and mediate activation, and an adjacent pleckstrin homology (PH) domain. The PH domain is thought to mediate membrane localization through lipid binding, but in addition, structural and biochemical evidence suggests that it might also directly affect the activity of the DH domain (**Figure 19**) (195). GAPs promote the hydrolysis of the bound GTP molecules, thus allowing the transfer of the GTPase back to the inactive state at the end of the stimulation cycle. (196, 198-200). GTPases in different branches exhibit structurally distinct but mechanistically similar GAPs and GEFs (198).

In addtion to the presence of these structural features, and regulatory proteins responsible for cycling between the inactive/active forms, RHO-GTPases need additional upstream signals in order to move from the cytosol to target membranes and subsequently to remain stably anchored in those structures. RHO GDIs play important roles in this regulatory context, because they hide the isoprenyl groups of the GTPases, thus resulting in the sequestration of the inactive GTPases in the cytosol. This property is also important for the removal of the GTPase from the plasma membrane at the end of the signaling process. Due to the interaction of RHO GDIs with the GTPase switch regions, they also block the release of GDP from the GTPase and consequently, contribute to the maintenance of the GTPases in an inactivate state in non-stimulated cells. The dissociation of the RHO GDI from the GTPase, an essential step for the activation of GTPases by GEFs and for their subsequent association with membranes, is regulated at different levels during signal transduction (**Figure 19**) (199, 200).

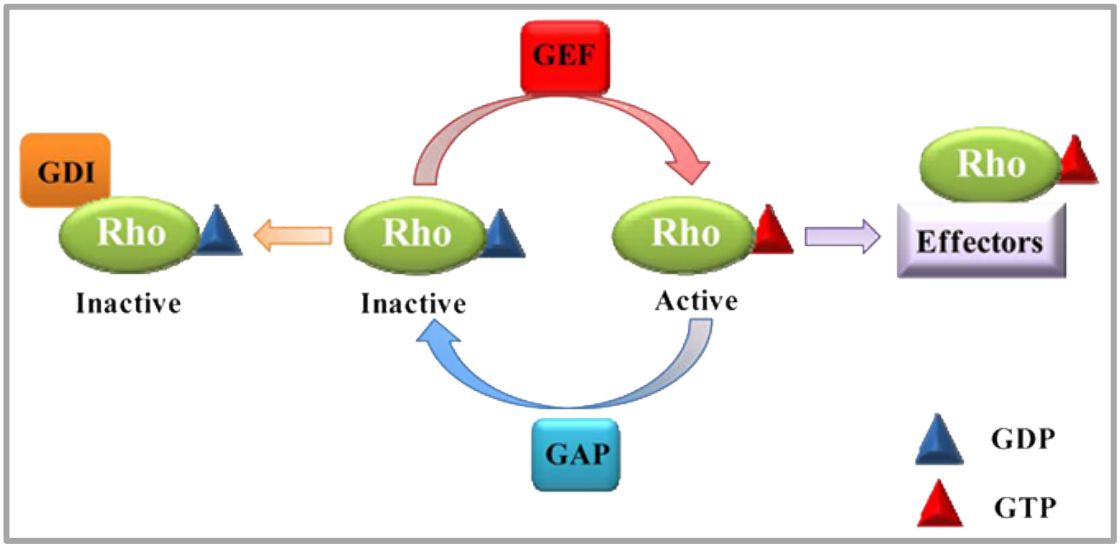

Figure 19. RHO-GTPases cycle between a GTP-bound and a GDP-bound conformation.
In the active (GTP-bound) state RHO-GTPases interact with several effector proteins. The cycle is highly regulated by guanine exchange factors (GEF) which catalyze nucleotide exchange and mediate activation; GTPase activating proteins (GAPs) regulate the switching from the GTP-bound active state to the inactive GDP-bound state, driving the GTPase activity; and guanine nucleotide dissociation inhibitors (GDIs) extract the inactive GTPase from membranes.

10.3 Effectors of RHO-GTPases

It is in the active form that RHO-GTPases can perform their regulatory function through a conformation-specific interaction with target (effector) proteins. There are several protein effectors that have been identified for RHO, RAC, and CD42 that include serine/threonine kinases, tyrosine kinases, lipid kinases, lipases, oxidases, and scaffold proteins (**Figure 20**).

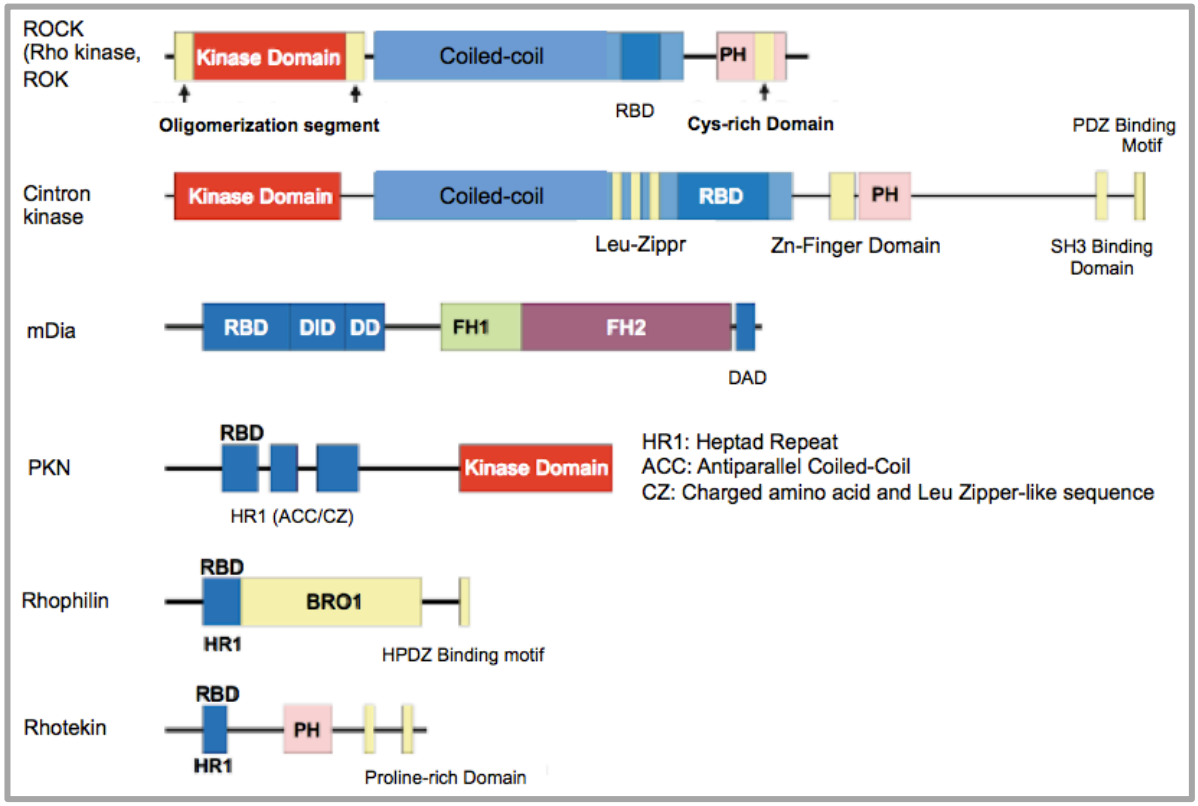

Figure 20. Schematic representation of domain structure of RHO effector molecules.

Source: Wittinghofer, A. 2014 (206)

From a structural characteristics, it is known that these effectors use distinct residues within the switch I and switch II regions as the major docking/recognition sites (200). A comparison of the RHOA-GDP and RHOA-GTP cristal structures reveals that the conformational differences between the GTP- and GDP-bound forms are restricted primarily to the switch I and II regions. Effector proteins must use these differences to discriminate between the GTP- and GDP-bound forms, though they also interact with other regions of the GTPase (195, 207). However, it is

possible that GTPases might also serve to recruit targets to specific locations or complexes (208).

Recently, there has been much interest in characterizing the contributions of specific effectors to different GTPase functions. The majority of the effectors identified so far (**Table 4**), some of which have a kinase activity, are activated by the best characterized RHO-GTPase proteins, RHOA, CDC42 and RAC1. Effectors of active CDC42 and RAC1 mediate cell-cell adhesion and cell polarization through actin polymerization at cell protrusions, stabilization and capture of microtubules, and also mediate arrangement of the cytoskeleton and organelles (e.g. Golgi, centrosomes and nucleus). The CDC42 and RAC effector proteins of p21-activated kinases (PAKs) are important mediators of cytoskeletal organization. Processes that are regulated downstream of active RHOA signaling includes membrane retraction by actomyosin-based stress fiber contraction, cell-cycle progression and cell division. For example, the RHO-associated coiled-coil-containing protein kinases (ROCKI and ROCKII) are RHOA effector kinases that influence cell adhesion and cell migration through regulation of actomyosin-mediated contractility, inducing stress fiber formation and assembly of focal contacts (processes that regulate the contractility of the actomyosin system) downstream of RHO (195, 207, 209). RHOA binding to the formin mammalian diaphanous 2 (mDia2/DIAPH2) or CDC42 binding to neural Wiskott-Aldrich syndrome protein (N-WASP) initiate the assembly of protein machineries required for actin polymerization (195). DIAPH belongs to the formin homology domain containing proteins (FH), which have emerged as important links between RHO and the actin cytoskeleton. This group of proteins includes p140Dia in mice, the Drosophila diaphanous gene product (mDia/DIAPH1 and 2), and the yeast proteins Bn1p and Fus1p. The FH1 domain is formed by long polyproline-rich motifs and has been implicated in binding profilin, a protein that has a complex effect on polymerized actin, its principal role is to sequester actin monomers but it can also promote the elongation of actin filaments (195, 207, 209). The PKNs is a subfamiliy of serine/threonine kinases that comprise PKN1, PKN2 and PKN3 (210, 211). Active RHOA is capable of binding PKNs enhancing their kinase activity. The physical interaction of PKN1 with transcription factors and the nuclear localization suggest a potential role for PKNs in transcriptional regulation (212-214).

Table 4. RHO-GTPases effectors

Effector	Protein type (alternate protein name)	Upstream GTPase	Main biological function
FilaminA	Actin binding protein	RhoA, Rac1, Cdc42	Cytoskeletal regulation, actin filament cross-linking
CopG2	Coatomer protein (γ2-Cop)	Cdc42	Vesicle trafficking (clathrin route)
DIAPH1,2	Formin	RhoA, Rac1	Cytoskeletal change via profilin and IRSp53
FHOD1	Formin	Rac1	Cytoskeletal and transcriptional regulation
FMNL1	Formin	Rac1	Cytoskeletal organization, cell polarity, cytokinesis
IP3R1	Inositol 1,4,5-triphosphate receptor	RhoA	Calcium entry in endothelial cells
PI4,5PK	Lipid kinase	RhoA	Phosphatidylinositol bisphosphate level modulation
CybA	NADPH oxidase complex subunit	Rac1	Superoxide production
NCF1,2	NADPH oxidase complex subunit	Rac1, Cdc42	Superoxide production
PLC-β2	Phospholipase, C type (PLC-β2)	Cdc42, Rac1	Production of second messengers
KCNA2	Potassium Channel subunit	RhoA	Potassium entry
PIK3R1	Regulatory p85 subunit of PIK3C	Rac1, Cdc42	Regulation of PIK3C activity, signal transduction
PPP1R12A	Regulatory subunit of phosphatase1	RhoA	MLC inactivation, cytoskeletal regulation
IQGAP1,2	RhoGAP and scaffold protein	Rac1, Cdc42	Cytoskeletal regulation, cell–cell contacts
ARFIP2	Scaffold protein (Por1)	Rac1	Cytoskeletal regulation
Cdc42SE1,2	Scaffold protein (Spec1,2)	Rac1, Cdc42	Modulation of GTPase signalling outputs
CYFIP1,2	Scaffold protein (Pir121)	Rac1	Regulation of the cytoskeleton via WASF proteins
MTSS1	Scaffold protein	Rac1	Cytoskeletal organization via WASF/WAVE
Kinectin1	Scaffold protein	RhoA, Rac1, Cdc42	Kinesin binding, microtubule vesicular trafficking
NCK1	Scaffold protein with SH2/3 domains	Rac1	Complex formation with WASP, signal transduction
NCKAP1	Scaffold protein (Nap125, Nap1)	Rac1	Regulation of the cytoskeleton via WASF proteins
N-WASP	Scaffold protein	Cdc42	Cytoskeletal regulation via Arp2/3 complex
Pard6 A,G	Scaffold protein (Par6α,γ)	Rac1, Cdc42	Cell polarity. Links GTPases and atypical PKCs
Trip10	Scaffold protein	Cdc42	Binding of WASP to microtubules
WASP	Scaffold protein	Rac1	Cytoskeletal regulation via the Arp2/3 complex
WAVE/Scar1,2	Scaffold protein	Cdc42, Rac1	Cytoskeletal regulation via the Arp2/3 complex
Cdc42bpgB	Serine/threonine kinase (MRCKβ)	Rac1, Cdc42	Cytoskeletal regulation
p70S6K	Serine/threonine kinase	Cdc42	Regulation of translation, cell cycle
PAK2	Serine/threonine kinase	Rac1, Cdc42	Cytoskeletal organization, kinase activation
PKCα	Serine/threonine kinase	RhoA, Rac1, Cdc42	Signal transduction
PKN1,2	Serine/threonine kinase (Prk)	RhoA	Vesicle recycling, PLD1 activation
ROCK1,2	Serine/threonine kinase (Rok α,β)	RhoA	Cytoskeleton, blockage of cell contact inhibition
Stat3	Transcriptional factor	Rac1, Cdc42	Transcription
α-Tubulin-1C	Tubulin	Rac1	Integral component of microtubules

Source: Goggs, R et al. 2015 (215)

10.4 Role of RHOA-GTPases in Gastric Cancer

As mentioned before, diffuse type gastric cancer (DGC) represents a subtype with poor prognosis (78-81); as a result, DGC has gained substantial public attention worldwide. DGC is histologically characterized as a poorly differentiated adenocarcinoma in which single isolated cancer cells or small collective masses of cancer cells massively infiltrate into adjacent tissue in a highly invasive manner with prominent scirrhous stromal reactions. DGC constitutes a poor-prognosis subgroup of gastric cancer with no known effective molecularly targeted therapies. Recent genomic characterization of gastric cancer by whole-exome sequencing showed that a large number of known cancer-related genes are frequently mutated in intestinal type gastric malignancies (185, 194). Because of DGC-specific molecular carcinogenesis mechanisms and druggable gene targets remains to be elucidated, Kakiuchi et al. (184) performed whole-exome sequencing on 30 DGC cases and they observed recurrent somatic mutations in 25.3% (22/87) of DGC samples in the *RHOA* gene. These somatic mutations were unevenly distributed across

the *RHOA* gene: mutational hotspots affected the Tyr42, Arg5 and Gly17 residues in the *RHOA* protein (**Figure 21a**). The Tyr42, Arg5, Gly17 and Leu57 residues in *RHOA*, which were identified as the most frequent sites of alteration in this study, are highly conserved among RHO family proteins. The Tyr42 residue is located within a region called the core effector domain, an important functional domain for physical interaction with effector molecules and/or RHO GEFs and RHO GAPs (**Figure 21b-c**). Over the past two decades, numerous biochemical and cell biological studies has focused on *RHOA* activities, there have also been a plenty of active discussion on the roles of *RHOA* in tumorigenesis, primarily based on gain- and loss-of-function experiments. *RHOA* is reported to participate in the formation and progression of many tumors, Karlsson *et al.* (216), and Chiba *et al*. (217) reported frequent somatic *RHOA* mutations in a distinct subtype of T-cell-type malignant lymphoma called angioimmunoblastic T-cell lymphoma (AITL), and other T-cell lymphoma with AITL-like features. Given the characteristic invasive growth pattern that are a hallmark of DGC, mutations in *RHOA* could be predicted to lead to constitutive activation of *RHOA*, enhancing activity of downstream mediators and increasing cellular invasion. Although not previously identified in cancer, the Tyr42 (Y42C) substitution in *RHOA* had been evaluated in earlier biochemical studies, which revealed attenuated activation of protein kinase N, while not affecting the bings of *RHOA* to other effectors tested (218). Therefore, here the role of PKN in the development of gastric cancer was investigated.

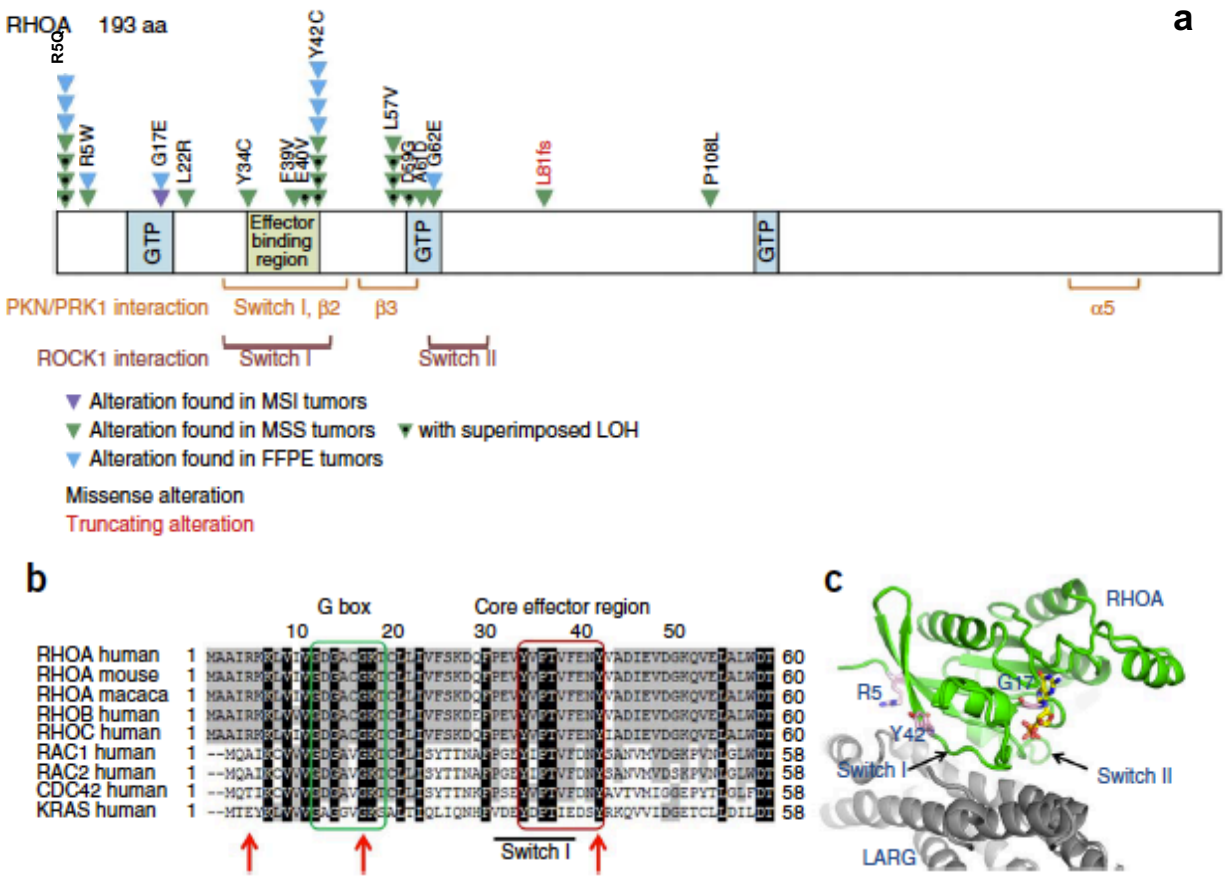

Figure 21. Distribution of RHOA alterations in DGC.

(**a**) Map of RHOA functional regions and the sites of the amino acid substitutions discovered by whole-exome sequencing analysis. Recurrent alterations are indicated by multiple triangles. (**b**) Amino acid alignment of RHOA and RHO family proteins (1–60 aa). The G box and core effector region are highly conserved across other mammalian RHOA and human RHO families, are highlighted by green and red boxes, respectively. Red arrows indicate the most frequently mutated positions Arg5, Gly17, Leu57 and Tyr42. (**c**) Structure of RHOA (green) and one of its representative RhoGEF proteins, LARG (gray), in its GDP-bound form. Tyr42, one of the most frequently mutated residues in this study, is located on an interaction surface of RHOA with RhoGEFs. Source: Kakiuchi *et al.* 2014 (184) and Wang *et al.* 2014 (185)

The two recent studies, which functionally interrogate these novel *RHOA* mutations found in DGC have reach opposite conclusions regarding the role of *RHOA* and its principal mutations play in the development of DGC.

First, Kakiuchi *et al.* (184) studied several cancer cell lines harboring *RHOA* mutations: the OE19 cell line (adenocarcinoma of the gastric cardia), the breast cancer cell line BT474, and the colorectal cancer cell line SW948. They showed that small interfering RNA (siRNA)-mediated silencing of *RHOA* significantly impairs *in vitro* proliferation in these mutant cell lines but does

not similarly impact gastric cancer cell lines with wild-type *RHOA*. Furthermore, they demonstrated that reintroduction of the codon 17 or 42 *RHOA* mutants, but not reintroduction of wild-type *RHOA* rescued cell proliferation effects of *RHOA* siRNA, suggesting tumor-promoting activity (gain-of-function activity) for these *RHOA* mutants.

On the other hand, the results from Wang *et al.* (185), provide additional insights into the potential role of mutant *RHOA*, using a RHO binding domain assay to immunoprecipitate RHOA-GTP, they showed that both the Y42C and L57V mutants significantly attenuate the GTP-associated form compared to wild-type protein, indicating a potential defect in *RHOA* activation with these mutants. They further used primary mouse intestinal organoids to study the impact of *RHOA* mutants Y42C and L57V upon anoikis (cell death induced when anchorage-dependent cells detach from the surrounding extracellular matrix). Inhibition of anoikis may represent a key requirement for DGC, because the loss of E-cadherin, leading to reduction in cellular adhesion has been shown to result in acute cell death via anoikis (219). Intestinal organoids stably expressing empty vector control, wild-type human *RHOA* or the *RHOA* mutants were dissociated into single cells, in the presence or absence of the ROCK inhibitor Y-27632, which is essential in preventing anoikis. Significantly higher organoid recovery with expression of the Y42C and L57V *RHOA* mutants than with vector control, whereas wild-type *RHOA* expression resulted in the opposite trend. In the absence of Y-27632, the complete cell death in organoids expressing the vector control and wild-type *RHOA* by day 10 was observed, whereas organoids expressing the mutants continued to survive and proliferate. Addition of Y-27632 increased the number of organoids in the mutants and also the size of the organoids compared with those expressing vector control or wild-type *RHOA*. These results confirm previous observations of a critical role for RHOA function in mediating anoikis (15, 220, 221) and show the functional relevance of the *RHOA* hotspot mutants in evading anoikis owing to their defective RHOA function. Through comprehensive genomic characterization, these studies demonstrated that, along with *CDH1* mutations, *RHOA* mutations are quite common in DGC but not in other variants of gastric cancer (184, 185). It remains to be clarified, however, whether *RHOA* mutations attenuate RHOA activity or if the mutations result in a gain-of-function effect. When taken together the results of these two studies underscore the need to carry out a more extensive characterization of the functional effects of these *RHOA* recurrent mutations in gastric cancer cells. Recently, our group has investigated the role of *RHOA* in colorectal cancer, and found that *RHOA* inactivation contributes to colorectal cancer progression/metastasis, largely through the activation of Wnt/β-catenin signaling, resulting in increased cell proliferation, invasion and dedifferentiation (222). *RHOA* inactivation in the murine intestine accelerates the tumorigenic process and reduced

RHOA levels were observed at metastatic sites compared with primary human colon tumors (222). Importantly, over the last few years we have also investigated the role of *RHOA* in diffuse type gastric cancer, and found that deletion of *RHOA* results in increased proliferation and invasion of diffuse gastric cancer cells "*in vitro*" and "*in vivo*" (unpublised, **Figure 22A-F**).

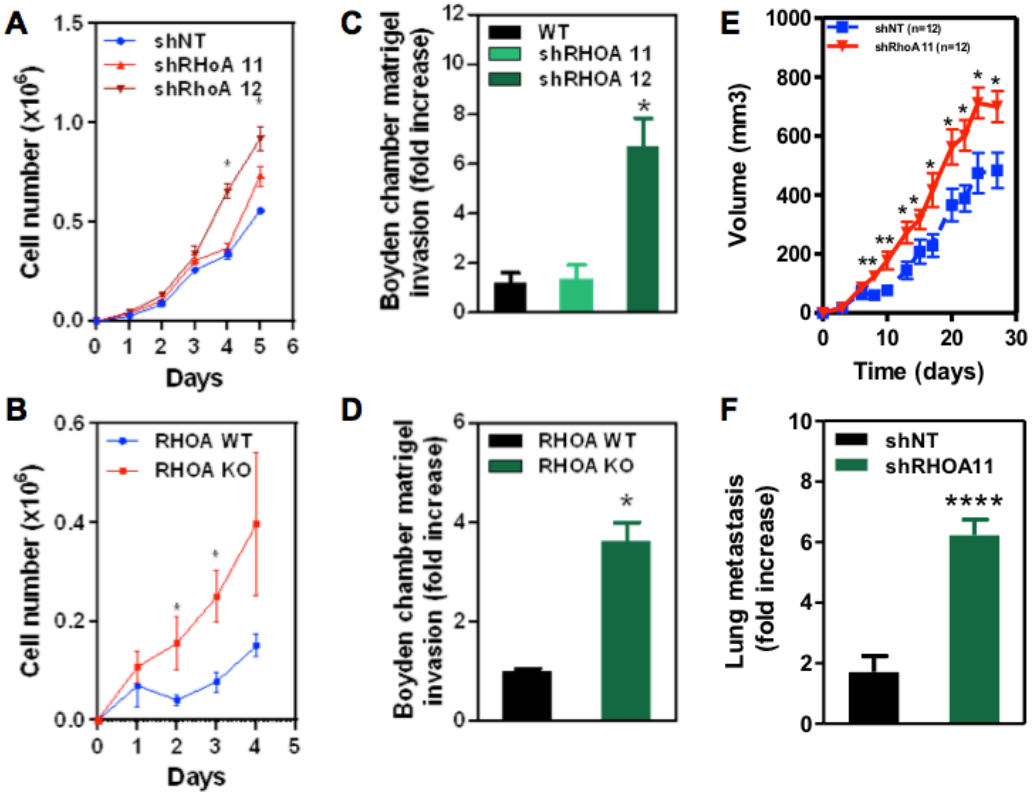

Figure 22. Effect of RHOA depletion in MKN45 gastric cancer cells.
Cellular proliferation *'in vitro'* of MKN45 cells with RHOA downregulation (A) and knockout (B). Invasion *'in vitro'* of MKN45 cells with RHOA downregulation (C) and knockout (D). Xenografts growth of MKN45 cells with RHOA downregulation (E) and lung metastasis formation of MKN45 cells with RHOA dowregulation (F).

The opposite effect is observed when it was overexpress the wild type or a constitutive activated (G14V) form of *RHOA* in diffuse gastric cell lines with low levels of RHOA (unpublised, **Figure 23A-B**). However, reintroduction of RHOA-Y42C into RHOA deficient diffuse gastric cancer cells significantly increased their growth (unpublised, **Figure 23C-E**). Moreover, in a large human gastric tumor collection it was observed that low levels of RHOA expression correlate with poor prognosis (unpublised, **Figure 23F**). Collectively, these results convincingly show that wild type *RHOA* has tumor suppressor activity in diffuse gastric cancer cells and that the recurrent hotspot

mutations observed in these tumors are oncogenic. These observations led to the hypothesis that *RHOA* hotspot mutations specifically inactivated a brach of *RHOA* signaling with tumor suppressor activity while preserving other *RHOA* signaling modules that have oncogenic activity. In this study, it was investigated the nature of the RHOA effector(s) that are tumor suppressive with the ultimate goal to exploit therapeutically this possible tumor vulnerability.

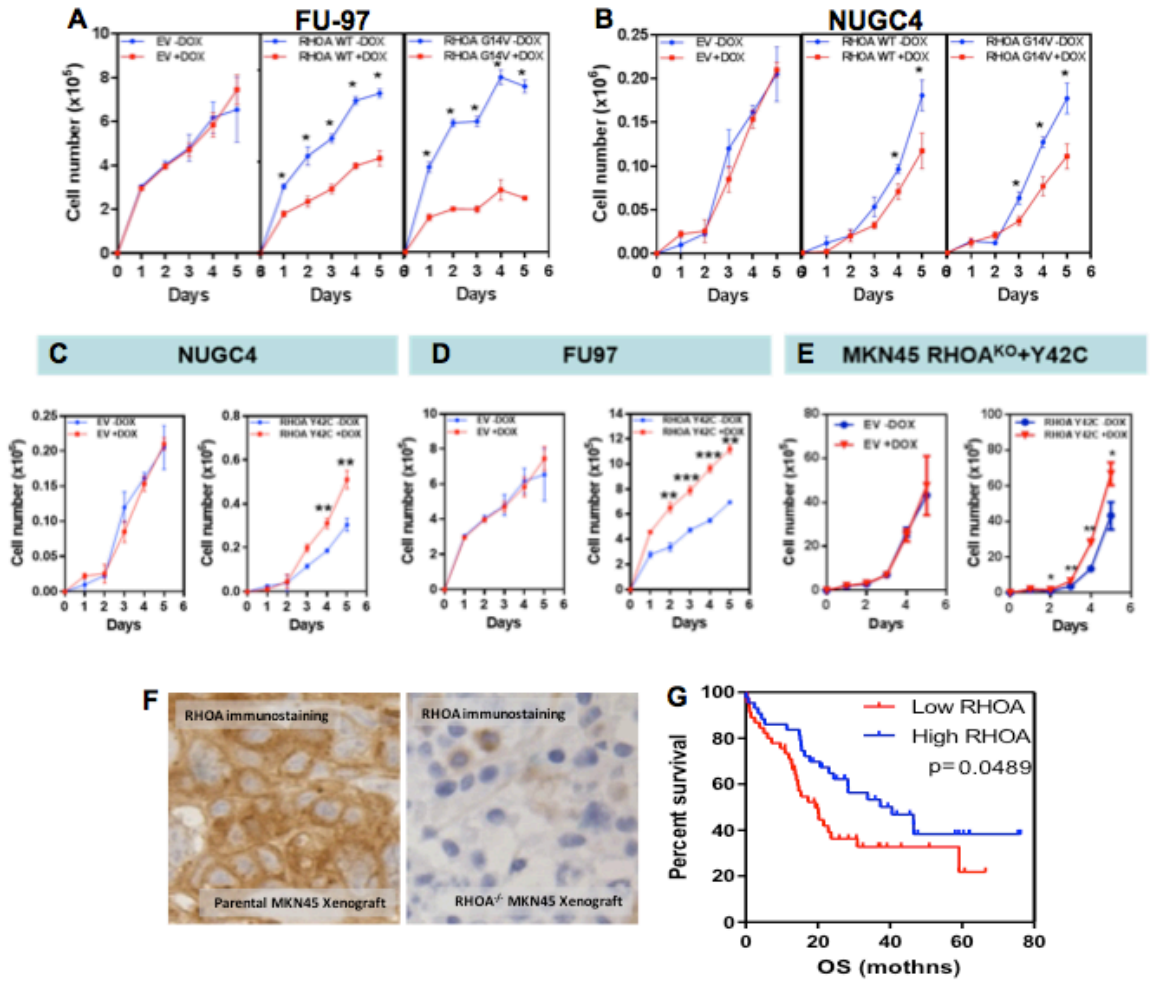

Figure 23. Effects of RHOA mutations on cell proliferation and RHOA protein expression in gastric tumors.
Cell proliferation with overexpression of RHOA wild type and constitutive active RHOA-G14V mutation in FU-97 (A) and NUGC4 (B). Cell proliferation with reintroduction of RHOA-Y42C mutation in NUGC4 (C), FU-97 (D) and MKN45 (E). F) Validation of Cell Signaling antibody rabbit monoclonal antibody anti-RHOA. G) Survival of 118 gastric cancer patients as a function of RHOA protein levels.

11. PKN protein family

11.1 Overview

Initially identified in 1994 (223), PKN (protein kinases N) family, also known as PRKs (protein kinase C-related kinases), belongs to the AGC family of kinases and consists of three members: PKN1/PRK1, PKN2/PRK2 and PKN3. The PKN enzymes are ~120 kDa proteins and has leucine zipper-like sequences (activation loop) in its amino terminal region, and contains a catalytic domain at the C-terminus region that are closely related to the novel isoforms of the protein kinase C (PKC) enzyme superfamily (**Figure 24**). PKN1–3 requires phosphorylation of the activation loop by phosphoinositide-dependent kinase 1 (PDK1), as well as turn motif phosphorylation for full catalytic activity (224). The primary amino acid sequence of the kinase domains of PKN2 and PKN3 are 87% and 70% conserved with PKN1, respectively, they differ to a large extent in their N-terminal regions, which have been shown to interact with RHO- and Rac-family GTPases, and these differences are probably related to the activation capability of each isoform (224). PKNs have been described to regulate intermediate filaments, for example vimentin glial fibrillary acidic protein as well as neurofilament proteins (225, 226).

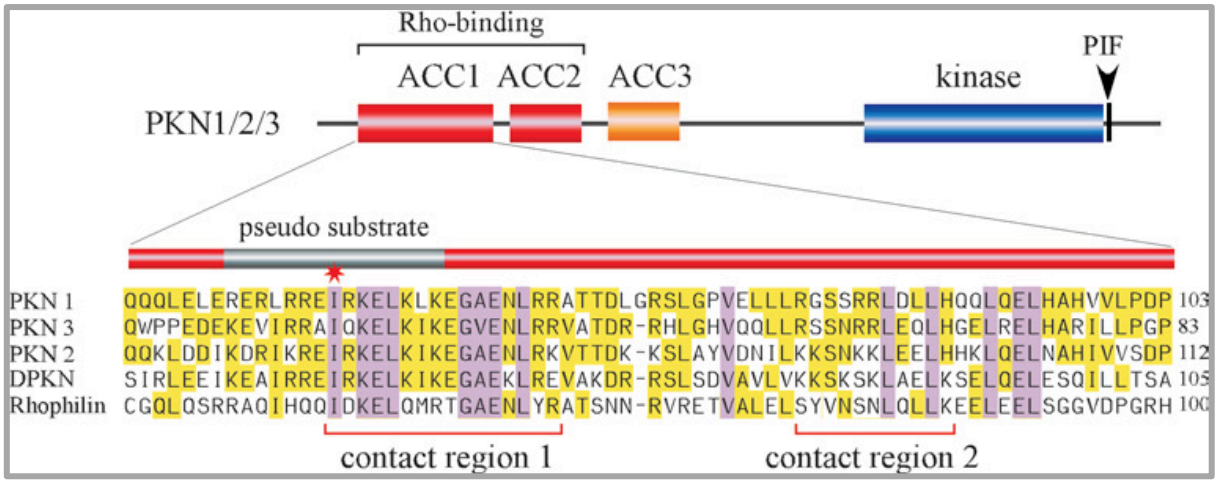

Figure 24. Domain structures of PKN family kinases.

PKNs contain three ACC structures at their N-termini and a catalytic domain at the C-terminus (blue). The hydrophobic 'PIF' motif is unusual in not requiring phosphorylation, unlike those in ROCK (RHO-kinase), MRCK (myotonin-related CDC42-binding kinase). The first two ACCs form the RHOA-binding domain (red) that overlaps a pseudo substrate region (gray), and (based on structural data) two RHOA contact regions marked by red lines. The RHOA-binding domain of PKN family kinases resembles that of a different RHOA effector, Rhophilin, as shown. A critical and conserved isoleucine residue that mimics the phosphoralatable residue is marked by a red star. Identical residues are shaded pink, and conservative substitutions in yellow. The accession numbers for sequences shown in

the alignment are BAA05169 (human PKNα/PKN1), BAA85625 (human PKNβ/PKN3), NP 006247 (human PKNγ /PKN2), NP 788291 (Drosophila DPKN) and AAL89809 (Rhophilin). Source: Zhao and Manser, 2005 (227).

11.2 Regulation of PKN activity

There is strong structural resemblance of the catalytic domains of PKN and PKC, and indeed PKN efficiently phosphorylates peptide substrates RXS/TXR/K, based on the pseudosubstrate sequence of PKC. PKN enzymes must be associated with membranes in order to be phosphorylated by PDK1. However, the mechanism of membrane anchoring differs from that of PKC in that it depends on several N-terminal HR1 domains (**Figure 20**) rather than on C1 and C2 domains (**Figure 25**). HR1 domains specifically interact with the small RHO-GTPase, which in its GTP-active form reversibly binds to membranes, thus providing a membrane-docking site for PKN. PKN1 is the first identified serine/threonine protein kinase that can bind to and be activated by a small RHO-GTPase, and it can also be activated by unsaturated fatty acids *in vitro* (228-230). In common with other GTPase-associated kinases, the interaction of RHO with the RHO binding domain in ACC1/2 in PKN appears to disrupt an auto-inhibitory intramolecular interaction, thereby allowing activation through an open conformation (231). The first ACC finger overlaps a putative pseudosubstrate site (**Figure 24**) corresponding to PKN1 residues 39–53, and the I46S substitution generates a potent substrate for PKN, thus competitive RHOA binding to the ACC1 finger domain could unmask an active catalytic domain of PKN (231). The interaction of RHO with PKN1 has been demonstrated to facilitate phosphorylation of the PKN1 activation loop by PDK1 (232, 233). Activation loop phosphorylation (on Thr-774 of PKN1 and Thr-816 of PKN2) is required for activity. Based on cotransfection experiments, an *in vivo* ternary complex of RHOA–PKN1–PDK1 was shown to be required for catalytic activation of PKN1 (233). PDK1 plays a role in the phosphorylation of equivalent residues on many other AGC kinases, such as PKCs (**Figure 25**). Thus, current models suggest that RHOA binds to PKN and induces a conformational change that is permissive for binding and phosphorylation by PDK1. The recruitment of PDK1 is likely to involve binding to the 'PIF' motif (FXXFDY) (234). This hydrophobic motif is unusual, since the acidic residue is occupied by a phosphorylatable Ser/Thr residue in most AGC kinases.

Interacting proteins that regulate PKNs are barely known; however, a proline-rich region between the C2-like region and the catalytic domain can bind various SH3 domain-containing proteins, including GRAF, a GTPase-activating protein for RHOA (235), which is suggested to

be a feedback loop to downregulate RHOA. PKN1–3 contains a Ca^{2+}-independent novel C2-domain between the N-terminal and kinase domains. The function of the C2-domain is not yet clear for the PKNs, but it may be involved in lipid binding and activation. Stimulation of PKN kinase activity in the presence of lipids *in vitro* is well documented (224, 228, 236, 237). The study to determined the kinetic mechanism and lipid sensitivity of each PKN isoform, used recombinant full-length human enzymes and a synthetic peptide substrate, it determined that PKN1–3 follows a sequential ordered Bi–Bi kinetic mechanism, where peptide substrate binding is preceded by ATP binding (229). This kinetic mechanism was confirmed by additional kinetic studies for product inhibition and affinity of small molecule inhibitors. In the same line, the study of PKN physiological substrates, enzymatic property and its regulation was first described by Mukai *et al.* (228), and they found that unsaturated fatty acids, such as arachidonic acid, linoleic acid and oleic acid increased the kinase activity of PKN. In a seminal study to determine the structural basis for lipid activation of PKN1 activity, Yoshinaga *et al.* (238) made a series of truncation mutants and found that while full-length PKN1 displayed low basal activity and demonstrated a dependence on Arachidonic acid, N-terminal truncation at residue 511 markedly increased specific activity and decreased Arachidonic acid sensitivity. A peptide corresponding to residues 455–511 inhibited PKN1 activity in a dose-dependent manner and was two-orders of magnitude less potent in the presence of Arachidonic acid. Thus, it was proposed that residues 455–511 composed an autoinhibitory domain within PKN1 that is released in the presence of lipids. This work addressed the hypothesis that interaction of lipids with the PKNs may free the protein from a compact, inhibited state, leading to enzymatic activation and downstream signalling, similar to the PKC kinases family (**Figure 25**).

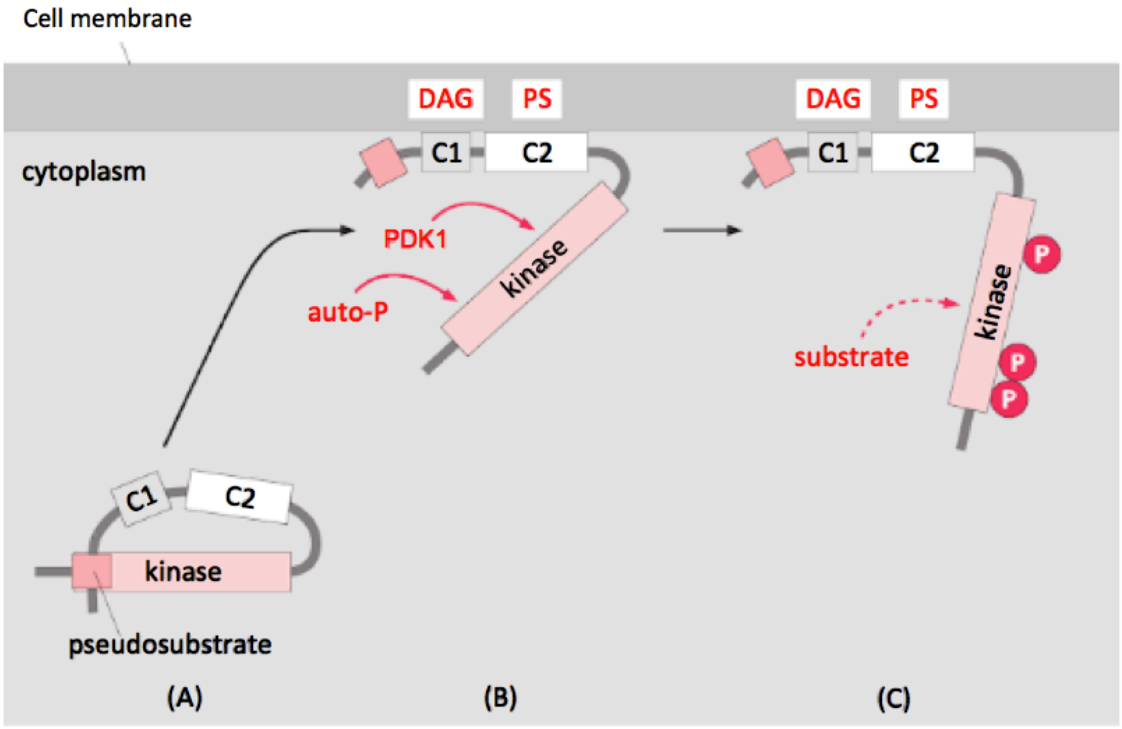

Figure 25. Activation of conventional protein kinase C.

Activation is a multistep process. (A) In the inactive enzyme, a pseudosubstrate motif occupies the binding sites for protein kinase PDK1 (which phosphorylates the activation loop of PKC) and for the substrates. (B) The blockade is lifted by binding to membrane-bound DAG and phosphatidylserine (PS). PKC can be transferred into the substrate-binding open conformation by autophosphorylation (auto-P) and phosphorylation by PDK1. (C) In the open conformation, PKC interacts with the substrates ATP and effector proteins. P= phosphate group. Source: Marks *et al.* (230).

11.3 PKN functions

PKN is widely distributed in various organisms such as mammal, frog, fly, and starfish. PKN1-3 in mammals, shows different enzymological properties, tissue distribution, and varied functions (224). As downstream effectors of RHO and Rac GTPases, once PKN has been activated, it mediates downstream signaling events involved in cytoskeletal reorganization, cell motility, apoptosis, as well as oncogenic processes. PKN1 activates a number of signaling pathways, including p38-MAPK, extracellular signal-regulated protein kinase, Jun N-terminal kinase, and the nuclear factor NF-κB (239, 240).

11.3.1 Cytoskeletal regulation

Vincent and Settleman (241) reported that the expression of a kinase-negative form of human PKN2 in microinjected NIH 3T3 fibroblasts results in the disruption of actin stress fibers, suggesting a normal role for PKN2 in regulating actin reorganization. Dong *et al.* (232) reported that the ectopic expression of PKN stimulates actin stress fiber depolymerization and membrane ruffling in 3T3 L1 and Rat1-IR fibroblasts. *In vivo* roles of PKN were first reported in *Drosophila* (242). This study showed that the loss of PKN as well as Rho mutation impairs the dorsal closure, suggesting that PKN works downstream of Rho and is required for the cell shape change during embryogenesis.

Since actin-cytoskeletal proteins such as caldesmon and G-actin are relatively preferred substrates for PKN1 *in vitro* (243), PKN1 might participate in the regulation of actin-cytoskeleton through phosphorylating these proteins by anchoring to α-actinin. PKN also directly binds to and phosphorylates the head-rod region of the intermediate filament proteins, another major cytoskeletal component, and inhibits the polymerization of some proteins *in vitro* like the subunits of neurofilament (NF) (226), vimentin, and glial fibrillary acidic protein (GFAP) (225). NF is known as one of the constituents of neurofibrillary tangles (NFTs). PKN can efficiently phosphorylate microtubule-associated protein (MAP) tau, another major constituent of NFTs, both *in vitro* and *in vivo* (244, 245). Immunocytochemical examination of postmortem human brain tissues showed that PKN is related with NFTs and abnormally modified tau in Alzheimer disease-affected neurons (246).

11.3.2 Cell adhesion

Rho-type GTPases play an important role as regulators of cell-cell adhesion in a manner which varies substantially depending on cell type and cellular context (247). A RHO V14-Y42C mutant which is selectively defective in PKN binding fails to promote recruitment of E-cadherin to cell–cell junctions in keratinocytes triggered by calcium treatment to induce keratinocyte differentiation (248). Overexpression of wild type PKN2 enhanced the cell–cell adhesion in keratinocytes triggered by calcium treatment. Tyr-phosphorylation of β- and γ-catenin and p120^{ctn}, and Fyn kinase activity are induced by overexpression of PKN2 in keratinocytes (248).

11.3.3 Vesicle transport

Electron microscopic analysis revealed that PKN1 is enriched in a subset of endoplasmic reticulum (ER) and ER-derived vesicles localized to the apical compartment of the juxtanuclear cytoplasm, as well as to late endosomes, multivesicular bodies, Golgi bodies, and secretory vesicles in neurons in human brain (246) suggesting that the enzyme is implicated in the

regulation of vesicle movement. Gampel et al. (249) reported that overexpression of RhoB retards the epidermal growth factor receptor (EGF-R) movement from early to late endosomal compartments after stimulation by EGF, and that a kinase-negative form of PKN mutant completely blocks this effect. Thus PKN1 may regulate the kinetics of EGF receptor trafficking.

11.3.4 Glucose transport

Insulin-stimulated glucose uptake is primarily mediated by the facilitative transporter Glut4, a member of a family of related transporters that are highly expressed in adipose tissue and skeletal and cardiac muscle (250). Insulin stimulates the translocation of a pool of Glut4 from vesicular compartments within the cell to the plasma membrane through a process of targeted exocytosis. In rat adipocytes, transient expression of wild-type PKN1 provokes an increase in the translocation of HA-Glut4 to the plasma membrane. However, kinase-negative PKN1 inhibits the effects of both insulin and GTPγS on HA-Glut4 translocation (251), suggesting that PKN1 contributes to Glut4 translocation during insulin and GTPγS action. PKN1 is reported to be involved in insulin-induced actin stress fiber breakdown and membrane ruffling, as described above (232). PKN1 might regulate Glut4 translocation by regulating actin cytoskeletal reorganization. Phospholipase D1 (PLD1) has been shown to localize with Glut4 vesicles and to potentiate the effects of insulin on Glut4 translocation (252). Recently PKN1 has been shown to bind to PLD1 and activate PLD1 in the presence of PIP2 (253). PKN might regulate PLD1 activity under insulin stimulation.

11.3.5 Apoptosis

Importantly, a constitutive active PKN (1-511) form contained the intact kinase domain and lacked the N-terminal regulatory domain was discovered after caspase-3-mediated proteolysis of PKN wild type (254) suggesting that constitutively active kinase activity may be a general phenomenon in apoptosis. In this context, it is of interest that PKN is expressed ubiquitously in human tissue (223), and relatively higher in testis, spleen, and thymus (237), where the apoptotic process is suggested to be active (255-257), although the physiological role of the cleavage products of PKN in apoptosis remains unknown. Possibly, PKN (1-511) constitutively phosphorylates substrates of PKN by escaping from the control of physiological regulators such as RhoA. As described above, PKN binds to and phosphorylates intermediate filaments, vimentin, and glial fibrillary acidic protein and the phosphorylation results in the inhibition of the filament assembly *in vitro* (225, 226). PKN also efficiently phosphorylates actin and caldesmon (a calmodulin binding protein) *in vitro* (243). Phosphorylation of such proteins by PKN (1-511)

might be involved in the morphological changes of the cells undergoing apoptosis, together with the caspase-mediated cleavage of cytoskeletal components (258). However, additional investigation will be required to clarify the role of the cleavage of PKN in apoptosis.

11.3.6 Regulation of meiotic maturation and embryonic cell cycles

During early development, oocytes arrest late in G2 of the first meiotic cell cycle. Hormonal stimulation results in the resumption of meiosis, known as meiotic maturation (259). In the case of starfish oocytes, meiotic maturation is characterized by the activation of Cdc2/CyclinB, breakdown of the germinal vesicle (GVBD), and the subsequent completion of meiosis I and II (260). PKN2 may regulate the early events during meiotic maturation, and the potential targets of PKN2 are the activation of Cdc2/cyclinB, translation initiation, and actin cytoskeletal changes (260). In the case of Xenopus embryos, microinjection of the active catalytic domain of PKN1 into the two-cell stage results in cell cleavage arrest in the injected blastomeres (261). On the other hand, microinjection of the kinase-negative form of PKN1 or active catalytic domain of PKCε, whose primary structure is very similar to that of PKN1, does not prevent normal cell division. Later, Yasui *et al.* (262) generated a PKN1 knockout mice and analyzed their phenotype. PKN1 knockout mice were born in a Mendelian ratio and exhibit normal appearance. However, after more than 30 weeks, they spontaneously form germinal centers in the spleen in the absence of immunization or infection and develop autoimmune-like disease, which was characterized by autoantibody production and glomerulonephritis. PKN1$^{-/-}$ B-cells were hyperresponsive and had increase phosphorylated Akt1 levels upon B-cell antigen receptor (BCR) stimulation. They found found that PKN1 negatively regulates Akt kinase downstream of the BCR and that this regulation is necessary for normal germinal centers development. PKN1 interacted with and inhibited Akt1 kinase and transforming activities. These results indicate that PKN1 down-regulation of BCR-activated Akt activity is critical for normal germinal centers B-cell survival. Recently, Quétier et al. (263) describe a murine model with knockouts of all three mouse PKN isoforms and reveal that PKN2, but not PKN1 or PKN3, is essential during mouse embryogenesis, PKN2 loss results in lethality at embryonic day 10 (E10), with associated cardiovascular and morphogenetic defects. Inducible systemic deletion of PKN2 after E7 resulted in the collapse of the embryonic mesoderm. Furthermore, mouse embryonic fibroblasts depend on PKN2 for proliferation and motility, these cellular defects were reflected *in vivo* as dependence on PKN2 for mesoderm proliferation and neural crest migration.

11.3.7 Signaling to the cell nucleus

PKN1 translocates from the cytosol to the nucleus in response to various stresses such as heat shock, and PKN2 translocates from the cytoplasm to germinal vesicles during meiotic maturation in starfish oocytes (260). However, the relevant nuclear targets of PKN have not been clearly identified. Co-expression of heat shock transcription factor 1 (HSF1) and the active catalytic domain of PKN1 in HeLa S3 cells and C6 glioma cells shows accumulation of small HSP αB-crystallin, whereas individual expression of HSF1 or PKN1 separately does not show accumulation of αB-cyrstallin (264). αB-crystallin is suggested to confer increased stress resistance, especially by associating with cytoskeletal elements to protect cellular integrity. Interestingly, inhibitors of cyclooxygenases and activators of phospholipase A2 stimulate the induction of αB-crystallin during heat and arsenite stress, suggesting that arachidonic acid stimulates the production of αB-crystallin (265). PKN may be implicated as a downstream effector of Rho in transcriptional responses in cardiomyocytes, which is associated with cardiac hypertrophy (266). Activated Rho can also stimulate c-jun expression and the activity of the c-jun promoter. PKN1, MKK3/MKK6, and ERK6 (p38γ) were reported to be involved in this signaling pathway, with consequent stimulation of transcription factors ATF2 and MEF2A, which act on the c-jun promoter through the jAP1 and MEF2 responsive elements (267). PKN1 may act as MAPKKKK and mediate Rho and lipid signals to the p38γ-MAP kinase cascade, by analogy to the Rac/PAK/p38 MAP kinase pathway (267). In addition to these reports, neuron-specific Helix-LooP-Helix (bHLH) transcription factor, NDRF/NeuroD2 were isolated as binding partners of PKN1. Transient transfection assays revealed that co-expression of a catalytically active form of PKN1 significantly enhances NDRF/NeuroD2-mediated transactivation activity (213). PKN might be involved in the mechanism of neuronal differentiation.

12. Role of PKN in Cancer

Individual PKN isoforms vary in tissue distribution, with PKN1 and PKN2 ubiquitously expressed, and PKN3 mainly restricted to various tumor tissues (224). Therefore, the PKNs have begun to be scrutinized as possible drug targets for the treatment of cancer, both with inhibitors and activators also for understanding PKN biology (229).

PKN1 has been linked to prostate cancer through its interaction with the androgen receptor (268, 269). Notably, PKN1 regulates endometrial cancer cell proliferation, migration, and invasiveness, by modulating TGF-β and epidermal growth factor (EGF) dependence (270). It has been reported that overexpression of PKN1 correlates with aggressive ovarian (271) and colorectal cancers (272). Other findings suggested that PKN1 has a role in the development of invasive

phenotypes of breast cancer cells (273). PKN2 was recently implicated in triple negative breast cancer (274) and in bladder tumor cells PKN2 has a critical role in the migration and invasion of these cells (275). PKN3 was found to be required for malignant growth in a prostate tumor model downstream of an activated phosphoinositide 3-kinase (PI3K) and was targeted using an RNAi (RNA interference) approach for solid tumors in Phase I clinical trials (276). Also, PKN1 and PKN2 contribute to motility pathways in human prostate cancer cells. Their activity is regulated by TORC2-dependent phosphorylation of the TM (turn-motif) PKNs (277). *In vivo*, triple knockout of Pten, Pkn1, and Pkn2 in mouse model results in squamous cell carcinoma, an uncommon but therapy-resistant form of prostate cancer (277).

The high risk human papillomaviruses (HPVs) are associated with carcinomas of cervix and other genital tumors (278). HPVs are categorized into low risk and high risk HPVs. Previous studies have identified two viral oncoproteins E6 and E7, which are expressed in the majority of HPV-associated carcinomas (279, 280). Only E6 and E7 genes are necessary for the immortalization activity of HPVs, in addition to E6-induced degradation of p53 tumor suppressor protein, other targets of E6 are required for mammary epithelial cells immortalization. Gao *et al.* (281) using the yeast two-hybrid system identified E6 oncoproteins of high risk HPVs (HPV16 and HPV18) preferentially interact with the C-terminal region of PKN1 as compared with the E6 protein of low risk HPVs (HPV6 and HPV11). Furthermore, all the immortalization-competent and many immortalization-non-competent E6 mutants retain the ability to interact with PKN1. These data suggest that binding to PKN may be required but not sufficient for immortalizing normal mammary epithelial cells. They also show that PKN phosphorylates E6, demonstrating that HPV E6 is a phosphoprotein. Further analysis is necessary to elucidate functional regulation between E6 and PKN. Despite these reports, there has been little work on the role of PKN proteins, specifically PKN1 in human DGC.

13. Current Gastric Cancer Therapeutic Approaches

Although therapeutic methods are improving with surgery combined with radiotherapy and chemotherapy, the benefits for advanced GC are far from optimal with the median survival rate of patients with advanced GC being still less than 12 months (47). The improvements in early diagnosis and the treatment of the GC may continue to be the most effective strategy for improving patient survival. Thus, seeking for more sensitive early detection approaches and effective therapeutic agents, particularly those targeting cancer progression mechanisms, are urgently needed.

Most of the strategies for testing the efficacy of gene therapy for gastric cancer have involved the use of adenoviral vectors. Some of the adenovirus-mediated approaches include transfer of p53, Bax, truncated dominant negative IGF-I receptor, enhancement of the c-Jun N-terminal kinase to reduce the level of P-glycoprotein, transduction of soluble VEGF-receptor (Flt-1) in peritoneal mesothelial cells to inhibit the angiogenesis and the dissemination of gastric cancer *in vivo* to increase the survival of treated animals (282-286).

DNA methylation (CpG) and histone deacetylation (HDAC) processes have assumed significance in recent years for risk assessment, detection, prognostic evaluation, and as therapeutic targets. In particular, the use of HDAC inhibitors that can reactivate transcriptionally silenced genes to induce cell differentiation, apoptosis, and growth suppression is an innovative approach in the treatment of gastric cancer (287). Nishigaki *et al.* (288) by using microarrays, identified 1,383 gene candidates reactivated in at least one cell line of eight gastric cancer cell lines after treatment with 5-aza-2'deoxycytidine and trichostatin A. The candidate gene R-RAS showed that demethylation of specific CpG sites within its first intron causes activation in more than half of gastric cancers. Then, introduction of siRNA into R-RAS-expressing cells resulted in the disappearance of the adhered cells, suggesting that functional blocking of the R-RAS signaling pathway has great potential for gastric cancer therapy.

So far, a couple of molecularly targeted drugs have been developed against gastric cancer, including HER2 antagonists. In the intestinal type of gastric cancer, the most common type, approximately 30% of tumors show positivity for HER2 protein expression; however, only fewer than 10% of DGC tumors show positivity for HER2 (289, 290). Thus, DGC constitutes a poor-prognosis subgroup of gastric cancer with very low effective molecularly targeted therapies.

As mentioned bebore, two independent genomic characterization of gastric cancer presented by Wang *et al.* (193) and Zang *et al.* (194) reported frequent mutations in *TP53*, *PTEN*, *ARID1A*, *APC*, *CTNNB1*, *CDH1, PI3KCA*, *KMT2C, FAT4*, and other genes. However, most of the sequenced tumors in these studies were intestinal-type gastric cancers (IGCs); given the need for new therapeutic targets for DGC, the recent whole-genome sequencing studies (173, 185) made an effort to determine if the role of RHOA activity and the novel RHOA mutants can be exploited as a therapeutic vulnerability.

RHO signaling has been widely reported to be oncogenic, and as such, different therapeutic approaches aimed at RHO inactivation have been proposed (**Figure 26**). First, RHO proteins require lipid modifications at their carboxyl termini to be active (**Figure 26a**); RHO mutants that sequester RHO–GEFs into non-functional complexes away from the endogenous RHO proteins have also proved to be a useful experimental strategy for regulation of RHO-protein function

(**Figure 26b**). In a similar manner, RHO-protein-binding domains have been used to sequester RHO-effector into nonfunctional complexes (**Figure 26c**). Finally, several of the RHO-effector pathways might be useful therapy targets, particularly, effector kinases such as PKN and ROCK (**Figure 26d**) (291).

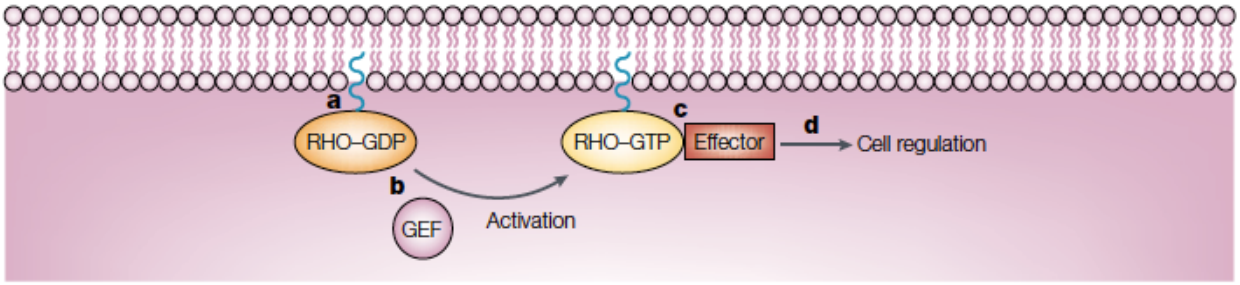

Figure 26. Methods of interfering with RHO-protein function.

a) Prevention of targeting of protein. Geranylgeranyltransferase inhibitors or farnesyltransferase inhibitors prevent the lipid modification of RHO proteins. **b)** Inhibition of RHO guanine nucleotide exchange factors (RHO–GEFs). RHO-protein mutants that only bind GDP interfere with RHO–GEF function and reduce endogenous RHO-protein activity. **c)** Disruption of RHO-protein–effector complexes. Overexpression of minimal RHO-protein binding domains can sequester GTP-bound RHO proteins away from their effectors. **d)** Inhibition of effector protein activity. The enzymatic functions of effector proteins can be targeted. Source: Sahai, E *et al.* 2002 (291)

However, our previous results (unpublished data, **Figure 22-23**) convincingly demonstrate that wild type RHOA is a strong tumor suppressor gene in gastric cancer, while hotspot RHOA mutations are oncogenic (unpublised data, **Figure 22-23**). Because the most frequent RHOA mutation in gastric tumors (Y42C) lacks the capacity to bind to the RHOA-GTPase effector PKN (292), the RHOA tumor-suppressor activity is propose to be mediated through PKN. Therefore, in this study I first investigate whether other hotspot RHOA mutations also interfere with the binding to PKN, and then it was characterized the potential tumor suppressor activity of PKN in gastric cancer cells. In addition, the portential therapeutic value of PKN reactivation in diffuse gastric cancer cells is also investigated. Because the RHOA hotspot mutations found in diffuse gastric cancer seem to inactivate the physiological activator of the putative tumor suppressor gene PKN, it was hypothesized that PKN is still present in these tumor cells, albeit inactive. This is in sharp contrast to most tumor suppressor genes, which are almost invariably directly inactivated by genetic mutations and their reactivation is not feasible. This unique situation potentially represents a true vulnerability of these gastric tumors that could be exploited

therapeutically if there were alternative mechanisms to reactivate this tumor suppressor signaling pathways. Importantly, PKN can be reactivated in these cells by arachidonic acid treatment, thus providing a novel therapeutic opportunity that is investigated here using *in vitro* systems and a preclinical mouse model of peritoneal deissemination of gastric cancer.

AIMS OF THE STUDY

CHAPTER II. AIMS OF THE STUDY

Recent results from our work have shown that RHOA has tumor suppressor activities in colon cancer (222) and also in gastric cancer (not published). In addition it has been reported by two independent groups that RHOA could be tumor suppressor or an oncogenic gene (184, 185), and the controversy needs to be solved. Also it has been reported that RHOA is frequently mutated in the diffuse type of gastric cancer, the most frequently mutation is the RHOA-Y42C which has already been described to inhibit RHOA binding to the effector PKN1 (292). Therefore, in this thesis we focus our investigation on the protein kinase N1, PKN1.
Little is known about the role of RHOA GTPase effector PKN1 in the development of gastric carcinogenesis and the possible mechanisms underlying in this process.

Therefore, the specific aims of this thesis are:

1. To investigate the effects of the most prevalent RHOA mutation observed in gastric cancer (RHOA-Y42C) using a novel murine model.

2. To investigate the effects of the most common gastric cancer hotspot RHOA mutations on the binding to effector proteins.

3. To investigate the role of PKN1 in gastric cancer using engineered *in vitro* systems.
   3.1 Study the effects on tumor growth
   3.2 Study the effects on metastasis

4. To assess the potential of PKN reactivation through arachidonic acid treatment, as a novel therapeutic target.

MATERIALS AND METHODS

CHAPTER III. MATERIALS AND METHODS

1. Materials

Human gastric cancer cell lines. A total of 9 diffuse type gastric cancer cell lines were used: FU-97, GCIY, KatoIII, MKN45, NUGC3, NUGC4, OCUM1, SNU-16, and SNU-5 were purchased from ATCC bank (https://www.atcc.org/). All cell lines were maintained on Dubelco's Modified Eagle's Medium (DMEM; SIGMA) containing 10% fetal bovine serum (Sigma) and 1x antibiotic-antimycotic (Life Technologies; 1000 U/mL streptomycin, 100 U/mL penicillin, and 0.25 µg/mL amphotericin B) at 37ºC and 5% CO_2. All the cell lines were tested to be negative for mycoplasma contamination by PCR Mycoplasma Detection Set (TaKaRa Bio, Inc. Kusatzu, Japan) every time before use.

Plasmids. Knockout cell line model: For this purpose, CRISPR/Cas9 technology was used. The sgRNA sequence targeting PKN1 exon 2 was designed using CRISPR design tool (http://crispr.mit.edu). The sgRNA was selected according to its on-target score (91.1 on a scale ranging from 0 to 100) and low probability of off-targets (5' GCTGCGGCGGGAAATCCGCA 3'). The predicted sequence was cloned into pSpCas9(BB)-2A-GFP (pX458, Addgene #48138) following the protocol described by Zhang's Lab (293). pINDUCER toolkit was used to generate cell lines with doxycycline-inducible overexpression or downregulation of PKN1 (294). **Downregulation cell line models:** two different shRNA sequences previously reported against PKN1 were used: sh1 (295), sh2 (296). As non-targeting control (shNT) an shRNA sequence against firefly luciferase was selected (**Table 5**). Then, using as backbone the mir30-shRNA, shRNA for PKN1 downregulation were designed using RNAi oligo retriever web server (http://cancan.cshl.edu/cgi-bin/Codex/Codex.cgi) and cloned into pINDUCER10 following the protocol described by Paddison *et al.* (297). **Overexpression cell line models:** A constitutively active PKN1 truncated form, containing 1-511 aa, was obtained from original PKN1 into pRC/CMV-FLAG-PKN1, a gift from Dr. Hideyuki Mukai (Biosignal Research Center, Kobe University, Japan), *EcoR*I and *BamH*I sites were used to cloned into pENTR-MCS-mCherry plasmid. Then, the sequence was transferred to pINDUCER20 through gateway cloning (Life technologies, USA). pINDUCER20 vector containing only the fluorescent protein mCherry was used as a control. **Lentiviral packaging plasmids:** pMD.G2 and psPAX packaging vectors for lentivirus production were obtained from Addgene (#12259 and #12260 respectively). **Yeast**

two-hybrid assay: Initially, the bait construct was prepared by designing primers with engineered *EcoR*I and *BamH*I restriction sites (**Table 5**); to generate the bait construct, the full open reading frame of RHOA was PCR-amplified from pDEST15-RHOA Clon5 with primers containing restriction sites for *EcoR*I and *BamH*I enzymes and then cloned into the pGBT9 vector. The mutant forms of RHOA (R5Q, L57V, Y42C or G17E) were generated using QuikChange mutagenesis kit (Agilent Technologies Inc.) according to manufacturer's specifications and cloned in frame with the yeast GAL4 transcription factor DNA-binding domain. The DNA oligos used for mutagenesis are shown in **Table 5**. The 'prey' to test interactions was done by mating the bait strain to a yeast strain pre-transformed with ROCK1, DIAPH2, full length PKN1 and Kinetin in a pGAD424 shuttle vector, all these vectors were a kind gift from Dr. Erik Sahai (Tumor Cell Biology Laboratory, Francis Crick Institute, London, UK). **Pull down assay:** The complete open reading frame of RHOA with *EcoR*I and *BamH*I restriction sites was cloned into a pGEX-4T vector, leading to the expression of GST-RHOA under the control of a *lac* promoter, inducible by the lactose analog isopropyl β-D-1-thiogalactopyranoside (IPTG). pGEX-Rhotekin GST plasmid, that contains the RHO binding domain of ROCK effector was used as a positive control. **Validation of RHOA-Y42C mutant expression:** Before being injected in the animals, the DNA construct used to generate the RHOA-Y42C mouse model was tested '*in vitro'* for RHOA protein overexpression*.* HEK293T cells were transiently transfected with pBabeGFP from Addgene, #10668 (Empty backbone for retroviral gene expression, to select recipient cells using GFP), pBabe-Cre a gift from Dr. Josep Villanueva (Tumor Biomarkers Program, Vall d'Hebron Institut of Oncology, Barcelona, Spain), LoxP-CAT a gift from Dr. Kazuto Kobayashi (Department of Molecular Genetics, Institute of Biomedical Sciences, Fukushima Medical University School of Medicine, Fukushima, Japan) and the newly generated LoxP-RhoA-Y42C.

Table 5. **DNA oligos used in this study**

Primer Name	Product Size (bp)	Sequence (5'to 3')	Application
APC-common		TTCCACTTTGGCATAAGGC	*Apc*^{min} mouse genotyping
APC-WT	600	GCCATCCCTTCACGTTAG	
APC-MIN	340	TTCTGAGAAAGACAGAAGTTA	
RHOA F	702	CAGGAGTCGCATAAGGGAGA	Y42C-RhoA mouse Genotyping
RHOA-DN-R		TCACAAGACAAGGCAACCAGATT	
Myo6 -WT-F	200	TTGGGATGTGAAATCCATGT	
Myo6-WT-R		CTGAACTTTCTTCCAGCGACT	
VIL-CRE-F	290	CAAGCCTGGCTCGACGGCC	VIL-CRE

VIL-CRE-R		CGCGAACATCTTCAGGTTCT	mouse Genotyping
PKN1 CRISPR EXON2 -F	385	CCACTGACCCTGTTCTGTCC	PKN1 exon2 sequencing
PKN1 CRISPR EXON2 -R		AGCCAGTGAGCAGTGGAATC	
shRNA1		AGCCCGGACCACGGGTGACATA	PKN1 Downregulation
shRNA2		CCGCCATCAAGGCTCTGAAGAA	
shRNA-NT		AGCTCCCGTGAATTGGAATCC	
PKN1 qPCR F		AAGCCGAGAACACCAGTGAAG	Quantitative PCR (qPCR)
PKN1 qPCR R		GCACCTCATGCCTCTCATTGT	
RHOA R5Q F1		CAATCACCAGTTTCTTCTGGATGGCAGCCATGGTT	RHOA mutagenesis
RHOA R5Q R1		AACCATGGCTGCCATCCAGAAGAAACTGGTGATTG	
RHOA G17EF		GAGCAAGCATGTCTTTTCACAGGCTCCATCACC	
RHOA G17E R		GGTGATGGAGCCTGTGAAAAGACATGCTTGCTC	
RHOA L57V F		CTGTGTCCCACACAGCCAACTCTACCTGCTTTCCA	
RHOA L57V R		TGGAAAGCAGGTAGAGTTGGCTGTGTGGGACACAG	
RHOAG14V F		GGTGATTGTTGGTGATGTAGCCTGTGGAAAGACAT	Yeast two-hybrid
RHOAG14V R		ATGTCTTTCCACAGGCTACATCACCAACAATCACC	
RHOA Y42C F		GATATCTGCCACACAGTTCTCAAACACTGTGGGCAC	Pull-down
RHOA Y42C R		GTGCCCACAGTGTTTGAGAACTGTGTGGCAGATATC	
RHOA G17E F		GAGCAAGCATGTCTTTTCACAGGCTACATCACC	Yeast two-hybrid
RHOA G17E R		GGTGATGTAGCCTGTGAAAAGACATGCTTGCTC	

Table 6. Primary antibodies used in this study

Antibody	**Source**	**Reference clone**	**Host**	**Application (dilution)**
PKN1 (H234)	Santa Cruz	sc-7161	Rabbit	Wb (1:200)
PKN1	LS Bio	LS-B13584	Rabbit	Wb (1:1000)
PKN1	Atlas Antibodies	HPA003982	Rabbit	Wb (1:200)
Anti-PRK3+PRK2+PRK1 (phospho T718 + T816 + T774 + T718 + T816 + T774) antibody	Abcam	ab187660	Rabbit	Wb (1:200)
PKN2	Atlas Antibodies	HPA034861	Rabbit	Wb (1:200)
β-tubulin	Sigma	T4026	Mouse	Wb (1:5000)
GAPDH	Santa Cruz	sc-32233	Mouse	Wb (1:5000)
BrdU	Developmental Studies Hybridoma Bank	G3G4	Mouse	HIC (1:15)
KRT19	Progen	61010	Mouse	IHC (1:500)
PG1	Atlas Antibodies	HPA031717	Rabbit	IHC (1:600)
Caspase 3 Active	R & D Systems	AF835	Rabbit	IHC (1:500)
Polyclonal Swine Anti-Rabbit Ig/HRP	Dako	P0217	Swine	Secondary Wb (1:10000)
Polyclonal Rabbit Anti-Human IgG/HRG	Dako	P0447	Goat	Secondary Wb (1:10000)

2. Methods

Knockout cell line model: MKN45 cells were transfected with pX458-sgRNA-PKN1 employing Lipofectamine (Lipofectamine™ 2000, Invitrogen). GFP positive cells were sorted 48 h after transfection, seeded at low density on a 10 cm plate ($5x10^3$ cells/plate) and grown until individual colonies were visible. Then, individual clones were picked and expanded. After DNA sequencing

and characterization by Western blot, four knockout clones were selected for experimental work and three wild type clones were selected as a negative control. **Stable PKN1 downregulation:** NUGC3 cells were stably transduced with short-hairpin RNAs by lentiviral infection (shRNA PKN1) and subsequently selected with puromycin. Production of lentiviral shRNA vectors and infection of the gastric cancer cell lines was carried out as follows: **Day 1**, TLA-HEK293T cells ($3x10^6$ cells) were plated on 10 cm poly-lysine coated plates/high adherence plates to have them ~80% confluent on the following day. **Day 2**, 2 hours prior transfection cell medium was replaced with 10 mL complete medium + 25 µM chloroquine. TLA-HEK293T cells were transfected with 10 µg of DNA of the viral vector, 3.5 µg of pMD.G2 and 2.75 µg of pPAX2, and up to complete 1000 µL with NaCl 150 mM. For transfection PEI (1 mg/mL) was used in 4:1 ratio to DNA. The transfection mixture was added to the cells in a drop wise manner, swirled slowly and incubated overnight. From this point on, biosecurity level-2 conditions were applied (298). **Day 3**, the medium was removed from the transfected cells and replaced with 6 mL reduced serum medium (2%) + 5 mM sodium butyrate. The cells were incubated at 37°C, 5% CO_2 for 24 h. **Day 4**, 24 h after medium change, 6 mL of supernatant containing the viral particles were collected from the plates, filtered with 0.45 µm filters and viral supernatants stored at 4°C. The medium was again replaced with new reduced serum medium + sodium butyrate and the cells were incubated at 37°C, 5% CO_2 for 24 h. The fourth day the target cells were seeded ($1x10^6$ cells) to assure that the cell confluence be at least 25-30% the day of infection. **Day 5**, 6 mL of supernatant containing the viral particles were collected from the plates, filtered with 0.45 µm filters. Both viral aliquots from day 4 and 5 were mixed. The medium from the target cells was removed and replaced with the viral supernatant mix containing polybrene (8 µg/mL) and incubated at 37°C, 5% CO_2 for 6 h. After 6 hours of cell infection the viral supernatant was replaced with new complete medium and kept for 72 h in culture for cell recovery. **Day 8**, the selective medium was added (puromycin diluted in complete DMEM to a final concentration of 9 µg/mL for NUGC3) and changed every 2 days. Once the selection period was finished, PKN1 inhibition was tested by Real-Time qPCR and Western blot 7 days after induction with 1 mg/mL doxycycline. **Inducible PKN1 overexpression:** FU-97 and NUGC4 cells were stable transduced with a pINDUCER20 vector expressing the constitutively active form of $PKN1^{1-511}$ under the control of doxycycline and subsequently selected with neomycin at 80 µg/mL for FU-97 cells and 750 µg/mL for NUGC4 cells determined previously with a killing curve. The cell infection protocol applied was the same as it is mentioned above. Low passage cells (<10) were used for all the experiments.

DNA extraction and sequencing. ***DNA extraction from cells:*** DNA from MKN45 clones was extracted using DNAzol® (Invitrogen) according to manufacturer's instructions. Exon 2 region CRISPR targeted was amplified using PKN1 CRISPR EXON2-F and PKN1 CRISPR EXON2-R primers (**Table 5**). After PCR, residual primers and nucleotides were removed from the reaction product by adding ExoSAP mix (0.1 U Exonuclease I, Fermentas and 0.056 U Shrimp Alkaline Phosphatase, Roche). Samples were sent to Macrogen for sequencing. ***DNA extraction from mice:*** Genomic DNA extraction was performed from ear or tail clips following HotShot protocol (299). Presence of $RhoA^{Y42C}$ mice was verified by sequencing after PCR amplification with the corresponding primers listed in **Table 5**. ExoSAP and sequencing was conducted as previously described.

RNA extraction and quantitative real-time PCR (qPCR). Total RNA was extracted with TRIZOL® (Invitrogen) according to the instructions of the manufacturer and retro-transcribed using the High Capacity cDNA Reverse Transcription Kit (Applied Biosystems). Real time PCR reactions were performed in duplicate on an ABI PRISM 7500 Real-Time System (Applied Biosystems) using the SYBR green method or TaqMan Gene Expression Assay for the 18S house-keeping gene. PKN1 mRNA was amplified using the primers described in **Table 5**. The relative mRNA levels were calculated using the comparative ΔΔCt method as previously described (300).

Protein extraction and quantification. To obtain whole protein cell lysates, cell cultures in the exponential growth phase were washed twice with ice-cold PBS 1X and harvested with a sterile rubber scraper. Pellets were collected in Eppendorf microtubes by centrifugation (Eppendorf centrifuge 5424 R) for 5 min, 3000 xg, at 4°C, and then resuspended in 50 µL of Small GTPase lysis buffer (25 mM Hepes pH 7.5, 150 mM NaCl, 5 mM $MgCl_2$, 1% NP-40, 1mM DTT, 10% Glycerol) supplemented with protease inhibitors cocktail (Complete™, Mini, EDTA-free Protease Inhibitor Cocktail, Roche). The lysate was centrifuged for 5 min, 16000 xg, at 4°C, and the supernatant was transferred into a new microtube and stored at -80°C. Protein concentration was quantified with a BCA™ Protein Assay Kit (Thermo Scientific). Briefly, 5 µL of test sample diluted in distilled water (final volume 25 µL) were mixed with 200 µL of BCA mixture in 96 well plate. A series of BSA protein standards diluted in distilled water was run alongside with the protein lysates to establish a standard curve. Samples were incubated in the dark at 37°C for 30 min. The absorbance was then read at 620 nm on a plate reader (Sunrise™ model, TECAN

Group Ltd.). Protein concentrations were determined by comparison with the BSA standard curve.

Western blot. ***Gel separation:*** protein separation was performed by one-dimensional SDS-PAGE electrophoresis assay as follows. Proteins were thawed on ice and 200 µg were mixed with Laemmli buffer 1X (25 mM Tris pH 6.8, 8% SDS, 40% Glycerol, 400 mM β-mercaptoethanol, 0.02% bromophenol blue) and denatured at 95°C for 5 minutes before being loaded into a polyacrylamide gel (4% stacking gel, 7.5% resolving gel). The electrophoresis chamber was filled with Runing buffer 1X (25 mM Tris, 192 mM glycine, 0.1% SDS). The power was set to 100 V and proteins were left to run until the loading dye reached the edge of the gel. **Protein transfer:** for the transfer of the separated proteins from the gel to a PVDF (PolyVinyliDene Fluoride) membrane, a wet blotting system was used. For this, the membrane and gel were set up as a "sandwich configuration" together with filter papers and sponges in the following order: sponge, filter paper, gel, membrane, filter paper and sponge. The setting up was run a 100V for 90 min in a transfer chamber filled with ice-cold transfer buffer (0.023M Tris and 0.19M Glycine). ***Blocking and Blotting:*** After protein transfer, the membrane was blocked with blocking buffer (5% skim milk in PBS-0.1% Tween-20) for 1 hour to avoid unspecific antibody binding. The membrane was then incubated overnight with the primary antibody at the corresponding dilution (**Table 6**). Next day, the membrane was extensively washed with PBS-0.1% Tween. The membrane was then incubated for 1 hour at room temperature (RT) with secondary antibody conjugated with horseradish peroxidase at the corresponding concentration (**Table 6**). ***Detection:*** Detection of protein by Western blotting was achieved using Enhanced Chemiluminescence system (ECL, GE Healthcare), a light-emitting non-radioactive substrate for the horseradish peroxidase. The membranes were incubated with an equal volume of detection reagent A and reagent B for 1 minute. Then, AGFA (CP-BU) films were exposed to the membrane to detect the chemiluminescent signal, and after automated film development the bands were visualized.

Flow cytometry analysis. mCherry reporter expression in FU-97-EV/PKN1$^{1-511}$ and NUGC4-EV/PKN1$^{1-511}$ and RFP in NUGC3-sh1, NUGC3-sh2, NUGC3-shNT were analyzed by flow cytometry (BD LSRFortessa™). Briefly, PKN1 overexpression or downregulation was induced with doxycycline (Dox; 0.1 µg/mL and 1 µg/mL respectively) for 48 h prior to trypsinization. Cells were filtered and then resuspended in PBS + 10% FBS for the analysis.

In vitro proliferation. Changes in cell proliferation were assessed using direct cell counting: Gastric cancer cell lines were seeded into 24-well flat-bottom plates in triplicate and allowed to adhere overnight. ***Knockout and downregulation cell line models:*** MKN45 wild type and knockout cell lines ($2.5x10^4$ cells) were seeded. To induce knockdown, NUGC3-sh1, NUGC3-sh2, and NUGC3-shNT cells were treated with or without Dox (1 µg/mL) for 7 days before seeding ($2x10^4$ cells). ***Overexpression cell line models:*** $1x10^5$ FU-97-EV/PKN1$^{1-511}$ and $2x10^4$ NUGC4-EV/PKN1$^{1-511}$ cells were treated with or without Dox (0.5 µg/mL) for 72 h before seeding, and then seeded as described. For cell count, cells were trypsinized and stained with trypan blue, viable cells were manually counted in a light-microscope every 24 h. Three independent experiments were carried out.

Clonogenicity assay. ***Knockout and downregulation cell line models:*** Five hundred MKN45 PKN1 wild type and PKN1 knockout cells were seeded in triplicate wells of 6-well plates. Control or Dox-containing medium was replaced twice per week. $1x10^3$ NUGC3-sh1, NUGC3-sh2, and NUGC3-shNT cells were treated with or without 1 µg/mL Dox as was described before and seeded into 6-well plates. Medium was renewed weekly with or without Dox, as corresponding. Once the colonies were visible, the plates were fixed with 1 mL methanol:acetic acid (3:1) for 5 min and stained with 5% crystal violet (Acros organics) in 1% methanol for 20 min. The number of macroscopically visible colonies was scored blinded from the sample identity using ImageJ software (https://imagej.nih.gov/ij/). ***Overexpression cell line models:*** $5x10^3$ FU-97-EV/PKN1$^{1-511}$ or NUGC4-EV/PKN1$^{1-511}$ cells were seeded into 6-well plates with medium containing or not Dox (0.1 µg/mL) and allowed to attach and grow as individual colonies. The medium was replaced twice per week (with or without Dox as corresponding). At least, three independent experiments were carried out in triplicate.

Soft-agar colony formation assay. ***Knockout and downregulation cell line models:*** $1x10^4$ MKN45 PKN1 wild type and PKN1 knockout cell lines were resuspended in complete DMEM medium containing 0.3% agar and then plated onto six-well plates on top of 0.6% agar in DMEM medium previously polymerized. Cultures were grown for 21 days at 37°C, 5% CO_2 until colonies were visible. The colonies were stained with nitro blue tetrazolium chloride (1mg/mL; Sigma-Aldrich) and the number of macroscopically visible colonies was scored using OpenCFU software (http://opencfu.sourceforge.net/). ***Overexpression cell line models:*** $2x10^5$ FU-97-EV/PKN1$^{1-511}$ and NUGC4-EV/PKN1$^{1-511}$ cells were resuspended in complete DMEM medium containing 0.3% agar with or without 0.1 µg/mL Dox and plated onto 6-well plates on top of 0.6%

agar in DMEM medium with or without 0.1 µg/mL Dox. For overexpression assay, complete DMEM supplemented with 20% FBS was used instead. Three independent experiments were carried out in triplicate.

Migration assay (Wound-Healing Method). ***Knockout and downregulation cell line models:*** $3x10^6$ MKN45 PKN1 wild type and PKN1 knockout cells were seeded into 6-well plates and allowed to grow until they reached 100% confluence. NUGC3-sh1, NUGC3-sh2, and NUGC3-shNT were treated with or without Dox (1 µg/mL) for 7 days prior seeding. Then, $2.5x10^6$ cells were seeded in 6-well plates. The cell monolayer was scratched with a sterile micropipette tip and the wound region was allowed to heal by cell migration. The area that remained clear of cells at different time points was quantified blinded from sample identity with TScratch software (http://www.cse-lab.ethz.ch/software/) and compared with the area of the wound at time zero. ***Overexpression cell line models:*** $3.5x10^6$ FU-97-EV/PKN1$^{1-511}$ and $4x10^6$ NUGC4-EV/PKN1$^{1-511}$ cells were seeded into 6-well plates with or without 0.1 µg/mL Dox and migration was quantified as described above. Three independent experiments were carried out in triplicate.

Invasion assay (Boyden Chamber Method). The ability of cells to invade through matrigel-coated filters was determined using a 24-well Boyden chamber (Beckton Dickinson; 8 µm pore size) covered with 100 µL of 1 mg/mL Matrigel (Beckton Dickinson). ***Knockout and downregulation cell line models:*** $1x10^5$ MKN45 PKN1 wild type and PKN1 knockout were seeded embedded in 100 µL of matrigel and 100 µL of DMEM containing 1% FBS was added on top after polymerization. The lower compartment was filled with DMEM with 10% FBS, acting as chemoattractant. NUGC3-sh1, NUGC3-sh2, and NUGC3-shNT cells were treated with or without Dox (1 µg/mL) for 7 days prior seeding. Then, $1x10^5$ NUGC3 derivative cells were seeded embedded in 100 µL of matrigel and 100 µL of DMEM containing 1% FBS was added on top after polymerization. The lower compartment was filled with DMEM with 10% FBS. After incubation for 48 h, 5% CO_2, at 37°C, the cells that were unable to pass through the filter were wiped out with a cotton swab, and the cells that had invaded the lower surface of the filter were fixed and stained with 5% crystal violet. Filters were mounted on microscope slides and the total number of invading cells was determined under the microscope (20X). The average of three independent experiments run in triplicate is shown. ***Overexpression cell line models:*** $2x10^5$ FU-97-EV/PKN1$^{1-511}$ and NUGC4-EV/PKN1$^{1-511}$ cells were seeded embedded in 100 µL of matrigel and 100 µL of DMEM containing 1% FBS was added on top after polymerization. The lower compartment was filled with DMEM with 10% FBS. After incubation for 72 h at 37°C in 5%

CO_2, the cells that had invaded the lower surface of the filter were fixed and stained as was previously described. The total number of invading cells was determined using the ImageJ software. The average of three independent experiments run in triplicate is shown.

Yeast two-Hybrid (Y2H) assay. Is a molecular biology technique used to discover protein–protein interactions (PPIs). Proteins of interest are expressed as fusions with a DNA-binding domain (BD) or activation domain (AD), making hybrid proteins. If the hybrid proteins bind to each other as a result of interaction between the proteins of interest, the BD and AD are brought together within the cell nucleus to lead the expression of a reporter gene. Whereas, in absence of interaction between the two proteins, the reporter gene is not expressed (301). Screening for interacting proteins of RHOA and the most common mutants found in gastric cancer was performed using the MATCHMAKER Two-Hybrid system 2 (CLONTECH®) according to the manufacturer's specifications. The pGTB9-RHOA wild type and RHOA mutants bait constructs (R5Q, L57V, Y42C or G17E), were transformed into *Saccharomyces cerevisiae* yeast strain GC-1945 for the screening. The baits were then used to detect the putative prey ligands. The prey DNA constructs encode fusion proteins consisting of the GAL4 activation domain (AD) fused to known RHOA-ligands binding domain (BD) PKN1, ROCK, Kinectin and DIAPH2. Following the bait-prey mating, the culture was plated onto primary selection Synthetic Defined (SD) media (-Leu, -Trp), which selected for diploid His^+ yeast cells successfully transformed with both plasmids. To assess the strength of the bait/prey interaction, at least five of these colonies were plated onto (SD/-Leu, -Trp, -His) supplemented with 3-amino-1,2,4 triazole (3-AT) at 0, 1, and 5 mM, and the plates were incubated at 30°C until colonies were visible (2-4 days). 3-AT is a competitive inhibitor of the product of the *HIS*3 gene was used to test the interaction strength. The higher 3-AT concentration is necessary to inhibit the yeast growth, stronger the interaction.

Pulldown assay. Is an *in vitro* method used to determine a physical interaction between two or more proteins, is also useful for both confirming the existence of a protein–protein interaction predicted by other research techniques (e.g., Y2H or co-immunoprecipitation) and as an initial screening assay for identifying previously unknown protein–protein interactions. To assay for GTP-bound (active) form of Small GTPases of the RHO superfamily in human gastric cancer cell lines but can also be applied to cells or tissues of other origins. The principle of assay is based on the property of these active GTPases to interact with their specific effectors (e.g. Rhotekin for RHOA). ***GST-fusion proteins purification:*** The most common RHOA mutations observed in diffuse gastric tumors (R5Q, G17E, Y42C and L57V) were generated as described in the

'Plasmids' section. The control empty vector pGEX-4T-GST, pGEX-Rhotekin-GST and the different pGEX-4T-GST-RHOA constructs were transformed by heat-sock into *E. coli* BL21. Transformed cells were grown in LB medium (1%Tryptone, 0.5%yeast extract, 1%NaCl) supplemented with 100 µg/mL ampicillin at 37ºC, 250 rpm, until $O.D._{600}$ reach 0.5. The GST-RHOA, GST-Rhotekin and GST-RHOA-mutants expression was induced with 400 µM IPTG at 30ºC for 3 h. The cells were harvested by centrifugation at 4000 xg, 20 min, and resuspended in 10 mL of buffer A [50 mM Tris-HCl pH 7.5, 1% Triton X-100, 150 mM NaCl, 5 mM $MgCl_2$, 1 mM 1,4-Dithiothreitol **(**DTT), 0.1 µg/mL aprotinin, 1 mM phenylmethylsulfonyl fluoride (PMSF), 200 µg/mL lysozyme (USB, Chicken egg white)] and incubated for 20 min on ice. The cells were disrupted by sonication on ice with a Fisher Sonic Dismembrator Model 100 (30 seconds constant duty cycle, output 4 and 1 min on ice, 4 cycles). Cell debris and high molecular weight DNA were removed by centrifugation at 10000 xg for 30 minutes and the supernatant was recovered. To equilibrate the glutathione sepharose beads (GSH-sepharose), it was washed twice with 400 µL of buffer A without lysozyme and finally resuspended in 200 µL complete buffer A. Then, 100 µL of glutathione sepharose beads was added to the supernatant and let them in rotation for 2 h at 4ºC. The beads were then centrifuged at 300 xg for 2 min at 4ºC, the supernatant was discarded and the beads were washed with 400 µL buffer B (50mM Tris pH 7.5, 0.5% triton X-100, 150mM NaCl, 5mM $MgCl_2$, 1mM DTT) 4 times, and once with 400 µL buffer C (50mM Tris HCl pH 7.2, 150mM NaCl, 5mM $MgCl_2$, 1mM DTT, 10% glycerol). Finally, the beads were resuspended in 300 µL buffer C to quantify the protein concentration. ***Pull-down:*** 20 µg of fusion proteins and 1-2 mg of fresh protein lysate obtained by mixing equal amounts from 9 diffuse type gastric cancer cell lines available in the lab (FU-97, GCIY, KatoIII, MKN45, NUGC3, NUGC4, OCUM1, SNU-16, and SNU-5), were mixed and incubated for 3 h at 4ºC in constant rotation. The beads were then pelleted by centrifugation, the supernatant discarded and the beads were washed 4 times with 1 mL of protein extraction buffer. Finally, the beads were resuspended in 110 µL of 50 µM Tris pH 7.5, 10 µM DTT as a reductor agent. 15 µL were mixed with 5 µL of Laemmli buffer, incubated at 95ºC for 5 min, and then loaded on a 10% Tris Glycine polyacrylamide gel. Western blotting was carried out as described above to detect the interacting proteins with RHOA. ***Rhotekin Pulldown:*** First, the cell lysates were processed as describe above, then 15 µL of GSH-sepharose were transfer into 100 µL of GST pull-down buffer A in a 1.5 mL Eppendorf tube. Mix and spin at 835 xg, 1 min. at room temperature. After the supernatant was discard and the washed GSH-sepharose beads were save for pre-clearing samples. For pre-clearing: 100 µg of crude cell lysates by adding into 300 µl of GST pull-down buffer A containing the washed GSH-sepharose and incubating with agitation at 4°C for 1 h. The

samples were centrifuge at 835 xg for 1 min at 4°C. The supernatant was transfer to a new 1.5 mL tube without disturbing the sepharose. An aliquot of the pre-cleared lysate was save as "input". To the supernatant 30 µL of glutathione beads bound with 30 µg GST-Rhotekin was added, mixing well and incubated at 4°C for 3 h with rocking. The samples were centrifuged at 835 xg for 1 min at 4°C to pellet the sepharose beads and the supernatant was discarded, the beads were washed three times by adding 300 µL 1x PBS at 4°C and then spin at 835 xg for 1 min at 4°C and aspirate supernatant. After washes the beads were boiled with Laemmli buffer for 5 min. and spin to harvest the pull-down proteins. Finally, the proteins were resolved by 10% SDS-PAGE and then Western blot analysis was performed using anti-RHOA antibody to detect active (pulldown) and total (input) GTPases.

Shotgun proteomics technique. Based on newly generated protein analysis (302), an additional experiment to identify the most important and specific GTPase RHOA effectors in gastric cancer context was performed through liquid chromatography-mass spectrometry (LC-MS) assay. Protein lysates from 9 gastric cancer cell lines were purified as described in Pulldown section. Then, the resulted product was processes for Liquid Chromatography/Mass Spectrometric analysis as was described (303). **Sample preparation and trypsin digestion:** Previous to LC-MS analysis, samples were digested in solution with trypsin. Samples were initially concentrated and buffer exchanged to 6 M Urea 50mM ammonium bicarbonate (AB) using 0.5 mL 3KDa cut-off Amicon Ultra ultrafiltration devices (Merck-Millipore). Total protein content was quantified using RCDC kit (Bio-Rad), and 8 µg of each sample were taken for tryptic digestion. Samples were first reduced with DTT to a final concentration of 10 mM, for 1 h at RT, and then alkylated with 20 mM of iodoacetamide (IAA) for 30 min at RT in the dark. Carbamidomethylation reaction was quenched by addition of N-acetyl-L-cysteine to final concentration of 35 mM followed by incubation for 15 min at RT in the dark. Samples were diluted with 50 mM AB to a final concentration of 1 M Urea, and then modified porcine trypsin (Promega Gold) was added in a ratio of 1:20 (w/w), and the mixture was incubated overnight at 37°C. The reaction was stopped with formic acid (FA) to a final concentration of 0.5%, and the digest was kept at -20ºC until further analysis. **Liquid chromatography-Mass spectrometry analysis (LC-MS):** Tryptic peptides from tricine gel sections and from RP-HPLC fractions of interest were analyzed on a LTQ Velos-Orbitrap mass spectrometer (ThermoFisher Scientific, Bremen, Germany) coupled to a nano-HPLC system (Proxeon Biosystems, Thermo Fisher Scientific, Bremen). Instrument control was performed using Xcalibur software package, version 2.2.0 (Thermo Fisher Scientific, Bremen, Germany). Peptide mixtures were initially concentrated

on an EASY-column, 2 cm long, 100 µm internal diameter (id), and packed with ReproSil C18, 5 µm particle size (Proxeon, Thermo Fisher Scientific), and subsequently chromatographed on an EASY-column, 75 µm id, 10 cm long, and packed with ReproSil-Pur C18-AQ, 3 µm particle size (Proxeon, Thermo Fisher Scientific). An ACN gradient (5− 35% ACN/0.1% formic acid in water, in 120 min, flow rate of 300 nL/min) was used to elute the peptides through a stainless steel nanobore emitter (Proxeon, Thermo Fisher Scientific) onto the nanospray ionization source of the LTQ Velos Orbitrap mass spectrometer. MS/MS fragmentation spectra (200 ms, 100− 2800 m/z) of 20 of the most intense ions, as detected from a 500 ms MS survey scan (300−1500 m/z), were acquired using a dynamic exclusion time of 20 s for precursor selection and excluding single-charged ions. Precursor scans were acquired in the Orbitrap analyzer at a mass resolution of 30,000. MS/MS spectra were acquired at the LTQ Velos analyzer using normalized collision energy of 35%. An intensity threshold of 1,000 counts was set for precursor selection. Orbitrap measurements were performed enabling the lock mass option (m/z 445.120024) for survey scans to improve mass accuracy. **Bioinformatics for protein identification:** LC-MS/MS data were analyzed using the Proteome Discoverer software (Thermo Fisher Scientific) to generate mgf files. Processed runs were loaded to ProteinScape software (Bruker Daltonics, Bremen, Germany) and peptides were identified using Mascot (Matrix Science, London UK) to search the SwissProt 20160108 database, restricting taxonomy to human proteins (20171 sequences). MS/MS spectra were searched with a precursor mass tolerance of 10 ppm, fragment tolerance of 0.8 Da, trypsin specificity with a maximum of 2 missed cleavages, cysteine carbamidomethylation set as fixed modification and methionine oxidation as variable modification. Significance threshold for the identifications was set to $p<0.05$ for the probability-based Mascot score, minimum ions score of 20, and the identification results were filtered to 1% FDR at peptide level, based on searches against a Decoy database. To identify and remove the contaminant proteins the crapome.org (Contaminant Repository for Affinity Purification Mass Spectrometry Data) database was used. Aggregating negative controls from multiple AP-MS studies were used to determinate the common contaminants across multiple experiments. Moreover, the proteins that were present also in the GST pulldown were also removed from the final list (**Supplementary Table 8**). LC-MS analysis was carried out at the Proteomics Core Facility, Vall d'Hebron Institut of Oncology, (VHIO).

Sulforhodamine B (SRB) method. Changes in cell growth with Arachidonic acid treatment was measured by SRB method. SRB dye stains protein content and the absorbance measurement at

510 nm can be used to assess relative differences in cell numbers (222, 304). $1x10^5$ MKN45 parental, MKN45-PKN1-2-wild type and MKN45-PKN1-2-knockout cells were seeded on a 96-well microtiter plate (8 replicates/cell line and condition). The plates were fixed 72 h after treatment with 30% Trichloroacetic Acid (TCA; Fisher Scientific). Once all plates were fixed, they were stained with 0.4% SRB (Sigma-Aldrich) in 1% acetic acid for 30 min under agitation and washed with 1% acetic acid. The stained plates were allowed to air dry during 24 h. The cell-bound SRB dye was dissolved in 10mM Tris pH10. Absorbance was measured at 510 nm and plotted versus time. Three independent experiments with each cell line were carried out.

Arachidonic acid treatment in cell lines. PKN1 activation. To investigate whether Arachidonic acid could activate PKN in gastric cancer cells, $6x10^6$ MKN45 parental cells were seeded on 10 cm plate, after 24 h the medium was replaced for fresh DMEM medium and Arachidonic acid (Abcam, UK) was added to a 30 µM final concentration. Cells were incubated at (0, 60, 120, 180) min, and then cells harvested on ice, pelleted was and snap frozen in liquid nitrogen. Cell lysis and protein quantification was carried out as described above in the 'Western blotting' section. Relative protein levels were assessed by Western blotting for PKN1, PKN2 and phospho-PKN1-2-3 (**Table 6**). **Determination of Arachidonic acid sensitivity (GI_{50}).** The dose resulting in 50% growth inhibition (GI_{50}) in the presence of Arachidonic acid, compared to the corresponding control, was determined as described (305, 306). Briefly, assays were performed in 96-well microtiter plates, each well receiving 200 µL of culture medium with $1x10^4$ cells. After 24 hours, the medium is removed from all wells and replaced by 200 µL of fresh medium in all wells with the corresponding concentration of Arachidonic acid. Arachidonic acid stock solution (750 µM) was prepared in complete DMEM to the corresponding final concentrations. For the assays, the compound is further diluted to the appropriate concentration using complete medium. The range concentration for Arachidonic acid was: 0, 1, 5, 10, 50, 100, 125, 174, 200, 300, 500, 750 µM. After 72 h of incubation the plates are inspected under an inverted microscope to assure growth of the controls and sterile conditions. Cells were fixed with 30% TCA and stained with SRB, as described in SRB method. One plate of each cell line was fixed to assess cell number at the time when Arachidonic acid treatment started (T_0). After absorbance was measured at 510 nm using a microplate reader (Sunrise, Tecan, Männedorf, Switzerland), the blank (medium incubated for 24 h or 72 h) was subtracted. In order to calculate the GI_{50}, three measurements are necessary: Ti=absorbance of cells after treatment (for each drug concentration), T_0= absorbance at the beginning of the treatment, and C= absorbance of cells without treatment (incubated with complete growth medium for 24 h). Using these

measurements, cellular responses was calculated for growth inhibition. The formula used is: If Ti ≥ T_0, the calculation is 100 x [(Ti - T_0)/ (C - T_0)]. If Ti ≤ T_0, cell killing has occurred and can be calculated from 100 x [([(Ti - T_0)/ T_0]. Thus, for Arachidonic acid, a dose-response curve was generated and growth inhibition of 50% (GI_{50}) was calculated from 100 x [(Ti - T_0)/ (C - T_0)] = 50, which is the drug concentration causing a 50% reduction of the total protein increase in control cells during the drug incubation (304, 307, 308). These experiments were carried out at least three times in quadruplicates and the calculations done with GraphPad Prism software.

Subcutaneous Xenograft model. 20 NOD/SCID (Harlan Laboratories) 7-8 weeks old female mice were s.c. injected with $1x10^6$ NUGC3-shNT (left flank) and NUGC3-sh1 (right flank) cells. The cells were treated with 1 µg/mL Dox for 7 days and then were resuspended in 100 µL of cold PBS for injection. The animals were then randomized in two groups (10 animals per group), one receiving Dox *ad libitum* in drinking water (1 mg/mL Dox and 2.5% sucrose; Sigma-Aldrich) or a control group (2.5% sucrose). In the case of MKN45 wild type and PKN1 knockout cells, 10 female NOD/SCID mice (Harlan Laboratories) 6-10 weeks old were s.c. injected with $2x10^6$ MKN45 PKN1 wild type (left flank) and MKN45 PKN1 knockout (right flank) resuspended in 100 µL of PBS. Tumor volume was calculated with the formula V = (L x W^2) x 0.5, where L is the length and W is the width of the xenograft. All animals were i.p. injected with 100 mg/kg Bromodeoxyuridine (BrdU) 2h before being sacrificed. At end-point of the experiment, the tumors were excised, formalin-fixed and paraffin-embedded for immunohistochemistry analysis. All animal experiments were carried out under protocols approved by the Institutional Ethical Committee and the appropriate governmental agency.

Lung metastasis model. $2x10^6$ MKN45 PKN1 wild type (MKN45-PKN1-WT) or PKN1 knockout (MKN45-PKN1-KO) cells resuspended in 100µl PBS were injected into the tail vein of 20 NOD/SCID mice (n=10 per group). At the end of the experiment animals were sacrificed and lungs were perfused with Formalin 1X; each lobe was separated and fixed overnight with 4% formalin and then abundantly washed with tap water and PBS 1X. The number of macroscopically visible tumors was scored under a dissecting microscope (OLYMPUS SZH stereo-zoom microscope, magnification 7.5X). Tissues were then embedded in paraffin, sectioned and stained with hematoxylin-eosin and the number of metastatic lesions scored.

Peritoneal carcinomatosis model. $1x10^6$ MKN45 parental cells resuspended in 400 µl PBS were intraperitoneally (i.p.) injected into 14 female 10-week-old NOD/SCID mice. After cell

inoculation animals were randomized into a control vehicle group (n=7) and a group of animals (n=7) treated with Arachidonic acid i.p. (2 mg/kg) three days per week. All animals were i.p. injected with 100 mg/kg Bromodeoxyuridine (BrdU) 2h before being sacrificed. At end-point of the experiment, the intraperitoneal tumors were excised, formalin-fixed and paraffin-embedded for immunohistochemistry analysis.

Mouse knockout strains. The *C57BL/6J-Apc^{min}/J* strain was obtained from the Jackson Laboratory (Maine, USA). These mice carry the heterozygous mutation *Apc^{min}* in the tumor-suppressor gene *Apc*. The mutation consists in the transversion point mutation T2549A, which converts codon 850 from one encoding a leucine to a stop codon. The transgenic *C57BL/6J-CAT-RhoA* were generated as described by Kobayashi et al. (309) in collaboration with Dr. Manuel Sánchez-Martin, Associate Professor. Department of Medicine. University of Salamanca (USAL). Before being injected in the animals, the DNA construct with RHOA-Y42C mutation was tested *'in vitro'* for protein overexpression. HEK293T cells were transfected with 10 µg of DNA, and up to complete 1000 µL with PBS. For transfection PEI (1 mg/mL) was used in 4:1 ratio to DNA. The transfection mixture was added to the cells in a drop wise manner, swirled slowly and incubated overnight. Next day, the medium was removed from the transfected cells and was replaced with fresh complete medium. After 72 h of incubation, the cells were processed for protein extraction, the protein lysates were assessed for RHOA detection by Western blot.
These transgenic mice (**Figure 27**) conditionally express the most common RhoA mutant observed in diffuse gastric tumors, *RhoA^{Y42C}*. Transgene expression is prevented by a 'stop cassette' (CAT-PA) upstream of *RhoA^{Y42C}* that is flanked by *loxP* sites (**Figure 27**). The B6.SJL-Tg (Vil-Cre) 997Gum/J mice hemizygous for the Villin-Cre transgene expressing *Cre* recombinase under the control of the *Villin 1* promoter (*Vil-Cre$^{TG/-}$*) (103) were obtained from the Jackson Laboratory (Maine, USA). *RhoA$^{Y42C/-}$* mice were crossed with animals carrying *Villin-Cre*, allowing for *Cre*-mediated recombination to occur in the villus and crypt cells of the small-large intestines and in progenitor cells of the stomach (13, 104), resulting in tissue specific expression of the Y42C mutant of RHOA (**Figure 27**).

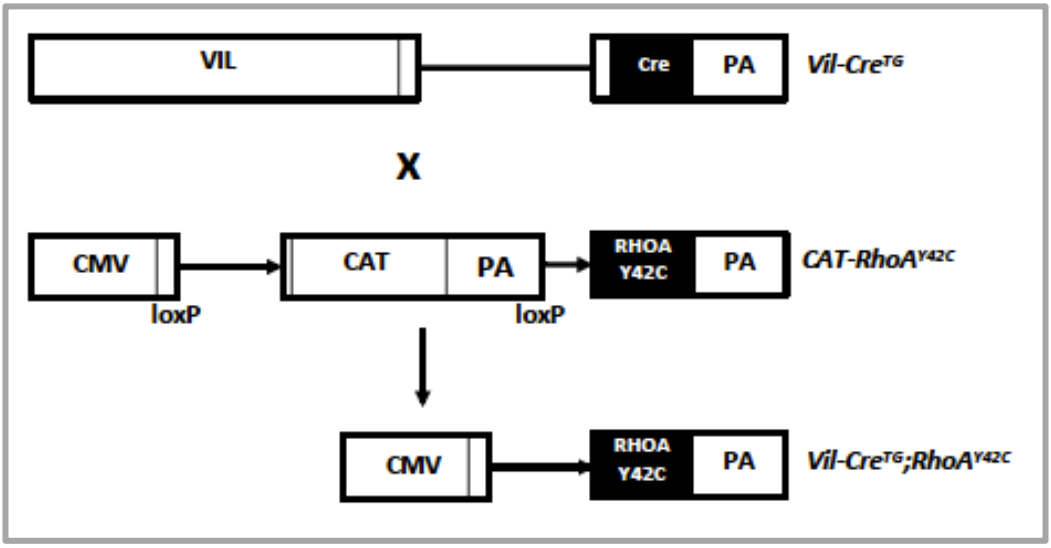

Figure 27. Expression of *RhoA-Y42C* using the Cre-*loxP*-mediated recombination.
Vil-Cre transgenic mice (*Vil-Cre*$^{TG/-}$) were crossed with CAT-RhoA-Y42C mice (*RhoA*$^{Y42/-}$). In the double transgenic mice (Vil-Cre$^{TG/-}$/RhoA$^{Y42C/-}$), Cre-loxP recombination deletes the CAT gene cassette in the progenitor cells of the stomach (and intestinal epithelial cells), therefore leading to the expression of the Y42C mutant form of RHOA. Adapted from Rodrigues et al. (222)

To verify for correct Cre mediated recombination in the generated offspring, intestinal protein lysates enriched in epithelial cells were collected from 6-week-old animals. Animal intestines were opened, washed twice with ice cold PBS and gently scraped with a microscope slide. This method was used to obtain protein from the intestinal epithelial layer; protein lysates were then used to perform WB and pull-down assays (as described in previous sections) to determine the overexpression of RHOA-Y42C in the intestine of the *Vil-Cre*$^{TG/-}$*;RhoA*$^{Y42C/-}$ mice compared to control *Vil-Cre*$^{-/-}$*;RhoA*$^{Y42C/-}$. To initiate tumorigenesis in the stomach of the animals, *Vil-Cre*^{TG} female animals, were crossed with male *Apc*$^{min/+}$*;Rho*$^{Y42C/-}$ mice and treated with the mutagenic compound N-methyl-N-nitrosourea (MNU, 240 ppm) in the drink water for a total of 5 weeks on alternative weeks in order to accelerated or cause tumor formation. It has been reported that MNU-treated *Apc*$^{min/+}$ mice significantly enhanced the tumor development (310).

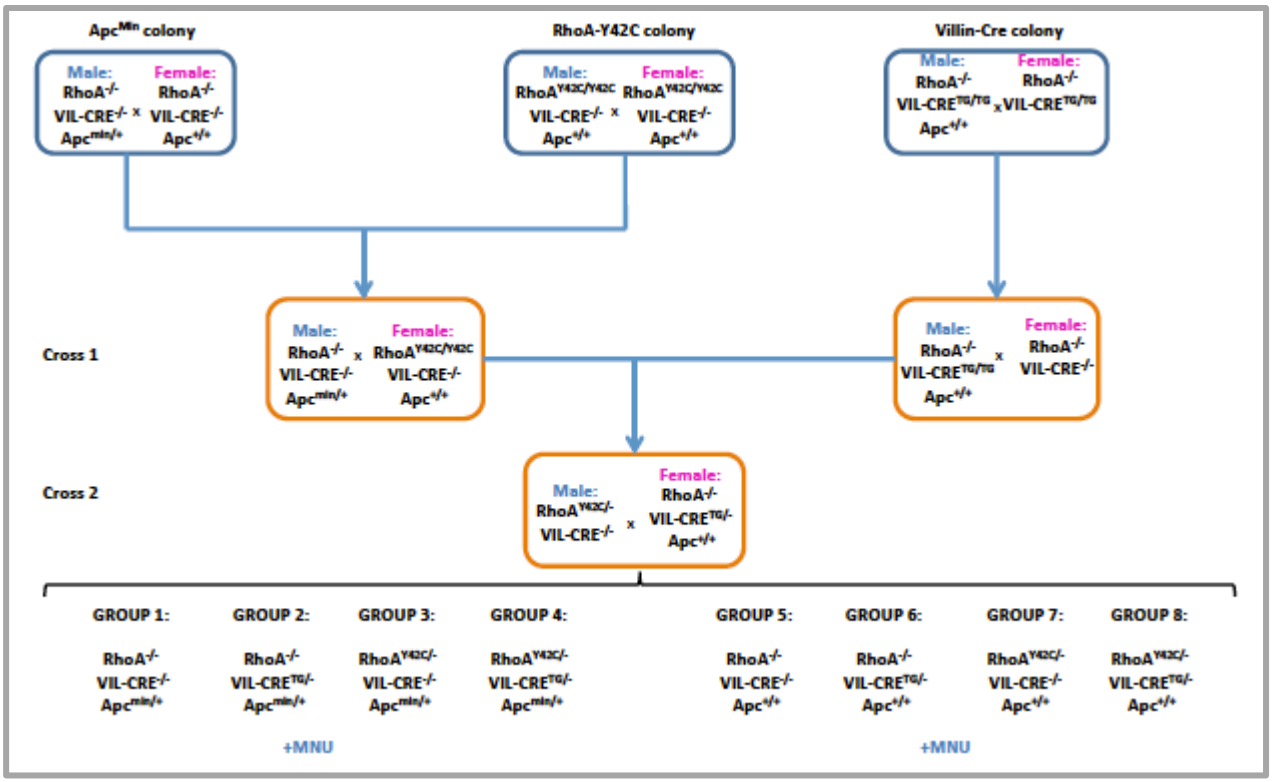

Figure 28. Genetic and chemical model for tumorigenesis initiation, experimental design.
In cross 1, *Apc* $^{min/+}$ male mice were crossed with *RhoA* $^{Y42C/Y42C}$ animals in order to generate *Apc* $^{min/-}$*/RhoA* $^{Y42C/Y42C}$ mice, which were then matted in cross 2 with *Vil-Cre* $^{TG/-}$ animals to generate offspring with expression of *Apc* $^{min/-}$*/Vil-Cre* $^{TG/-}$*/RhoA* $^{Y42C/-}$ mice) and the respective control animals where neither the Y42C-RHOA mutant nor the *Apc* $^{min/-}$ is expressed.

The treatment strategy was designed in two different set up, first in which *Apc* $^{min/+}$ mice with or without RhoA $^{Y42C/-}$ mutation were treated with MNU during 5 weeks and sacrificed at 19-week-old (the time-period established was determined by pain curve of the animals); and second in which *Apc* wild type mice were also treated for 5 weeks with MNU but sacrificed at longer time (35- and 50-week-old) (**Figure 29**). There were in total eight experimental groups (n=10, **Figure 28**). At the end of the experiments, the stomach of these animals was processed for histological analysis (formalin fixation and paraffin embedding). All animals were i.p. injected with 100 mg/Kg Bromodeoxyuridine (BrdU) 2h before being sacrificed allowing the assessment of changes in proliferation in the stomach tumors by inmunohistochemical analysis.

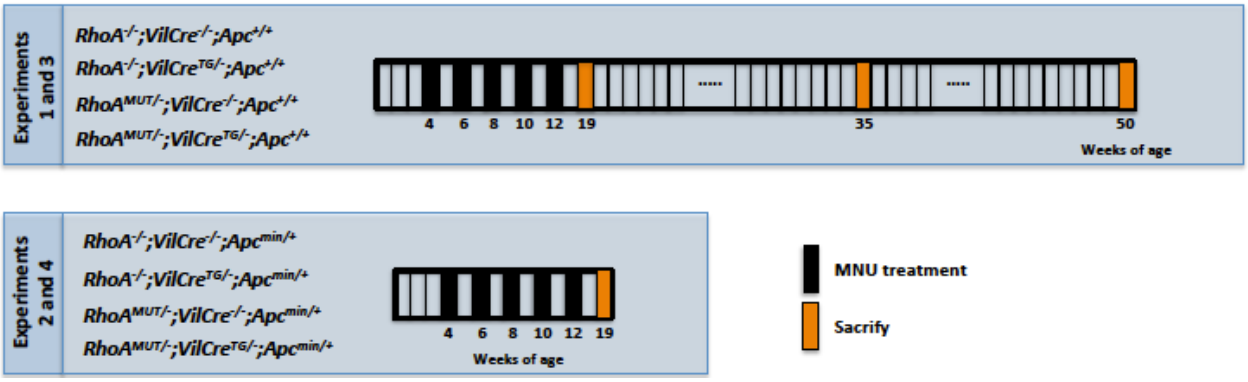

Figure 29. **MNU administration protocol.**

All animals were treated with MNU (240ppm in water) in alternate weeks during 5 weeks, starting at 4 weeks of age. Groups of animals (at least, n=10) were euthanized at week 35 and 50 (animals wild type *Apc*), and week 19 (animals $Apc^{min/-}$).

Immunohistochemistry. To assess cell proliferation in the subcutaneous xenograft tumors and stomach tissue of MNU-treated mice, the animals were i.p. injected with 100 mg/Kg BrdU 2 hours before being sacrificed. The number of cells in S-phase of the cell cycle during this time was assessed by anti-BrdU immunohistochemistry. In brief, for **BrdU immunostaining**, citrate buffer pH 6.0 for 4 min at 120°C in a pressure cooker was used for sample antigen retrieval and then incubated with mouse monoclonal anti-BrdU primary antibody at 4°C, overnight (hybridoma supernatant Developmental Studies Hybridoma Bank) **Table 6,** using a commercial kit (Novolink Polymer Detection System, Leica Microsystems, UK). Slides were counterstained with haematoxylin, dehydrated and mounted with DPX mounting medium. To quantify the number of proliferating cells in the subcutaneous tumors of the animals, the number of BrdU-positive cells and the total number of tumor cells per field was counted. Three fields per animal in ten different animals per group were counted. For **active Caspase 3 and KT19 immunostaining** (**Table 6**), the same procedure was performed as described for BrdU staining**.** To quantify the number of apoptotic cells in the tumors, the number of Caspase 3 positive cells present in subcutaneous xenografts from MKN45 cells lacking of PKN1 and from the PKN1 wild type control cells were quantified. The total number of cells and the number of Caspase 3 positive cells in at least 3 images per tumor was scored using ImageJ, blinded from the animal identity. To quantify the percentage of BrdU and active Caspase 3 positive cells, pictures from subcutaneous xenografts of MKN45 wild type and PKN1 knock out cells were obtained. For **PG1 immunostaining**, antigen retrieval was performed in EDTA Buffer 1mM, pH 9.0 in the pressure cooker at 120°C for 4 min. Samples were incubated with the corresponding antibody (**Table 6**), at 4°C, overnight.

Slides were counterstained with haematoxylin, dehydrated and mounted with DPX mounting medium. To quantify PG1 levels in gastric glands, three fields per animal in three animals per genotype were scored (0=no stain, 1=stain) and the percentage of PG1 stain glands was determined.

Statistical analysis. Assay for characterizing phenotype of cells were analyzed by Student's test. Statistical GraphPad Prism 5 was used to analyze data. A p value of <0.05 was considered statistically significant. *p <0.05; **p <0.01; ***p <0.001; ****p <0.0001.

RESULTS

CHAPTER IV. RESULTS

1. The recurrent RHOA-Y42C mutation enhances gastric tumorigenesis in a novel transgenic mouse model

Recent findings published by Wang *et al.* (185) and Kakiuchi *et al.* (184) identified frequent (14-24%) mutations in the small GTPase RHOA in diffuse-type gastric tumors, although based on these genetic data it is difficult to conclude whether RHOA signaling prevents or promotes the oncogenic process.

Recently, in our laboratory we have also investigated the role of RHOA in diffuse-type gastric cancer, and found that deletion of RHOA results in increased proliferation and invasion of diffuse gastric cancer cells "*in vitro*" and "*in vivo*" (unpublished, **Figure 22A-F**). The opposite effect is observed when we overexpress the wild type or a constitutive activated (G14V) form of RHOA in diffuse gastric cell lines with low endogenous levels of RHOA (unpublished, **Figure 23A-B**). However, reintroduction of RHOA-Y42C into RHOA deficient diffuse gastric cancer cells significantly increased their growth (unpublised, **Figure 23C-E**). Moreover, in a large human gastric tumor collection we observed that low levels of RHOA expression correlate with poor prognosis (unpublised, **Figure 23F-G**). To further investigate the possible oncogenic role of the RHOA-Y42C mutant frequently observed in diffuse gastric tumors in the context of a full organism, we generated mice with the frequent RHOA-Y42C mutation found in gastric tumors in the gastric epithelium by crossing new transgenic mice with *Cre*-dependent expression of RHOA-Y42C, with mice expressing *Cre* recombinase under the control of the *Villin 1* promoter that is expressed in gastric progenitor cells (104), (*Vil-Cre*^{TG}; **Figure 27**).

The *C57BL/6J-CAT-RHOA-Y42C* mice carrying a point mutation Y42C of RHOA (*RhoA*$^{Y42C/-}$) preceded by a CMV-CAT-PA cassette in which the CAT-PA region is flanked by *loxP* sites, were generated as described by Kobayashi *et al.* (309). Briefly, a 0.9 kb DNA fragment containing the cytomegalovirus (CMV) early gene promoter was fused to the rabbit β-globin second intron and chloramphenicol acetyltransferase (CAT) gene cassette connected to a polyadenylation signal (PA) both ends of which were flanked by *loxP* sites. Another polyadenylation signal was connected downstream of the second *loxP* site, making a unique *ClaI* site between the *loxP* site and the 5′-end of the polyadenylation signal to generate pCMV-CAT-PA. A 0.6 kb DNA fragment encoding the Y42C mutant of *RhoA* or *RhoA*^{Y42C}, was inserted into the *ClaI* site of pCMV-CAT-PA, resulting in pCAT-*RhoA*^{Y42C} (**Figure 30)**.

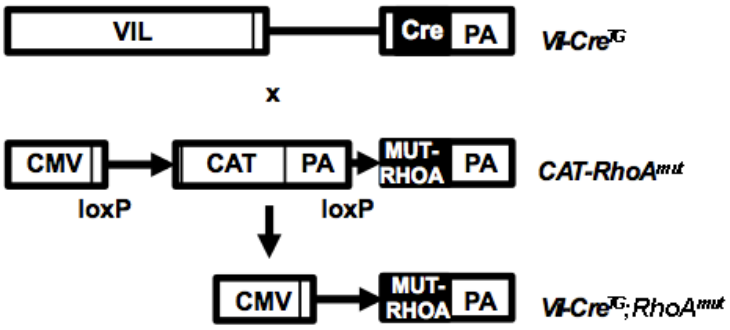

Figure 30. Generation of a mouse model conditionally expressing *RhoA*^{Y42C}.
Mice expressing *Cre* recombinase under the control of the promoter of Villin 1 (*Vil-Cre*) were crossed with *RhoA*^{Y42C} mice. In the double transgenic mice (*RhoA*$^{Y42C/—}$;*Vil-Cre*$^{TG/—}$) Cre-loxP recombination deletes the chloramphenicol acetyltransferase (CAT) cassette in villin 1 expressing cells, and RhoA^{Y42C} is then expressed.

Before being introduced in the animals, this DNA construct was tested '*in vitro'* for RHOA protein overexpression. HEK293T cells were transiently co-transfected with the newly generated pCAT-*RhoA*^{Y42C} and the pBabe-Cre vector, constitutively expressing *Cre* recombinase, and increased total and active (GTP-bound) RHOA was observed (see lane 4 in **Figure 31**). As a control, no changes in RHOA levels were observed in HEK293 cells transfected with the empty vector pCAT, or the pBabe-GFP (see lanes 1-3 in **Figure 31**), thus indicating that Cre-LoxP recombination of the *RhoA*^{Y42C} cassette works as expected.

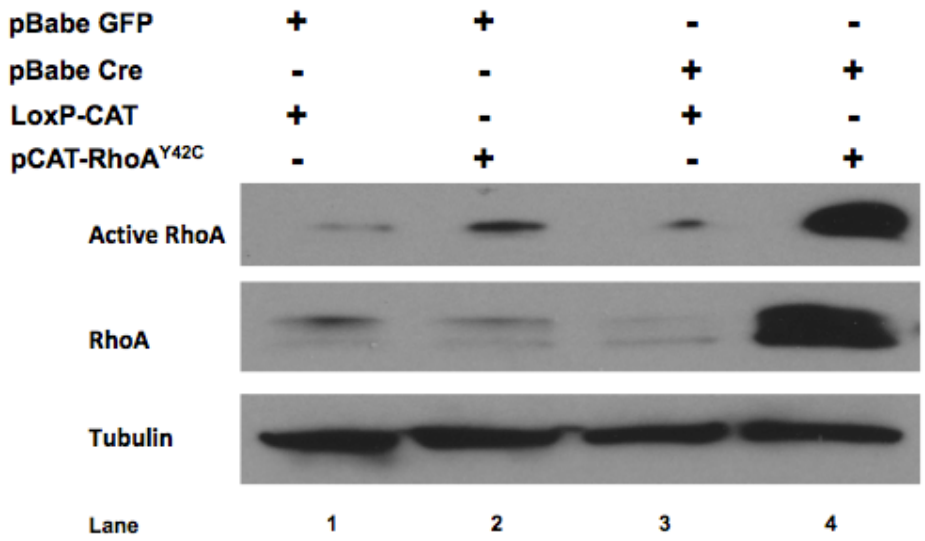

Figure 31. Validation of DNA construct pCAT-*RhoA*^{Y42C} to generate the *RhoA*^{Y42C} transgenic mice.
HEK293T cells co-transfected with pBabeCre and pCAT-*RhoA*^{Y42C} (Lane 4) or different controls (Lane 1, 2 and 3). Total and GTP-bound active RHOA levels were assessed after 72h by Western blotting to confirm RHOA overexpression. Tubulin expression was used as a loading control.

The generation of the transgenic mice was conducted by our collaborator Dr. Manuel Sánchez-Martin (Department of Medicine, University of Salamanca). Briefly, the newly generated vector pCAT-*RhoA*^{Y42C} was linearized with *SalI* and *XhoI* restriction enzymes, the resulting DNA insert CMV/loxP/pCAT-RhoA^{Y42C} was purified. The transgene was finally microinjected into fertilized mouse eggs, which were then implanted in pseudopregnant females. Transgenic mice were identified by PCR genotyping of genomic DNA prepared from tail clips with the oligos previously described (**Table 5**). Three founders were obtained, but only one of them was able to pass the transgene to the offspring, meaning that when this founder was mating with *Cre*-mouse the F1 generation exhibited a clear RHOA overexpression (**Figure 32**). Therefore, this founder was selected to establish the new RHOA-Y42C colony that was used in this study.

The B6.SJL-Tg(*Vil-Cre*)997Gum/J mice hemizygous for the *Villin-Cre* transgene expressing *Cre* recombinase under the control of the *Villin 1* promoter (*Vil-Cre*$^{TG/-}$) (103) and were obtained from the Jackson Laboratory (Maine, USA; Stock number: 004586). *RhoA*$^{Y42C/-}$ *mice* were crossed with animals carrying *Villin-Cre*, allowing for *Cre*-mediated recombination to occur in the villi and crypt cells of the small-large intestines and in progenitor cells of the stomach (13, 104) resulting in tissue specific expression of *RhoA*^{Y42C} (**Figure 32**).

Because in the stomach epithelium, only a small proportion of progenitor cells express Villin 1, *RhoA*^{Y42C} expression was confirmed in intestinal epithelial cells of the generated double

transgenic mice (*RhoA*$^{Y42C/-}$;*Vil-Cre*$^{TG/-}$) widely expressing Villin 1 protein, thus facilitating the assessment of transgene expression in these mice. Robust RHOA overexpression and increased GTP-bound active RHOA levels were observed in *RhoA*$^{Y42C/-}$;*Vil-Cre*$^{TG/-}$ compared to control *RhoA*$^{Y42C/-}$;*Vil-Cre*$^{-/-}$ (**Figure 32**). *RhoA*$^{Y42C/-}$ animals were born at Mendelian ratios, the number of animals expected *vs* the animals observed were compared with a Chi-square analysis, no significant differences was observed, p=0.8802: the number of animals with the genotype *RhoA*$^{-/-}$;*Vil-Cre*$^{-/-}$ was 25/93 *(27%),* with *RhoA*$^{-/-}$;*Vil-Cre*$^{TG/-}$ genotype 21/93 *(23%),* with *RhoA*$^{Y42C/-}$;*Vil-Cre*$^{-/-}$ genotype 23/93 *(25%),* and with *RhoA*$^{Y42C/-}$;*Vil-Cre*$^{TG/-}$ genotype 18/93 (19%) (**Figure 33A**). Mice had no overt phenotype and no differences were observed in the weight of the animals at 5 weeks of age (**Figure 33B**).

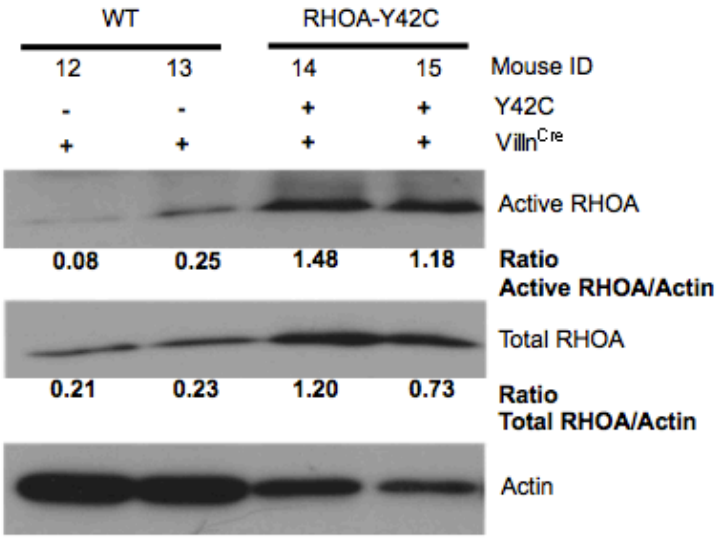

Figure 32. Generation and validation of a mouse model conditionally expressing *RhoA*^{Y42C}

B) Total protein extracted from intestinal epithelial cells of *RhoA*$^{-/-}$;*Vil-Cre*$^{TG/-}$ or *RhoA*$^{Y42C/-}$;*Vil-Cre*$^{TG/-}$ and relative total and active RHOA expression was assessed by Western blot. Actin levels was used as a loading control.

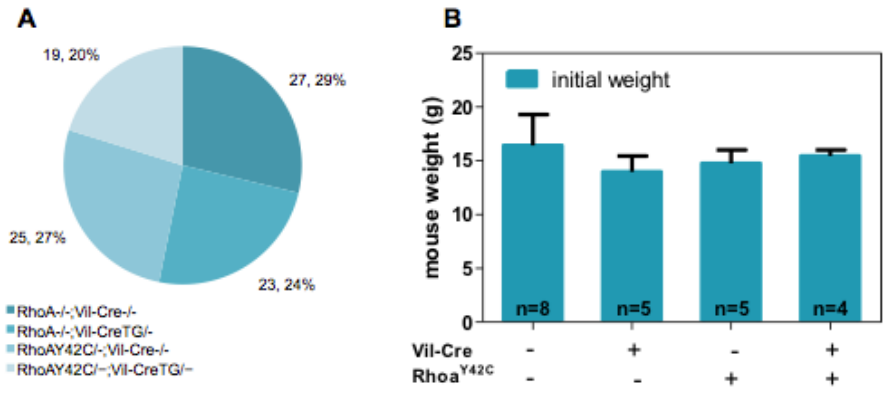

Figure 33. Mendelian ratios and body weight of *RhoA*^{Y42C} mice and control animals.
A) Mendelian inheritance ratios of *RhoA*^{Y42C} are shown as a percentage of the 87 mice (total colony population) Chi-square= 0.6702, p=0.8802. B) Body weight of *RhoA*^{Y42C} and control mice at 5-week-old was measured. The mean (±SEM) is shown.

Next, the role of RHOA-Y42C in gastric tumorigenesis was investigated using a model where the oncogenic process is initiated by N-methyl-N-nitrosourea (MNU) treatment for 5-weeks in alternative weeks, as described previously (104). Because the *Apc*^{min} mutation (T2549A introducing a premature stop codon) has been shown to initiate the tumorigenic process in the stomach of mice (310), *RhoA*$^{Y42C/-}$*;Vil-Cre*$^{TG/-}$*;Apc*$^{min/+}$ mice and control mice (*RhoA*$^{-/-}$*;Vil-Cre*$^{-/-}$*;Apc*$^{min/+}$ *or RhoA*$^{-/-}$*;Vil-Cre*$^{TG/-}$*;Apc*$^{min/+}$ *or RhoA*$^{TG/-}$*;Vil-Cre*$^{-/-}$*;Apc*$^{min/+}$) were treated with MNU and the number of tumors assessed. However, *Apc*$^{min/+}$ mice have a short lifespan (**Figure 34A**) due to the large number of tumors present in their intestine, and the animals had to be sacrificed at 19 weeks of age to assess possible differences in the number of gastric tumors. The incidence of gastric tumors in *Apc*$^{min/+}$ mice with *RhoA*^{Y42C} expression or control mice was small at 19 weeks of age. Gastric tumors were detected in 3 of 13 *RhoA*^{Y42C} mice (23% incidence) and in 8 of 38 mice (21% incidence) control animals (**Figure 34B**). No significant differences in the number of gastric tumors were observed between any of the experimental groups (**Figure 36A**).

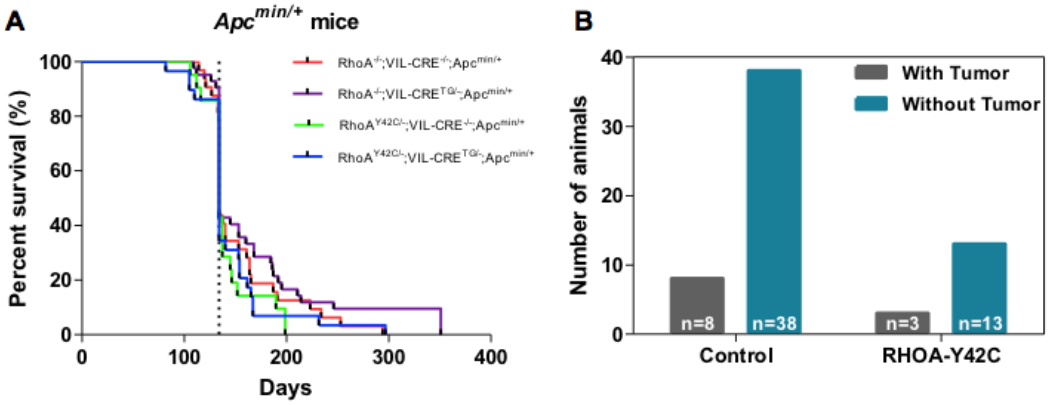

Figure 34. Lifespan and gastric tumor incidence in *Apc*^{min} mice with *RhoA*^{Y42C} overexpression.
A) Survival curve for mice with heterozygous mutations of the tumor suppressor *Apc* gene (Apc$^{min/+}$) with normal levels of RhoA (*RhoAY42C/-;Vil-Cre-/-;Apcmin/+*, n=20; or *RhoA-/-; Vil-Cre-/-; Apcmin/+*, n= 32; or *RhoA-/-;Vil-Cre-TG/-;Apcmin/+*, n=40) or RhoA^{Y42C} mutant expression (*RhoAY42C/-;Vil-Cre-TG/-;Apcmin/+*, n= 28). The vertical dashed line indicated 19 weeks. B) Tumor incidence in the combined control groups (21%) compared to *RhoA*^{Y42C} mutant mice (23%) is shown.

Next, the role of *RhoA*^{Y42C} in gastric tumorigenesis was assessed in *Apc* wild type mice with (*RhoA*$^{Y42C/-}$*;Vil-Cre*$^{TG/-}$) and without (*RhoA*$^{-/-}$*;Vil-Cre*$^{-/-}$ *or RhoA*$^{-/-}$*;Vil-Cre*$^{TG/-}$ *or RhoA*$^{TG/-}$*;Vil-Cre*$^{-/-}$) *RhoA*^{Y42C} overexpression at 35 or 50 weeks of age after MNU treatment. The histological examination of gastric tumors was conducted by an experienced pathologist. MNU treatment resulted in formation of gastric adenomas (**Figure 35**). The adenomatous lesions demonstrated enlarged and deformed glandular structures which led to additional branching, and interglandular messy pattern.

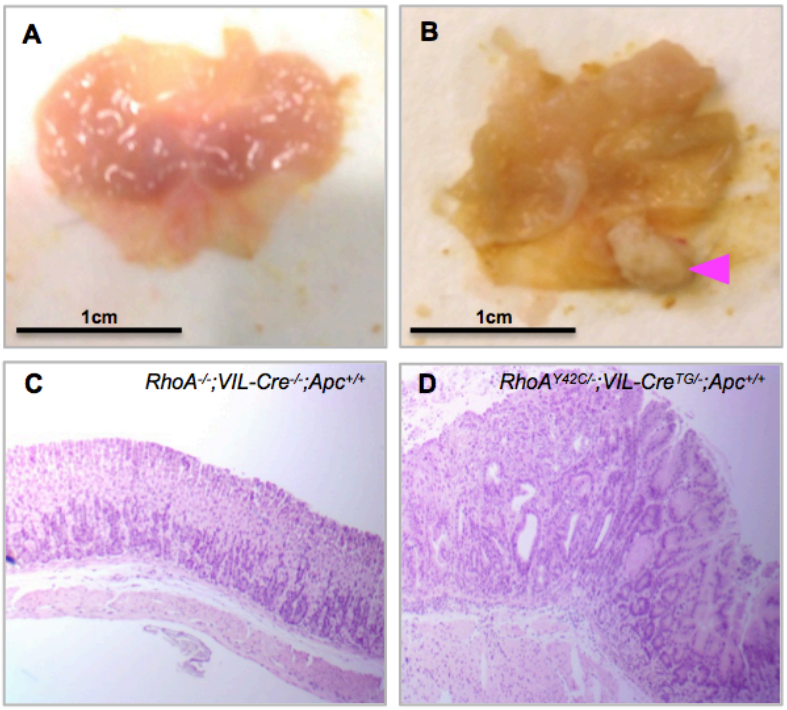

Figure 35. Gastric tumor development in the stomach of *RhoA*^{Y42C} mouse model after MNU treatment.
(A, B) Gross morphology of stomachs obtained from 50-week-old *RhoA*$^{-/-}$*;Vil-Cre*$^{-/-}$ control mice and *RhoA*$^{Y42C/-}$*;Vil-Cre*$^{TG/-}$ (RhoA^{Y42C} overexpression) mice. A visible tumor mass in a *RhoA*^{Y42C} mouse stomach is indicated by a pink arrow. Representative photographs of microscopic view of normal gastric mucosa of a 50-week-old *RhoA*$^{-/-}$*;Vil-Cre*$^{-/-}$ animal (C) and a tumor present in a *RhoA*$^{Y42C/-}$*;Vil-Cre*$^{TG/-}$ mouse (D), both treated with MNU. H&E staining is shown. 4X magnification.

The expression of RhoA^{Y42C} in gastric progenitor cells results in a significant increase in the number of tumors in the *RhoA*$^{Y42C/-}$*;Vil-Cre*$^{TG/-}$ 50-week-old mice treated with MNU compared to control *RhoA*$^{-/-}$*;Vil-Cre*$^{-/-}$, *RhoA*$^{-/-}$*;Vil-Cre*$^{TG/-}$ or *RhoA*$^{Y42C/-}$*;Vil-Cre*$^{-/-}$ mice (**Figure 36C**). Although no differences were observed in the number of gastric tumors in 35-week-old mice treated with MNU (**Figure 36B**), it was observed that Pepsinogen 1 (PG1) expression was significantly reduced in animals with RhoA^{Y42C} transgene expression at 35-weeks of age compared to control mice (**Figure 37**). PG1 is expressed in mucus cells and their levels have been studied as a marker of gastric malignancies. Low PG1 has been reported in atrophic gastritis, a pre-cancerous condition (311-313).

In summary, the results obtained with the novel *RhoA*^{Y42C} transgenic mouse model indicate that at least this mutation, which is the most prevalent RHOA mutation observed in diffuse gastric cancer tumors, can accelerate the oncogenic process initiated by the gastric carcinogen MNU.

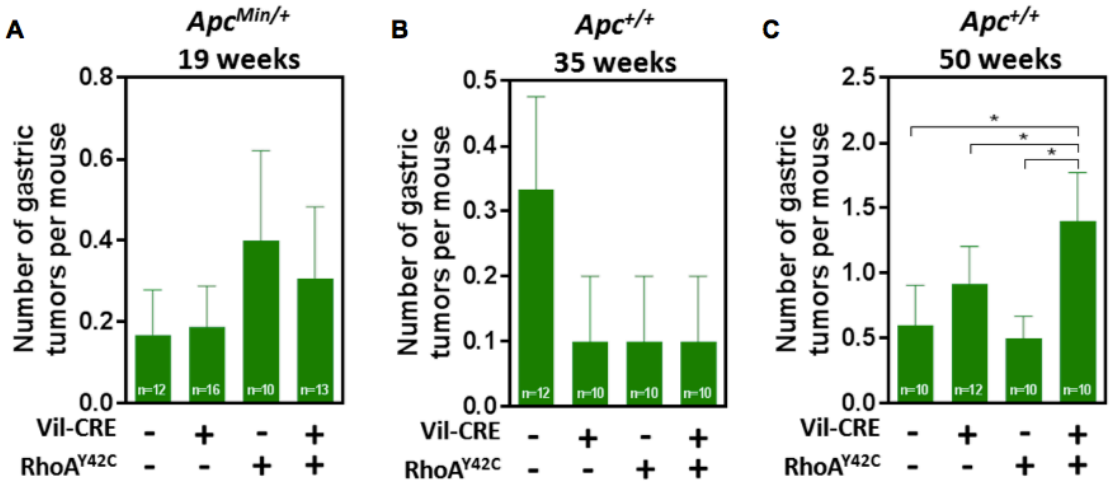

Figure 36. Effect of conditionally-expressed RhoA^{Y42C} mutant in gastric tumorigenesis.

Animals expressing the RhoA^{Y42C} mutant and *Cre* recombinase under the control of the gastrointestinal-specific *Villin 1* promoter, or control animals carrying only RHOA-Y42C, *Vil-Cre* or neither of these transgenes, were treated with the stomach-specific carcinogen N-Nitroso-N-methylurea (MNU) for 5 weeks. In some animals (A), mutations in the tumor-suppressor gene *Apc* were used in an attempt to accelerate tumorigenesis in MNU treated animals. Animals were sacrificed at the age of 19 (A), 35 (B) or 50 (C) weeks, and the number of gastric tumors were scored in histological sections. n=number of animals per group. The mean (±SEM) is shown, Student's t-test *p<0.05.

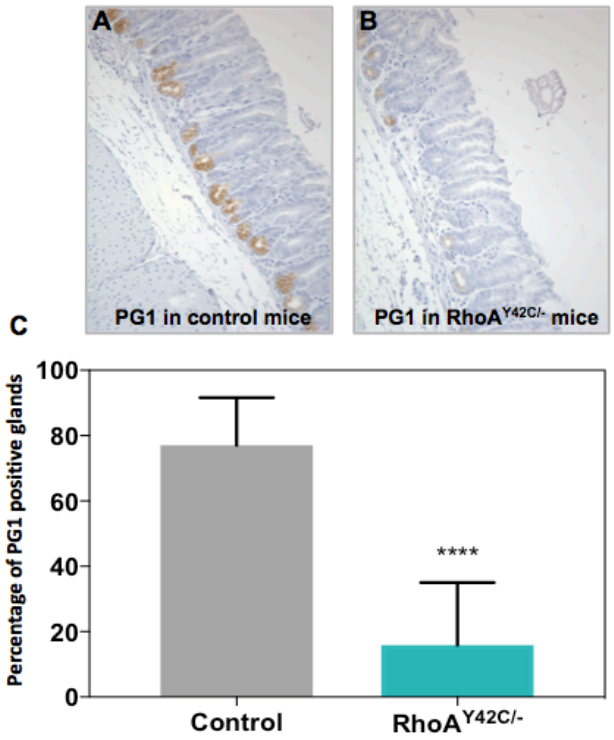

Figure 37. Relative levels of Pepsinogen 1 (PG1) in gastric glands of *RhoA*^{Y42C} transgenic mice.
(A-B) Representative photographs of gastric glands for PG1 immunodetection (IHC) in control and *RhoA*$^{Y42C/-}$ mice are shown. 20X magnification. At least 20 glands from 3 different regions and from 6 animals per group were scored. C) The percentage of the positive PG1 staining glands in the stomach of 35-week-old *RhoA*$^{Y42C/-}$*;Vil-Cre*$^{-/-}$ and *RhoA*$^{Y42C/-}$*;Vil-Cre*$^{TG/-}$ mice was determined. The mean (±SEM) is shown. Student's t-test, ****p<0.0001.

2. Characterization of the interactome of wild type RHOA and the RHOA mutants frequently found in gastric tumors

RHOA is an important molecular switch that acts through binding and activation of several downstream effectors (195). Interestingly, high frequency of point RHOA mutations has been reported in diffuse gastric cancer (184, 185), however the effects of these mutations are currently unknown. Moreover, the most recurrent RHOA-Y42C mutation found in diffuse gastric tumors has been shown to affect the binding capacity to its known effector PKN1, while not affecting the interaction of RHOA with other effectors (292). Therefore, to investigate changes in the RHOA binding capacity caused by its most frequent mutations reported in diffuse gastric tumors, the interactome of these RHOA mutants was investigated.

2.1 Yeast two-hybrid screening of effector binding to wild type and mutant RHOA

To study the effects of the frequent RHOA mutations found in gastric tumors on the binding capacity of RHOA to its known effectors, a yeast two-hybrid (Y2H) screening was performed. This assay is used to identify interacting proteins where the proteins of interest are expressed in yeast as a fusion to the DNA-binding domain (BD) or activation domain (AD) of a transcription factor, creating hybrid proteins. If there is an interaction between the two hybrid proteins, the BD and AD are brought together within the cell nucleus to lead the expression of a reporter gene. Whereas, in the absence of interaction the reporter gene will be not expressed (301). As previously reported (292), the RHOA mutations G14V and I90S were introduced in the coding sequence of RHOA and used as a bait in this assay, as these two mutations allow the protein to be active and inhibits the membrane-anchorage capacity, respectively. The RHOA protein carrying these two mutations (G14V and I90S) is henceforth referred to as the wild type RHOA (i.e., not carrying any of the recurrent mutations found in gastric tumors) and the capacity to interact with some of the best characterized RHOA effectors, namely, PKN1 (236, 314), ROCK (315-318), DIAPH2 (319), and Kinectin (319, 320), was compared to RHOA mutants carrying the RHOA mutations most frequently found in gastric tumors, R5Q, G17E, Y42C and L57V (184, 185).

As expected, no yeast colonies were observed in agar plates when the empty pGTB9 vector was used (**Figure 9**), and robust growth was observed to all the tested RHOA interactors (PKN1, ROCK1, DIAPH2 and Kinectin) when the wild type RHOA was used as a bait, even in the presence of the highest concentration (5mM) of 3-amino-1,2,4-triazole (3-AT), a competitive inhibitor of the product of the *HIS*3 gene that allows a semiquantitative assessment of the strength of RHOA binding to these effectors (i.e., stronger interactions require higher concentrations of 3-AT to inhibit yeast growth; **Figure 38** and **Table 7**). We were able to confirmed as previously reported (292) that RHOA-Y42C was unable to bind to PKN1 even in the absence of 3-AT (-), while retaining its binding capacity to almost all the RHOA effectors tested (+++) (DIAPH2, ROCK1 and Kinectin; **Figure 38** and **Table 7**). Moreover, it was observed that all mutants, except R5Q, are unable to bind to PKN1. Interestingly, RHOA-G17E mutant did not bind neither to PKN1, ROCK nor Kinectin. However, there was a moderate binding between RHOA-G17E mutant to DIAPH2 (++), but in the highest 3-AT concentration the interaction was lost, suggesting that at least this G17E mutant decrease the binding capacity or produce an unstable interaction with DIAPH2 effector. Further investigations are necessary to analyze this effect. Finally, we observed robust colony formation even in the highest 3-AT concentration for RHOA-R5Q, -Y42C and -L57V mutants, each interacting with ROCK, DIAPH2 and Kinectin,

which strongly suggest that these mutations do not affect the binding capacity to the effectors tested. Collectively, these results demonstrated that the most frequent RHOA mutations found in DGC and specifically RHOA-Y42C interfere with PKN1 interaction. Also, these new mutants give the opportunity to further investigate its role in GC. The summary of the results is shown in **Table 7**.

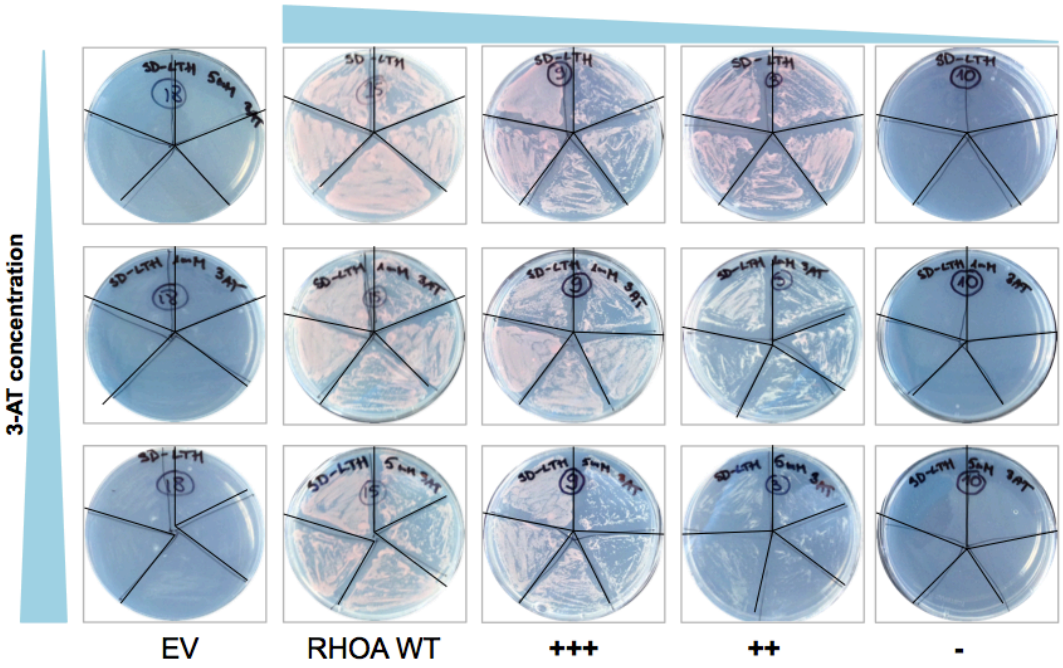

Figure 38. Yeast growth for testing protein-protein interaction between wild type and mutant RHOA to different effectors.

Yeast two-hybrid system was performed to evaluated protein-protein interaction of wild type RHOA and the most frequent RHOA mutations found in DGC to the most known effectors (PKN1, ROCK, DIAPH2 and Kinectin). Representative images of the binding as example with EV-DIAPH2, RHOA WT-DIAPH2, L57V-DIAPH2 (+++), G17E-DIAPH2 (++) and G17E-Kinectin (-) are shown. At least 5 colonies were picked to growth in SD conditional media. 3-AT concentration from the top to above 0, 1 and 5 □M respectivey, is shown. *+++ Robust growth with 0mM, 1mM and 5mM 3-amino-1,2,4-triazole (3-AT); ++ Robust growth with 0mM and 1mM 3-AT; - No growth with or without 3-AT*

Table 7. Interaction of RHOA mutants with downstream effectors

	EV	RHOA-WT	RHOA-R5Q	RHOA-G17E	RHOA-Y42C	RHOA-L57V
PKN1	-	++	++	-	-	-
ROCK	-	+++	+++	-	+++	+++
DIAPH2	-	+++	+++	++	+++	+++
Kinectin	-	+++	+++	-	+++	+++

+++ Robust growth with 0mM, 1mM and 5mM 3-amino-1,2,4-triazole (3-AT), a competitive inhibitor of the product of the *HIS3* gene

++ Robust growth with 0mM and 1mM 3-AT

- No growth with or without 3-AT

2.2 Mass spectrometry screening of effector binding to wild type and mutant RHOA

As an independent and unbiased method to identify changes in the RHOA interactome caused by the recurrent RHOA mutations found in DGC (184, 185), a pulldown assay coupled with liquid chromatography/mass spectrometry (LC/MS) analysis was performed (**Figure 39**). Wild type RHOA (not carrying the G14V or the I90S mutations needed for the yeast two-hybrid assay, or any of the GC hotspot mutations) or the RHOA-R5Q, -G17E, -Y42C or -L57V mutants were produced in bacteria as a fusion protein with GST. These proteins were purified and used as 'bait' to identify binding proteins in a protein lysate obtained from mixing equal amounts of total protein extracted from 9 different diffuse gastric cancer cell lines, used here as a protein lysate representative of human gastric tumors with diffuse histology (**Figure 39A**). RHOA and interacting proteins were pulled down with glutation sepharose beads and binding proteins were eluted and identified using liquid chromatography/mass spectrometry analysis (LC/MS; **Figure 39B**).

As expected, wild type RHOA was found to bind to multiple proteins that are known RHOA interactors, including PKN2, RALY, CBX1, NHP2L1 and H2AFY (**supplementary Table 8**). Interestingly, there are some notable absences on that such as ROCK and DIAPH1, which are among the best known RHOA effectors, but this might be due to these proteins not being expressed at significant levels in diffuse gastric cancer cell lines. Further analysis needs to be done in order to address this question.

Importantly, a significant number of proteins binding to wild type RHOA but not to any of the RHOA mutants investigated were identified (**supplementary Table 8**). PKN2 was found to be

the most abundant protein interacting with wild type RHOA but not with any of the RHOA mutants investigated (**Figure 39C; supplementary Table 8**). To validate these results, we tested by Western blot the levels of PKN2 in the pulldown with the different mutations of RHOA. In good agreement with the mass spectrometry results we observed robust biding of wild type RHOA to PKN2, whereas no binding of PKN2 was detected to the recurrent hotspot mutations found in gastric tumors (**Figure 39D**). Moreover, we showed that in MKN45 and NUGC3 cells that PKN1 binds to wild type RHOA but not to Y42C, in good agreement with the Y2H data (**Figure 40**).

In addition, multiple proteins were found that do not bind to wild type RHOA but consistently bind to all the RHOA mutants investigated, including PSPC1, FARSA, FARS8 and WDR11 (**supplementary Table 8**).

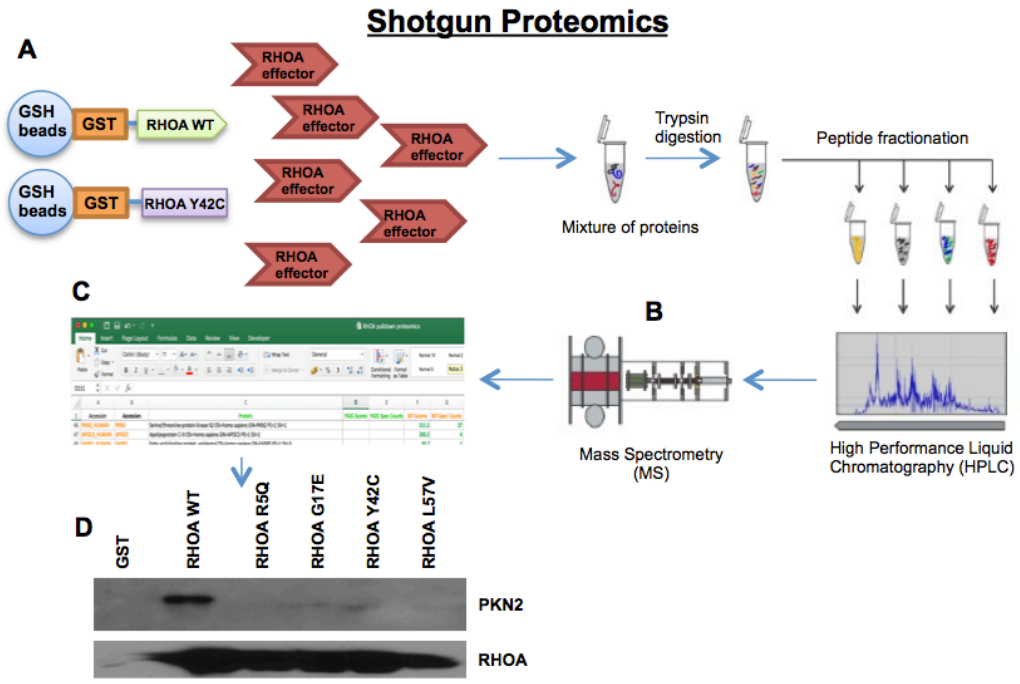

Figure 39. Identification of RHOA interactors using mass spectrometry.

A) GST fused to wild type RHOA or the most common RHOA mutants found in diffuse gastric tumors (R5Q, G17E, Y42C and L57V) were produced in bacteria as GST-RHOA fusion proteins and after purification were used to pulldown RHOA interacting proteins binding to wild type or mutants RHOA. B) The RHOA interacting proteins were identified using mass spectrometry. C) PKN2 was found to be the most abundant protein binding to wild type RHOA and not binding to either of the four RHOA mutants tested. D) PKN2 binding to wild type RHOA and the lack of interaction with the RHOA mutants was confirmed by Western blotting.

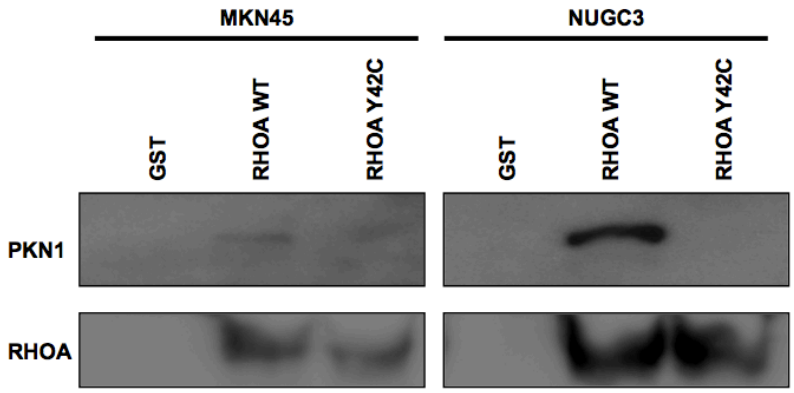

Figure 40. PKN1 and RHOA pulldown in gastric cancer cells.
PKN1 binding to wild type RHOA and the lack of interaction with the RHOA-Y42C mutant was confirmed by Western blot in MKN45 and NUGC3 cells. RHOA Ab was used as a positve control.

Recent data from our laboratory has shown that RHOA has tumor suppressor activity in DGC cells (unpublished data, **Figure 22-23**) and RHOA hotspot mutations found in diffuse gastric tumors, such as RHOA-Y42C, are oncogenic (see the results obtained with the RHOA-Y42C transgenic mouse model in Results Section 1; and additional unpublished data). Therefore, in this study it is postulated that RHOA mutations interfere with a branch of RHOA signaling with strong tumor suppressive activities, while leaving unaffected other signaling pathways downstream of RHOA that are oncogenic. Interestingly, RHOA-PKN binding was found to be suppressed by the RHOA mutations more commonly found in DGC. These results led us to formulate the hypothesis that the tumor suppressive RHOA effects observed in gastric cancer are mediated by downstream PKN signaling. This hypothesis is investigated in the following sections of this Thesis.

3. Investigation of the role of PKN1 in gastric cancer

The gastric and intestinal epithelium shows the fastest renewal rate among all the tissues in the body. Uncontrolled cell growth represents a critical initial event for cancer development (37), and spreading of the disease to distant organs represents the major cause of cancer death. Therefore, to investigate the role of PKN1 in the growth and metastatic potential of diffuse gastric cancer cells, we generated isogenic cell lines.

3.1 Generation of isogenic cell lines models with modulation of PKN1 expression

To assess possible phenotypic changes resulting from the manipulation of PKN1 in diffuse gastric cancer cells, it was generated isogenic cell line models where PNK1 expression was downregulated or knocked out in cell lines with high endogenous levels of the protein and then PKN1 was overexpressed in cell lines with low endogenous levels.

3.1.1 Assessment of the expression of RHOA and PKN in gastric cancer cell lines

To select cell line models for the modulation of PKN expression, first the mRNA expression of RHOA, PKN1 and PKN2 were analyzed in a panel of 14 gastric cancer cell lines, 9 diffuse-type cancer cell lines and 5 intestinal-type cancer cell lines (**Figure 41A-C**) available from *'Genentech gastric cell line sequencing'* (Dataset stable ID: EGAD00001001013), a database of RNAseq and exome sequencing of gastric cancer cell lines available in the 'European Genome-phenome Archive'. Then, the protein levels of expression of total and active RHOA, PKN1 and PKN2 were further studied in a panel of 9 diffuse-type gastric cancer cell lines (**Figure 41F**).

Correlation analysis was performed between mRNA levels of RHOA and mRNA of PKNs (**Figure 41D-E**), and a significant correlation was observed between RHOA and PKN2 expression in the subset of 9 diffuse-type cancer cell lines (Pearson's r=0.47, p=0.04, **Figure 41E**). Overall, the average of mRNA levels of RHOA, PKN1 and PKN2 are higher in diffuse-type cancer cell lines than the intestinal-type cell lines, although these values are not different between both types of cell lines. As it is known, according Lauren's classification, gastric cancer distinguishes intestinal (differentiated) type GC and diffuse (undifferentiated) type GC. Several investigations around the world are trying to identify specific markers genes to early predict gastric carcinogenesis and to elucidate the molecular mechanism behind the disease. Interestingly, the screening of a vast number of genes, such as *cadherin* family genes (321, 322), human *mucin* genes (323), *vimentin* (324) and *cathepsin* family genes (325-327), whose expressions have been reported to be different between intestinal and diffuse type GC. Therefore, it could be further investigated whether RHOA and PKN proteins could be good markers in GC and also the tumor suppressive potential of RHOA and PKN family proteins in both intestinal and diffuse-type gastric cancer.

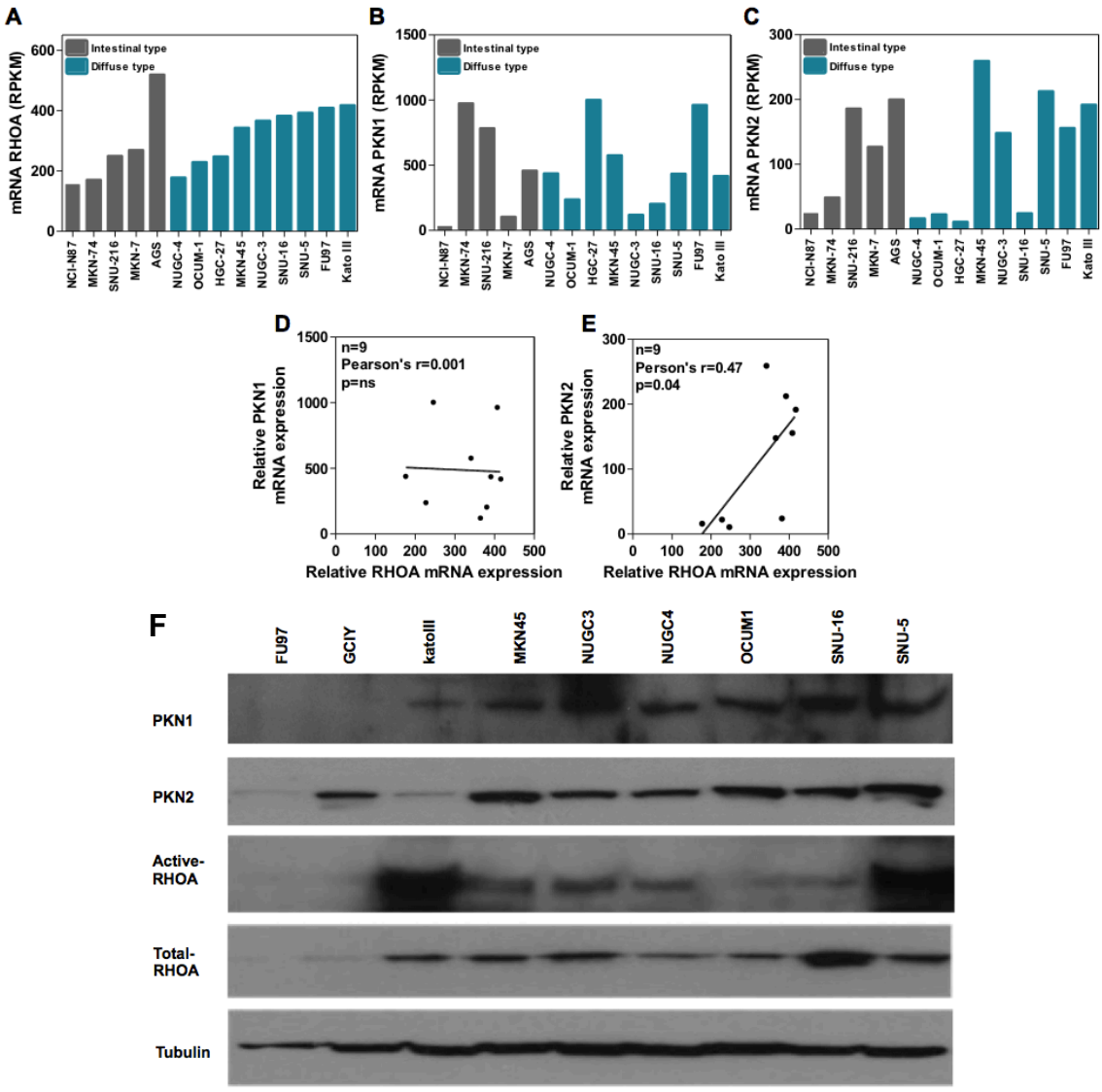

Figure 41. Expression levels of RHOA, PKN1 and PKN2 in a panel of 14 intestinal and diffuse gastric cancer cell lines. A-C) The relative mRNA expression levels of RHOA, PKN1 and PKN2 in gastric cancer cell lines did not show difference between intestinal and diffuse gastric cancer cell lines, Dataset stable ID: EGAD00010001013. Relative mRNA levels of PKN1 (D) and PKN2 (E) were correlated with mRNA levels of RHOA, and a significant correlation was observed between mRNA RHOA levels and mRNA PKN2 levels (Pearson's r=0.47, p=0.04). F) The expression of active RHOA, total RHOA, PKN1 and PKN2 proteins was assessed by Western blotting in a panel of 9 different gastric cancer cell lines derived from intestinal and diffuse type human gastric cancer tumors.

3.1.2 Downregulation of PKN1 in gastric cancer cell lines

MKN45 (MSS) and NUGC3 (MSI-high) were selected as models for PKN1 downregulation since they show high relative expression of endogenous PKN1 mRNA and protein levels (**Figure 41F**). The MKN45 cell line was selected for PKN1 knockout using CRISPR/Cas9 technology. Parental

MKN45 cells were transiently transfected with a pX458 plasmid expressing Cas9 and GFP in addition to a sgRNA (described in methods) against PKN1. Transfected GFP-positive cells were sorted by FACS, seeded at low density and allowed to form individual colonies. After expansion of 24 clones, DNA sequencing of the targeted exon 2 showed a total of 13 clones (45%) with PKN1 mutations, and other 11 clones (38%) were wild type (**Figure 42A**). PKN1 protein levels were detected by Western blot (**Figure 42B**). Western blot analysis demonstrated complete loss of PKN1 protein expression in four clones (henceforth referred as knockout, KO), and three of the wild type clones (henceforth referred as WT) were selected as a negative control **(Figure 42B)**.

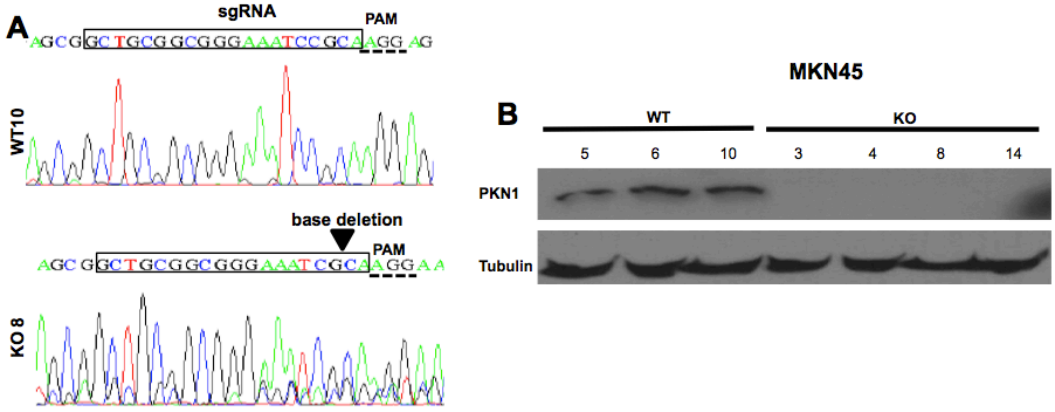

Figure 42. Validation of MKN45 isogenic *in vitro* model for the study of PKN1 role in gastric cancer by CRISPR/Cas9 technology.

A) Chromatogram showing PKN1 exon 2 region targeted for the parental cell line and a representative example of the mutant clones obtained. sgRNA and PAM sequences are indicated in the figure. The presence of double picks after the target sequence (black arrowhead) indicates the presence of an insertion/deletion for each of the alleles. B) Relative PKN1 protein expression in MKN45 wild type (WT) and knockout clones (KO). Tubulin levels are shown as a loading control.

Because it was not possible to get individual clones from NUGC3 cells that could then be expanded after CRISPR/Cas9-based inactivation, an approach based on lentiviral transduction and RNA interference was used to downregulate PKN1 expression in this cell line. Therefore, NUGC3 cells were stably transduced with doxycycline-inducible vectors containing two different shRNA sequences targeting PKN1 (sh1, sh2) and a control non-target shRNA (shNT). After puromycin selection, the percentage of RFP-positive cells was determined by flow cytometry to

be above 90% (**Figure 43A-B**). Downregulation of PKN1 was confirmed by Western blotting after treatment of the different derivative NUGC3 cell lines with 1 µg/mL Doxycycline (Dox) for 7 days of treatment (**Figure 43C**).

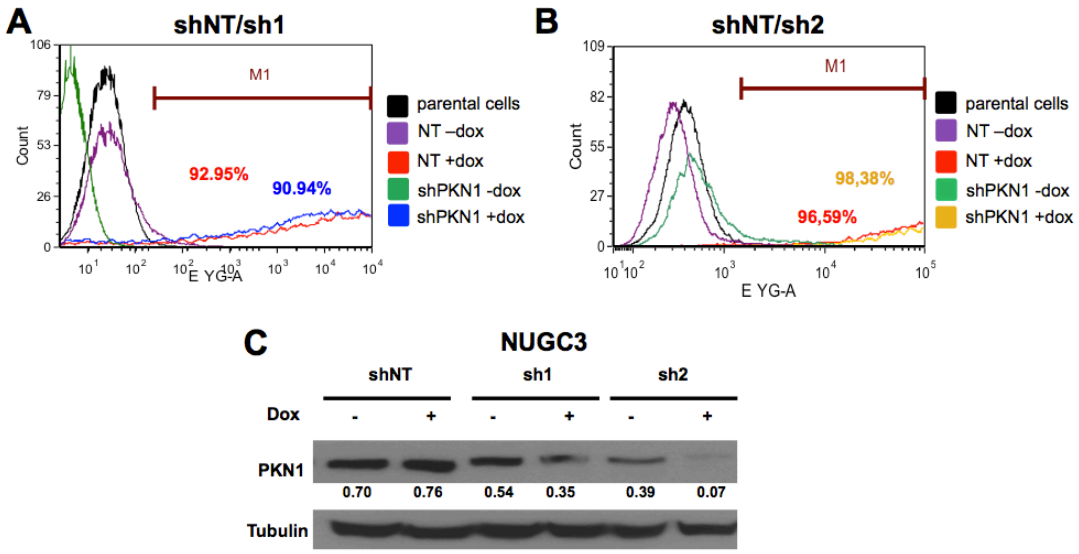

Figure 43. Validation of isogenic *in vitro* NUGC3 models for the study of PKN1 role in gastric cancer by RNA interference.

A-B) Flow cytometry analysis (FACS) of the Doxycycline-inducible model for PKN1 downregulation in NUGC3 cells (sh1 and sh2) and its corresponding shNT control. The percentage of RFP-positive cells is shown. C) Relative PKN1 protein expression in control shNT, sh1 and sh2 NUGC3 derivative cell lines is shown after Dox treatment, -sh1 and -sh2 showed a 33% and 82% reduction in PKN1 expression, respectively. Tubulin levels are shown as loading control.

3.1.3 Overexpression of PKN1 in gastric cancer cell lines

In addition, novel isogenic cell line systems with inducible expression of a constitutively active form of PKN1 were engineered using the pINDUCER lentiviral toolkit (294). We chose two diffuse gastric cancer cell lines, FU-97 (MSS) and NUGC4 (MSS). FU-97 cells show undetectable levels of PKN1 protein expression and NUGC4 cells show moderate endogenous levels of PKN1 as determined by Western blotting (**Figure 41F**). FU-97 and NUGC4 parental cells were stably transduced (lentiviral infection) with a vector expressing a constitutively active deletion mutant of PKN1 lacking amino acids 512 to 942, fused to a reporter mCherry gene at its N-terminal region [fused-protein PKN kept its proper function (328)] or the corresponding empty vector as a control (EV) expressing mCherry. After neomycin selection, PKN1 overexpression was assessed. First, the overexpression of $PKN1^{1-511}$ was confirmed at mRNA level by qPCR

(**Figure 44A-B**). Then, detection of mCherry fluorescence in the derivative cell lines was analyzed by flow cytometry (FACS), and the percentage of mCherry-positive cells was 93.6% and 90.3% for FU-97-EV and FU-97-PKN1$^{1-511}$, respectively (**Figure 44C**), and 74.4% and 96.1% for NUGC4-EV and NUGC4-PKN1$^{1-511}$, respectively (**Figure 44D**). Doxycycline-dependent expression of PKN1$^{1-511}$ was confirmed by Western blotting with a range of different Dox concentrations (**Figure 45A-B**) for both cell lines. Finally, 72h of incubation with 0.5 μg/mL of Dox was selected as the appropriate conditions to use for further experiments in both cases (**Figure 45C-D**).

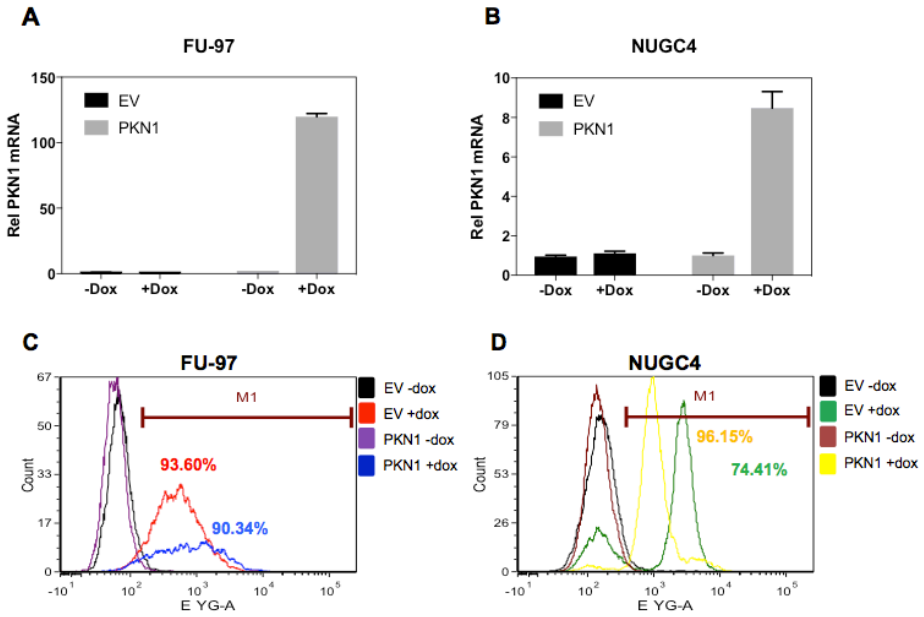

Figure 44. Validation of isogenic FU-97 and NUGC4 *in vitro* models for constitutively active PKN1$^{1-511}$ overexpression by qPCR and flow cytometric analysis.

A-B) Relative levels of PKN1 mRNA in FU-97 cells (A) and NUGC4 (B) with/without Dox treatment were determined by qPCR. C-D) Flow cytometry analysis (FACS) of mCherry-PKN1$^{1-511}$ overexpression in FU-97 (C) and NUGC4 (D) cells and their corresponding mCherry EV-control are shown.

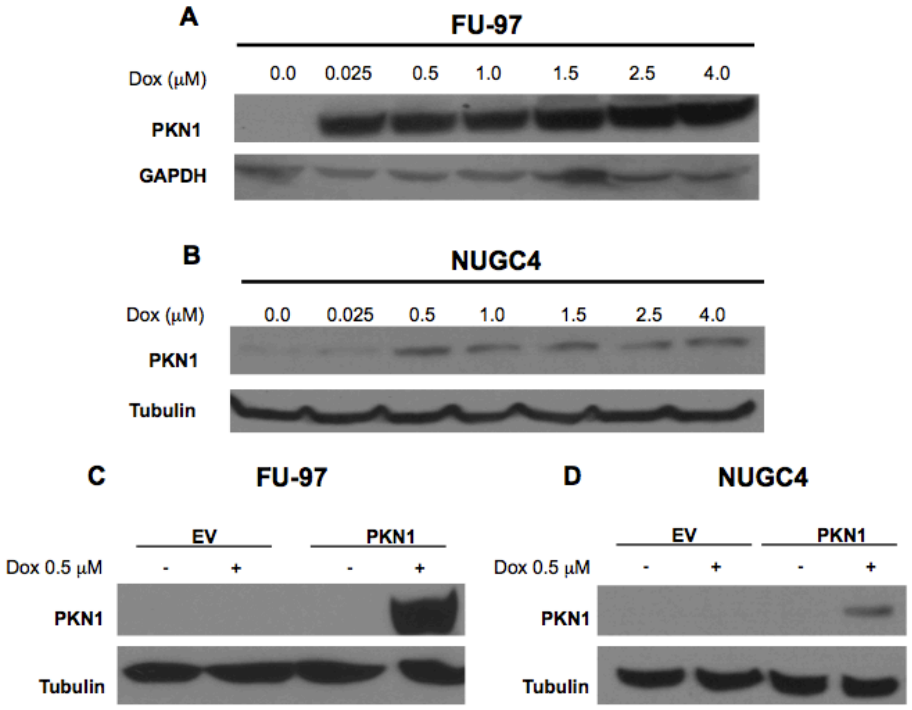

Figure 45. Validation of isogenic *in vitro* models for constitutively active PKN1 overexpression by Western blot.
A-B) Western blot showing ectopic PKN1$^{1-511}$ protein expression in FU-97 (A) and NUGC4 (B) cells after exposure to different concentrations of Doxycycline for 72h. C-D) Protein expression of PKN1$^{1-511}$ after 72h of incubation with 0.5 μg/mL Doxycycline in FU-97 (C) and NUGC4 (D) cells and their respective EV-control.

4. Investigation of the role of PKN1 in gastric tumorigenesis using the isogenic cell line models generated

4.1 Investigation of the role of PKN1 on the growth of diffuse gastric cancer cells

Uncontrolled cell growth represents a critical initial event for cancer development (37). Therefore, the molecular pathways behind this complex process need to be thoroughly investigated. To further study the role of PKN1 on the growth of diffuse gastric cancer cells, all the novel isogenic cell line systems previously generated were characterized through different *'in vivo'* and *'in vitro'* approaches, such as clonogenic, anchorage-dependent and anchorage-independent growth.

4.1.1 PKN1 and growth of diffuse gastric cancer cells

First, the effect of PKN1 knockout in MKN45-PKN1-KO cells (**Figure 46A**) and PKN1 downregulation in NUGC3 cells using doxycycline-inducible shRNAs (**Figure 46B**) was assessed. The results show a significant increase in their proliferation capacity for both cell lines, measured by direct cell-count compared to their respective controls. In addition, the effect of the doxycycline-controlled overexpression of constitutively active $PKN1^{1-511}$ into FU-97 and NUGC4 cell lines was studied (**Figure 46C-D**). In good agreement with the previous results, the proliferation rate showed a significant decrease compared to their respective controls in both FU-97 and NUGC4 cell lines. Taken together, these results demonstrate that PKN1 inhibits cell proliferation *'in vitro'*.

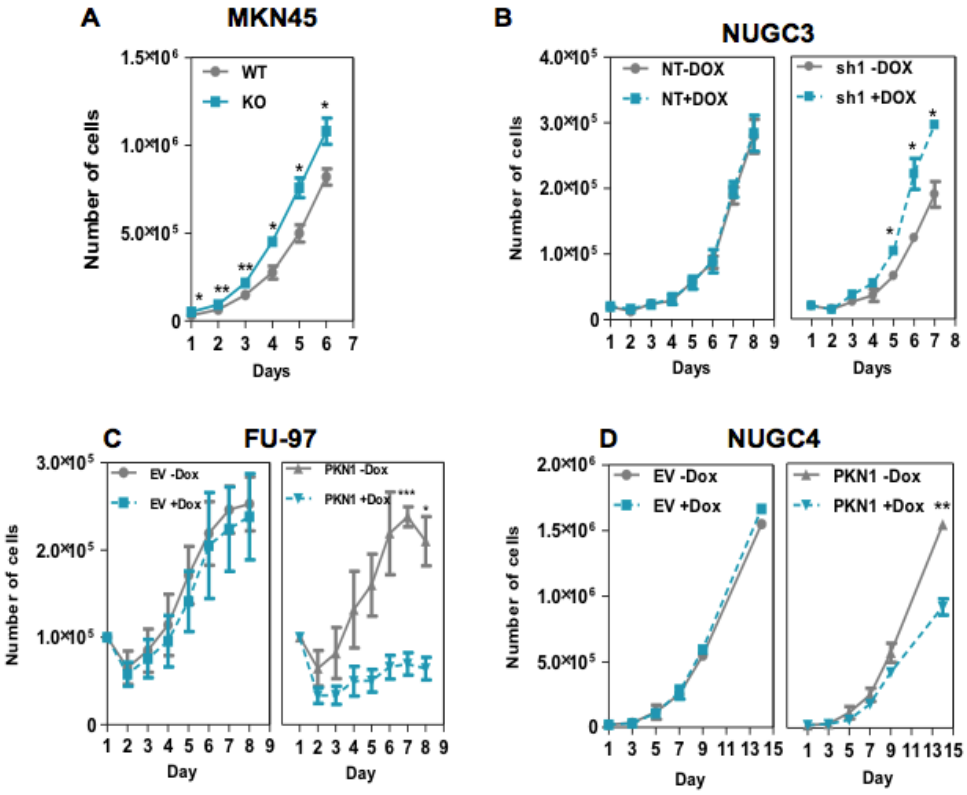

Figure 46. Role of PKN1 on the proliferation rate of gastric cancer cells on attachment conditions.

A) The effect of targeted deletion of PKN1 on the average growth of four different PKN1 knockout clones of MKN45 cells compared with the average growth of three PKN1 wild type clones. B) Effects of PKN1 downregulation in NUGC3-sh1 compared to the NUGC3-shNT control cells. C-D) The effects of constitutively active $PKN1^{1-511}$ overexpression in the growth of FU-97 and NUGC4 compared to the corresponding EV control lines. Proliferation was measured by directly counting the number of cells over time using a Fuchs-Rosenthal chamber. The mean (±SEM) of three independent experiments with three technical replicates each is shown. Student's t-test. * $p<0.05$; ** $p<0.01$; *** $p<0.001$

4.1.2 PKN1 and the clonogenic potential of diffuse gastric cancer cells

The capacity of tumor cells to survive as single cells and continue to divide forming a macroscopic colony is associated with its long-term proliferative capacity. The clonogenic potential of the isogenic cell line models generated was studied. In the case of MKN45-PKN1-KO cells (**Figure 47A**) no differences were observed in their ability to form colonies compared with the MKN45-PKN1-WT controls. However, in NUGC3-sh1 cells with PKN1 downregulation there was a significant increase in the number of colonies observed 15 days after seeding the cells at low density (**Figure 47B**). In good agreement, overexpression of the constitutively active $PKN1^{1-511}$ in FU-97 (**Figure 47C**) and NUGC4 (**Figure 47D**) cells resulted in a significant

decrease in the number of colonies compared with the corresponding EV controls. Taken together these results demonstrate that PKN1 negatively can regulate the long-term clonogenic potential of diffuse gastric cancer cells.

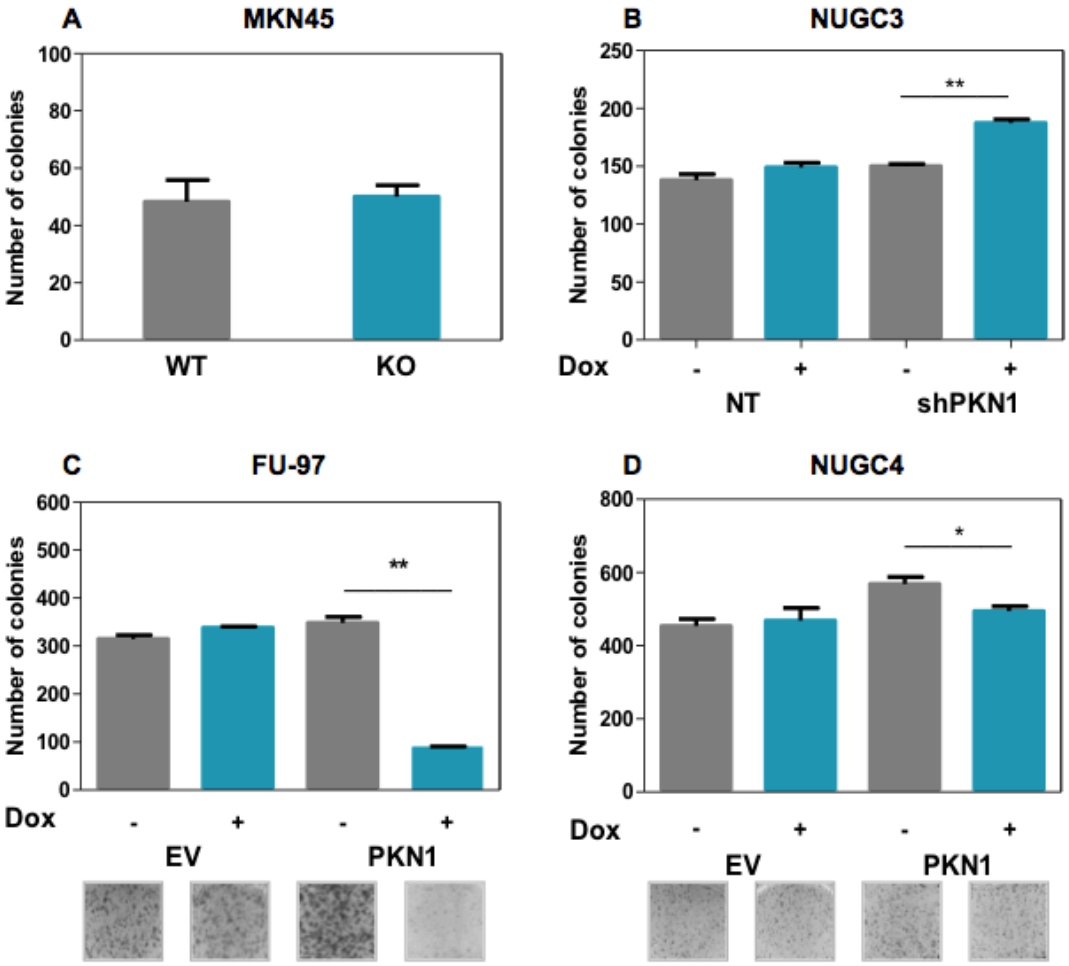

Figure 47. Effect of PKN1 on the clonogenicity of gastric cancer cells.

A) The average number of colonies observed 15 days after seeding 500 cells on tissue culture plates is shown for 4 MKN45-PKN1-KO clones and 3 MKN45-PKN1-WT clones. The mean (±SEM) of WT and KO clones is shown. (B) The average number of colonies for NUGC3-shNT and NUGC3-sh1 with/without 1 µg/mL Dox is shown. C-D) Number of colonies observed in the clonogenic assay for FU-97 and NUGC4 cell lines with inducible constitutively active $PKN1^{1-511}$ overexpression and the corresponding EV control, treated with/without 0.5 µg/mL Dox. Representative pictures of the number of colonies formed by each of the lines/conditions are shown under the corresponding histogram bars. The mean (±SEM) of at least three independent experiments each carried out in triplicate is shown. Student's t test *p<0.05; **p<0.01; ***p<0.001

4.1.3 PKN1 and the anchorage-independent growth potential of diffuse gastric cancer cells

The ability to exhibit anchorage-independent cell growth (colony forming capacity in soft agar semisolid media) has been associated with a more aggressive phenotype '*in vivo*' such as tumorigenic and metastatic potentials, and is also used '*in vitro*' as a marker of transformation (329, 330). Therefore, we next investigated whether modulation of PKN1 expression affected the anchorage-independent growth of diffuse gastric cancer cells. The deletion of PKN1 did not to affect the anchorage-independent growth capacity of MKN45-PKN1-KO cells compared to MKN45-PKN1-WT cells (**Figure 48A**). Although NUGC3 cells were unable to grow under these conditions and are therefore not amenable for this assay, forced overexpression of a constitutively active form of $PKN1^{1-511}$ in FU-97 and NUGC4 cells resulted in a significant reduction in their anchorage-independent growth, compared to the corresponding EV control lines (**Figure 48B-C**). These results show that ectopic expression of $PKN1^{1-511}$ can interfere with the anchorage-independent growth capacity of diffuse gastric cancer cells.

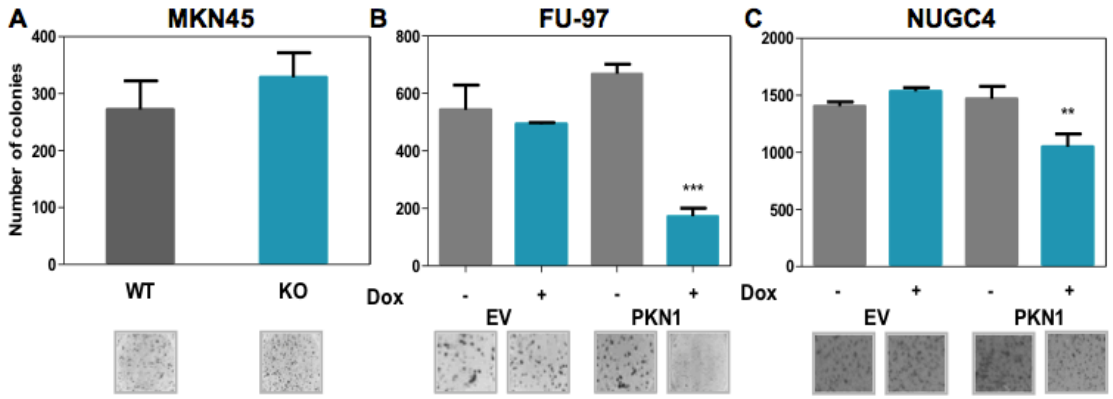

Figure 48. Effect of PKN1 on the anchorage-independent growth of gastric cancer cells.

A) Anchorage-independent cell growth of the MKN45-PKN1-KO and MK45-PKN1-WT cells in soft agar, the average of 4 wild type clones and three knockout clones is shown. B-C) Anchorage-independent cell growth for $PKN1^{1-511}$ overexpressing FU-97 and NUGC4 cells and the corresponding EV controls is shown. The mean (±SEM) of at least three independent experiments each carried out in triplicate is shown. Student's t test **p<0.01; ***p<0.001

4.1.4 PKN1 and growth of diffuse gastric cancer cells 'in vivo'

Uncontrolled cell growth represents a critical initial event for cancer development (37). Xenograft models, where tumor cells are subcutaneously implanted in immunodeficient mice, are often used to study the growth of human cancer cells '*in vivo*' and to determine the '*in vivo*' activity of

new anti-cancer therapeutics prior to clinical development and testing in humans. Therefore, the role of PKN1 on the *'in vivo'* growth of gastric cancer cells was further investigated using a subcutaneous xenograft in a NOD/SCID mouse model. All animals (n = 10) were subcutaneously injected with the pool of 3 MKN45-PKN1-WT clones and 4 MKN45-PKN1-KO clones ($1x10^6$ cells) in order to minimize the clonal effect, in the right and left flank, respectively. Tumor growth was monitored for 40 days, and targeted deletion of PKN1 in MKN45-PKN1-KO cells resulted in significantly faster tumor growth compared to the contralateral wild type MKN45-PKN1-WT cells (**Figure 49A**). Consistently, the weight of xenografts was measured at the end of the experiment and there was a significant increase in the weight of the tumors formed by the MKN45-PKN1-KO cells compared to the tumors derived from MK45-PKN1-WT cells (**Figure 49B**). In good agreement, an increase in the number of proliferative cells (BrdU-positive cells) was observed in tumors formed by MKN45-PKN1-KO cells compared to the MKN45-PKN1-WT cells (**Figure 49C**), although no differences were observed in the number of apoptotic cells (Caspase 3-positive cells) in MKN45-PKN1-KO and MKN45-PKN1-WT tumors (**Figure 49D**).

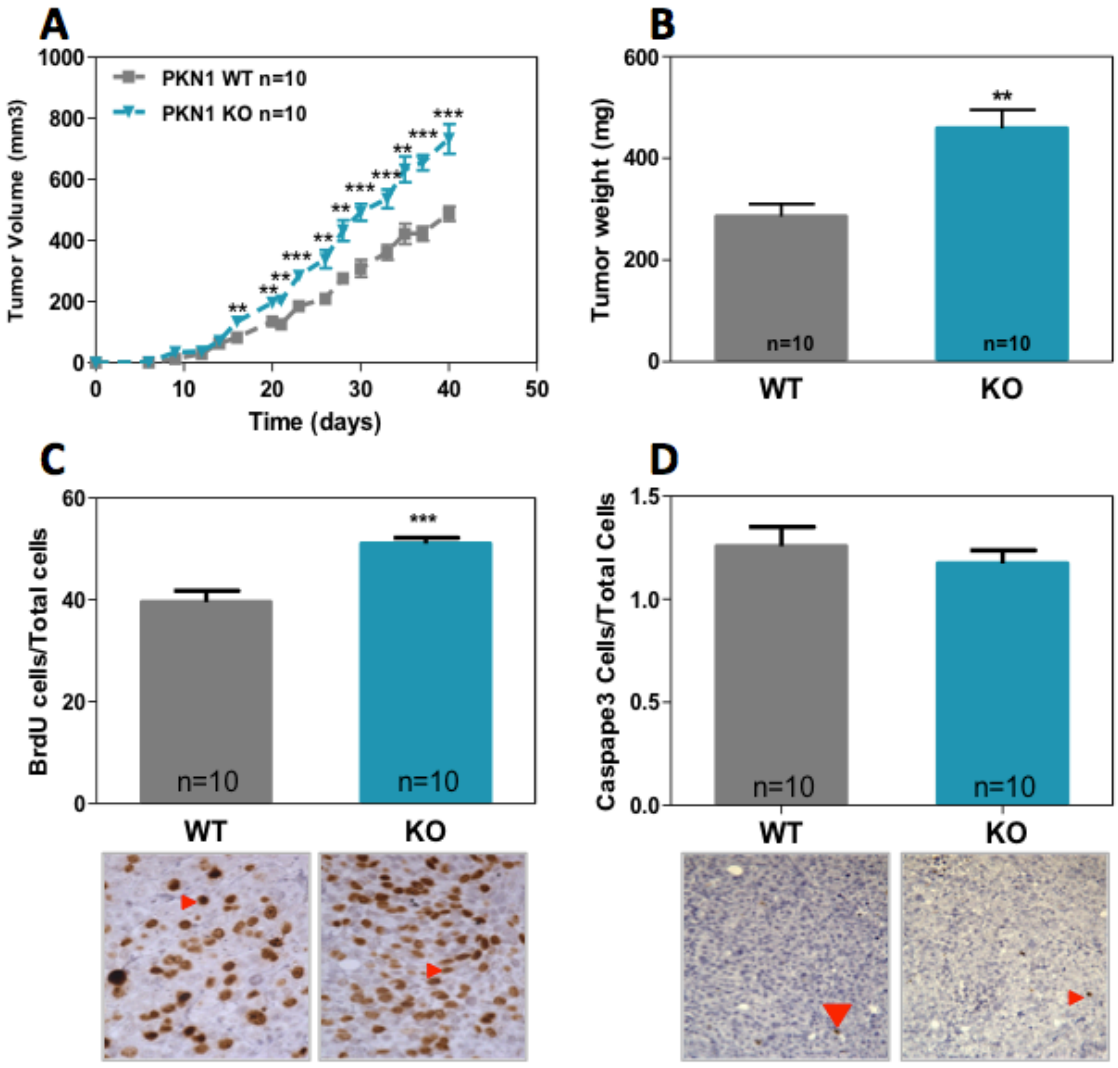

Figure 49. Effect of PKN1 in the growth of MKN45 gastric cancer cells *in vivo*.

A) 10 NOD/SCID mice were injected ($1x10^6$ cells) subcutaneously in left flank with MKN45-PKN1-WT cells and MKN45-PKN1-KO cells in the right flank and the volume of the subcutaneous tumors formed was monitored over time. B) The average weight (±SEM) of the tumors formed by the MKN45-PKN1-WT and MKN45-PKN1-KO cells at the end of the experiment is shown. The tumor samples were formalin-fixed and paraffin-embedded, tissue sections were cut (4□m) and processed for IHC detection. The average number (±SEM) of proliferative cells (C; BrdU-positive immunostaining, 40X magnification) and apoptotic cells (D; active Caspase 3-positive immunostaining, 20X magnification) was quantified in the tumors formed by MKN45-PKN1-WT and MKN45-PKN1-KO cells. At least 200 tumor cells were scored per mouse and there were n=10 mice per group. Panels A, B, C and D shown the average (±SEM). Student's t test **p<0.01; ***p<0.001

To further investigate the role of PKN1 downregulation in diffuse gastric cancer cells, NUGC3-shNT and NUGC3-sh1 cells were subcutaneously injected in the left or right flank, respectively, of a total of 20 NOD/SCID immunodeficient mice. Animals were then randomized into two groups (n=10) that were treated or not with 1 mg/mL Dox in the drinking water. No significant differences were observed in the growth of the xenografts formed by control NUGC3-shNT and NUGC3-sh1 cells (**Figure 50A**). The weight of tumors was determined at the end of the experiment and no differences were observed between control NUGC3-shNT and NUGC3-sh1 tumors (**Figure 50B**). However, the quantification of the levels of PKN1 in the tumors at the end of the experiment failed to demonstrate a reduction in PKN1 expression in the NUGC3-sh1 tumors from animals treated with Dox (**Figure 50C**). Importantly, since we have subsequently confirmed that PKN1 downregulation is more robust using a second shRNA targeting PKN1 (NUGC3-sh2; **Figure 43C**), it would be interesting to repeat these experiments using NUGC3-sh2 cells to further evaluate the effects of PKN1 downregulation on the growth of diffuse gastric cells "*in vivo*".

Collectively, the results obtained demonstrate that PKN1 can regulate the clonogenic potential and the growth of diffuse gastric cancer cells under attachment and non-attachment conditions as well as in a subcutaneous xenograft model.

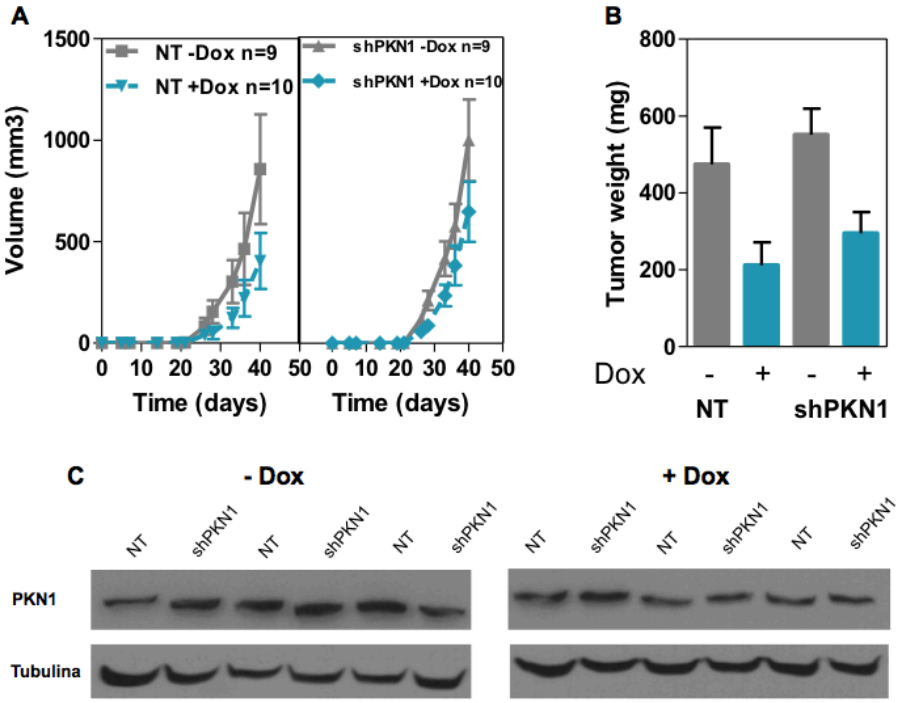

Figure 50. Effect of PKN1 in the proliferation of NUGC3 gastric cancer cells *in vivo*.

A) Volume of subcutaneous tumors with downregulation of PKN1 (NUGC3-sh1) vs control (NUGC3-shNT) over time. All the cell lines were subcutaneously injected in 20 NOD/SCID animals. Then, the animals were randomized in two groups (n=10). The animals were treated with/without 1 mg/mL Dox in the drinking water. B) Tumor weight of NUGC3-sh1 and NUGC3-shNT xenografts with/without Dox at final point. C) Levels of PKN1 expression in tissue extracts from subcutaneous xenografts formed by NUGC3-shPKN1 and NUGC3-shNT cells with/without Dox treatment. The average tumor size (±SEM) and average tumor weight (±SEM) is shown. 'n' indicates number of animals per group.

4.2 Investigation of the role of PKN1 on the metastatic potential of diffuse gastric cancer cells

In the tumorigenic evolution of cancer, the reorganization and reassembly of the actin cytoskeleton is a key step for invasive cell behavior, such as the dissolution of cell-cell contacts and motility (331). This behavior allows cancer cells to spread to distant organs causing metastasis and leading ultimately to the death of the patient. Diffuse gastric tumors show a very invasive phenotype that is directly linked to its increased metastatic potential and to the poorer prognosis found in patients with this subtype of gastric cancer. However, the mechanism underlying in this behavior is largely unknown. Because of that, it is important to investigate the possible role of PKN1 in the motility and invasive capacity in the diffuse gastric cell lines.

4.2.1 PKN1 and migration capacity of diffuse gastric cancer cells

Invasive carcinoma cells acquire a migratory phenotype associated with increased expression of several genes involved in cell motility (332, 333). Cancer cells are often observed moving linearly in association with the extracellular matrix (ECM) fibers. Given that some of the ECM fibers converge onto blood vessels, these fibers function as a path for carcinoma cells to migrate toward blood vessels. Directed migration of cancer cells is mediated by chemoattractants diffusing from blood vessels and produced by other cell types. The metastatic process of the carcinoma cells comprises local invasion, intravasation, survival in the blood/lymph, extravasation and finally the colonization to distant metastatic sites (334).

A wound-healing assay was used to assess possible changes in the motility of gastric cancer cells due to PKN1 modulation in the isogenic cell line systems engineered. Downregulation of PKN1 in MKN45 (**Figure 51A**) and NUGC3 (**Figure 51B**) cells or overexpression of $PKN1^{1-511}$ in NUGC4 cells (**Figure 51C**) did not affect their motility under the conditions assayed. However, reintroduction of $PKN1^{1-511}$ into FU-97 cells resulted in a significant reduction in the migratory capacity of these cells (**Figure 51D**), indicating that PKN1 can regulate the motility of gastric cancer cells.

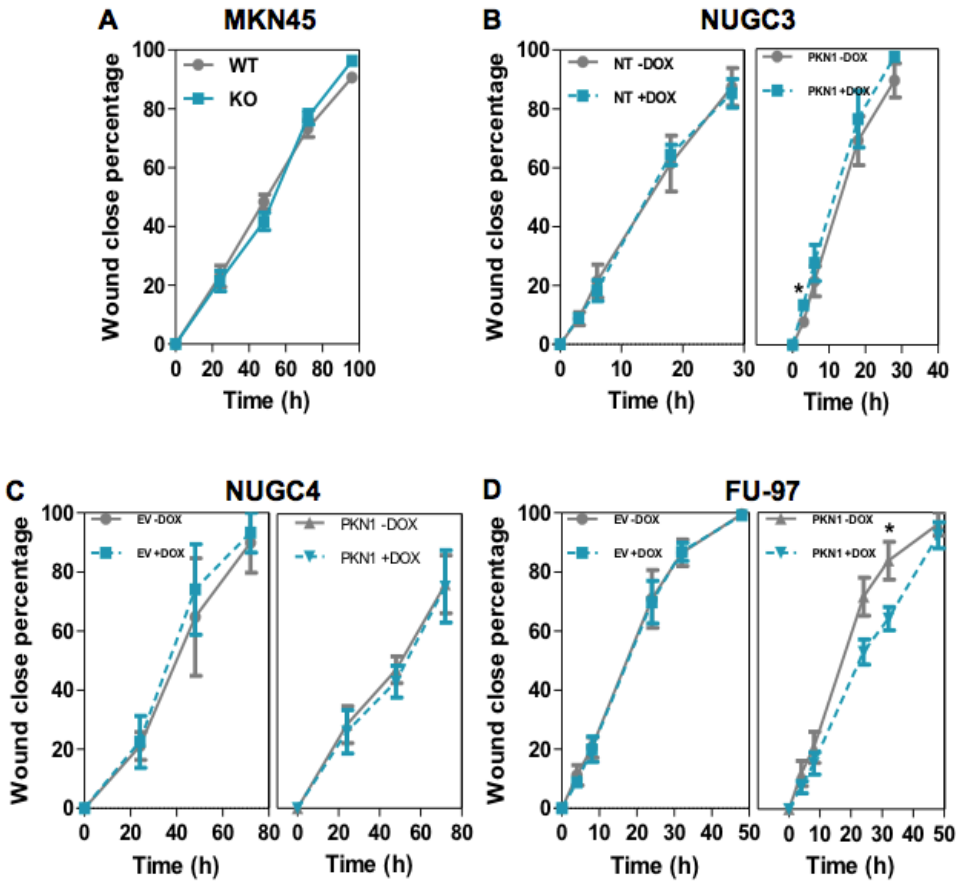

Figure 51. Effects of PKN1 on the migration capacity of gastric cancer cells.

The migration rate was measured in a wound healing assay as the percentage of wounded area closed over a time course. A-B) Downregulation of PKN1 by CRISPR/Cas9-targeted inactivation in MKN45 cells (A) or shRNA-mediated downregulation in NUGC3 cells (B), did not affect the motility of the cells. C) Overexpression of constitutively active $PKN1^{1-511}$ in NUGC4 cells did not affect cell motility. D) Ectopic expression constitutively active $PKN1^{1-511}$ in FU-97 cells significantly reduced cell migration. The mean (±SEM) of three independent experiments, each in triplicate is shown. Student's t-test *p <0.05

4.2.2 PKN1 and invasion capacity of diffuse gastric cancer cells

Invasion of cancer cells into the normal surrounding tissue and the vasculature is an initial step in tumor metastasis. This requires chemotactic migration of cancer cells, steered by protrusive activity of the cell membrane and its attachment to the extracellular matrix (334). A Boyden chamber assay (335) was used to assess the effects of PKN1 modulation on the invasive capacity of gastric cancer cells. Cells were seeded on top of a transwell with 8µm diameter pores covered with matrigel (an extracellular matrix secreted by Engelbreth-Holm-Swarm (EHS) mouse sarcoma cells) and the number of cells invading into the lower chamber was determined to assess the capacity of the cells to degrade and migrate through it.

MKN45-PKN1-KO cells showed a significant increase in their invasive capacity compared to MKN45-PKN1-WT control (**Figure 52A**). Although no significant differences between NUGC3-shNT and NUGC3-sh1 cells treated with Dox (**Figure 52B**) were observed, there was a clear tendency (Student's T-test p=0.2517) that is consistent with the MKN45 cells. On the other hand, the invasion capacity of FU-97 cells was significantly reduced when constitutively active $PKN1^{1-511}$ was overexpressed (**Figure 52C**). In NUGC4 cells there was a decrease in invasion capacity upon $PKN1^{1-511}$ overexpression, although this difference did not reach statistical significance (Student's T-test p=0.1555; **Figure 52D**). In summary, the results show that PKN1 deletion contributes to cellular invasion and the PKN1 overexpression can decrease the invasion capability of the cells.

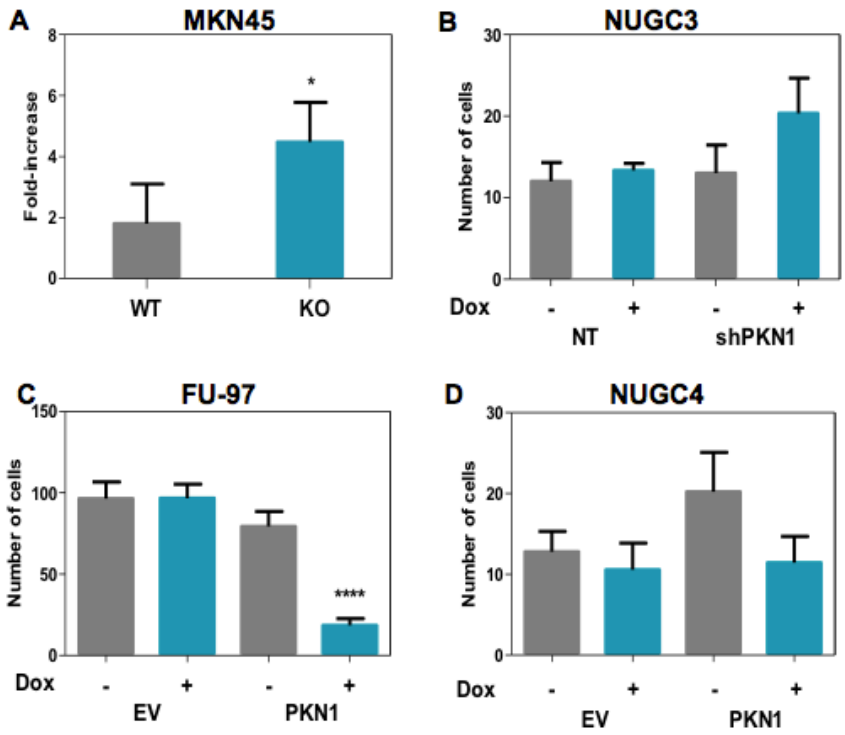

Figure 52. Effects of PKN1 on the invasion capacity of gastric cancer cells.

The effects of PKN1 modulation on invasion capacity of the cells was assessed using a Boyden chamber assay. (A) In MKN45-PKN1-KO cells increased the invasion capacity compared to MKN45-PKN1-WT control. (B) In NUGC3, although no significant differences where observed. (C) FU-97 cells with constitutively active $PKN1^{1-511}$ overexpression show decreased invasion capacity compared to controls. (F) Overexpression of constitutively active $PKN1^{1-511}$ in NUGC4 did not show significant effect on the invasion capacity. Three independent experiments each in triplicate were carried out. The mean (±SEM) is shown. Student's t-test, *p <0.05; ****p <0.0001

4.2.3 PKN1 and metastatic capacity of diffuse gastric cancer cells

Metastasis, the dissemination of cancer cells from the primary tumor to a distant organ, is the most frequent cause of death for patients with cancer. However, the molecular mechanisms of the metastatic process are poorly understood as a result of their complexity. Cancer cell migration and invasion into adjacent tissues and intravasation into blood/lymphatic vessels are required for metastasis of adenocarcinomas, the most common human cancers (336, 337). Invasive carcinoma cells acquire a migratory phenotype associated with increased expression of several genes involved in cell motility (332, 333). This allows carcinoma cells to respond to cues from the microenvironment that trigger tumor invasion. However, most studies on cell motility are performed in two-dimensional culture systems, which limits the similarity of mechanisms of cell migration in *'in vivo'* context, as cells use different cell migration strategies in physiological three-dimensional conditions (338, 339). The regulation of cancer cell invasion *in vivo* is more complicated, involving chemoattractants, the extracellular matrix, and signaling interactions with stromal cells (337).

To directly assess the role of PKN1 in the metastatic process, we used a model of experimental lung metastasis where pooled ($2x10^6$ cells) MKN45-PKN1-WT clones and a pool of MKN45-PKN1-KO clones, both at low passage resuspended in 100 µL of PBS were injected into the caudal vein of 20 immunosuppressed NOD/SCID mice. After 36 days (**Figure 53A**) the animals were sacrificed and the number of lung metastasis was determined in histological sections with Hematoxylin-eosin staining (**Figure 53B-C**). The average number of metastasis observed in mice injected with MKN45-PKN1-KO cells was higher than in animals injected with MKN45-PKN1-WT cells, although the difference was not statistically significant (**Figure 53D**). Also, the size of the tumors was measured in MKN45-PKN1-KO and MKN45-PKN1-WT groups and the average of relative ratios of tumor areas was compared, although not significant differences were observed (**Figure 53E**).

Collectively, the previous results show that PKN1 overexpression decreased significantly cell motility and invasion capacity *in vitro*. Although PKN1 deletion in MKN45-PKN1-KO cells resulted in increased invasive potential '*in vitro'*, no significant differences in the number/size of lung metastasis could be observed compared to MKN45-PKN-WT cells, suggesting that PKN1 inactivation may contribute to the early steps of the metastatic process of gastric cancer cells. However, these results need to be confirmed with some of the additional isogenic cell line models available.

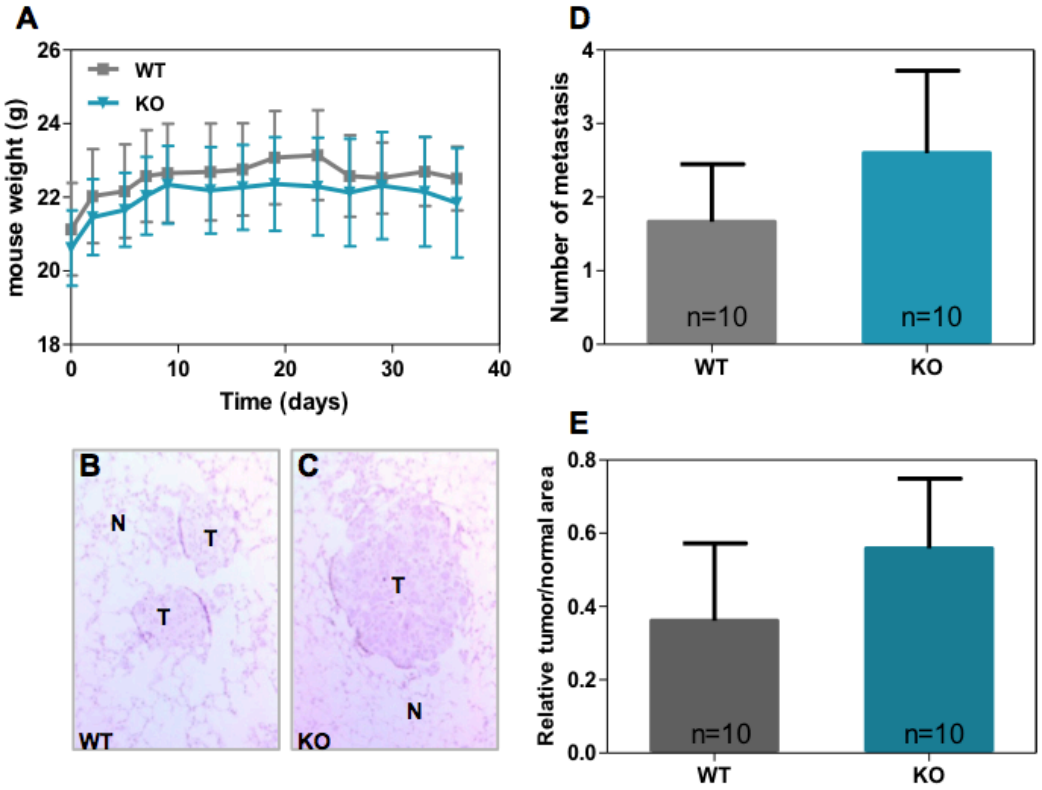

Figure 53. Mouse model of experimental lung metastasis.

The metastatic potential of MKN45 cells was assessed *in vivo* by using a lung metastasis model. $2x10^6$ MKN45-PKN1-KO and MKN45-PKN1-WT cells were injected into the tail vein of NOD/SCI mice. A) Body weight of animals was monitored over the course of the experiment. B-C) Representative microscopic images of the tumors formed by the MKN45-PKN1-WT and MKN45-PKN1-KO cells, in H&E-stained sections, 10X magnification. D) Average number of lung metastasis per mouse was determined in H&E stained tissue sections. E) Further analysis of the relative ratio of tumor area (size of the tumors) to the complete area of lung assessed in each section were determined in WT and KO mice groups. n= number of animals per group. N: normal; T: tumor. The mean (±SEM) is shown. Student's t-test was performed.

5. PKNs as a new therapeutic target for gastric cancer treatment

The results presented above convincingly demonstrate that PKN1 negatively regulates the growth and the invasion of diffuse type gastric cancer cells. Importantly, in a significant proportion of gastric tumors with diffuse histology, PKNs are present in the cells although they remain inactive due the recurrent mutations reported in RHOA, the physiological activator of PKN. It was therefore hypothesized that reactivation of PKNs in this subset of gastric tumors, could have therapeutic application by inhibiting tumor growth and invasion. Importantly, PKN1

and PKN2 proteins can be activated by fatty acids such as arachidonic acid, oleic acid or linoleic acid (229). These fatty acids unfold the auto-inhibitory N-terminal domain of PKN1 and PKN2 and allow its activation by PDK1 (phosphoinositide-dependent kinase 1). Arachidonic acid is an Omega-6 fatty acid present in the diet and could potentially be safely administrated to patients with gastric cancer with limited side effects, alone or in combination with other therapeutic agents approved for these patients.

To investigate the potential therapeutic value of PKN reactivation, first the ability of arachidonic acid to activate PKN1 and PKN2 was assessed in gastric cancer cells. Indeed, treatment with 30 µM of arachidonic acid increased the phosphorylation levels of PKN1 and PKN2 (as a surrogate of PKN activation) after one, two or three hours of treatment in diffuse gastric MKN45 cells (**Figure 54**).

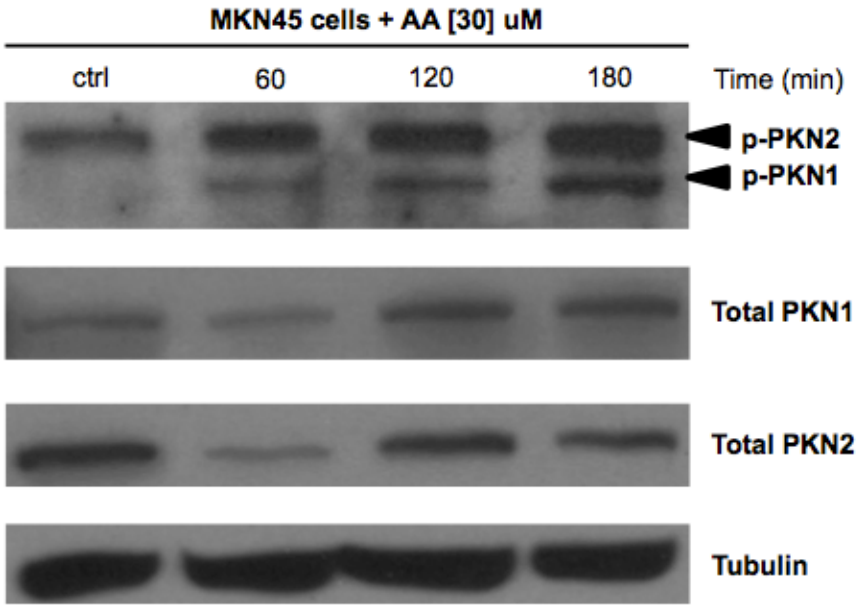

Figure 54. PKN1 activation with arachidonic acid treatment in gastric cancer cell.
Treatment of MKN45 cells with 30 µM of Arachidonic acid increased phospho-PKN1 and phospho-PKN2 levels over time. Total PKN1 and PKN2 levels are also shown. Tubulin was used as a loading control.

Moreover, treatment of MKN45 cells with arachidonic acid resulted in a significant reduction in the growth of the cells and cell death through apoptosis (**Figure 55C**). Quantification of the proportion of apoptotic cells by PI staining and flow cytometric analysis showed that exposure of

MKN45 cells to different concentrations of Arachidonic acid resulted in an increased of apoptosis that was concentration-dependent (**Figure 55A-C**).

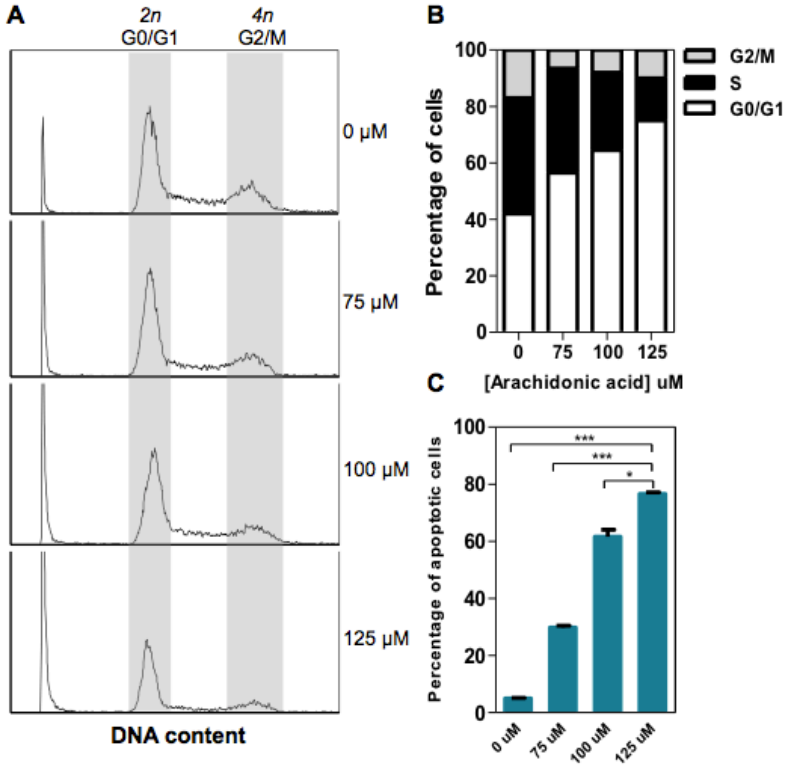

Figure 55. Effect of Arachidonic acid on cell cycle.

A) The cell cycle distribution of MKN45 cells was determined after treatment for 72 h with different concentrations of arachidonic acid. Representative experiments are shown. B) The number of cells in G0/G1, S phase and G2/M were quantified by PI staining and flow cytometric analysis. C) The percentage of apoptotic MKN45 cells after exposure to different concentrations of arachidonic acid were quantified by PI staining and flow cytometric analysis. Mean (±SEM) of three experiments is shown in panels B and C.

To assess whether the activation of PKN1 and/or PKN2 contribute to the cytotoxic effects caused by arachidonic acid we tested if the targeted deletion of these proteins led to increased resistance to arachidonic acid treatment. Consistently, the deletion of PKN1 or PKN2 resulted in significantly reduced sensitivity to arachidonic acid, as revealed by the total area under the GI50 curve, that represents an increased concentration of arachidonic acid required to reduce cell growth by 50%, (GI50 dose; **Figure 56A-D**). Together these results demonstrate that arachidonic acid activates PKN1 and PKN2, inhibiting the growth of diffuse gastric cancer cells

and inducing apoptosis. Importantly, these effects are at least partially dependent on PKN activity.

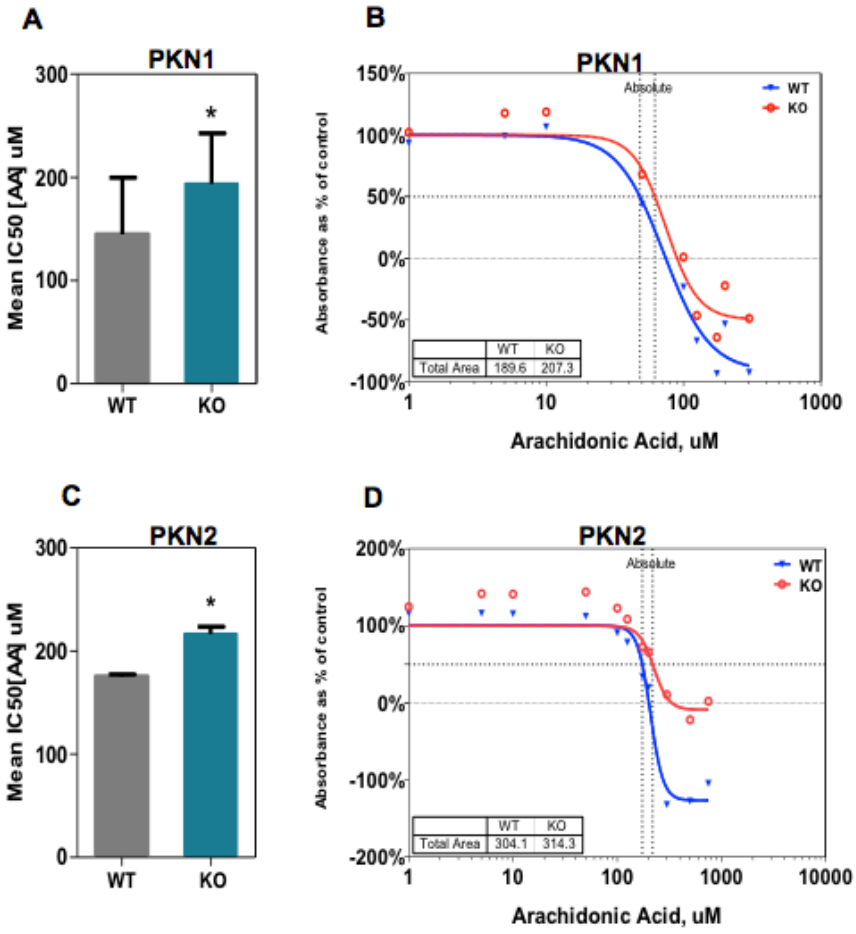

Figure 56. Treatment of MKN45 gastric cancer cells and PKN activation with Arachidonic acid.
Deletion of PKN1 (A) or PKN2 (C) in MKN45 cells reduced the sensitivity to arachidonic acid. The total area under the curve is shown in the representative arachidonic acid GI50 growth curve for MKN45 cells with knockout of PKN1 (B) and PKN2 (D). The average (±SEM) of three independent experiments, each carried out in triplicate is shown in panels D-E. Student's t-test *p <0.05

To further investigate the therapeutic value of PKN reactivation with arachidonic acid, we used a preclinical mouse model of peritoneal carcinomatosis, the most frequent pattern of metastatic dissemination of gastric cancer. MKN45 cells ($1x10^6$) were intraperitoneally (i.p.) injected into 14 female 10-week-old NOD/SCID mice. After cell inoculation animals were randomized into a control vehicle group (n=7) and a group of animals (n=7) treated with arachidonic acid i.p. (2

mg/kg) three days per week. Over the course of the experiment (3 weeks), all animals developed widespread tumor growth throughout the peritoneal cavity (**Figure 57A-B**). Moreover, immunohistochemical staining with Hematoxylin-eosin (**Figure 57C**) and an antibody specifically recognizing cytokeratin 19 of human origin, demonstrated the presence of MKN45-derived peritoneal metastases (**Figure 57D-E**). All macroscopic tumor masses were dissected from the animals, and a 37% reduction in the average tumor weight was observed in the group treated with arachidonic acid compared to the vehicle group (**Figure 57F**).

Collectively, all these results show that arachidonic acid can 1) activate PKN, 2) reduce the growth and 3) induce apoptosis of gastric cancer cells *in vitro*. Moreover, arachidonic acid treatment in a model of peritoneal carcinomatosis demonstrates the potential therapeutic value of PKN reactivation in diffuse-type gastric cancer, a subtype of tumors with poor prognosis and limited treatment options.

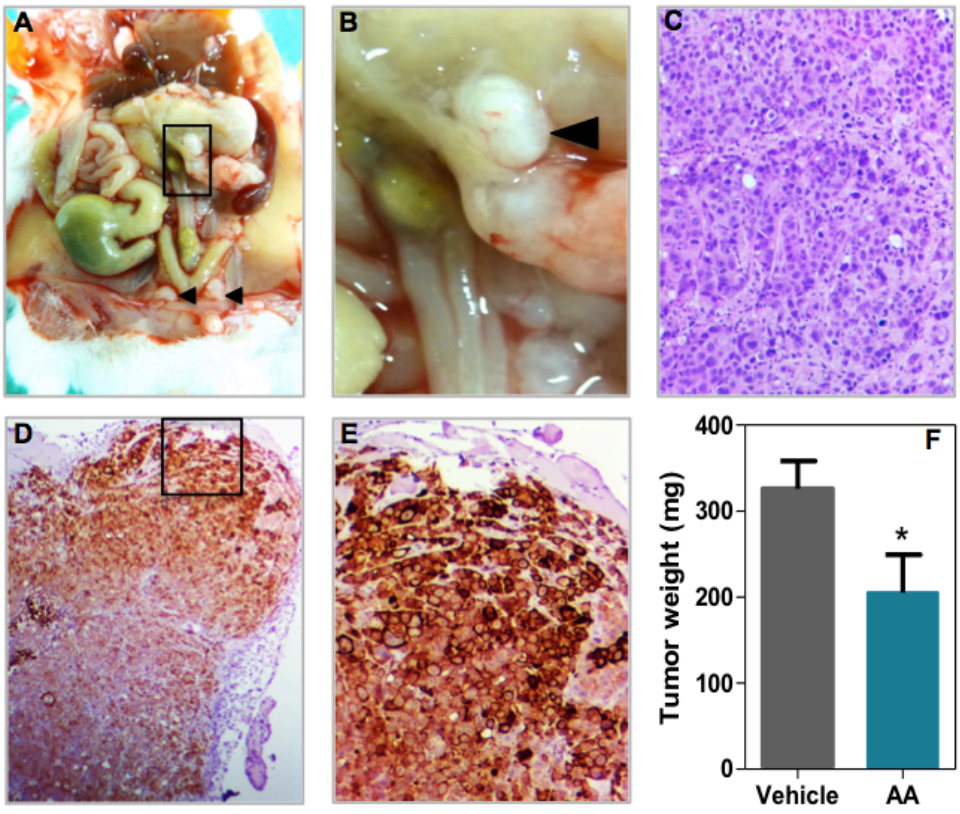

Figure 57. Mouse model of peritoneal carcinomatosis with MKN45 cells and arachidonic acid treatment.

(A-B) Representative photographs of tumor dissemination in the peritoneal cavity of the mouse. C) Tumor samples were processed for H&E staining, 10X magnification. (D-E) Immunohistochemical staining with cytokeratin 19 antibody, demonstrated the presence of MKN45-derived peritoneal metastasis, (D) 4X and (E) 10X magnification. F)

Tumor weight from vehicle and treated mice at the end point of the experiment. The mean (±SEM) is shown. Student's t-test *$p<0.05$

DISCUSSION

CHAPTER V. DISCUSSION

Gastric cancer (GC) is the fifth most common cancer and third leading cause of cancer death, constituting a major health issue worldwide. More than 90% of the tumors are adenocarcinomas. There is a poor prognosis with an average 5-year survival rate of less than 20%. The diagnosis generally occurs at advanced stages because the symptoms are clinically silent. However, if the tumor detection and treatment starts before it invades the muscular layer of the stomach, the 5-year survival rate can reach 90% (340). GC is caused by multiple factors, including infectious agents like *H. pylori* or EBV; environmental factors, as tobacco and high dietary salt consumption; genetic factors, as genetic polymorphisms of genes linked to the inflammatory response and/or tumoral suppressor activity (340). Based on Lauren's histologic classification, there are 2 types of GC: intestinal and diffuse (341). Both types are associated with *H. pylori* infection, but diffuse carcinoma cells lack cohesion and invade tissues independently or in small clusters, is more common in young patients and behaves more aggressively than the intestinal type. As summarized in the diagram in **Figure 58**, before cancer becomes clinically apparent, a prolonged precancerous process takes place, with relative well-defined sequential stages: chronic active gastritis → chronic atrophic gastritis → intestinal metaplasia, first complete or small intestinal type and then incomplete or colonic → dysplasia (intraepithelial neoplasia), → invasive carcinoma. As the oncogenic process advances, genetic abnormalities accumulate, such as mutations in the *APC*, *SMAD4*, *TP53* and *KRAS* genes; or frequent somatic mutations of *CDH1 in diffuse type* (**Figure 58**). *H. pylori* infection induces a transition from normal mucosa to chronic superficial gastritis, which then leads to atrophic gastritis. As a consequence of inflammation and regeneration cycling, the gastric mucosa can undergo intestinal metaplasia. Activation of intestine-specific *CDX2* is one of the most likely candidates linked with the induction of intestinal metaplasia. *APC/β-catenin* mutations can induce formation of gastric adenomas, although the frequency of this conversion is low. Another set of genetic changes, such as methylation of the *MLH1* promoter, microsatellite instability (MSI) and *TGF-β* type II receptor (*TGF-βRII*) gene mutations have been associated with a small subset of intestinal-type gastric cancers (MSI subtype). *TP53* alterations could be involved in the development of both intestinal and diffuse type gastric cancers (342).

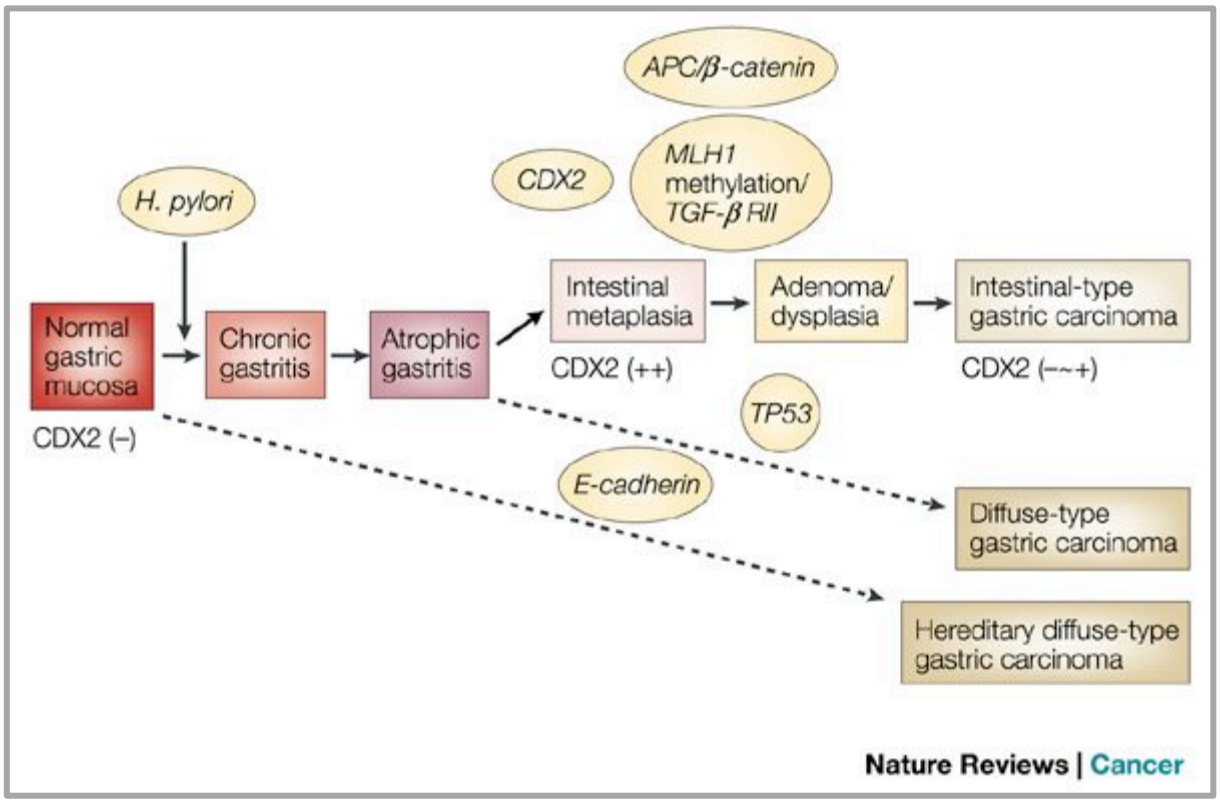

Figure 58. Models of the gastric carcinogenic progression.

Gastric cancer according to its histological pattern is classified into two main types: the intestinal and diffuse types. Lost of *E-cadherin* function are strongly associated with diffuse-type gastric cancer, which develops through a shorter, unidentified sequence of events from gastric epithelial cells. Intestinal type gastric cancer is defined by well-characterized sequential stages. (–) meaning no expression of protein; (+) meaning expression of protein; (– ~ +) indicates no or low expression of protein. Source: Yuasa, Y.(342)

Moreover, changes in the expression of specific genes with important roles in diverse cellular functions, such as cell adhesion, cell differentiation, signal transduction, development, metastasis, DNA repair and glycosylation happen in gastric cancer development (126). Over the past several years, it has been clearly demonstrated that multiple genetic alterations were responsible for the development and progression of gastric cancer (91). However, despite recent advances in the understanding of the molecular events of gastric cancer, the precise mechanisms that contributes to malignant phenotypes of the disease remains largely unknown. Therefore, a better understanding of the molecular changes during gastric carcinogenesis is certainly needed to lead new perspectives and possible improvements in cancer prevention, diagnosis and treatment. The recently published molecular classification by TCGA of gastric

cancer is expected to improve patient stratification and selection for clinical trials and provide a guideline for future drug development (343).

Over the past decade in our laboratory we have focused mainly on the study of colorectal cancer field, putting a lot of effort on elucidating the role of new discovered tumor suppressor genes. For example, we have already described the importance of *RHOA* (344, 345) as a tumor suppressor gene in colon cancer. In addition, recent next-generation sequencing analysis has also highlighted *RHOA* to exhibit recurrent mutations in diffuse-type/genome-stable GCs (184, 185, 343). The intriguing premise here is that *RHOA* mutations are localized to N-terminal hotspot regions (Tyr42, Arg5, Gly17 and Leu57), which most probably are affecting its normal function (184, 185).

Recent studies in our laboratory provided clear evidence of the tumor suppressor role of RHOA in gastric cancer (unpublished data). For example, the downregulation or deletion of RHOA results in the increase of cell proliferation and invasion both "*in vitro*" and "*in vivo*" studies. Moreover, the opposite effect is observed when we overexpress the wild type or the constitutively active (G14V) form of RHOA in diffuse gastric cell lines with low endogenous levels of RHOA protein. The results from '*in vivo*' and '*in vitro*' experiments presented in this thesis are in agreement with this evidence. As mentioned above, RHOA is frequently mutated in diffuse type gastric tumors. Because at least the most prevalent RHOA mutation observed in this type of tumors (Y42C) has previously been reported to interfere specifically with the RHOA effector PKN1 (218), here silencing of PKN1 signaling is postulated to have an important role in gastric tumorigenesis. Moreover, reactivation of PKN signaling in RHOA-mutant tumors is hypothesized to provide a new therapeutic opportunity for diffuse type gastric cancer, an aggressive subtype of tumors with limited therapeutic options.

1. RHOA-Y42C mutation enhances gastric tumorigenesis in a new transgenic mouse model

As discussed above, diffuse type gastric cancer (DGC) represents a subtype with poor prognosis (78-81). The recently published data showed that 14%–24% of DGC tumors has *RHOA* mutations (184, 185). For example, Kakiuchi *et al.* observed recurrent somatic mutations in 7/30 of DGC samples in the RHOA gene, interestingly, mutation encoding Tyr42Cys (Y42C) was detected in four of the seven mutated cases (184).

Therefore, to investigate the role of RHOA mutations in gastric tumorigenesis, we generated a new transgenic CRE-inducible mouse model expressing the frequent RHOA-Y42C mutation in gastric tumors by crossing new transgenic mice with *Cre*-dependent expression of RHOA-Y42C, with mice expressing *Cre* recombinase under the control of the *Villin 1* promoter that is expressed in gastric progenitor cells (104). The generation of the transgenic mice was came out in colaboration with Dr. Manuel Sánchez-Martin. Associate Professor. Department of Medicine. University of Salamanca (USAL). Transgenic mice were identified by PCR genotyping. Three founders were obtained, and it was confirmed they were able to pass the transgene to the offspring. Therefore, one founder was selected to establish the new RHOA-Y42C colony and all animals used were progeny from this founder. The animals were born at Mendelian ratios. Overall, mice had no overt phenotype and the weight of the animals at 5 weeks of age was very similar between groups.

The mice with ectopic expression of RhoA-Y42C were treated with N-Nitroso-N-Methylurea (MNU) to initiate the tumorigenic process as described before (104). We found that the expression of RHOA-Y42C in the gastric epithelium of mice ($RhoA^{Y42C/-};Vil\text{-}Cre^{TG/-}$) led to an increase in the number of tumors when compared to the control animals (with all the genotypes combinations: wild type, $RhoA^{-/-};Vil\text{-}Cre^{-/-}$, *Vil-Cre expression,* $RhoA^{-/-};Vil\text{-}Cre^{TG/-}$, and RhoA-Y42C mutant, $RhoA^{Y42C/-};Vil\text{-}Cre^{-/-}$) in 50 week-old mice treated with MNU. Although, no differences in the number of tumors in 35 week-old mice were observed, the histological IHC examination of Pepsinogen 1 (PG1) expression was significantly reduced in animals with RhoA-Y42C transgene expression at 35-weeks of age, which is an indicative of a premalignant gastric lesion. PG1 is expressed in mucus cells and their levels have been studied as a marker of gastric malignancies. Low PG1 has been reported in atrophic gastritis, a pre-cancerous condition (311-313). Therefore it could be suggested that RHOA-Y42C mutation also requires longer time frame (advanced age) for gastric tumor formation. Taken together, these results suggested that RHOA-Y42C mutation lead to a development of gastric tumors in mice and given the time frame for tumor formation, our model is highly relevant to advanced stages of human gastric cancer. Morevover, the role of the additional hotspot RHOA mutations in gastric cancer can be further investigated *in vivo,* through the generation of new mice models.

Moreover, an alternative model using a combination of genetic and carcinogenic tumorigenesis was used. Because the *Apc min* mutation (T2549A introducing a premature stop codon) has been shown to initiate the tumorigenic process in the stomach of mice (310). $RhoA^{Y42C/-};Vil\text{-}Cre^{TG/-};Apc^{min/+}$ mice and control mice were treated with MNU and the number of tumors assessed. These $Apc^{min/+}$ mice have short lifespan due to the presence of multiple intestinal

tumors, which eventually leads to an intestinal obstruction, therefore the animals had to be sacrificed at 19 weeks of age to assess possible differences in the number of gastric tumors. No differences were observed in the number of tumors in 19-week-old mice carrying *Apc* mutation. However, the incidence of gastric tumors in $Apc^{min/+}$ mice with RHOA-Y42C expression or control mice was low at 19 weeks of age (~20%). Due to $Apc^{min/+}$ mice could not live longer, and the MNU-treatment experiments suggest that a longer time is needed to gastric tumor formation, this could be the reason why no differences in the number of gastric tumors were observed in 19-week-old MUN-treated mice. These results suggested that time frame it is an important factor for gastric tumor development even with the presence of *Apc* and/or *RHOA* mutations.

Interestingly, somatic mutations of *APC* gene are less frequent in gastric tumors (12/57 of tumor samples analyzed) than in the intestinal tumors (346), and the mutations in *Apc* are less frequent in poorly differentiated (diffuse type) gastric tumors. Therefore, the results obtained with the novel RHOA-Y42C transgenic mouse model indicate that at least this mutation, which is the most prevalent RHOA mutation observed in diffuse gastric cancer tumors, can accelerate the oncogenic process initiated by the gastric carcinogen MNU even in *Apc* wild type background different to the observed in the intestinal tumorigenesis.

2. RHOA mutations can affect the binding to PKN

As mentioned before, RHOA is an important molecular switch that acts through binding and activation of several downstream effectors (195). Whole-exome sequencing analysis revealed that RHOA mutations are located in hotspots such as Tyr42, Arg5, Gly17 and Lue57 of RHOA protein (184, 185). Previous studies carried out in our laboratory convincingly demonstrate a strong tumor suppressor activity of RHOA in diffuse gastric cancer cells (unpublished data, see **Figures 22-23**). It was therefore hypothesized that this tumor suppressive activity was specifically mediated by some of the RHOA effectors. To investigate changes in the effector binding capacity caused by the most frequent RHOA mutations in diffuse gastric tumors, the interactome of RHOA and its frequent mutants in DGC was characterized. The RHOA mutants studied were R5Q, G17E, Y42C and L57V, accounting for up to 24% of the RHOA mutations observed in diffuse gastric tumors.

The effects of the frequent RHOA mutations on binding effectors were assessed through a yeast two-hybrid (Y2H) screening, which allowed us to assess interactions of the different RHOA mutants (R5Q, G17E, Y42C and L57V) to its more common effectors (ROCK, DIAPH2, PKN1,

and Kinectin). First, we were able to confirm as previously reported (292) that RHOA-Y42C was unable to bind to PKN1, while retaining its binding capacity to almost all the RHOA effectors tested (ROCK, DIAPH2 and Kinectin). Moreover, we also demonstrated that wild type RHOA binds to all effectors tested including PKN1. Interestingly, we also found that all RHOA mutants inhibited the binding capacity to PKN1, whereas the binding capacity to the other effectors ROCK, DIAPH2 and Kinectin remained and these data had not been shown before.

Additionally, as an independent-unbiased method to identify changes in the RHOA interactome caused by the recurrent RHOA mutations, a pulldown assay coupled with liquid chromatography/mass spectrometry (LC/MS) analysis was performed. First, wild type RHOA or the RHOA-R5Q, -G17E, -Y42C or -L57V mutants as a fusion protein with GST were purified and used as 'bait' to identify binding proteins in a protein lysate obtained from 9 different diffuse gastric cancer cell lines, used as a protein lysate representative of human gastric tumors with diffuse histology. Interacting proteins were pulled down with glutation sepharose beads and binding proteins were eluted and identified using liquid chromatography/mass spectrometry analysis. As expected, wild type RHOA was found to bind to multiple proteins that are known RHOA interactors, including PKN2 and other interactors that have not been previously reported. Interetingly, these proteins were interacting with wild type RHOA but not with any of the RHOA mutants investigated (**Supplementary Table 8**). Surprisingly, some known interactors of RHOA were not detected in this assay, for example ROCK or DIAPH2. Some of these proteins may not be expressed at significant levels in diffuse gastric cancer cell lines, therefore it would not be possible to detect them. Moreover, multiple proteins were also found that do not bind to wild type RHOA but consistently bind to all the RHOA mutants investigated including PSPC1, FARSA, FARS8 and WDR11 (**Supplementary Table 8**). For example, FARSA has shown to be expressed in a tumor-selective and specific cell cycle stages, this could have an important biological implication suggesting that RHOA mutations can activate genes, signaling pathways and other molecular factors involved in oncogenic process. Interestingly, in RHOA interactome we did not found PKN1, ROCK or DIAPH2, well known RHOA-binding proteins, as expected, but instead PKN2 it was found as the most abundant protein interacting with wild type RHOA. For PKN1, this could be explained by the fact that gene expression is low (both, at protein and mRNA levels) in gastric cancer cell lines used in our study (**Figure 41**), compared to PKN2 levels. Therefore, low amount of PKN1 peptides could be masked by higher amount of PKN2 peptides. However, in pulldown assay we were able to detect the RHOA binding to PKN1 in cell lines with high levels of PKN. Thus, further analysis needs to be done to solve these unexpected results. The fact that only wild type RHOA was able to interact with PKN2, whereas the binding

with all the mutants was completely lost confirmed that RHOA-PKN interaction is a key event deregulated in the gastric cancer. These results led us to formulate the hypothesis that the tumor suppressive RHOA effects observed in gastric cancer are mediated by downstream PKN signaling.

Before the high frequency of RHOA mutations was identified in diffuse gastric tumors, Sahai *et al.* (1998) investigated the effects of different RHOA effector-loop mutants on the binding to different effectors, and found that the RHOA-Y42C mutant failed to bind to PKN1, while retaining its capacity to interact with other effectors investigated (292). Taken all together, these results demonstrated that the mutations found commonly in gastric tumors lack the ability to bind and therefore activate PKN family proteins. Therefore, it was established the importance to focus on the study of PKN role in gastric cancer.

3. The differential of expression of RHOA and PKN in gastric cancer cell lines could be associated with diffuse gastric cancer

The results described above strongly suggests an important role of PKN in gastric cancer. Therefore, to investigate the role of PKN1 in the growth and metastatic potential of gastric cancer cells, we generated isogenic cell lines where PNK1 expression was downregulated or knocked out in cell lines with high endogenous levels of the protein and PKN1 was overexpressed in cell lines with low endogenous levels. First, the mRNA level of PKN protein and the mRNA level of small GTPase RHOA in a panel of 14 gastric cancer cell lines (9 diffuse-type cancer cell lines and 5 intestinal-type cancer) were investigated in the dataset 'European Genome-phenome Archive'. Interestingly, a significant variability of mRNA levels of RHOA, PKN1 and PKN2 was observed in diffuse and intestinal type cell lines. Also, it was a trend of increased expression of these proteins in the diffuse type cells compared to intestinal type cells and this data has not been reported before. Moreover, a significant correlation was observed between mRNA RHOA levels and mRNA PKN2 levels in the subset of 9 diffuse-type cancer cell lines ($p<0.05$). Big efforts in many laboratories across the world are trying to identify specific markers to early predict gastric carcinogenesis. According to the literature, the expression of several genes is negatively or positively regulated regarding the tumor-type in gastric cancer. The expression of cadherin, mucin, vimentin and cathepsin family genes has been reported to be different between intestinal and diffuse type GC (321-327). Some of these family genes are also implicated in other type of cancers. For example, increased mucin production occurs in

many adenocarcinomas, including cancers of the pancreas, lung, breast, ovary and colon. The pathological implication of MUC1 and MUC4 in the disease process have been extensively studied (347, 348). High levels of vimentin gene methylation have also been observed in certain upper gastrointestinal pathologies such as Barrett's esophagus which is a premalignant condition of esophageal adenocarcinoma, and intestinal type gastric cancer (349). Moreover, Cathepsin B, D and L have been shown to play an important role in matrix degradation and cell invasion (350). Also, some of these genes are under investigation as possible diagnostic markers for malignancies in which they are most commonly over- or down-expressed (351, 352). Therefore, it could be further investigated whether RHOA and PKN proteins could be good markers in GC and also the tumor suppressive potential of RHOA and PKN family proteins in both intestinal and diffuse-type gastric cancer.

3.1 PKN1 regulates the proliferation of gastric cancer cells

Although uncontrolled cell growth represents a critical initial event for cancer development (37), the molecular pathways involved in this process are not completely understood. However, there is a lot of investigations focus on the study of key genes that are specifically implicated in cancer development. Therefore, we have investigated the role of PKN1 on the growth of diffuse gastric cancer cells.

Interestingly, PKN1 overexpression has been reported to be correlated with the development and progression of many tumors including colorectal (272), breast cancer (353), and renal cell carcinoma (354). Some other studies have demonstrated that depletion of PKN1 also promotes programmed cell death in melanoma cells (355). Whereas, in prostate cancer (PC-3M-luc2) cells it has been demonstrated that PKN1 controls migration and invasion but not proliferation (356). Other studies have reported that PKN1 is overexpressed in prostate tumors (269) and in certain cohorts of malignant melanoma (355). The high risk human papillomaviruses (HPVs) are associated with cervix carcinoma and other genital tumors (278). Previous studies have identified two viral oncoproteins E6 and E7, which are expressed in the majority of HPV-associated carcinomas (279, 280). In recent years, it has become clear that in addition to E6-induced degradation of p53 tumor suppressor protein, other E6 targets are necessary for mammary epithelial cells immortalization. Gao, *et al.* identified a novel interaction of HPV16 E6 with protein kinase PKN (281). They showed direct binding of high risk HPV E6 proteins to PKN *'in vitro'* and *'in vivo'*. Importantly, E6 proteins of high risk HPVs but not low risk HPVs were able to bind to PKN. Also, they showed that PKN phosphorylates E6 protein, these results indicate that a cellular phosphorylation cascade is mediating HPV E6-dependent oncogenic process.

Other study showed that reducing the levels of PKN1 with siRNAs significantly enhances activation of β-catenin-activated reporter and increases apoptosis in melanoma cell lines (355). Also, they found that PKN1 is present in a protein complex with a WNT3A receptor, Frizzled 7, as well as with proteins that co-purify with Frizzled 7. These data establish that PKN1 inhibits Wnt/β-catenin signaling and sensitizes melanoma cells to cell death stimulated by WNT3A (355).

These previous works partly explained the molecular mechanism of PKN1 contributing to carcinogenesis, suggesting the oncogenic role of PKN1. Therefore, the possible role of PKN in gastric cancer has not been investigated. Here we show that proliferation of gastric cancer cells can be enhanced by depletion of PKN1 and conversely, PKN1 overexpression reduces the growth of diffuse gastric cancer cells. In this study, using two different isogenic gastric cancer cell line models, it was found that PKN1 inactivation through complete (knockout) or partial (downregulation) depletion of the protein led to significantly faster growth *in vitro* (cell culture) and *in vivo* (mouse *xenografts*). In good agreement, we found that the overexpression of constitutive active form of $PKN1^{1-511}$ in two different cell lines with low endogenous PKN1 levels, results in a significant growth inhibition. At the molecular level, PKN has previously been linked to several signaling pathways, which can affect cell proliferation. The available literature describes opposite observations to what we obtained. For example, PKN2 is known to downregulates the protein kinase activities of Akt leading to the inhibition of the downstream signaling *in vivo* and therefore inhibiting pro-survival signaling (357). PKN1 is a component of the mitogen-activated protein kinase (MAPK), JUN N-terminal kinase (JNK), steroid hormone receptor, and nuclear factor κβ (NFκβ) signaling pathways, which have all been associated with oncogenesis (358). PKNs family activates MEK as well as RAF1 by phosphorylating them on serine 298 and serine 338, respectively (359-361). Thus, activating gene expression of these effectors that culminate in the proliferative cellular response (358). The increase of Ras-induced fibroblast transformation by PKN1 correlated with its effects on signaling through the extracellular signal-regulated kinase (ERK)–MAPK pathway, and was dissociable from effects on the JNK or p38–MAPK pathways (362). In melanoma, β-catenin levels decrease during the progression of the disease and higher expression of β-catenin in tumors at the time of diagnosis correlates with improved patient survival in melanoma, contrary to the correlation observed in colorectal tumors (363-366). James *et al.* demonstrated that depletion of PKN1 and PKN2 increase WNT3A-dependent activation of Wnt/β-catenin, thus increasing cell apoptosis (355). Based on these data, we could hypothesized that Wnt signaling is activated in gastric cancer cells due to PKN1 deletion, leading to cell proliferation. Therefore PKN1 activation could inhibit

Wnt/β-catenin pathway which finally sensitizes gastric cells to cell death. Further experiments are necessary to test this hypothesis. In this study we were able to thoroughly characterize the phenotype of both depletion- and overexpression- of PKN1 models and these results confirmed that PKN1 significantly contributes to proliferative capacity of gastric cancer cells and that PKN1 could have tumor suppressor activity in gastric cancer.

Tumor suppressor genes code for proteins that normally operate to restrict cellular growth and division or even promote apoptosis. Examples include inhibitors of cell cycle progression, factors involved in maintenance of cell cycle checkpoints, and proteins required for apoptosis induction.

The role of PKN1 in cell cycle regulation, an uncontrolled process in cancer, has not been deeply investigated. Some studies reported that PKN1 activation in breast cancer cells results in cyclin D1 upregulation, therefore enhanced cell-cycle progression (367). Other studies show that knockdown of the PKN1 led to G2/M cell cycle arrest in gastric cancer cells leading to cyclin B1 downregulation (368). At G2/M phase, ERK5 stimulates downstream NF-κB, allowing it to translocate into the nucleus and activate expression of cyclin B1 (369). Recently, NF-κB has been shown to modulate cyclin B1 expression. Moreover, PKN1 is required for the upstream stimulus-dependent activation of the NF-κB transcription factor, and also constitutively-active PKN1 stimulates NF-κB activity (370). Additionally, proteolytic analysis revealed that Caspase 3-induced cleavage of PKN1 to produce N-terminally truncated isoform (constitutively-active isoform), which may contribute to signal transduction, eventually leading to apoptosis (254). In Caspase-regulated apoptotic cell death, the MAPK signaling pathway, which involves ERK1/2, p38, and JNK, coordinately regulates diverse cellular programs, such as proliferation, apoptosis and differentiation in human cancers (371).

Some studies have highlighted the importance of the effect of p38-MAPK activation in the control of cell cycle (372). Depending on the cell type, p38-MAPK can either induce progression or inhibition at G1/S transition by positive or negative regulation of specific cyclin levels (cyclin A or D1) as well as by phosphorylation of the retinoma protein (pRb), which is a hallmark of G1/S progression (373, 374). JNK pathway is also involved in many forms of stress-induced apoptosis. JNK has a pro-apoptotic function in stress-induced neural cell damage through transcriptional activation of c-Jun, whereas depletion of JNK in embryonic fibroblasts has been shown to be antiapoptotic (375, 376). Under specific circumstances, JNK plays a protective role and supports cell survival. Probably, these diverse functions of JNK pathway are possible because JNK operates in a cell-type, stimulus, and context dependent manner (377). In conclusion, as we induced the constitutively active $PKN1^{1-511}$ form to study the PKN1 role in gastric cancer cells, our results suggests that the tumor suppressor activity of PKN1 could be

mediated apoptosis by its cleavage (or activation) by Caspase 3. However, further research to clarify how PKN1 regulates cell proliferation dynamics may greatly enhance our understanding of the molecular mechanisms of gastric cancer.

4. PKN1 might be involved in migration, invasion and metastatic process

In the Western world, gastric cancer is most often diagnosed at an advanced stage, after becoming metastatic at distant sites. Patients with advanced disease (locally advanced or metastatic) have a poor prognosis (47). Moreover, formation of metastasis is a multistage process that requires active tumor cell migration and invasion (378), and the role of PKN1 in the metastatic process of gastric cancer cells had not been investigated.

RHO-GTPases family are known for their roles in the cytoskeleton reorganization and cell migration activity (379), and these activities are mediating by a number of downstream effectors (200), such as PKN1 (380). Here we show that constitutively active $PKN1^{1-511}$ overexpression significantly decreases the motility (migration) and invasion capacity of gastric cancer cells *in vitro*. Moreover, although PKN1 downregulation did not have an effect on cell motility it increased the invassive capacity of diffuse gastric cancer cells. In this study the mechanisms behind these observations have not been elucidated but might be related to alterations in the capability to reorganize the actin cytoskeleton due to altered PKN1 signaling, leading to an inhibition in the migratory phenotype. Opposite results to our observations has been reported in other tumor types. For example, some studies showed that both PKN1 and PKN2 are able to control cellular migration and invasion in bladder tumor 5637 cells (275, 381). Whereas, in prostate PC3 cells PKN3, but not PKN1 or PKN2 was shown to play a role in invasion of a 3D matrix (382). The mechanism of action and regulation of each isoform is still controversial. But the role of PKN in gastric cancer cells seems to be uniquely different compared to other tumor types. Although, the *in vivo* experiments showed that depletion of PKN1 alone did not cause statistically significant changes in the number of lung metastasis in the intravenous model. Based on the literature, it could be claimed that in *'in vivo'* context, additional genetic and molecular factors might be necessary for PKN1 to have an impact in the migratory and invasive capacity. In addition, the tumor progressed was measured by the relative ratio of the tumor areas to the whole lung, which represents the volume of the tumor (size). There was a trend to larger and the number of tumors lacking of PKN1.

Current knowledge in metastatic process, implies that in cancer cell integrins together with receptor tyrosine kinases confers positional control of migrating tumor cells for the attachment to

the extracellular matrix (ECM) (383). Integrin adaptors such as enhancer of filamentation/neural precursor cell expressed developmentally down-regulated 9 (NEDD9) whose expression is regulated by PKN1, influence signaling pathways, actin cytoskeleton reorganization, and ECM degradation (383, 384). Furthermore, regulation of cell motility, site-specific extracellular signaling and cell protrusion, is controlled by focal adhesion (FA) (378). It has been reported that PKN1 stimulates angiogenesis in the FA regulation of vascular wall from smooth muscle cells (385).

PKN1 was shown to bind the actin bundling protein α-actinin (243). This protein helps to shape dorsal and ventral stress fibers which are anchored with one or both ends in focal adhesions and the disruption of the PKN-actinin interaction could result in defective focal adhesions and reduce cell motility (386). It is possible therefore, that cells depleted of PKN1 have modified focal adhesions that make them adhere stronger to the substrate and might result in a delayed detraction of the cell body during cell migration, which in part could explain our *in vitro* results for PKN1 depletion. However, in FU-97 cells the constitutive active $PKN1^{1-511}$ overexpression also resulted in low cell motility, which is contrary to what was explained before. But it can be claimed that this reduction in cell motility is mainly due to cell death, because the constitutive active form of PKN1 is closely related to Caspase 3-induced apoptosis.

Although, the role of PKN1 in cancer cells generally appears to be pro-oncogenic, we showed that PKN1 overexpression decreases the migration and invasion capability of the cells. These results indicate that PKN1 may have tumor type-dependent activities, thus possibly contributing to metastasis in some tissues such as breast and prostate cancer (353, 356), while suppressing the spread of gastric cancer cells.

5. PKNs as new therapeutic targets in gastric cancer

The results present above we have clearly demonstrated that PKN1 is an important mediator in tumor suppressor activities, possibly upstream signaling RHOA participates in such effects and also many other pathways could be involved. Interestingly, recent reports show that RHOA is frequently mutated in diffuse gastric tumors (184, 185, 343). In addition, mutations in PKN1 and PKN2 in gastric tumors are not common (PKN1, 2.79% and PKN2, 4.53%). However, these mutations are significantly found together (TCGA data: Log Odds Ratio: 2.094; p=0.046) (**Figure 59**).

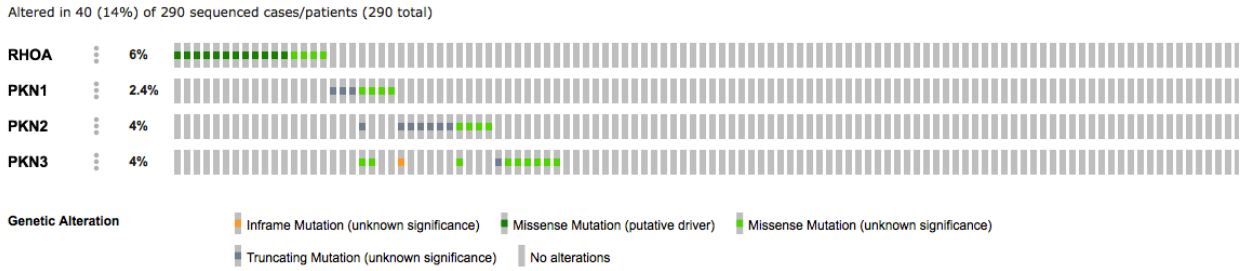

Figure 59. **Percent of RHOA, PKN1, PKN2 and PKN3 mutations found in gastric cancer patients.** Source: Stomach Adenocarcinoma (TCGA, Nature 2014). www.cbioportal.org

This indicates that direct inactivation of PKNs is a rare but an important event, however the higher mutation rate found in RHOA (24%) is suggesting that it is more likely to occur a single mutation in RHOA rather than several mutations in two or more genes. In this logic, we have hypothesized that a single mutation in RHOA (Y42C) is enough and more likely to occur to inactivate downstream effector PKN, instead of several mutations in the three different genes of PKN family proteins to inactivate them. This phenomenon extend a unique opportunity to strike gastric cancer, where PKN pathway is inactivated upstream but the leading proteins PKNs are still fully functional and can be activated in a RHOA-independent manner.

Considering that tumor suppressor genes are inactivated by mutations, and therefore difficult to reactivate them, this allow evasion of tumor cell death mechanisms and rapid tumor progression. For example, the tumor suppressor gene *TP53* is the most frequently mutated gene in cancer (387, 388). TP53 wild type form can suppress tumor development by regulation of multiple pathways, however the mutations (missense-mutant and nonsense-mutant) and the resultant inactivation of the gene cause tumor progression. Therefore, recent investigations on pharmacological reactivation of *TP53* are being conducted (389). Nevertheless, most *TP53* mutations are missense mutations that have been demonstrated to have oncogenic activity (390-392). In addition, some of these mutants show extensive structural distortion and reduced thermostability (393), therefore they have been considered as undruggable targets. However, several small molecules that promote proper folding and/or reactivation of common missense-mutant TP53 proteins have been identified but only very few have reached clinical trials phase so far, mainly because *in vitro* experimental phase may not have favorable solubility and hydrophobicity properties and/or may have general toxicity in cells regardless of *p53* status.

Collectively, the results presented before convincingly demonstrate that PKN1 negatively regulates the growth and the invasion capacity of diffuse type gastric cancer cells. Moreover, it

has been shown that in a significant proportion of gastric tumors with diffuse histology, PKNs are present in the cells but its activity remain in 'off-state' due to the recurrent mutations reported in RHOA, the principal activator of PKNs family. Therefore, in this study it is proposed that the reactivation of PKN in diffuse gastric tumors could have a therapeutic application by inhibiting tumor growth and invasion.

It has already been described that PKN family proteins can be activated through lipid exposure, such as arachidonic acid, oleic acid or linoleic acid (224, 228, 229, 236, 237, 394-397). For the first time Mukai, *et al.* (228) and Kitagawa *et al.* (237) purified PKN protein from COS-7 cells transiently transfected with the cDNA construct encoding human PKN for enzymatic characterization of the protein. Interestingly, they found that in the presence of 40 μM arachidonic acid, linoleic acid, and oleic acid the kinase activity, measured by the phosphate incorporation, increased by several tens-fold compared to control-transfected cells. Later, Amano *et al.* through the stimulation of Swiss 3T3 cells by lysophosphatidic acid (LPA) showed the phosphorylation increase of PKN by two-fold compared with untreated cells (236). Recently, Falk, *et al.* (229) expressed and purified full-lenght human PKN1-3 from HEK-293 cells for enzymatic characterization. They found that these proteins to be phosphorylated at two key sites of regulation, the threonine-774 in the activation loop, and the threonine/serine in the turn motif. In addition, it was shown that PKN1 and PKN2 kinase activity (phosphotylation level) was increased by the presence of phosphatidylinositol-4,5-bisphosphate (PIP2) and arachidonic acid. These fatty acids unfold the auto-inhibitory N-terminal domain of PKN1 and PKN2 and allow the activation of the protein by phosphoinositide-dependent kinase (PDK1) (229). Arachidonic acid is a major component of the cell membrane, suggesting that PKN1 and PKN2 might be associated with plasma membrane remodeling.

As an important proof of concept, we tested *in vitro* PKNs reactivation in the diffuse gastric cancer cells by the exposure to arachidonic acid, our results confirmed that PKN1 and PKN2 was activated (increase phospho-PKN1-2 levels) by the presence of 30 μM arachidonic acid. In addition, PKN1 or PKN2 isogenic knockout gastric cancer MKN45 cells were significantly more resistant to arachidonic acid treatment. Moreover, here we showed that exposure of MKN45 cells to different concentrations of arachidonic acid induced an arrest of proliferating cells in the G2/M phases of the cell cycle. Consistently with this result, we observed that apoptosis was increased in a concentration-dependent manner. Apoptotic cell death-based therapy is the preferred anti-cancer strategy for eliminating malignant cancer cells due to its irreversibility. Therefore, several therapeutic agents have been proposed with a significant anti-cancer activity capable of inducing apoptosis in cancer cells. However the molecular mechanisms underlying

the cytotoxic effects of these agents are still being elucidated. We demonstrate here that exposure of proliferating gastric cancer cells to arachidonic acid induces a G2/M arrest consistent with an increase of cellular apoptosis. Together, these results suggest that arachidonic acid could be assessed as a new therapeutic anti-cancer agent. Although, further experiments are required to deeply understand the molecular mechanisms involved in the induction of apoptosis after exposure to arachidonic acid.

Arachidonic acid is the major n-6 polyunsaturated fatty acid (PUFA) that is present in cell membrane and is thought to have an important role in maintaining cellular functions (398). Most of the effects of arachidonic acid are due to its metabolic conversion by oxygenases (COX, LOX, and Cyt P450) into several lipid mediators, such as prostaglandin E_2 (PGE_2) and lipoxin A_4 (LXA_4) (**Figure 60**) (399). In human body, arachidonic acid is synthesized from Linoleic acid and the average intake of adults is around 50-250 mg/day of arachidonic acid from daily diet (400-402). Also, clinical trials of arachidonic acid supplementation have been conducted in healthy elderly subjects without adverse effects (403). Moreover, arachidonic acid is essential for perinatal and neonatal development due to conversion rate from linoleic acid in infants is low and it declines with age (404, 405). Arachidonic acid supplementation in elderly has been reported to improve cognitive response and brain functions (398, 406, 407), and cardiovascular functions (408). Several *in vivo* animal studies support these findings and also have demonstrated that arachidonic acid can be safely administered with no secondary effects (409-414). However, it should be noted that arachidonic acid serves as a precursor to pro- and anti-inflammatory eicosanoids. But the effects of arachidonic acid supplementation in inflammation colitis models has been evaluated and the results demonstrated that arachidonic acid ingest does not increase inflammation parameters, such as C-reactive proteins, interleukin-6 (IL-6) and tumor necrosis factor-α (TNF-α) (399, 409, 415). There are some clinical trials of arachidonic acid supplementation in adults, for example, among healthy males who consumed 1.5 g/day of arachidonic acid for 50 days (416, 417) or 838 mg/day for 4 weeks (418) in randomized controlled studies, showing that platelet aggregation did not change and adverse effects did not occur.

Our results with arachidonic acid treatment in a model of peritoneal carcinomatosis showed a 37% reduction in the average tumor weight in the group treated with arachidonic acid compared to the vehicle group. Collectively, all the results show that arachidonic acid can: 1) activate PKN, 2) reduce the tumor growth *in vivo* and 3) induce apoptosis of gastric cancer cells *in vitro*. This also demonstrates the potential therapeutic value of PKN reactivation in diffuse gastric cancer, a subtype of tumors with high frequency of RHOA mutations, poor prognosis and limited treatment

options. Interestingly, to consider whether this alternative of treatment can be extended to other tumor types it might be required further analysis, regarding RHOA and PKN status, disease staging and overall patient status. In conclusion, arachidonic acid could be safely administrated to early or advanced diffuse gastric cancer patients as a complementary treatment without adverse effects and maintaining the conventional treatment.

As mentioned above, arachidonic acid is converted by COX, LOX and Cyt P450 oxygenases into several lipid mediators, such as prostaglandins (PGs), lipoxins (LXs), leukotrienes, endocannabinoids and epoxyeicosatetranoates (399). Moreover, the results presented before certainly demonstrates that arachidonic acid can activate PKNs. In addition, we have shown that PKN inactivation significantly increases the growth of gastric cancer cells, and ectopic overexpression of $PKN1^{1-511}$ reduced proliferation of gastric cancer cells. Thus, as an additional strategy for PKN reactivation, we have hypothesized that pharmacological modulation of the cellular metabolism of arachidonic acid will lead to its intracellular accumulation, which will reactivate PKN (increasing phospho PKN levels) and finally a robust tumoral suppressor effect might be observed. Therefore, treatment with FDA-approved inhibitors of the enzymes that regulate the conversion of arachidonic acid to other intermediate biosynthetic and signaling derivatives (COX, LOX and Cyt P450; **Figure 60**) should lead to the elevation of cytosolic arachidonic acid and PKN activation, which should in turn result in growth arrest and apoptosis.

Several inhibitors of COX, LOX and Cyt P450 are currently undergoing clinical trials to determine their therapeutic potential in different tumor types and different settings. The discovery and characterization of new biomarkers capable of identifying cohorts of patients with increased sensitivity (such as RHOA mutations) would constitute a major advantage for the clinical use of these agents. The study of the effects of treating gastric cancer cells with some of these compounds is currently ongoing (**Figure 60**). Although, the present results positively suggest that arachidonic acid is a good therapy for gastric cancer patients, further investigations are needed to finally respond this question.

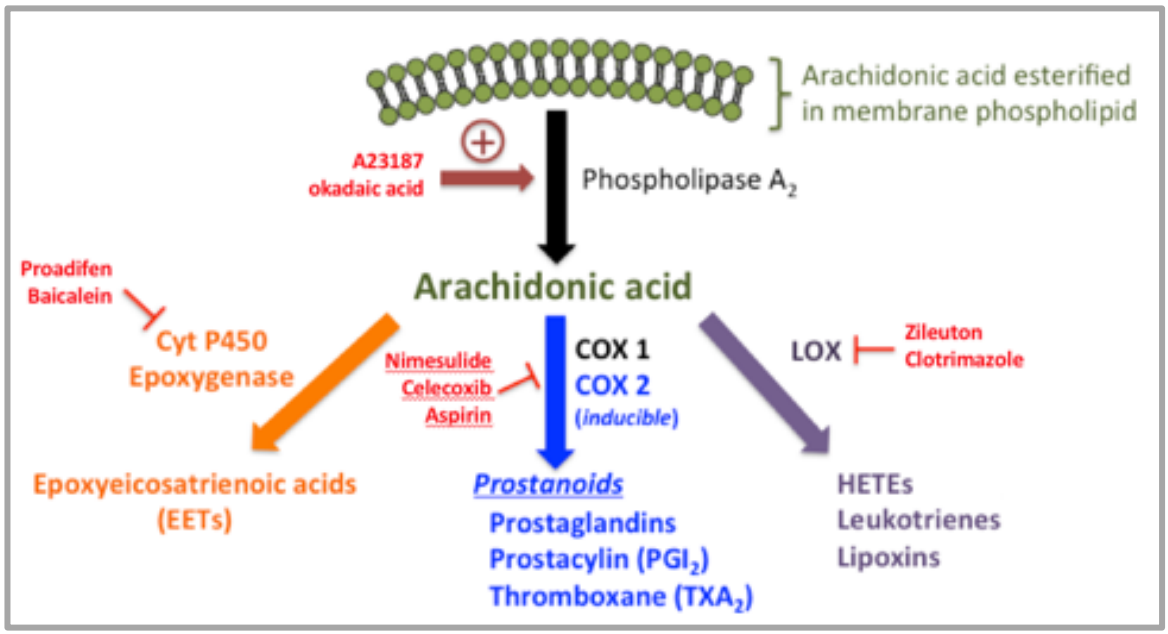

Figure 60. **Cellular metabolism of Arachidonic acid.**

Schematic representation of the different metabolic pathways for Arachidonic acid. Inhibition of COX, LOX or Cytochrome P450, or the activation of phospholipase A2, can lead to the elevation of cytosolic Arachidonic acid levels. The gastric cancer cells treatments with the compounds indicated in red, is currently ongoing. Source: http://tmedweb.tulane.edu

CONCLUSIONS

CHAPTER VI. CONCLUSIONS

In this study, we have investigated the effects of the frequent RhoA-Y42C mutation in gastric cancer, which also lacks the ability to bind and therefore activate the effector kinase PKN1. Moreover, we performed a functional characterization of the role of PKN1 in gastric cancer.

The main conclusions of this study are:

1. In mice, the expression of RHOA-Y42C mutation in the gastric epithelial cells increased the number of gastric tumors.

2. Hotspot RHOA mutations found in gastric cancer affect specifically its binding to the effector PKN.

3. PKN1 has a tumor suppressor activity in gastric cancer cells.
   3.1 PKN1 negatively regulates gastric cancer cell proliferation.
   3.2 PKN1 inactivation may contribute to the early steps of the metastatic process of gastric cancer cells.

4. PKN signaling can be reactivated by arachidonic acid treatment and constitutes a novel candidate therapeutic target for a subset of patients with DGC.

This study demonstrates the oncogenic nature of RHOA hotspot mutations and the tumor suppressor role of PKN1 in gastric cancer thus contributing to elucidate the molecular pathways involved in the disease development. In addition, it has been proposed a new therapeutic approach for GC treatment.

Table 8. **RHOA interacting proteins identified by MS analysis.**

Accession	Protein	Scores GST	# Spec Counts GST	Scores WT	# Spec Counts WT	Scores R5Q	# Spec Counts R5Q	Scores G17E	# Spec Counts G17E	Scores Y42C	# Spec Counts Y42C	Scores L57V	# Spec Counts L57V	User Input	Mapped Gene Symbol
PKN2_HUMAN	Serine/threonine-protein kinase N2			227,2	16									PKN2_HUMAN	PKN2
RALY_HUMAN	RNA-binding protein Raly			90,7	5									RALY_HUMAN	RALY
CBX1_HUMAN	Chromobox protein homolog 1			71,4	2									CBX1_HUMAN	CBX1
NH2L1_HUMAN	NHP2-like protein 1			68,9	4									NH2L1_HUMAN	NHP2L1
H2AY_HUMAN	Core histone macro-H2A.1			56,1	2									H2AY_HUMAN	H2AFY
BOP1_HUMAN	Ribosome biogenesis protein BOP1			47,6	4									BOP1_HUMAN	BOP1
ARHGB_HUMAN	Rho guanine nucleotide exchange factor 11			41,4	2									ARHGB_HUMAN	ARHGEF11
ACINU_HUMAN	Apoptotic chromatin condensation inducer in the nucleus			33,6	4									ACINU_HUMAN	ACIN1
PSPC1_HUMAN	Paraspeckle component 1					56,8	3	228,4	12	257,3	15	108,4	9	PSPC1_HUMAN	PSPC1
SYFA_HUMAN	Phenylalanine--tRNA ligase alpha subunit					38,8	1	158,3	9	136,5	8	36,5	3	SYFA_HUMAN	FARSA
SYFB_HUMAN	Phenylalanine--tRNA ligase beta subunit					29,3	1	101,9	7	103,2	10	51,6	4	SYFB_HUMAN	FARSB
WDR11_HUMAN	WD repeat-containing protein 11					30,6	1	112,1	9	97,7	5	52,8	4	WDR11_HUMAN	WDR11
RT18B_HUMAN	28S ribosomal protein S18b, mitochondrial					51,8	2	86,3	8	94,1	6	45	4	RT18B_HUMAN	MRPS18B
F120A_HUMAN	Constitutive coactivator of PPAR-gamma-like protein 1					55,8	3	258,7	13	72,9	6	52,1	4	F120A_HUMAN	FAM120A
DHX36_HUMAN	ATP-dependent RNA helicase DHX36					44,6	3	186,1	11	70,5	4	67,7	3	DHX36_HUMAN	DHX36
ELOA1_HUMAN	Transcription elongation factor B polypeptide 3					38,2	1	66	3	63,8	2	48,2	1	ELOA1_HUMAN	TCEB3

CYFP1_HUMAN	Cytoplasmic FMR1-interacting protein 1	41,9	2	70,2	3	62,6	3	36,7	2	CYFP1_HUMAN	CYFIP1
F91A1_HUMAN	Protein FAM91A1	33,6	1	86,6	3	62,4	2	39,3	2	F91A1_HUMAN	FAM91A1
PTCD3_HUMAN	Pentatricopeptide repeat domain-containing protein 3, mitochondrial	34	1	59,4	1	62,2	1	44	1	PTCD3_HUMAN	PTCD3
DJC21_HUMAN	DnaJ homolog subfamily C member 21	26,2	1	33,8	1	49,4	1	31,6	1	DJC21_HUMAN	DNAJC21
SMC3_HUMAN	Structural maintenance of chromosomes protein 3	46	1	60,8	8	48,2	5	44,8	2	SMC3_HUMAN	SMC3
MARK3_HUMAN	MAP/microtubule affinity-regulating kinase 3	55,8	3	127	6	47,1	3	54,6	3	MARK3_HUMAN	MARK3
RM49_HUMAN	39S ribosomal protein L49, mitochondrial	64,8	1	111,6	2	47	1	49,8	1	RM49_HUMAN	MRPL49
AHR_HUMAN	Aryl hydrocarbon receptor	35,2	1	66	2	43,8	2	44,2	1	AHR_HUMAN	AHR
LYSC_HUMAN	Lysozyme C	123,5	3	83	2	41,7	1	34,5	1	LYSC_HUMAN	LYZ
CC154_HUMAN	Coiled-coil domain-containing protein 154	40,5	79	51,8	92	39,5	84	37,9	88	CC154_HUMAN	CCDC154
DDX47_HUMAN	Probable ATP-dependent RNA helicase DDX47	35,8	2	38,2	2	39,3	1	56,5	1	DDX47_HUMAN	DDX47
TRI56_HUMAN	E3 ubiquitin-protein ligase TRIM56	32,7	1	105,1	8	38,6	3	51	3	TRI56_HUMAN	TRIM56
LEG4_HUMAN	Galectin-4	45,9	1	39,6	2	37,3	2	47,1	2	LGALS4	LGALS4
DHX30_HUMAN	Putative ATP-dependent RNA helicase DHX30	44,6	3	117,4	8	37,1	3	40,4	7	DHX30_HUMAN	DHX30
NSUN5_HUMAN	Probable 28S rRNA (cytosine-C(5))-methyltransferase	33	1	113,8	2	36,6	2	36,9	1	NSUN5_HUMAN	NSUN5
ESF1_HUMAN	ESF1 homolog	40	1	46,4	1	36,1	1	32,9	1	ESF1_HUMAN	ESF1
MOV10_HUMAN	Putative helicase MOV-10	47,4	1	94,9	3	33,4	2	37,4	1	MOV10_HUMAN	MOV10
MACF1_HUMAN	Microtubule-actin cross-linking factor 1, isoforms 1/2/3/5	37,1	1	52,8	2	31,6	1	30,6	2	MACF1_HUMAN	MACF1

BIBLIOGRAPHY

CHAPTER VII. BIBLIOGRAPHY

1. Rogers K. The Human Body The Digestive System. First ed. New York, NY: Britannica Educational Publishing; 2011. 251 p.

2. Lee E, Trasler J, Dwivedi S, Leblond C. Division of the mouse gastric mucosa into zymogenic and mucous regions on the basis of gland features. Am J Anat. 1982;164(3):187-207.

3. Karam S, Leblond C. Dynamics of epithelial cells in the corpus of the mouse stomach. I. Identification of proliferative cell types and pinpointing of the stem cell. Anat Rec. 1993;236(2):259-79.

4. Karam S. A focus on parietal cells as a renewing cell population. World J Gastroenterol. 2010;16(5):538-46.

5. Leblond C. The life history of cells in renewing systems. Am J Anat. 1981;160(2):114-58.

6. Karam S. Lineage commitment and maturation of epithelial cells in the gut. Front Biosci. 1999(4):D286-98.

7. Vries R, Huch M, Clevers H. Stem cells and cancer of the stomach and intestine. Mol Oncol. 2010;4(5):373-84.

8. He S, Nakada D, Morrison S. Mechanisms of stem cell self-renewal. Annu Rev Cell Dev Biol. 2009(25):377-406.

9. Lobo N, Shimono Y, Qian D, Clarke M. The biology of cancer stem cells. Annu Rev Cell Dev Biol. 2007(23):675-99.

10. Myoung-Eun H, Sae-Ock O. Gastric stem cells and gastric cancer stem cells. Anat Cell Biol. 2013;46(1):8-18.

11. Huh W, Pan X, Mysorekar I, Mills J. Location, allocation, relocation: isolating adult tissue stem cells in three dimensions. Curr Opin Biotechnol. 2006;17(5):511-7.

12. Khurana S, Mills J. The gastric mucosa development and differentiation. Prog Mol Biol Transl Sci. 2010(96):93-115.

13. Qiao X, Ziel J, McKimpson W, Madison B, Todisco A, Merchant J, et al. Prospective identification of a multilineage progenitor in murine stomach epithelium. 2007. 2007;133(6):1989-98.

14. Quante M, Marrache F, Goldenring J, Wang T. TFF2 mRNA transcript expression marks a gland progenitor cell of the gastric oxyntic mucosa. Gastroenterology. 2010;139(6):2018-27.e2. .

15. Barker N, Huch M, Kujala P, van de Wetering M, Snippert H, van Es J, et al. Lgr5(+ve) stem cells drive self-renewal in the stomach and build long-lived gastric units in vitro. Cell Stem Cell. 2010;6(1):25-36.

16. Arnold K, Sarkar A, Yram M, Polo J, Bronson R, Sengupta S, et al. Sox2(+) adult stem and progenitor cells are important for tissue regeneration and survival of mice. Cell Stem Cell. 2011;9(4):317-29.

17. Stange D, Koo B, Huch M, Sibbel G, Basak O, Lyubimova A, et al. Differentiated Troy+ chief cells act as reserve stem cells to generate all lineages of the stomach epithelium. Cell. 2013;155(2):357-68.

18. Hayakawa Y, Ariyama H, Stancikova J, Sakitani K, Asfaha S, Renz B, et al. Mist1 Expressing Gastric Stem Cells Maintain the Normal and Neoplastic Gastric Epithelium and Are Supported by a Perivascular Stem Cell Niche. Cancer Cell. 2015;28(6):800-14.

19. Karam S, Leblond C. Dynamics of epithelial cells in the corpus of the mouse stomach. III. Inward migration of neck cells followed by progressive transformation into zymogenic cells. Anat Rec. 1993;236(2):297-313.

20. Karam S, Leblond C. Dynamics of epithelial cells in the corpus of the mouse stomach. II. Outward migration of pit cells. Anat Rec. 1993;236(2):280-96.

21. Fukaya M, Isohata N, Ohta H, Aoyagi K, Ochiya T, Saeki N, et al. Hedgehog signal activation in gastric pit cell and in diffuse-type gastric cancer. Gastroenterology. 2006;131(1):14-29.

22. Nomura S, Settle S, Leys C, Means A, Peek RJ, Leach S, et al. Evidence for repatterning of the gastric fundic epithelium associated with Ménétrier's disease and TGFalpha overexpression. Gastroenterology. 2005;128(5):1292-305.

23. Ramsey V, Doherty J, Chen C, Stappenbeck T, Konieczny S, Mills J. The maturation of mucus-secreting gastric epithelial progenitors into digestive-enzyme secreting zymogenic cells requires Mist1. Development. 2007;134(1):211-22.

24. Tian X, Jin R, Bredemeyer A, Oates E, Błazewska K, McKenna C, et al. RAB26 and RAB3D are direct transcriptional targets of MIST1 that regulate exocrine granule maturation. Mol Cell Biol. 2010;30(5):1269-84.

25. Karam S, John R, Alpers D, Ponery A. Retinoic acid stimulates the dynamics of mouse gastric epithelial progenitors. Stem Cells. 2005;23(3):433-41.

26. Stepan V, Ramamoorthy S, Nitsche H, Zavros Y, Merchant J, Todisco A. Regulation and function of the sonic hedgehog signal transduction pathway in isolated gastric parietal cells. The Journal of biological chemistry. 2005;280(16):15700-8.

27. Shinohara M, Mao M, Keeley T, El-Zaatari M, Lee H, Eaton K, et al. Bone morphogenetic protein signaling regulates gastric epithelial cell development and proliferation in mice. Gastroenterology. 2010;139(6):2050-60.e2.

28. Wang T, Koh T, Varro A, Cahill R, Dangler C, Fox J, et al. Processing and proliferative effects of human progastrin in transgenic mice. J Clin Invest. 1996;98(8):1918-29.

29. Creamer B, Shorter R, Bamforth J. The turnover and shedding of epithelial cells. Gut. 1961;2(2):110-6.

30. McDonald S, Greaves L, Gutierrez-Gonzalez L, Rodriguez-Justo M, Deheragoda M, Leedham S, et al. Mechanisms of field cancerization in the human stomach: the expansion and spread of mutated gastric stem cells. Gastroenterology. 2008;134(2):500-10.

31. Nomura S, Esumi H, Job C, Tan S. Lineage and clonal development of gastric glands. Dev Biol. 1998;204(1):124-35.

32. Tatematsu M, Fukami H, Yamamoto M, Nakanishi H, Masui T, Kusakabe N, et al. Clonal analysis of glandular stomach carcinogenesis in C3H/HeN<==>BALB/c chimeric mice treated with N-methyl-N-nitrosourea. Cancer Lett. 1994;83(1-2):37-42.

33. Thompson M, Fleming K, Evans D, Fundele R, Surani M, Wright N. Gastric endocrine cells share a clonal origin with other gut cell lineages. Development. 1990;110(2):477-81.

34. Karam S. Dynamics of epithelial cells in the corpus of the mouse stomach. IV. Bidirectional migration of parietal cells ending in their gradual degeneration and loss. Anat Rec. 1993;236(2):314-32.

35. Lee E. Dynamic histology of the antral epithelium in the mouse stomach: III. Ultrastructure and renewal of pit cells. Am J Anat. 1985;172(3):225-40.

36. Lee E, Leblond C. Dynamic histology of the antral epithelilum in the mouse stomach: IV. Ultrastructure and renewal of gland cells. Am J Anat. 1985;172(3):241-59.

37. Hanahan D, Weinberg R. Hallmarks of cancer: the next generation. Cell. 2011;144(5):646-74.

38. Ferlay J, Soerjomataram I, Ervik M, Dikshit R, Eser S, Mathers C, et al. GLOBOCAN 2012 v1.0, Cancer Incidence and Mortality Worldwide: IARC CancerBase No. 11 [online]. http://globocan.iarc.fr: International Agency for Research on Cancer. ; 2013 [

39. Torre L, Bray F, Siegel R, Ferlay J, Lortet-Tieulent J, Jemal A. Global cancer statistics, 2012. CA: a cancer journal for clinicians. 2015;65(2):87-108.

40. SEER. National Cancer Institute. Cancer Stat Facts: Stomach Cancer 2018 [Available from: https://seer.cancer.gov/statfacts/html/stomach.html.

41. Song Y, Wang Y, Tong C, Xi H, Zhao X, Wang Y, et al. A unified model of the hierarchical and stochastic theories of gastric cancer. Br J Cancer. 2017;116(8):973-89.

42. Cunningham D, Starling N, Rao S, Iveson T, Nicolson M, Coxon F, et al. Capecitabine and oxaliplatin for advanced esophagogastric cancer. N Engl J Med. 2008;358(1):36-46.

43. Kang Y, Kang W, Shin D, Chen J, Xiong J, Wang J, et al. Capecitabine/cisplatin versus 5-fluorouracil/cisplatin as first-line therapy in patients with advanced gastric cancer: a randomised phase III noninferiority trial. Ann Oncol. 2009;20(4):666-73.

44. Janowitz T, Thuss-Patience P, Marshall A, Kang J, Connell C, Cook N, et al. Chemotherapy vs supportive care alone for relapsed gastric, gastroesophageal junction, and oesophageal adenocarcinoma: a meta-analysis of patient-level data. Br J Cancer. 2016;114(4):381-7.

45. Howlader N, Noone A, Krapcho M, Miller D, Bishop K, Kosary C, et al. American Joint Committee on Cancer. Stomach Cancer. In: Springer, editor. AJCC Cancer Staging Manual. 8th ed. New York, NY.2017. p. 117-21.

46. Smyth E, Verheij M, Allum W, Cunningham D, Cervantes A, Arnold D, et al. Gastric cancer: ESMO Clinical Practice Guidelines for diagnosis, treatment and follow-up. Ann Oncol. 2016;27(suppl 5):v38-v49.

47. Digklia A, Wagner A. Advanced gastric cancer: Current treatment landscape and future perspectives. World J Gastroenterol. 2016;22(8):2403-14.

48. Bang Y, Van Cutsem E, Feyereislova A, Chung H, Shen L, Sawaki A, et al. Trastuzumab in combination with chemotherapy versus chemotherapy alone for treatment of HER2-positive advanced gastric or gastro-oesophageal junction cancer (ToGA): a phase 3, open-label, randomised controlled trial. Lancet. 2010;376(9742):687-97.

49. Chua C, Tan I, Yamada Y, Rha S, Yong W, Ong W, et al. Phase II study of trastuzumab in combination with S-1 and cisplatin in the first-line treatment of human epidermal growth factor receptor HER2-positive advanced gastric cancer. Cancer Chemother Pharmacol. 2015;76(2):397-408.

50. Ryu M, Yoo C, Kim J, Ryoo B, Park Y, Park S, et al. Multicenter phase II study of trastuzumab in combination with capecitabine and oxaliplatin for advanced gastric cancer. Eur J Cancer. 2015;51(4):482-8.

51. Okines A, Norman A, McCloud P, Kang Y, Cunningham D. Meta-analysis of the REAL-2 and ML17032 trials: evaluating capecitabine-based combination chemotherapy and infused 5-fluorouracil-based combination chemotherapy for the treatment of advanced oesophago-gastric cancer. Ann Oncol. 2009;20(9):1529-34.

52. Al-Batran S, Hartmann J, Hofheinz R, Homann N, Rethwisch V, Probst S, et al. Biweekly fluorouracil, leucovorin, oxaliplatin, and docetaxel (FLOT) for patients with metastatic adenocarcinoma of the stomach or esophagogastric junction: a phase II trial of the Arbeitsgemeinschaft Internistische Onkologie. Ann Oncol. 2008;19(11):1882-7.

53. Dank M, Zaluski J, Barone C, Valvere V, Yalcin S, Peschel C, et al. Randomized phase III study comparing irinotecan combined with 5-fluorouracil and folinic acid to cisplatin combined with 5-fluorouracil in chemotherapy naive patients with advanced adenocarcinoma of the stomach or esophagogastric junction. Ann Oncol. 2008;19(8):1450-7.

54. Guimbaud R, Louvet C, Ries P, Ychou M, Maillard E, André T, et al. Prospective, randomized, multicenter, phase III study of fluorouracil, leucovorin, and irinotecan versus epirubicin, cisplatin, and capecitabine in advanced gastric adenocarcinoma: a French intergroup (Fédération Francophone de Cancérologie Digestive, Fédération Nationale des Centres de Lutte Contre le Cancer, and Groupe Coopérateur Multidisciplinaire en Oncologie) study. J Clin Oncol. 2014;32(31):3520-6.

55. Thuss-Patience P, Kretzschmar A, Bichev D, Deist T, Hinke A, Breithaupt K, et al. Survival advantage for irinotecan versus best supportive care as second-line chemotherapy in gastric cancer--a randomised phase III study of the Arbeitsgemeinschaft Internistische Onkologie (AIO). Eur J Cancer. 2011;47(15):2306-14.

56. Ford H, Marshall A, Bridgewater J, Janowitz T, Coxon F, Wadsley J, et al. Docetaxel versus active symptom control for refractory oesophagogastric adenocarcinoma (COUGAR-02): an open-label, phase 3 randomised controlled trial. Lancet Oncol. 2014;15(1):78-86.

57. Kang J, Lee S, Lim D, Park K, Oh S, Kwon H, et al. Salvage chemotherapy for pretreated gastric cancer: a randomized phase III trial comparing chemotherapy plus best supportive care with best supportive care alone. J Clin Oncol. 2012;30(13):1513-8.

58. Roy A, Park S, Cunningham D, Kang Y, Chao Y, Chen L, et al. A randomized phase II study of PEP02 (MM-398), irinotecan or docetaxel as a second-line therapy in patients with locally advanced or metastatic gastric or gastro-oesophageal junction adenocarcinoma. Ann Oncol. 2013;24(6):1567-73.

59. Okines A, Asghar U, Cunningham D, Ashley S, Ashton J, Jackson K, et al. Rechallenge with platinum plus fluoropyrimidine +/- epirubicin in patients with oesophagogastric cancer. Oncology. 2010;79(1-2):150-8.

60. Satoh T, Xu R, Chung H, Sun G, Doi T, Xu J, et al. Lapatinib plus paclitaxel versus paclitaxel alone in the second-line treatment of HER2-amplified advanced gastric cancer in Asian populations: TyTAN--a randomized, phase III study. J Clin Oncol. 2014;32(19):2039-49.

61. Hecht J, Bang Y, Qin S, Chung H, Xu J, Park J, et al. Lapatinib in Combination With Capecitabine Plus Oxaliplatin in Human Epidermal Growth Factor Receptor 2-Positive Advanced or Metastatic Gastric, Esophageal, or Gastroesophageal Adenocarcinoma: TRIO-013/LOGiC--A Randomized Phase III Trial. J Clin Oncol. 2016;34(5):443-51.

62. Comprehensive molecular characterization of gastric adenocarcinoma. Nature. 2014;513(7517):202-9.

63. Nagini S. Carcinoma of the stomach: A review of epidemiology, pathogenesis, molecular genetics and chemoprevention. World J Gastrointest Oncol. 2012;4(7):156-69.

64. Forman D, Burley V. Gastric cancer: global pattern of the disease and an overview of environmental risk factors. Best Pract Res Clin Gastroenterol. 2006;20(4):633-49.

65. Noto J, Gaddy J, Lee J, Piazuelo M, Friedman D, Colvin D, et al. Iron deficiency accelerates Helicobacter pylori-induced carcinogenesis in rodents and humans. J Clin Invest. 2013;123(1):479-92.

66. Murphy G, Pfeiffer R, Camargo M, Rabkin C. Meta-analysis shows that prevalence of Epstein-Barr virus-positive gastric cancer differs based on sex and anatomic location. Gastroenterology. 2009;137(3):824-33.

67. Peleteiro B, Bastos A, Ferro A, Lunet N. Prevalence of Helicobacter pylori infection worldwide: a systematic review of studies with national coverage. Dig Dis Sci. 2014;59(8):1698-709.

68. Nomura A, Wilkens L, Henderson B, Epplein M, Kolonel L. The association of cigarette smoking with gastric cancer: the multiethnic cohort study. Cancer Causes Control. 2012;23(1):51-8.

69. Dyke G, Craven J, Hall R, Garner R. Smoking-related DNA adducts in human gastric cancers. Int J Cancer. 1992;52(6):847-50.

70. Kneller R, You W, Chang Y, Liu W, Zhang L, Zhao L, et al. Cigarette smoking and other risk factors for progression of precancerous stomach lesions. J Natl Cancer Inst. 1992;84(16):1261-6.

71. McLean M, El-Omar E. Genetics of gastric cancer. Nat Rev Gastroenterol Hepatol. 2014;11(11):664-74.

72. Noone A, Howlader N, Krapcho M, Miller D, Brest A, Yu M, et al. SEER Cancer Statistics Review, 1975-2015, National Cancer Institute. Bethesda, MD, https://seer.cancer.gov/csr/1975_2015/, based on November 2017 SEER data submission, posted to the SEER web site, April 2018.

73. LAUREN P. THE TWO HISTOLOGICAL MAIN TYPES OF GASTRIC CARCINOMA: DIFFUSE AND SO-CALLED INTESTINAL-TYPE CARCINOMA. AN ATTEMPT AT A HISTO-CLINICAL CLASSIFICATION. Acta Pathol Microbiol Scand. 1965;64:31-49.

74. Correa P. Helicobacter pylori and gastric carcinogenesis. Am J Surg Pathol. 1995;19 Suppl 1:S37-43.

75. Yakirevich E, Resnick M. Pathology of gastric cancer and its precursor lesions. Gastroenterol Clin North Am. 2013;42(2):261-84.

76. Piazuelo M, Correa P. Gastric cancer: Overview. Colomb Med (Cali). 2013;44(3):192-201.

77. Kaneko S, Yoshimura T. Time trend analysis of gastric cancer incidence in Japan by histological types, 1975-1989. Br J Cancer. 2001;84(3):400-5.

78. Kong X, Wang J, Chen H, Fang J. Comparison of the clinicopathological characteristics of young and elderly patients with gastric carcinoma: a meta analysis. J Surg Oncol. 2012;106(3):346-52.

79. Warneke V, Behrens H, Hartmann J, Held H, Becker T, Schwarz N, et al. Cohort study based on the seventh edition of the TNM classification for gastric cancer: proposal of a new staging system. J Clin Oncol. 2011;29(17):2364-71.

80. Chiaravalli A, Klersy C, Vanoli A, Ferretti A, Capella C, Solcia E. Histotype-based prognostic classification of gastric cancer. World J Gastroenterol. 2012;18(9):896-904.

81. Stiekema J, Cats A, Kuijpers A, van Coevorden F, Boot H, Jansen E, et al. Surgical treatment results of intestinal and diffuse type gastric cancer. Implications for a differentiated therapeutic approach? Eur J Surg Oncol. 2013;39(7):686-93.

82. Bosman F, Carneiro F, Hruban R, Theise N. WHO Classification of Tumours of the Digestive System: IARC; 2010.

83. Almeida R, Silva E, Santos-Silva F, Silberg D, Wang J, De Bolós C, et al. Expression of intestine-specific transcription factors, CDX1 and CDX2, in intestinal metaplasia and gastric carcinomas. J Pathol. 2003;199(1):36-40.

84. Goldenring J, Nomura S. Differentiation of the gastric mucosa III. Animal models of oxyntic atrophy and metaplasia. Am J Physiol Gastrointest Liver Physiol. 2006;291(6):G999-1004.

85. Goldenring J, Nam K. Oxyntic atrophy, metaplasia, and gastric cancer. Prog Mol Biol Transl Sci. 2010(96):117-31.

86. Karin M. Inflammation and cancer: the long reach of Ras. 2005. 2005;11(1):20-1.

87. Taketo M. Mouse models of gastrointestinal tumors. Cancer Sci. 2006;97(5):355-61.

88. Choi S, Aid S, Bosetti F. The distinct roles of cyclooxygenase-1 and -2 in neuroinflammation: implications for translational research. Trends Pharmacol Sci. 2009;30(4):174-81.

89. Echizen K, Hirose O, Maeda Y, Oshima M. Inflammation in gastric cancer: Interplay of the COX‐2/prostaglandin E2 and Toll‐like receptor/MyD88 pathways. Cancer Sci. 2016;107(4):391-7.

90. Oshima H, Oshima M, Inaba K, Taketo M. Hyperplastic gastric tumors induced by activated macrophages in COX-2/mPGES-1 transgenic mice. The EMBO journal. 2004;23(7):1669-78.

91. Tan P, Yeoh K. Genetics and Molecular Pathogenesis of Gastric Adenocarcinoma. Gastroenterology. 2015;149(5):1153-62.

92. Kreso A, Dick J. Evolution of the cancer stem cell model. Cell Stem Cell. 2014;14(3):275-91.

93. Notta F, Mullighan C, Wang J, Poeppl A, Doulatov S, Phillips L, et al. Evolution of human BCR-ABL1 lymphoblastic leukaemia-initiating cells. Nature. 2011;469(7330):362-7.

94. Chow K, Shin D, Jenkins M, Miller E, Shih D, Choi S, et al. Epigenetic states of cells of origin and tumor evolution drive tumor-initiating cell phenotype and tumor heterogeneity. Cancer Res. 2014;74(17):4864-74.

95. Baer C, Claus R, Plass C. Genome-wide epigenetic regulation of miRNAs in cancer. Cancer Res. 2013;73(2):473-7.

96. Klutstein M, Nejman D, Greenfield R, Cedar H. DNA Methylation in Cancer and Aging. Cancer Res. 2016;76(12):3446-50.

97. Elowitz M, Levine A, Siggia E, Swain P. Stochastic gene expression in a single cell. Science. 2002;297(5584):1183-6.

98. Kaern M, Elston T, Blake W, Collins J. Stochasticity in gene expression: from theories to phenotypes. Nat Rev Genet. 2005;6(6):451-64.

99. Spencer S, Gaudet S, Albeck J, Burke J, Sorger P. Non-genetic origins of cell-to-cell variability in TRAIL-induced apoptosis. Nature. 2009;459(7245):428-32.

100. Plaks V, Kong N, Werb Z. The cancer stem cell niche: how essential is the niche in regulating stemness of tumor cells? Cell Stem Cell. 2015;16(3):225-38.

101. Medema J, Vermeulen L. Microenvironmental regulation of stem cells in intestinal homeostasis and cancer. Nature. 2011;474(7351):318-26.

102. Borovski T, De Sousa E, Vermeulen L, Medema J. Cancer stem cell niche: the place to be. Cancer Res. 2011;71(3):634-9.

103. Madison B, Dunbar L, Qiao X, Braunstein K, Braunstein E, Gumucio D. Cis elements of the villin gene control expression in restricted domains of the vertical (crypt) and horizontal (duodenum, cecum) axes of the intestine. The Journal of biological chemistry. 2002;277(36):33275-83.

104. Li Q, Jia Z, Wang L, Kong X, Li Q, Guo K, et al. Disruption of Klf4 in villin-positive gastric progenitor cells promotes formation and progression of tumors of the antrum in mice. Gastroenterology. 2012;142(3):531-42.

105. Craig S, Powell L. Regulation of actin polymerization by villin, a 95,000 dalton cytoskeletal component of intestinal brush borders. Cell. 1980;22(3):739-46.

106. Braunstein E, Qiao X, Madison B, Pinson K, Dunbar L, Gumucio D. Villin: A marker for development of the epithelial pyloric border. Dev Dyn. 2002;224(1):90-102.

107. van den Brink G, Hardwick J, Nielsen C, Xu C, ten Kate F, Glickman J, et al. Sonic hedgehog expression correlates with fundic gland differentiation in the adult gastrointestinal tract. Gut. 2002;51(5):628-33.

108. van den Brink G, Hardwick J, Tytgat G, Brink M, Ten Kate F, Van Deventer S, et al. Sonic hedgehog regulates gastric gland morphogenesis in man and mouse. Gastroenterology. 2001;121(2):317-28.

109. Berman D, Karhadkar S, Maitra A, Montes De Oca R, Gerstenblith M, Briggs K, et al. Widespread requirement for Hedgehog ligand stimulation in growth of digestive tract tumours. Nature. 2003;425(6960):846-51.

110. van den Brink G. Hedgehog signaling in development and homeostasis of the gastrointestinal tract. Physiol Rev. 2007;87(4):1343-75.

111. Xiao C, Ogle S, Schumacher M, Orr-Asman M, Miller M, Lertkowit N, et al. Loss of parietal cell expression of Sonic hedgehog induces hypergastrinemia and hyperproliferation of surface mucous cells. Gastroenterology. 2010;138(2):550-61, 61.e1-8.

112. Xiao C, Ogle S, Schumacher M, Schilling N, Tokhunts R, Orr-Asman M, et al. Hedgehog signaling regulates E-cadherin expression for the maintenance of the actin cytoskeleton and tight junctions. Am J Physiol Gastrointest Liver Physiol. 2010;299(6):G1252-65.

113. Martin J, Donnelly J, Houghton J, Zavros Y. The role of sonic hedgehog reemergence during gastric cancer. Dig Dis Sci. 2010;55(6):1516-24.

114. Song Z, Yue W, Wei B, Wang N, Li T, Guan L, et al. Sonic hedgehog pathway is essential for maintenance of cancer stem-like cells in human gastric cancer. PloS one. 2011;6(3):e17687.

115. Han M, Lee Y, Baek S, Kim B, Kim J, Oh S. Hedgehog signaling regulates the survival of gastric cancer cells by regulating the expression of Bcl-2. Int J Mol Sci. 2009;10(7):3033-43.

116. Lee S, Han H, Lee K, Hwang T, Kim J, Sung I, et al. Sonic hedgehog expression in gastric cancer and gastric adenoma. Oncol Rep. 2007;17(5):1051-5.

117. Yoo Y, Kang M, Kim J, Oh S. Sonic hedgehog signaling promotes motility and invasiveness of gastric cancer cells through TGF-beta-mediated activation of the ALK5-Smad 3 pathway. Carcinogenesis. 2008;29(3):480-90.

118. Merchant A, Matsui W. Targeting Hedgehog--a cancer stem cell pathway. Clin Cancer Res. 2010;16(12):3130-40.

119. Giannakis M, Stappenbeck T, Mills J, Leip D, Lovett M, Clifton S, et al. Molecular properties of adult mouse gastric and intestinal epithelial progenitors in their niches. The Journal of biological chemistry. 2006;281(16):11292-300.

120. Radulescu S, Ridgway R, Cordero J, Athineos D, Salgueiro P, Poulsom R, et al. Acute WNT signalling activation perturbs differentiation within the adult stomach and rapidly leads to tumour formation. Oncogene. 2013;32(16):2048-57.

121. Watanabe H, Enjoji M, Yao T, Ohsato K. Gastric lesions in familial adenomatosis coli: their incidence and histologic analysis. Hum Pathol. 1978;9(3):269-83.

122. Bianchi L, Burke C, Bennett A, Lopez R, Hasson H, Church J. Fundic gland polyp dysplasia is common in familial adenomatous polyposis. Clin Gastroenterol Hepatol. 2008;6(2):180-5.

123. Cai C, Zhu X. The Wnt/β-catenin pathway regulates self-renewal of cancer stem-like cells in human gastric cancer. Mol Med Rep. 2012;5(5):1191-6.

124. Wu W, Cho C, Lee C, Fan D, Wu K, Yu J, et al. Dysregulation of cellular signaling in gastric cancer. Cancer Lett. 2010;295(2):144-53.

125. Clements W, Wang J, Sarnaik A, Kim O, MacDonald J, Fenoglio-Preiser C, et al. beta-Catenin mutation is a frequent cause of Wnt pathway activation in gastric cancer. Cancer Res. 2002;62(12):3503-6.

126. Tahara E. Molecular biology of gastric cancer. World J of Surgery. 1995;19(4):484-8.

127. Kim T, Shivdasani R. Notch signaling in stomach epithelial stem cell homeostasis. J Exp Med. 2011;208(4):677-88.

128. Jensen J, Pedersen E, Galante P, Hald J, Heller R, Ishibashi M, et al. Control of endodermal endocrine development by Hes-1. Nature genetics. 2000;24(1):36-44.

129. Yeh T, Wu C, Hsu K, Liao W, Yang M, Li A, et al. The activated Notch1 signal pathway is associated with gastric cancer progression through cyclooxygenase-2. Cancer Res. 2009;69(12):5039-48.

130. Fiske W, Threadgill D, Coffey R. ERBBs in the gastrointestinal tract: recent progress and new perspectives. Exp Cell Res. 2009;315(4):583-601.

131. Hoffmann W. Stem cells, self-renewal and cancer of the gastric epithelium. Curr Med Chem. 2012;19(35):5975-83.

132. Tang L, Modlin I, Lawton G, Kidd M, Chinery R. The role of transforming growth factor alpha in the enterochromaffin-like cell tumor autonomy in an African rodent mastomys. Gastroenterology. 1996;111(5):1212-23.

133. Gravalos C, Jimeno A. HER2 in gastric cancer: a new prognostic factor and a novel therapeutic target. Ann Oncol. 2008;19(9):1523-9.

134. Yoshida K, Tsuda T, Matsumura T, Tsujino T, Hattori T, Ito H, et al. Amplification of epidermal growth factor receptor (EGFR) gene and oncogenes in human gastric carcinomas. Virchows Arch B Cell Pathol Incl Mol Pathol. 1989;57(2):285-90.

135. Matsubara J, Yamada Y, Hirashima Y, Takahari D, Okita N, Kato K, et al. Impact of insulin-like growth factor type 1 receptor, epidermal growth factor receptor, and HER2 expressions on outcomes of patients with gastric cancer. Clin Cancer Res. 2008;14(10):3022-9.

136. Mishra L, Derynck R, Mishra B. Transforming growth factor-beta signaling in stem cells and cancer. Science. 2005;310(5745):68-71.

137. Miyazono K, Suzuki H, Imamura T. Regulation of TGF-beta signaling and its roles in progression of tumors. Cancer Sci. 2003;94(3):230-4.

138. Chang T, Ito K, Ko T, Liu Q, Salto-Tellez M, Yeoh K, et al. Claudin-1 has tumor suppressive activity and is a direct target of RUNX3 in gastric epithelial cells. Gastroenterology. 2010;138(1):255-65.e1-3.

139. Maloum F, Allaire J, Gagné-Sansfaçon J, Roy E B, K , Sarret P, Morisset J, et al. Epithelial BMP signaling is required for proper specification of epithelial cell lineages and gastric endocrine cells. Am J Physiol Gastrointest Liver Physiol. 2011;300(6):G1065-79.

140. Bleuming S, Kodach L, Garcia Leon M, Richel D, Peppelenbosch M, Reitsma P, et al. Altered bone morphogenetic protein signalling in the Helicobacter pylori-infected stomach. J Pathol. 2006;209(2):190-7.

141. Wen X, Akiyama Y, Baylin S, Yuasa Y. Frequent epigenetic silencing of the bone morphogenetic protein 2 gene through methylation in gastric carcinomas. Oncogene. 2006;25(18):2666-73.

142. Wen X, Miyake S, Akiyama Y, Yuasa Y. BMP-2 modulates the proliferation and differentiation of normal and cancerous gastric cells. Biochem Biophys Res Commun. 2004;316(1):100-6.

143. Spehlmann ME EL. Nuclear factor-kappa B in intestinal protection and destruction. Curr Opin Gastroenterol. 2009;25(2):92-9.

144. Yasumoto K, Okamoto S, Mukaida N, Murakami S, Mai M, Matsushima K. Tumor necrosis factor alpha and interferon gamma synergistically induce interleukin 8 production in a human gastric cancer cell line through acting concurrently on AP-1 and NF-kB-like binding sites of the interleukin 8 gene. The Journal of biological chemistry. 1992;267(31):22506-11.

145. Kang M, Ryu B, Lee M, Han J, Lee J, Ha T, et al. NF-kappaB activates transcription of the RNA-binding factor HuR, via PI3K-AKT signaling, to promote gastric tumorigenesis. Gastroenterology. 2008;135(6):2030-42, 42.e1-3.

146. Liu C, Wang M, Chi C, Wu C, Chen J. Rho/Rhotekin-mediated NF-kappaB activation confers resistance to apoptosis. Oncogene. 2004;23(54):8731-42.

147. Sakamoto K, Hikiba Y, Nakagawa H, Hayakawa Y, Yanai A, Akanuma M, et al. Inhibitor of kappaB kinase beta regulates gastric carcinogenesis via interleukin-1alpha expression. Gastroenterology. 2010;139(1):226-38.e6.

148. Matsumoto Y, Marusawa H, Kinoshita K, Endo Y, Kou T, Morisawa T, et al. Helicobacter pylori infection triggers aberrant expression of activation-induced cytidine deaminase in gastric epithelium. Nat Med. 2007;13(4):470-6.

149. Liu X, Wang X, Zhang J, Lam E, Shin V, Cheng A, et al. Warburg effect revisited: an epigenetic link between glycolysis and gastric carcinogenesis. Oncogene. 2010;29(3):442-50.

150. Cho S, Park J, Kang J, Kim W, Juhnn Y, Lee J, et al. Nuclear factor-kappaB dependency of doxorubicin sensitivity in gastric cancer cells is determined by manganese superoxide dismutase expression. Cancer Sci. 2008;99(6):1117-24.

151. Hinohara K, Kobayashi S, Kanauchi H, Shimizu S, Nishioka K, Tsuji E, et al. ErbB receptor tyrosine kinase/NF-κB signaling controls mammosphere formation in human breast cancer. Proc Natl Acad Sci U S A. 2012;109(17):6584-9.

152. Mimeault M, Johansson S, Batra S. Pathobiological implications of the expression of EGFR, pAkt, NF-κB and MIC-1 in prostate cancer stem cells and their progenies. PloS one. 2012;7(2):e31919.

153. Nogueira L, Ruiz-Ontañon P, Vazquez-Barquero A, Lafarga M, Berciano M, Aldaz B, et al. Blockade of the NFκB pathway drives differentiating glioblastoma-initiating cells into senescence both in vitro and in vivo. Oncogene. 2011;30(32):3537-48.

154. Nishimura T. Total number of genome alterations in sporadic gastrointestinal cancer inferred from pooled analyses in the literature. Tumour Biol. 2008;29(6):343-50.

155. Oliveira C, Pinheiro H, Figueiredo J, Seruca R, Carneiro F. Familial gastric cancer: genetic susceptibility, pathology, and implications for management. Lancet Oncol. 2015;16(2):e60-70.

156. Zanghieri G, Di Gregorio C, Sacchetti C, Fante R, Sassatelli R, Cannizzo G, et al. Familial occurrence of gastric cancer in the 2-year experience of a population-based registry. Cancer. 1990;66(9):2047-51.

157. Palli D, Galli M, Caporaso NE, Cipriani F, Decarli A, Saieva C, et al. Family history and risk of stomach cancer in Italy. Cancer Epidemiol Biomarkers Prev. 1994;3(1):15-8.

158. Hansford S, Kaurah P, Li-Chang H, Woo M, Senz J, Pinheiro H, et al. Hereditary Diffuse Gastric Cancer Syndrome: CDH1 Mutations and Beyond. JAMA Oncol. 2015;1(1):23-32.

159. Mimata A, Fukamachi H, Eishi Y, Yuasa Y. Loss of E-cadherin in mouse gastric epithelial cells induces signet ring-like cells, a possible precursor lesion of diffuse gastric cancer. Cancer Sci. 2011;102(5):942-50.

160. Worthley D, Phillips K, Wayte N, Schrader K, Healey S, Kaurah P, et al. Gastric adenocarcinoma and proximal polyposis of the stomach (GAPPS): a new autosomal dominant syndrome. Gut. 2012;61(5):774-9.

161. Rahner N, Steinke V, Schlegelberger B, Eisinger F, Hutter P, Olschwang S. Clinical utility gene card for: Lynch syndrome (MLH1, MSH2, MSH6, PMS2, EPCAM) - update 2012. Eur J Hum Genet. 2013;21(1).

162. Lipton L, Tomlinson I. The genetics of FAP and FAP-like syndromes. Fam Cancer. 2006;5(3):221-6.

163. Vasen H, Möslein G, Alonso A, Aretz S, Bernstein I, Bertario L, et al. Guidelines for the clinical management of familial adenomatous polyposis (FAP). Gut. 2008;57(5):704-13.

164. Li F, Fraumeni JJ. Rhabdomyosarcoma in children: epidemiologic study and identification of a familial cancer syndrome. J Natl Cancer Inst. 1969;43(6):1365-73.

165. Malkin D, Li F, Strong L, Fraumeni JJ, Nelson C, Kim D, et al. Germ line p53 mutations in a familial syndrome of breast cancer, sarcomas, and other neoplasms. Science. 1990;250(4985):1233-8.

166. Allen B, Terdiman J. Hereditary polyposis syndromes and hereditary non-polyposis colorectal cancer. Best Pract Res Clin Gastroenterol. 2003;17(2):237-58.

167. Howe J, Sayed M, Ahmed A, Ringold J, Larsen-Haidle J, Merg A, et al. The prevalence of MADH4 and BMPR1A mutations in juvenile polyposis and absence of BMPR2, BMPR1B, and ACVR1 mutations. J Med Genet. 2004;41(7):484-91.

168. Hudler P. Genetic aspects of gastric cancer instability. ScientificWorldJournal. 2012;2012:761909.

169. Liang H, Kim Y. Identifying molecular drivers of gastric cancer through next-generation sequencing. Cancer Lett. 2013;340(2):241-6.

170. The National Institutes of Health. The Cancer Genome Atlas [online] 2014 [Available from: http://www.cancergenome.nih.gov.

171. Wellcome Trust Sanger Institute. Cancer Genome Project [online] 2014 [Available from: http://www.sanger.ac.uk/research/projects/cancergenome.

172. International Cancer Genome Consortium (ICGC). International Cancer Genome Projects [online] 2014 [Available from: https://icgc.org/.

173. Network CGAR. Comprehensive molecular characterization of gastric adenocarcinoma. Nature. 2014;513(7517):202-9.

174. Lengauer C, Kinzler K, Vogelstein B. Genetic instabilities in human cancers. Nature. 1998;396(6712):643-9.

175. Garattini S, Basile D, Cattaneo M, Fanotto V, Ongaro E, Bonotto M, et al. Molecular classifications of gastric cancers: Novel insights and possible future applications. World J Gastrointest Oncol. 2017;9(5):194-208.

176. Pedrazzani C, Corso G, Velho S, Leite M, Pascale V, Bettarini F, et al. Evidence of tumor microsatellite instability in gastric cancer with familial aggregation. Fam Cancer. 2009;8(3):215-20.

177. Velho S, Fernandes M, Leite M, Figueiredo C, Seruca R. Causes and consequences of microsatellite instability in gastric carcinogenesis. World J Gastroenterol. 2014;20(44):16433-42.

178. Falchetti M, Saieva C, Lupi R, Masala G, Rizzolo P, Zanna I, et al. Gastric cancer with high-level microsatellite instability: target gene mutations, clinicopathologic features, and long-term survival. Hum Pathol. 2008;39(6):925-32.

179. Fang W, Chang SC, Lan YT, Huang KH, Chen JH, Lo SS, et al. Microsatellite instability is associated with a better prognosis for gastric cancer patients after curative surgery. World J Surg. 2012;36(9):2131-8.

180. Comprehensive molecular characterization of human colon and rectal cancer. Nature. 2012;487(7407):330-7.

181. Integrated genomic characterization of endometrial carcinoma. Nature. 2013;497(7447):67-73.

182. The somatic genomic landscape of glioblastoma. Cell. 2013;155(2):462-77.

183. Zhang W. TCGA divides gastric cancer into four molecular subtypes: implications for individualized therapeutics. Chin J Cancer. 2014;33(10):469-70.

184. Kakiuchi M, Nishizawa T, Ueda H, Gotoh K, Tanaka A, Hayashi A, et al. Recurrent gain-of-function mutations of RHOA in diffuse-type gastric carcinoma. Nature genetics. 2014;46(6):583-7.

185. Wang K, Yuen ST, Xu J, Lee SP, Yan HH, Shi ST, et al. Whole-genome sequencing and comprehensive molecular profiling identify new driver mutations in gastric cancer. Nature genetics. 2014;46(6):573-82.

186. Cristescu R, Lee J, Nebozhyn M, Kim K, Ting J, Wong S, et al. Molecular analysis of gastric cancer identifies subtypes associated with distinct clinical outcomes. Nat Med. 2015;21(5):449-56.

187. Gonzalgo M, Jones P. Mutagenic and epigenetic effects of DNA methylation. Mutat Res. 1997;386(2):107-18.

188. Hanazono K, Natsugoe S, Stein H, Aikou T, Hoefler H, Siewert J. Distribution of p53 mutations in esophageal and gastric carcinomas and the relationship with p53 expression. Oncol Rep. 2006;15(4):821-4.

189. Lei Z, Tan I, Das K, Deng N, Zouridis H, Pattison S, et al. Identification of molecular subtypes of gastric cancer with different responses to PI3-kinase inhibitors and 5-fluorouracil. Gastroenterology. 2013;145(3):554-65.

190. Grabsch H, Tan P. Gastric cancer pathology and underlying molecular mechanisms. Dig Surg. 2013;30(2):150-8.

191. Jaiswal B, Kljavin N, Stawiski E, Chan E, Parikh C, Durinck S, et al. Oncogenic ERBB3 mutations in human cancers. Cancer Cell. 2013;23(5):603-17.

192. Chen K, Yang D, Li X, Sun B, Song F, Cao W, et al. Mutational landscape of gastric adenocarcinoma in Chinese: implications for prognosis and therapy. Proc Natl Acad Sci U S A. 2015;112(4):1107-12.

193. Wang K, Kan J, Yuen S, Shi S, Chu K, Law S, et al. Exome sequencing identifies frequent mutation of ARID1A in molecular subtypes of gastric cancer. Nature genetics. 2011;43(12):1219-23.

194. Zang ZJ, Cutcutache I, Poon SL, Zhang SL, McPherson JR, Tao J, et al. Exome sequencing of gastric adenocarcinoma identifies recurrent somatic mutations in cell adhesion and chromatin remodeling genes. Nature genetics. 2012;44(5):570-4.

195. Bishop A, Hall A. Rho GTPases and their effector proteins. The Biochemical journal. 2000;348(2):241-55.

196. Van Aelst L, D'Souza-Schorey C. Rho GTPases and signaling networks. Genes & development. 1997;11(18):2295-322.

197. Etienne-Manneville S, Hall A. Rho GTPases in cell biology. Nature. 2002;420(6916):629-35.

198. Wennerberg K, Rossman K, Der C. The Ras superfamily at a glance. J Cell Sci. 2005;118(5):843-6.

199. Heasman S, Ridley A. Mammalian Rho GTPases: new insights into their functions from in vivo studies. Nat Rev Mol Cell Biol. 2008;9(9):690-701.

200. Bustelo X, Sauzeau V, Berenjeno I. GTP-binding proteins of the Rho/Rac family: regulation, effectors and functions in vivo. Bioessays. 2007;29(4):356-70.

201. Kawano Y, Kaneko-Kawano T, Shimamoto K. Rho family GTPase-dependent immunity in plants and animals. Front Plant Sci. 2014(5):522.

202. Rossman K, Der C, Sondek J. GEF means go: turning on RHO GTPases with guanine nucleotide-exchange factors. Nat Rev Mol Cell Biol. 2005;6(2):167-80.

203. Moon S, Zheng Y. Rho GTPase-activating proteins in cell regulation. Trends Cell Biol. 2003;13(1):13-22.

204. Olofsson B. Rho guanine dissociation inhibitors: pivotal molecules in cellular signalling. Cellular signalling. 1999;11(8):545-54.

205. Dopeso H, Rodrigues P, Bilic J, Bazzocco S, Cartón-García F, Macaya I, et al. Mechanisms of inactivation of the tumour suppressor gene RHOA in colorectal cancer. Br J Cancer. 2018;118(1):106-16.

206. Wittinghofer A. Ras Superfamily Small G Proteins: Biology and Mechanisms 1 General Features, Signaling. New York NY: Springer; 2014.

207. Burridge K, Wennerberg K. Rho and Rac take center stage. Cell. 2004;116(2):167-79.

208. Jaffe A, Hall A. Rho GTPases: biochemistry and biology. Annu Rev Cell Dev Biol. 2005(21):247-69.

209. Aspenström P. Effectors for the Rho GTPases. Curr Opin Cell Biol. 1999;11(1):95-102.

210. Mukai H, Mori K, Takanaga H, Kitagawa M, Shibata H, Shimakawa M, et al. Xenopus PKN: cloning and sequencing of the cDNA and identification of conserved domains. Biochim Biophys Acta. 1995;1995(1261):2.

211. Palmer R, Ridden J, Parker P. Cloning and expression patterns of two members of a novel protein-kinase-C-related kinase family. Eur J Biochem. 1995;227(1-2):344-51.

212. Metzger E, Yin N, Wissmann M, Kunowska N, Fischer K, Friedrichs N, et al. Phosphorylation of histone H3 at threonine 11 establishes a novel chromatin mark for transcriptional regulation. Nat Cell Biol. 2008;10(1):53-60.

213. Shibata H, Oda H, Mukai H, Oishi K, Misaki K, Ohkubo H, et al. Interaction of PKN with a neuron-specific basic helix-loop-helix transcription factor, NDRF/NeuroD2. Brain Res Mol Brain Res. 1999;74(1-2):126-34.

214. Takanaga H, Mukai H, Shibata H, Toshimori M, Ono Y. PKN interacts with a paraneoplastic cerebellar degeneration-associated antigen, which is a potential transcription factor. Exp Cell Res. 1998;241(2):363-72.

215. Goggs R, Williams C, Mellor H, Poole A. Platelet Rho GTPases-a focus on novel players, roles and relationships. The Biochemical journal. 2015;466(3):431-42.

216. Karlsson R, Pedersen E, Wang Z, Brakebusch C. Rho GTPase function in tumorigenesis. Biochim Biophys Acta. 2009;1796(2):91-8.

217. Chiba S, Enami T, Ogawa S, Sakata-Yanagimoto M. G17V RHOA: Genetic evidence of GTP-unbound RHOA playing a role in tumorigenesis in T cells. Small GTPases. 2015;6(2):100-3.

218. Sahai E, Alberts A, Treisman R. RhoA effector mutants reveal distinct effector pathways for cytoskeletal reorganization, SRF activation and transformation. The EMBO journal. 1998;17(5):1350-61.

219. Kantak S, Kramer R. E-cadherin regulates anchorage-independent growth and survival in oral squamous cell carcinoma cells. The Journal of biological chemistry. 1998;273(27):16953-61.

220. Sato T, Vries R, Snippert H, van de Wetering M, Barker N, Stange D, et al. Single Lgr5 stem cells build crypt-villus structures in vitro without a mesenchymal niche. Nature. 2009;459(7244):262-5.

221. Watanabe K, Ueno M, Kamiya D, Nishiyama A, Matsumura M, Wataya T, et al. A ROCK inhibitor permits survival of dissociated human embryonic stem cells. Nat Biotechnol. 2007;25(6):681-6.

222. Rodrigues P, Macaya I, Bazzocco S, Mazzolini R, Andretta E, Dopeso H, et al. RHOA inactivation enhances Wnt signalling and promotes colorectal cancer. Nat Commun. 2014;5(5458).

223. Mukai H, Ono Y. A novel protein kinase with leucine zipper-like sequences: its catalytic domain is highly homologous to that of protein kinase C. Biochem Biophys Res Commun. 1994;199(2):897-904.

224. Mukai H. The structure and function of PKN, a protein kinase having a catalytic domain homologous to that of PKC. Journal of biochemistry. 2003;133(1):17-27.

225. Matsuzawa K, Kosako H, Inagaki N, Shibata H, Mukai H, Ono Y, et al. Domain-specific phosphorylation of vimentin and glial fibrillary acidic protein by PKN. Biochem Biophys Res Commun. 1997;234(3):621-5.

226. Mukai H, Toshimori M, Shibata H, Kitagawa M, Shimakawa M, Miyahara M, et al. PKN associates and phosphorylates the head-rod domain of neurofilament protein. The Journal of biological chemistry. 1996;271(16):9816-22.

227. Zhao Z, Manser E. PAK and other Rho-associated kinases--effectors with surprisingly diverse mechanisms of regulation. The Biochemical journal. 2005;386(2):201-14.

228. Mukai H, Kitagawa M, Shibata H, Takanaga H, Mori K, Shimakawa M, et al. Activation of PKN, a novel 120-kDa protein kinase with leucine zipper-like sequences, by unsaturated fatty acids and by limited proteolysis. Biochem Biophys Res Commun. 1994;204(1):348-56.

229. Falk M, Liu W, Bolanos B, Unsal-Kacmaz K, Klippel A, Grant S, et al. Enzyme kinetics and distinct modulation of the protein kinase N family of kinases by lipid activators and small molecule inhibitors. Biosci Rep. 2014;34(2).

230. Marks F, Klingmüller U, Müller-Decker K. Cellular Signal Processing. An Introduction to the Molecular Mechanisms of Signal Transduction New York, NY: Garland Science, Taylor and Francis Group, LLC; 2009.

231. Kitagawa M, Shibata H, Toshimori M, Mukai H, Ono Y. The role of the unique motifs in the amino-terminal region of PKN on its enzymatic activity. Biochem Biophys Res Commun. 1996;220(3):963-8.

232. Dong L, Landa L, Wick M, Zhu L, Mukai H, Ono Y, et al. Phosphorylation of protein kinase N by phosphoinositide-dependent protein kinase-1 mediates insulin signals to the actin cytoskeleton. Proc Natl Acad Sci U S A. 2000;97(10):5089-94.

233. Flynn P, Mellor H, Casamassima A, Parker P. Rho GTPase control of protein kinase C-related protein kinase activation by 3-phosphoinositide-dependent protein kinase. The Journal of biological chemistry. 2000;275(15):11064-70.

234. Biondi R, Kieloch A, Currie R, Deak M, Alessi D. The PIF-binding pocket in PDK1 is essential for activation of S6K and SGK, but not PKB. The EMBO journal. 2001;20(16):4380-90.

235. Shibata H, Oishi K, Yamagiwa A, Matsumoto M, Mukai H, Ono Y. PKNbeta interacts with the SH3 domains of Graf and a novel Graf related protein, Graf2, which are GTPase activating proteins for Rho family. Journal of biochemistry. 2001;130(1):23-31.

236. Amano M, Mukai H, Ono Y, Chihara K, Matsui T, Hamajima Y, et al. Identification of a putative target for Rho as the serine-threonine kinase protein kinase N. Science. 1996;271(5249):648-50.

237. Kitagawa M, Mukai H, Shibata H, Ono Y. Purification and characterization of a fatty acid-activated protein kinase (PKN) from rat testis. The Biochemical journal. 1995;310 (Pt 2):657-64.

238. Yoshinaga C, Mukai H, Toshimori M, Miyamoto M, Ono Y. Mutational analysis of the regulatory mechanism of PKN: the regulatory region of PKN contains an arachidonic acid-sensitive autoinhibitory domain. Journal of biochemistry. 1999;126(3):475-84.

239. Frost J, Steen H, Shapiro P, Lewis T, Ahn N, Shaw P, et al. Cross-cascade activation of ERKs and ternary complex factors by Rho family proteins. The EMBO journal. 1997;16(21):6426-38.

240. Bagrodia S, Dérijard B, Davis R, Cerione R. Cdc42 and PAK-mediated signaling leads to Jun kinase and p38 mitogen-activated protein kinase activation. The Journal of biological chemistry. 1995;270(47):27995-8.

241. Vincent S, Settleman J. The PRK2 kinase is a potential effector target of both Rho and Rac GTPases and regulates actin cytoskeletal organization. Mol Cell Biol. 1997;17(4):2247-56.

242. Yu L, Settleman J. The Drosophila Pkn protein kinase is a Rho/Rac effector target required for dorsal closure during embryogenesis. Genes & development. 1999;13(9):1168-80.

243. Mukai H, Toshimori M, Shibata H, Takanaga H, Kitagawa M, Miyahara M, et al. Interaction of PKN with alpha-actinin. The Journal of biological chemistry. 1997;272(8):4740-6.

244. Taniguchi T, Kawamata T, Mukai H, Hasegawa H, Isagawa T, Yasuda M, et al. Phosphorylation of tau is regulated by PKN. The Journal of biological chemistry. 2001;276(13):10025-31.

245. Isagawa T, Mukai H, Oishi K, Taniguchi T, Hasegawa H, Kawamata T, et al. Dual effects of PKNalpha and protein kinase C on phosphorylation of tau protein by glycogen synthase kinase-3beta. Biochem Biophys Res Commun. 2000;273(1):209-12.

246. Kawamata T, Taniguchi T, Mukai H, Kitagawa M, Hashimoto T, Maeda K, et al. A protein kinase, PKN, accumulates in Alzheimer neurofibrillary tangles and associated endoplasmic reticulum-derived vesicles and phosphorylates tau protein. J Neurosci. 1998;18(18):7402-10.

247. Hall A. Rho GTPases and the actin cytoskeleton. Science. 1998;279(5350):509-14.

248. Calautti E, Grossi M, Mammucari C, Aoyama Y, Pirro M, Ono Y, et al. Fyn tyrosine kinase is a downstream mediator of Rho/PRK2 function in keratinocyte cell-cell adhesion. J Cell Biol. 2002;2002(156):1.

249. Gampel A, Parker P, Mellor H. Regulation of epidermal growth factor receptor traffic by the small GTPase rhoB. Curr Biol. 1999;9(17):955-8.

250. James D, Brown R, Navarro J, Pilch P. Insulin-regulatable tissues express a unique insulin-sensitive glucose transport protein. Nature. 1988;333(6169):183-5.

251. Standaert M, Bandyopadhyay G, Galloway L, Ono Y, Mukai H, Farese R. Comparative effects of GTPgammaS and insulin on the activation of Rho, phosphatidylinositol 3-kinase, and protein kinase N in rat adipocytes. Relationship to glucose transport. The Journal of biological chemistry. 1998;273(13):7470-7.

252. Emoto M, Klarlund J, Waters S, Hu V, Buxton J, Chawla A, et al. A role for phospholipase D in GLUT4 glucose transporter translocation. The Journal of biological chemistry. 2000;275(10):7144-51.

253. Oishi K, Takahashi M, Mukai H, Banno Y, Nakashima S, Kanaho Y, et al. PKN regulates phospholipase D1 through direct interaction. The Journal of biological chemistry. 2001;276(21):18096-101.

254. Takahashi M, Mukai H, Toshimori M, Miyamoto M, Ono Y. Proteolytic activation of PKN by caspase-3 or related protease during apoptosis. Proc Natl Acad Sci U S A. 1998;95(20):11566-71.

255. Billig H, Furuta I, Rivier C, Tapanainen J, Parvinen M, Hsueh A. Apoptosis in testis germ cells: developmental changes in gonadotropin dependence and localization to selective tubule stages. Endocrinology. 1995;136(1):5-12.

256. Parry S, Hasbold J, Holman M, Klaus G. Hypercross-linking surface IgM or IgD receptors on mature B cells induces apoptosis that is reversed by costimulation with IL-4 and anti-CD40. J Immunol. 1994;152(6):2821-9.

257. Murphy K, Heimberger A, Loh D. Induction by antigen of intrathymic apoptosis of CD4+CD8+TCRlo thymocytes in vivo. Science. 1990;250(4988):1720-3.

258. Kothakota S, Azuma T, Reinhard C, Klippel A, Tang J, Chu K, et al. Caspase-3-generated fragment of gelsolin: effector of morphological change in apoptosis. Science. 1997;278(5336):294-8.

259. Masui Y, Clarke H. Oocyte maturation. Int Rev Cytol. 1979;57:185-282.

260. Stapleton G, Nguyen C, Lease K, Hille M. Phosphorylation of protein kinase C-related kinase PRK2 during meiotic maturation of starfish oocytes. Dev Biol. 1998;193(1):36-46.

261. Misaki K, Mukai H, Yoshinaga C, Oishi K, Isagawa T, Takahashi M, et al. PKN delays mitotic timing by inhibition of Cdc25C: possible involvement of PKN in the regulation of cell division. Proc Natl Acad Sci U S A. 2001;98(1):125-9.

262. Yasui T S-YK, Nishimura T, Morita K, Tada S, Mosialos G, Kieff E, Kikutani H. Protein kinase N1, a cell inhibitor of Akt kinase, has a central role in quality control of germinal center formation. Proc Natl Acad Sci U S A. 2012;109(51):21022-7.

263. Quétier I, Marshall J, Spencer-Dene B, Lachmann S, Casamassima A, Franco C, et al. Knockout of the PKN Family of Rho Effector Kinases Reveals a Non-redundant Role for PKN2 in Developmental Mesoderm Expansion. Cell Rep. 2016;14(3):440-8.

264. Kitagawa M, Mukai H, Takahashi M, Ono Y. The role of PKN in the regulation of alphaB-crystallin expression via heat shock transcription factor 1. Biochem Biophys Res Commun. 1998;252(3):561-5.

265. Derham B, Harding J. Alpha-crystallin as a molecular chaperone. Prog Retin Eye Res. 1999;18(4):463-509.

266. Morissette M, Sah V, Glembotski C, Brown J. The Rho effector, PKN, regulates ANF gene transcription in cardiomyocytes through a serum response element. Am J Physiol Heart Circ Physiol. 2000;278(6):H1769-74.

267. Marinissen M, Chiariello M, Gutkind J. Regulation of gene expression by the small GTPase Rho through the ERK6 (p38 gamma) MAP kinase pathway. Genes & development. 2001;15(5):535-53.

268. Turner E, Kavanagh D, Mulvaney E, McLean C, Wikström K, Reid H, et al. Identification of an interaction between the TPalpha and TPbeta isoforms of the human thromboxane A2 receptor with protein kinase C-related kinase (PRK) 1: implications for prostate cancer. The Journal of biological chemistry. 2011;286(17):15440-57.

269. Metzger E, Müller J, Ferrari S, Buettner R, Schüle R. A novel inducible transactivation domain in the androgen receptor: implications for PRK in prostate cancer. The EMBO journal. 2003;22(2):270-80.

270. Attarha S, Rao Saini R, Andersson S, Mints M, Souchelnytskyi S. PKN1 modulates TGFβ and EGF signaling in HEC-1-A endometrial cancer cell line. Onco Targets Ther. 2014(7):1397-408.

271. Galgano M, Conaway M, Spencer A, Paschal B, Frierson HJ. PRK1 distribution in normal tissues and carcinomas: overexpression and activation in ovarian serous carcinoma. Hum Pathol. 2009;40(10):1434-40.

272. Carter J, Douglass L, Deddens J, Colligan B, Bhatt T, Pemberton J, et al. Pak-1 expression increases with progression of colorectal carcinomas to metastasis. Clin Cancer Res. 2004;10(10):3448-56.

273. Adam L, Vadlamudi R, Mandal M, Chernoff J, Kumar R. Regulation of microfilament reorganization and invasiveness of breast cancer cells by kinase dead p21-activated kinase-1. The Journal of biological chemistry. 2000;275(16):12041-50.

274. Brough R, Frankum J, Sims D, Mackay A, Mendes-Pereira A, Bajrami I, et al. Functional viability profiles of breast cancer. Cancer Discov. 2011;1(3):260-73.

275. Lachmann S, Jevons A, De Rycker M, Casamassima A, Radtke S, Collazos A, et al. Regulatory domain selectivity in the cell-type specific PKN-dependence of cell migration. PloS one. 2011;6(7):e21732.

276. Strumberg D, Schultheis B, Traugott U, Vank C, Santel A, Keil O, et al. Phase I clinical development of Atu027, a siRNA formulation targeting PKN3 in patients with advanced solid tumors. Int J Clin Pharmacol Ther. 2012;50(1):76-8.

277. Yang C, Melhuish T, Spencer A, Ni L, Hao Y, Jividen K, et al. The protein kinase C super-family member PKN is regulated by mTOR and influences differentiation during prostate cancer progression. Prostate. 2017;77(15):1452-67.

278. zur Hausen H. Papillomaviruses in human cancer. Cancer. 1987;59(10):1692-6.

279. Hawley-Nelson P, Vousden K, Hubbert N, Lowy D, Schiller J. HPV16 E6 and E7 proteins cooperate to immortalize human foreskin keratinocytes. The EMBO journal. 1989;8(12):3905-10.

280. Münger K, Phelps W, Bubb V, Howley P, Schlegel R. The E6 and E7 genes of the human papillomavirus type 16 together are necessary and sufficient for transformation of primary human keratinocytes. J Virol. 1989;63(10):4417-21.

281. Gao Q, Kumar A, Srinivasan S, Singh L, Mukai H, Ono Y, et al. PKN binds and phosphorylates human papillomavirus E6 oncoprotein. The Journal of biological chemistry. 2000;275(20):14824-30.

282. Ohashi M, Kanai F, Ueno H, Tanaka T, Tateishi K, Kawakami T, et al. Adenovirus mediated p53 tumour suppressor gene therapy for human gastric cancer cells in vitro and in vivo. Gut. 1999;44(3):366-71.

283. Tsunemitsu Y, Kagawa S, Tokunaga N, Otani S, Umeoka T, Roth J, et al. Molecular therapy for peritoneal dissemination of xenotransplanted human MKN-45 gastric cancer cells with adenovirus mediated Bax gene transfer. Gut. 2004;53(4):554-60.

284. Min Y, Adachi Y, Yamamoto H, Imsumran A, Arimura Y, Endo T, et al. Insulin-like growth factor I receptor blockade enhances chemotherapy and radiation responses and inhibits tumour growth in human gastric cancer xenografts. Gut. 2005;54(5):591-600.

285. Zhou J, Liu M, Aneja R, Chandra R, Lage H, Joshi H. Reversal of P-glycoprotein-mediated multidrug resistance in cancer cells by the c-Jun NH2-terminal kinase. Cancer Res. 2006;66(1):445-52.

286. Sako A, Kitayama J, Koyama H, Ueno H, Uchida H, Hamada H, et al. Transduction of soluble Flt-1 gene to peritoneal mesothelial cells can effectively suppress peritoneal metastasis of gastric cancer. Cancer Res. 2004;64(10):3624-8.

287. Park J, Jung Y, Kim T, Kim S, Jong H, Lee J, et al. Class I histone deacetylase-selective novel synthetic inhibitors potently inhibit human tumor proliferation. Clin Cancer Res. 2004;10(15):5271-81.

288. Nishigaki M, Aoyagi K, Danjoh I, Fukaya M, Yanagihara K, Sakamoto H, et al. Discovery of aberrant expression of R-RAS by cancer-linked DNA hypomethylation in gastric cancer using microarrays. Cancer Res. 2005;65(6):2115-24.

289. Tanner M, Hollmén M, Junttila T, Kapanen A, Tommola S, Soini Y, et al. Amplification of HER-2 in gastric carcinoma: association with Topoisomerase IIalpha gene amplification, intestinal type, poor prognosis and sensitivity to trastuzumab. Ann Oncol. 2005;16(2):273-8.

290. Bang Y, Chung H, Xu J, Lordick F, Sawaki A, Al-Sakaff N, et al. Pathological features of advanced gastric cancer (GC): Relationship to human epidermal growth factor receptor 2 (HER2) positivity in the global screening programme of the ToGA trial J Clin Oncol. 2009(27):4556.

291. Sahai E, Marshall C. RHO-GTPases and cancer. Nat Rev Cancer. 2002;2(2):133-42.

292. Sahai E, Alberts A, Treisman R. RhoA effector mutants reveal distinct effector pathways for cytoskeletal reorganization, SRF activation and transformation. The EMBO journal. 1998;17(5):1350-61.

293. Ran F, Hsu P, Wright J, Agarwala V, Scott D, Zhang F. Genome engineering using the CRISPR-Cas9 system. Nat Protoc. 2013;8(11):2281-308.

294. Meerbrey K, Hu G, Kessler J, Roarty K, Li M, Fang J, et al. The pINDUCER lentiviral toolkit for inducible RNA interference in vitro and in vivo. Proc Natl Acad Sci U S A. 2011;108(9):3665-70.

295. Yang W, Xia Y, Hawke D, Li X, Liang J, Xing D, et al. PKM2 Phosphorylates Histone H3 and Promotes Gene Transcription and Tumorigenesis. Cell. 2012;150(4):685-96.

296. Kim J, Banerjee T, Vinckevicius A, Luo Q, Parker J, Baker M, et al. A Role for WDR5 in Integrating Threonine 11 Phosphorylation to Lysine 4 Methylation on Histone H3 during Androgen Signaling and in Prostate Cancer. Molecular Cell. 2014;54(4):613-25.

297. Paddison P, Cleary M, Silva J, Chang K, Sheth N, Sachidanandam R, et al. Cloning of short hairpin RNAs for gene knockdown in mammalian cells. Nat Methods. 2004;1(2):163-7.

298. Duane EG. A Practical Guide to Implementing a BSL-2+ Biosafety Program in a Research Laboratory. Appl Bio. 2013;18(1):30-6.

299. Truett G, Heeger P, Mynatt R, Truett A, Walker J, Warman M. Preparation of PCR-quality mouse genomic DNA with hot sodium hydroxide and tris (HotSHOT). Biotechniques. 2000;29(1):52-4.

300. Bazzocco S, Dopeso H, Carton-Garcia F, Macaya I, Andretta E, Chionh F, et al. Highly Expressed Genes in Rapidly Proliferating Tumor Cells as New Targets for Colorectal Cancer Treatment. Clin Cancer Res. 2015;21(16):3695-704.

301. Luker K, Piwnica-Worms D. Optimizing Luciferase Protein Fragment Complementation for Bioluminescent Imaging of Protein–Protein Interactions in Live Cells and Animals. In: Inc. E, editor. Methods in enzymology. 3852004.

302. García-Mata R WK, Arthur WT, Noren NK, Ellerbroek SM, Burridge K. Analysis of activated GAPs and GEFs in cell lysates. Methods in enzymology. 2006(406):425-37.

303. Llombart V, Trejo S, Bronsoms S, Morancho A, Feifei M, Faura J, et al. Profiling and identification of new proteins involved in brain ischemia using MALDI-imaging-mass-spectrometry. J Proteomics. 2017;152:243-53.

304. Skehan P, Storeng R, Scudiero D, Monks A, McMahon J, Vistica D, et al. New colorimetric cytotoxicity assay for anticancer-drug screening. J Natl Cancer Inst. 1990;82(13):1107-12.

305. Mariadason JM AD, Shi Q, Wilson AJ, Corner GA, Nicholas C, Aranes MJ, Lesser M, Schwartz EL, Augenlicht LH. Gene expression profiling-based prediction of response of colon carcinoma cells to 5-fluorouracil and camptothecin. Cancer Res. 2003;63(24):8791-812.

306. Dopeso H, Mateo-Lozano S, Elez E, Landolfi S, Ramos Pascual F, Hernández-Losa J, et al. Aprataxin tumor levels predict response of colorectal cancer patients to irinotecan-based treatment. Clin Cancer Res. 2010;16(8):2375-82.

307. Monks A, Scudiero D, Skehan P, Shoemaker R, Paull K, Vistica D, et al. Feasibility of a high-flux anticancer drug screen using a diverse panel of cultured human tumor cell lines. J Natl Cancer Inst. 1991;83(11):757-66.

308. Vichai V, Kirtikara K. Sulforhodamine B colorimetric assay for cytotoxicity screening. Nat Protoc. 2006;1(3):1112-6.

309. Kobayashi K, Takahashi M, Matsushita N, Miyazaki J, Koike M, Yaginuma H, et al. Survival of developing motor neurons mediated by Rho GTPase signaling pathway through Rho-kinase. J Neurosci. 2004;24(14):3480-8.

310. Tomita H, Yamada Y, Oyama T, Hata K, Hirose Y, Hara A, et al. Development of gastric tumors in Apc(Min/+) mice by the activation of the beta-catenin/Tcf signaling pathway. Cancer Res. 2007;67(9):4079-87.

311. Sipponen P, Graham D. Importance of atrophic gastritis in diagnostics and prevention of gastric cancer: application of plasma biomarkers. Scand J Gastroenterol. 2007;42(1):2-10.

312. Sipponen P. Biomarkers in clinical practice: a tool to find subjects at high risk for stomach cancer. A personal view. Adv Med Sci. 2006;51:51-3.

313. Guariso G, Basso D, Bortoluzzi C, Meneghel A, Schiavon S, Fogar P, et al. GastroPanel: evaluation of the usefulness in the diagnosis of gastro-duodenal mucosal alterations in children. Clin Chim Acta. 2009;402(1-2):54-60.

314. Watanabe G, Saito Y, Madaule P, Ishizaki T, Fujisawa K, Morii N, et al. Protein kinase N (PKN) and PKN-related protein rhophilin as targets of small GTPase Rho. Science. 1996;271(5249):645-8.

315. Leung T, Manser E, Tan L, Lim L. A novel serine/threonine kinase binding the Ras-related RhoA GTPase which translocates the kinase to peripheral membranes. The Journal of biological chemistry. 1995;270(49):29051-4.

316. Leung T, Chen X, Manser E, Lim L. The p160 RhoA-binding kinase ROK alpha is a member of a kinase family and is involved in the reorganization of the cytoskeleton. Mol Cell Biol. 1996;16(10):5313-27.

317. Nakagawa O, Fujisawa K, Ishizaki T, Saito Y, Nakao K, Narumiya S. ROCK-I and ROCK-II, two isoforms of Rho-associated coiled-coil forming protein serine/threonine kinase in mice. FEBS Lett. 1996;392(2):189-93.

318. Ishizaki T, Naito M, Fujisawa K, Maekawa M, Watanabe N, Saito Y, et al. p160ROCK, a Rho-associated coiled-coil forming protein kinase, works downstream of Rho and induces focal adhesions. FEBS Lett. 1997;404(2-3):118-24.

319. Alberts A, Bouquin N, Johnston L, Treisman R. Analysis of RhoA-binding proteins reveals an interaction domain conserved in heterotrimeric G protein beta subunits and the yeast response regulator protein Skn7. The Journal of biological chemistry. 1998;273(15):8616-22.

320. Hotta K, Tanaka K, Mino A, Kohno H, Takai Y. Interaction of the Rho family small G proteins with kinectin, an anchoring protein of kinesin motor. Biochem Biophys Res Commun. 1996;225(1):69-74.

321. Mayer B, Johnson J, Leitl F, Jauch K, Heiss M, Schildberg F, et al. E-cadherin expression in primary and metastatic gastric cancer: down-regulation correlates with cellular dedifferentiation and glandular disintegration. Cancer Res. 1993;53(7):1690-5.

322. Grötzinger C, Kneifel J, Patschan D, Schnoy N, Anagnostopoulos I, Faiss S, et al. LI-cadherin: a marker of gastric metaplasia and neoplasia. Gut. 2001;49(1):73-81.

323. Wakatsuki K, Yamada Y, Narikiyo M, Ueno M, Takayama T, Tamaki H, et al. Clinicopathological and prognostic significance of mucin phenotype in gastric cancer. J Surg Oncol. 2008;98(2):124-9.

324. Otsuki S, Inokuchi M, Enjoji M, Ishikawa T, Takagi Y, Kato K, et al. Vimentin expression is associated with decreased survival in gastric cancer. Oncol Rep. 2011;25(5):1235-42.

325. Matsuo K, Kobayashi I, Tsukuba T, Kiyoshima T, Ishibashi Y, Miyoshi A, et al. Immunohistochemical localization of cathepsins D and E in human gastric cancer: a possible correlation with local invasive and metastatic activities of carcinoma cells. Hum Pathol. 1996;27(2):184-90.

326. Saku T, Sakai H, Tsuda N, Okabe H, Kato Y, Yamamoto K. Cathepsins D and E in normal, metaplastic, dysplastic, and carcinomatous gastric tissue: an immunohistochemical study. Gut. 1990;31(11):1250-5.

327. Watanabe M, Higashi T, Watanabe A, Osawa T, Sato Y, Kimura Y, et al. Cathepsin B and L activities in gastric cancer tissue: correlation with histological findings. Biochem Med Metab Biol. 1989;42(1):21-9.

328. Torbett N, Casamassima A, Parker P. Hyperosmotic-induced Protein Kinase N 1 Activation in a Vesicular Compartment Is Dependent upon Rac1 and 3-Phosphoinositide-dependent Kinase 1. The Journal of biological chemistry. 2003;278(34):32344-51.

329. Cifone M, Fidler I. Correlation of patterns of anchorage-independent growth with in vivo behavior of cells from a murine fibrosarcoma. Proc Natl Acad Sci U S A. 1980;77(2):1039-43.

330. Mori S, Chang J, Andrechek E, Matsumura N, Baba T, Yao G, et al. An Anchorage-Independent Cell Growth Signature Identifies Tumors with Metastatic Potential. Oncogene. 2009;28(31):2796-805.

331. Nürnberg A, Kitzing T, Grosse R. Nucleating actin for invasion. Nat Rev Cancer. 2011;11(3):177-87.

332. Wang W, Goswami S, Lapidus K, Wells A, Wyckoff J, Sahai E, et al. Identification and testing of a gene expression signature of invasive carcinoma cells within primary mammary tumors. Cancer Res. 2004;64(23):8585-94.

333. Wang W, Goswami S, Sahai E, Wyckoff J, Segall J, Condeelis J. Tumor cells caught in the act of invading: their strategy for enhanced cell motility. Trends Cell Biol. 2005;15(3):138-45.

334. Yamaguchi H, Wyckoff J, Condeelis J. Cell migration in tumors. Curr Opin Cell Biol. 2005;17(5):559-64.

335. BOYDEN S. The chemotactic effect of mixtures of antibody and antigen on polymorphonuclear leucocytes. J Exp Med. 1962;115:453-66.

336. Chambers A, Groom A, MacDonald I. Dissemination and growth of cancer cells in metastatic sites. Nat Rev Cancer. 2002;2(8):563-72.

337. Friedl P, Wolf K. Tumour-cell invasion and migration: diversity and escape mechanisms. Nat Rev Cancer. 2003;3(5):362-74.

338. Wolf K, Mazo I, Leung H, Engelke K, von Andrian U, Deryugina E, et al. Compensation mechanism in tumor cell migration: mesenchymal-amoeboid transition after blocking of pericellular proteolysis. J Cell Biol. 2003;160(2):267-77.

339. Sahai E, Marshall C. Differing modes of tumour cell invasion have distinct requirements for Rho/ROCK signalling and extracellular proteolysis. Nat Cell Biol. 2003;5(8):711-9.

340. Correa P. Gastric cancer: overview. Gastroenterol Clin North Am. 2013;42(2):211-7.

341. Lauren P. The two histological main types of gastric carcinoma: Diffuse and so-called intestinal-type carcinoma. An attempt at a histo-clinical classification. Acta Pathol Microbiol Scand. 1965(64):31-49.

342. Yuasa Y. Control of gut differentiation and intestinal-type gastric carcinogenesis. Nat Rev Cancer. 2003;3(8):592-600.

343. The Cancer Genome Atlas Research Network. Comprehensive molecular characterization of gastric adenocarcinoma. Nature2014 [Available from: http://dx.doi.org/10.1038/nature13480.

344. Rodrigues P, Macaya I, Bazzocco S, Mazzolini R, Andretta E, Dopeso H, et al. RHOA inactivation enhances Wnt signalling and promotes colorectal cancer. Nat Commun. 2014(5):5458.

345. Arango D, Laiho P, Kokko A, Alhopuro P, Sammalkorpi H, Salovaara R, et al. Gene-expression profiling predicts recurrence in Dukes' C colorectal cancer. Gastroenterology. 2005;129(3):874-84.

346. Nakatsuru S, Yanagisawa A, Ichii S, Tahara E, Kato Y, Nakamura Y, et al. Somatic mutation of the APC gene in gastric cancer: frequent mutations in very well differentiated adenocarcinoma and signet-ring cell carcinoma. Hum Mol Genet. 1992;1(8):559-63.

347. Singh A, Moniaux N, Chauhan S, Meza J, Batra S. Inhibition of MUC4 expression suppresses pancreatic tumor cell growth and metastasis. Cancer Res. 2004;64(2):622-30.

348. Singh A, Chauhan S, Bafna S, Johansson S, Smith L, Moniaux N, et al. Aberrant expression of transmembrane mucins, MUC1 and MUC4, in human prostate carcinomas. Prostate. 2006;66(4):421-9.

349. Moinova H, Leidner R, Ravi L, Lutterbaugh J, Barnholtz-Sloan J, Chen Y, et al. Aberrant Vimentin Methylation Is Characteristic of Upper Gastrointestinal Pathologies. Cancer Epidemiol Biomarkers Prev. 2012;21(4):594-600.

350. Nomura T, Katunuma N. Involvement of cathepsins in the invasion, metastasis and proliferation of cancer cells. J Med Invest. 2005;52(1-2):1-9.

351. Singh A, Chaturvedi P, Batra S. Emerging roles of MUC4 in cancer: a novel target for diagnosis and therapy. Cancer Res. 2007;67(2):433-6.

352. Leader M, Collins M, Patel J, Henry K. Vimentin: an evaluation of its role as a tumour marker. Histopathology. 1987;11(1):63-72.

353. Vadlamudi R, Adam L, Wang R, Mandal M, Nguyen D, Sahin A, et al. Regulatable expression of p21-activated kinase-1 promotes anchorage-independent growth and abnormal organization of mitotic spindles in human epithelial breast cancer cells. The Journal of biological chemistry. 2000;275(46):36238-44.

354. O'Sullivan G, Tangney M, Casey G, Ambrose M, Houston A, Barry O. Modulation of p21-activated kinase 1 alters the behavior of renal cell carcinoma. Int J Cancer. 2007;121(9):1930-40.

355. James R, Bosch K, Kulikauskas R, Yang P, Robin N, Toroni R, et al. Protein kinase PKN1 represses Wnt/β-catenin signaling in human melanoma cells. The Journal of biological chemistry. 2013;288(48):34658-70.

356. Jilg C, Ketscher A, Metzger E, Hummel B, Willmann D, Rüsseler V, et al. PRK1/PKN1 controls migration and metastasis of androgen-independent prostate cancer cells. Oncotarget. 2014;5(24):12646-64.

357. Koh H, Lee K, Kim D, Kim S, Kim J, Chung J. Inhibition of Akt and its anti-apoptotic activities by tumor necrosis factor-induced protein kinase C-related kinase 2 (PRK2) cleavage. The Journal of biological chemistry. 2000;275(44):34451-8.

358. Kumar R, Gururaj A, Barnes C. p21-activated kinases in cancer. Nat Rev Cancer. 2006;6(6):459-71.

359. Slack-Davis J, Eblen S, Zecevic M, Boerner S, Tarcsafalvi A, Diaz H, et al. PAK1 phosphorylation of MEK1 regulates fibronectin-stimulated MAPK activation. JBC. 2003;162(2):281.

360. Eblen S, Slack J, Weber M, Catling A. Rac-PAK signaling stimulates extracellular signal-regulated kinase (ERK) activation by regulating formation of MEK1-ERK complexes. Mol Cell Biol. 2002;22(17):6023-33.

361. King A, Sun H, Diaz B, Barnard D, Miao W, Bagrodia S, et al. The protein kinase Pak3 positively regulates Raf-1 activity through phosphorylation of serine 338. Nature. 1998;396:180-3.

362. Tang Y, Chen Z, Ambrose D, Liu J, Gibbs J, Chernoff J, et al. Kinase-deficient Pak1 mutants inhibit Ras transformation of Rat-1 fibroblasts. Mol Cell Biol. 1997;17(8):4454-64.

363. Kageshita T, Hamby C, Ishihara T, Matsumoto K, Saida T, Ono T. Loss of beta-catenin expression associated with disease progression in malignant melanoma. Br J Dermatol. 2001;145(2):210-6.

364. Bachmann I, Straume O, Puntervoll H, Kalvenes M, Akslen L. Importance of P-cadherin, beta-catenin, and Wnt5a/frizzled for progression of melanocytic tumors and prognosis in cutaneous melanoma. Clin Cancer Res. 2005;11(24 Pt 1):8606-14.

365. Gould Rothberg B, Berger A, Molinaro A, Subtil A, Krauthammer M, Camp R, et al. Melanoma prognostic model using tissue microarrays and genetic algorithms. J Clin Oncol. 2009;27(34):5772-80.

366. Maelandsmo G, Holm R, Nesland J, Fodstad Ø, Florenes V. Reduced beta-catenin expression in the cytoplasm of advanced-stage superficial spreading malignant melanoma. Clin Cancer Res. 2003;9(9):3383-8.

367. Balasenthil S, Sahin A, Barnes C, Wang R, Pestell R, Vadlamudi R, et al. p21-activated kinase-1 signaling mediates cyclin D1 expression in mammary epithelial and cancer cells. The Journal of biological chemistry. 2004;279(2):1422-8.

368. Liu F, Li X, Wang C, Cai X, Du Z, Xu H, et al. Downregulation of p21-activated kinase-1 inhibits the growth of gastric cancer cells involving cyclin B1. Int J Cancer. 2009;125(11):2511-9.

369. Cude K, Wang Y, Choi H, Hsuan S, Zhang H, Wang C, et al. Regulation of the G2–M cell cycle progression by the ERK5–NFκB signaling pathway. J Cell Biol. 2007;177(2):253-64.

370. Frost J, Swantek J, Stippec S, Yin M, Gaynor R, Cobb M. Stimulation of NFkappa B activity by multiple signaling pathways requires PAK1. The Journal of biological chemistry. 2000;275(26):19693-9.

371. Zhang H, Tan S, Wang J, Chen S, Quan J, Xian J, et al. Musashi2 modulates K562 leukemic cell proliferation and apoptosis involving the MAPK pathway. Exp Cell Res. 2014;320(1):119-27.

372. Cuenda A, Rousseau S. p38 MAP-kinases pathway regulation, function and role in human diseases. Biochim Biophys Acta. 2007;1773(8):1358-75.

373. Brancho D, Tanaka N, Jaeschke A, Ventura J, Kelkar N, Tanaka Y, et al. Mechanism of p38 MAP kinase activation in vivo. Genes & development. 2003;17(16):1969-78.

374. Ambrosino C, Nebreda A. Cell cycle regulation by p38 MAP kinases. Biology of the cell / under the auspices of the European Cell Biology Organization. 2001;93(1-2):47-51.

375. Xia Z, Dickens M, Raingeaud J, Davis R, Greenberg M. Opposing effects of ERK and JNK-p38 MAP kinases on apoptosis. Science. 1995;270(5240):1326-31.

376. Tournier C, Hess P, Yang D, Xu J, Turner T, Nimnual A, et al. Requirement of JNK for stress-induced activation of the cytochrome c-mediated death pathway. Science. 2000;288(5467):870-4.

377. Davis R. Signal transduction by the JNK group of MAP kinases. Cell. 2000;103(2):239-52.

378. Ridley A, Schwartz M, Burridge K, Firtel R, Ginsberg M, Borisy G, et al. Cell migration: integrating signals from front to back. Science. 2003;302(5651):1704-9.

379. Raftopoulou M, Hall A. Cell migration: Rho GTPases lead the way. Dev Biol. 2004;265(1):23-32.

380. Palmer R, Parker P. Expression, purification and characterization of the ubiquitous protein kinase C-related kinase 1. The Biochemical journal. 1995;309(Pt 1):315-20.

381. Turner E, Kavanagh D, Mulvaney E, McLean C, Wikstrom K, Reid H, et al. Identification of an interaction between the TPalpha and TPbeta isoforms of the human thromboxane A2 receptor with protein kinase C-related kinase (PRK) 1: implications for prostate cancer. The Journal of biological chemistry. 2011;286(17):15440-57.

382. Leenders F, Möpert K, Schmiedeknecht A, Santel A, Czauderna F, Aleku M, et al. PKN3 is required for malignant prostate cell growth downstream of activated PI 3-kinase. The EMBO journal. 2004;23(16):3303-13.

383. Cabodi S, del Pilar Camacho-Leal M, Di Stefano P, Defilippi P. Integrin signalling adaptors: not only figurants in the cancer story. Nat Rev Cancer. 2010;10(12):858-70.

384. Han B, Xiao H, Xu J, Lodyga M, Bai X, Jin T, et al. Actin filament associated protein mediates c-Src related SRE/AP-1 transcriptional activation. FEBS Lett. 2011;585(3):471-7.

385. Romer L, Birukov K, Garcia J. Focal Adhesions Paradigm for a Signaling Nexus. Circ Res. 2006(98):606-16.

386. Naumanen P, Lappalainen P, Hotulainen P. Mechanisms of actin stress fibre assembly. J Microsc. 2008;231(3):446-54.

387. Kandoth C, McLellan M, Vandin F, Ye K, Niu B, Lu C, et al. Mutational landscape and significance across 12 major cancer types. Nature. 2013;502(7471):333-9.

388. Soussi T, Wiman K. TP53: an oncogene in disguise. Cell Death Differ. 2015;22(8):1239-49.

389. Bykov V, Eriksson S, Bianchi J, Wiman K. Targeting mutant p53 for efficient cancer therapy. Nat Rev Cancer. 2018;18(2):89-102.

390. Lang G, Iwakuma T, Suh Y, Liu G, Rao V, Parant J, et al. Gain of function of a p53 hot spot mutation in a mouse model of Li-Fraumeni syndrome. Cell. 2004;119(6):861-72.

391. Olive K, Tuveson D, Ruhe Z, Yin B, Willis N, Bronson R, et al. Mutant p53 gain of function in two mouse models of Li-Fraumeni syndrome. Cell. 2004;119(6):847-60.

392. Morton J, Timpson P, Karim S, Ridgway R, Athineos D, Doyle B, et al. Mutant p53 drives metastasis and overcomes growth arrest/senescence in pancreatic cancer. Proc Natl Acad Sci U S A. 2010;107(1):246-51.

393. Bullock A, Henckel J, Fersht A. Quantitative analysis of residual folding and DNA binding in mutant p53 core domain: definition of mutant states for rescue in cancer therapy. Oncogene. 2000;19(10):1245-56.

394. Mukai H OY. Purification and kinase assay of PKN. Methods in enzymology. 2006(406):234-50.

395. Oishi K, Mukai H, Shibata H, Takahashi M, Ona Y. Identification and characterization of PKNbeta, a novel isoform of protein kinase PKN: expression and arachidonic acid dependency are different from those of PKNalpha. Biochem Biophys Res Commun. 1999;261(3):808-14.

396. Yu W, Liu J, Morrice N, Wettenhall R. Isolation and characterization of a structural homologue of human PRK2 from rat liver. Distinguishing substrate and lipid activator specificities. The Journal of biological chemistry. 1997;272(15):10030-4.

397. Palmer R, Dekker L, Woscholski R, Le Good J, Gigg R, Parker P. Activation of PRK1 by phosphatidylinositol 4,5-bisphosphate and phosphatidylinositol 3,4,5-trisphosphate. A comparison with protein kinase C isotypes. The Journal of biological chemistry. 1995;270(38):22412-6.

398. Tokuda H, Kontani M, Kawashima H, Akimoto K, Kusumoto A, Kiso Y, et al. Arachidonic acid-enriched triacylglycerol improves cognitive function in elderly with low serum levels of arachidonic acid. J Oleo Sci. 2014;63(3):219-27.

399. Tateishi N, Kakutani S, Kawashima H, Shibata H, Morita I. Dietary supplementation of arachidonic acid increases arachidonic acid and lipoxin A_4 contents in colon, but does not affect severity or prostaglandin E_2 content in murine colitis model. Lipids Health Dis. 2014;13(30).

400. Linseisen J, Schulze M, Saadatian-Elahi M, Kroke A, Miller A, Boeing H. Quantity and quality of dietary fat, carbohydrate, and fiber intake in the German EPIC cohorts. Ann Nutr Metab. 2003;47(1):37-46.

401. Sioen I, Pynaert I, Matthys C, De Backer G, Van Camp J, De Henauw S. Dietary intakes and food sources of fatty acids for Belgian women, focused on n-6 and n-3 polyunsaturated fatty acids. Lipids 2006;41(5):415-22.

402. Kawabata T, Hirota S, Hirayama T, Adachi N, Hagiwara C, Iwama N, et al. Age-related changes of dietary intake and blood eicosapentaenoic acid, docosahexaenoic acid, and arachidonic acid levels in Japanese men and women. Prostaglandins Leukot Essent Fatty Acids. 2011;84(5-6):131-7.

403. Kakutani S, Ishikura Y, Tateishi N, Horikawa C, Tokuda H, Kontani M, et al. Supplementation of arachidonic acid-enriched oil increases arachidonic acid contents in plasma phospholipids, but does not increase their metabolites and clinical parameters in Japanese healthy elderly individuals: a randomized controlled study. Lipids Health Dis. 2011(10):241.

404. Fleith M, Clandinin M. Dietary PUFA for preterm and term infants: review of clinical studies. Crit Rev Food Sci Nutr. 2005;45(3):205-29.

405. Maniongui C, Blond J, Ulmann L, Durand G, Poisson J, Bézard J. Age-related changes in delta 6 and delta 5 desaturase activities in rat liver microsomes. Lipids. 1993;28(4):291-7.

406. Ishikura Y, Ikeda G, Akimoto K, Hata M, Kusumoto A, Kidokoro A, et al. Arachidonic acid supplementation decreases P300 latency and increases P300 amplitude of event-related potentials in healthy elderly men. Neuropsychobiology. 2009;60(2):73-9.

407. Kotani S, Sakaguchi E, Warashina S, Matsukawa N, Ishikura Y, Kiso Y, et al. Dietary supplementation of arachidonic and docosahexaenoic acids improves cognitive dysfunction. Neurosci Res. 2006;56(2):159-64.

408. Oe H, Hozumi T, Murata E, Matsuura H, Negishi K, Matsumura Y, et al. Arachidonic acid and docosahexaenoic acid supplementation increases coronary flow velocity reserve in Japanese elderly individuals. Heart. 2008;94(3):316-21.

409. Naito Y, Ji X, Tachibana S, Aoki S, Furuya M, Tazura Y, et al. Effects of arachidonic acid intake on inflammatory reactions in dextran sodium sulphate-induced colitis in rats. Br J Nutr. 2015;114(5):734-45.

410. Canseva M, Wurtmana R. Chronic administration of docosahexaenoic acid or eicosapentaenoic acid, but not arachidonic acid, alone or in combination with uridine, increases brain phosphatide and synaptic protein levels in gerbils. Neuroscience. 2007;148(2):421-31.

411. Kotani S, Nakazawa H, Tokimasa T, Akimoto K, Kawashima H, Toyoda-Ono Y, et al. Synaptic plasticity preserved with arachidonic acid diet in aged rats. Neurosci Res. 2003;46(4):453-61.

412. Okaichi Y, Ishikura Y, Akimoto K, Kawashima H, Toyoda-Ono Y, Kiso Y, et al. Arachidonic acid improves aged rats' spatial cognition. Physiol Behav. 2005;84(4):617-23.

413. Fukaya T, Gondaira T, Kashiyae Y, Kotani S, Ishikura Y, Fujikawa S, et al. Arachidonic acid preserves hippocampal neuron membrane fluidity in senescent rats. Neurobiol Aging. 2007;28(8):1179-86.

414. Nakano D, Ishii F, Fujii K, Ishikura Y, Akimoto K, Kontani M, et al. Effects of dietary arachidonic acid supplementation on age-related changes in endothelium-dependent vascular responses. J Nutr Sci Vitaminol (Tokyo). 2007;53(1):75-81.

415. Ramakers J, Mensink R, Verstege M, te Velde A, Plat J. An arachidonic acid-enriched diet does not result in more colonic inflammation as compared with fish oil- or oleic acid-enriched diets in mice with experimental colitis. Br J Nutr. 2008;100(2):347-54.

416. Nelson G, Schmidt P, Bartolini G, Kelley D, Kyle D. The effect of dietary arachidonic acid on platelet function, platelet fatty acid composition, and blood coagulation in humans. Lipids. 1997;32(4):421-5.

417. Ferretti A, Nelson G, Schmidt P, Kelley D, Bartolini G, Flanagan V. Increased dietary arachidonic acid enhances the synthesis of vasoactive eicosanoids in humans. Lipids. 1997;32(4):435-9.

418. Kusumoto A, Ishikura Y, Kawashima H, Kiso Y, Takai S, Miyazaki M. Effects of arachidonate-enriched triacylglycerol supplementation on serum fatty acids and platelet aggregation in healthy male subjects with a fish diet. Br J Nutr. 2007;98(3):626-35.

AGRADECIMIENTOS

Llegar a este momento, es como estar ya en el final de una carrera de resistencia con toda clase de obstáculos pero ciertamente muy emocionante. Para mi, plasmar en papel y transmitir con palabras este sentimiento no es fácil, pero lo único que resta es agradecer a quienes de manera directa e indirecta han colaborado en este proyecto.

A mi asesor de Tesis, el Dr. Diego Arango, por permitirme trabajar y formar parte de este equipo, y a mi co-asesor Dr. Jose Dopeso por su invaluable apoyo y guía en este trabajo. Las charlas y el desarrollo de ideas originales dirigidas hacia este proyecto, sin duda fueron esenciales para la obtención de este trabajo.

A mis compañeros de laboratorio, gracias por brindarme su amistad y apoyo, por todas las charlas de despacho, los comentarios en seminarios y reuniones de trabajo que de manera constructiva han contribuido en mi crecimiento profesional y personal.

Al equipo administrativo y operativo de CIBBIM, VHIR, UB, VHIO gracias por brindarme siempre un buen servicio y con la mejor disposición.

Especialmente quiero agradecer desde el corazón a todas las personas que me han acompañado en esta aventura desde México, a quienes van conmigo siempre en el pensamiento, papá creo que estarás orgulloso de verme ahí donde estés, como cuando me decías que una acción vale más que mil palabras, esta es mi acción para ti. Mamá, mi mejor amiga, no hay nada que no te haya dicho ya y ni la mejor poesía describe mi amor por ti, quédate conmigo siempre. Ale, mi ejemplo de todo, te quiero tanto, siempre tan lejos pero a la vez tan cerca, gracias por hacer crecer esta familia y mi amor por ellos. A toda mi familia mexicana, que ya con solo esas dos palabras se describe a si misma, por transmitirme todo su apoyo, motivación, alegría y aquella fuerza que traspasa fronteras, literalmente derribaremos muros, gracias por hacerme sentir orgullosa de mi tierra y sepan que…¡tenemos una gran fiesta pendiente! Finalmente pero nunca menos importante, a los amigos que hice aquí y que al igual que yo se encontraban viviendo su propia aventura, gracias a la vida por hacernos coincidir y a ustedes por el honor de su amistad Marijose (Ecuador es el paraíso?), Ana (pero, ¡soy de Aragón baby!) y Alfonso (nos queda Calamocha) y a TODAS las personas que conocí a través de ellos, gracias por todos los momentos compartidos, viajes, quedadas, risas y llantos, etc., gracias infinitas por acudir a rescatarme siempre que lo necesité, por su incondicional apoyo y generosidad, nunca imaginé que al otro lado del mundo encontraría también personas maravillosas y que a tantos kilómetros de distancia de mi hogar encontraría otro. Por favor, recuerden que en México y en mi casa son bienvenidos *any time, allways*. Espero que alguna

vez podamos ser de nuevo compañeros de viajes, porque ahora soy adicta a ellos!!! ☺ ✈✈✈ GRACIAS A USTEDES.